■ **DOCTORAL THESIS**

LIGNOCELLULOSIC FRACTIONS FROM RICE AND COFFEE HUSKS TO IMPROVE FUNCTIONALITY OF FILMS BASED ON STARCH AND POLYLACTIC ACID

UNIVERSITAT POLITÈCNICA DE VALÈNCIA

Instituto Universitario de Ingeniería de Alimentos

para el Desarrollo

Sofía Collazo Bigliardi

Supervisors:

Dra. Amparo Chiralt Boix

Dr. Rodrigo Ortega Toro

Valencia, May 2019

Dra. Amparo Chiralt Boix, Catedrática de Universidad, perteneciente al Departamento de Tecnología de Alimentos de la Universitat Politècnica de València (Valencia, España).

Dr. Rodrigo Ortega Toro, Profesor de Universidad, perteneciente a la Facultad de Ingeniería de la Universidad de Cartagena (Cartagena de Indias, Colombia).

Hacen constar que:

La memoria titulada "**LIGNOCELLULOSIC FRACTIONS FROM RICE AND COFFEE HUSKS TO IMPROVE FUNCTIONALITY OF FILMS BASED ON STARCH AND POLYLACTIC ACID**" que presenta **Dª Sofía Collazo Bigliardi** para optar al grado de Doctor por la Universitat Politècnica de València, ha sido realizada en el Instituto de Ingeniería de Alimentos para el Desarrollo (IuIAD – UPV) bajo su dirección y que reúne las condiciones para ser defendida por su autora.

Valencia, May 2019

Fdo. Dra. Amparo Chiralt Boix

Fdo. Dr. Rodrigo Ortega Toro

A María José

y mi querido Coco.

ACKNOWLEDGEMENTS

Gracias a **Amparo Chiralt** por haberme dado la oportunidad de realizar el doctorado, y aceptarme en este grupo de investigación tan prestigioso. Fue una gran fortuna poder aprender de ti durante todos estos años; la pasión que trasmites por el conocimiento es admirable, eres un ejemplo a seguir en una infinidad de aspectos. Gracias a **Rodrigo Ortega** por confiar en mí y ayudarme a entrar en el área de la investigación, sin tu predisposición y pasión por el mundo académico no hubiera sido posible; me has enseñado que con esfuerzo, trabajo y dedicación todo se puede conseguir.

Gracias a mis compañer@s de laboratorio **Cristina, Emma, Raquel, Amalia, Eva y Ramón** por todos los buenos momentos y anécdotas compartidas. **Emma**, gracias por ser tan buena persona y estar dispuesta a ayudar sin esperar nada a cambio. Gracias a **Carol** por el apoyo y la alegría transmitida. Gracias a **Caro** y **Martina** por la felicidad y buena onda que me han dado durante el tiempo que estuvieron con nosotr@s; ¡Son divinas!

Gracias en especial a **Mayra y Alina**, mis queridas Sapper y Tampau. Sin duda son lo más bonito que me llevo de esta aventura. Hermoso todo lo que hemos vivido juntas, son unas bellísimas y auténticas personas. Gracias **Johana** por brindarme siempre buenas palabras, alegría, energía positiva, humildad y bondad; cualidades que te hacen una persona maravillosa, fuerte y admirable. Chicas, están muy adentro de mi corazón.

La distancia me enseñó que el corazón es más fuerte que los kilómetros. Gracias a **Rodrigo** por darme amor, confianza y ánimo. Hemos vivido experiencias muy enriquecedoras que nos enseñaron que prevalece el amor y el equilibrio, ante todo. Gracias por enseñarme a conservar la calma y mantener siempre una actitud positiva frente a las situaciones.

Gracias **Mariajo**, mi sensei, mi gran amiga. Siempre me has trasmitido fuerza, has estado pendiente de mí, dándome ánimo, haciéndome sentir que podía con todo. Eres una persona increíble. Te mereces todo.

Gracias totales a **Laura, Sergio y Agu**; mi hermosa loca familia. Mi mejor ejemplo de trabajo, fuerza, lucha, energía, crecimiento, apoyo y amor de familia. Mamá y papá, les admiraré y agradeceré siempre lo valiente que fueron al hacer todo lo que hicieron por nosotros cuatro. A mi hermano, gracias porque solo tengo uno y no tengo que compartirte con nadie, desde siempre me has enseñado a “pensar alto”. ¡¡Vamos!!

Una vez leí: “Gracias a todos por todo, porque todo ha sido necesario para que se diera este momento”.

ABSTRACT

The massive use of synthetic plastics, especially in the field of packaging, has provoked serious environmental problems, which, alongside the problems associated with their non-renewable origin, requires that strategies be put into practice to minimize their use. Of the different approaches to reducing this problem, one of the most interesting is the development of biodegradable compositions (preferably renewable) to replace conventional plastics. Starch and polylactic acid (PLA) are biodegradable polymers obtained from natural resources which could be used for food packaging purposes due to their ability to form food contact plastic materials with a competitive cost. Nevertheless, some of their functional properties, such as water sensitivity (starch), low oxygen barrier capacity (PLA) or mechanical performance, need to be adapted for the packaging requirements. In this sense, lignocellulosic residues constitute a source of reinforcing materials (cellulose fibres or nanocrystals) and active compounds (antioxidant/antimicrobial) which can be used to improve the functional properties of biodegradable plastics.

This Doctoral Thesis has focused on the isolation and characterisation of cellulosic materials and active extracts from coffee and rice husks, and their incorporation into starch films and starch-PLA compatibilised blend films in order to improve their functional properties as food packaging materials.

Cellulose fibres were obtained through alkali and bleaching treatment with a final yield of 41 and 53 g fibres/100 g husk, respectively for rice and coffee husks. Cellulose nanocrystals were isolated from the bleached fibres by acid hydrolysis, with a yield of 5% with respect to bleached fibres, in both cases, with high crystallinity (90-92%), thermal resistance and aspect ratio (L/d: 20-40). The active compounds were obtained by hydrothermal extraction (180 ^{o}C, 9.5 bar) with yields of 17 -18 g/100 g husks. They exhibited antioxidant properties (EC_{50}: 5.37-5.29 mg extract solids/mg DPPH) and antibacterial activity against *L. innocua* (MIC: 48-52 mg powder/mL) and *E. coli (*MIC: 50-66 mg powder/mL*),* which were quantified in terms of the minimal inhibitory concentration.

Cellulosic material from rice and coffee husks were incorporated into thermoplastic starch films (TPS) by melt blending and compression moulding. The elastic modulus increased by 186 and 121% when 1 wt% of cellulose nanocrystals (CNC) from rice and coffee husks, respectively, was incorporated into the matrix. Likewise, cellulose fibres (CF) were incorporated into TPS films at 1, 5 and 10 wt%. Both CF increased the film stiffness while reducing its stretchability. However, CF from coffee husk better maintained the film ductility at 1 and 5 wt%. The water vapour permeability of TPS films was not reduced in composites, although oxygen permeability was lowered by about 17%. When active extracts were

incorporated into starch films, they improved the tensile properties; the elastic modulus increased by about 350%, while films became less stretchable. The cellulosic fibres from both residues were more effective as reinforcing agents in films containing extract solids than in net starch films.

Starch-PLA blend films were also studied using grafted polycaprolactone with maleic anhydride and/or glycidyl methacrylate (PCL_{MG} or PCL_G) as compatibilisers. The effect of both the PLA ratio in the blend (20 and 40% with respect to starch) and the amount of both compatibilisers (2.5 and 5%) on the film properties was analysed. The analyses of microstructure, thermal behaviour and functional properties (mechanical, optical and barrier) of the films led to the conclusion that substituting 20% of the starch by PLA, and incorporating 5% of PCL_G would be a good strategy to obtain films suitable for food packaging. The effect of the addition of cellulosic fillers (CF and CNC) and antioxidant aqueous extract from coffee husk to compatibilised starch-PLA blends was also studied. The antioxidant properties of the films were tested through their efficacy at preserving sunflower oil from oxidation. Significant differences were observed in the functional properties of the films when CNC was incorporated by two different methods. The reinforcing effect of cellulosic materials in S-PLA blends was less noticeable than in starch films, probably due to the overlapping of the PLA reinforcing effect. The antioxidant extract did not improve the mechanical performance in the blends, but conferred antioxidant capacity suitable for food packaging applications.

RESUMEN

El uso masivo de plásticos sintéticos, especialmente en el área de envases, ha provocado serios problemas ambientales que, junto con el inconveniente asociado a su carácter no renovable, hace necesario el desarrollo de diferentes estrategias para minimizar su uso. Uno de los enfoques más interesantes para reducir este problema, es el desarrollo de materiales biodegradables (preferentemente renovables) para reemplazar los plásticos convencionales. El almidón y el ácido poliláctico (PLA) son polímeros biodegradables obtenidos de recursos naturales, los cuales pueden utilizarse para el envasado de alimentos debido a su capacidad para formar materiales plásticos aptos para contacto con alimentos, a precio competitivo. Sin embargo, algunas de sus propiedades funcionales, tales como su sensibilidad al agua (almidón), su baja capacidad barrera al oxígeno (PLA) o sus limitadas propiedades mecánicas, deben adaptarse a los requerimientos de envasado. En este sentido, los residuos lignocelulósicos son una fuente de agentes de refuerzo (fibras o nanocristales de celulosa) y compuestos activos (antioxidantes/ antimicrobianos), que se pueden utilizar para mejorar las propiedades funcionales de los plásticos biodegradables.

La presente Tesis Doctoral se ha centrado en el aislamiento y caracterización de materiales celulósicos y extractos activos, procedentes de las cascarillas de arroz y café, y su incorporación a películas de almidón y mezclas compatibilizadas de almidón-PLA, para mejorar sus propiedades funcionales como materiales para el envasado de alimentos.

Las fibras de celulosa (CF) se obtuvieron mediante tratamiento alcalino y de blanqueo, con un rendimiento de 41 y 53 g fibras/100 g cascarilla, respectivamente para cascarilla de arroz y café. Los nanocristales de celulosa (CNC) se aislaron de las fibras mediante hidrólisis ácida, con un rendimiento del 5% respecto a las fibras y con alta cristalinidad (90-92%), resistencia térmica y relación de aspecto (L/d: 20-40). Los compuestos activos se obtuvieron mediante extracción hidrotérmica (180 ^{o}C; 9,5 bares), con un rendimiento de 17-18 g/ 100 g de cascarilla. Dichos extractos exhibieron capacidad antioxidante (EC_{50}: 5,37-5,29 mg sólidos extraídos/ mg DPPH) y antimicrobiana (cuantificada en términos de concentración mínima inhibitoria: MIC) frente a *L. innocua* (MIC: 48-52 mg polvo/mL) y *E. coli (*MIC: 50-66 mg polvo/mL*)*.

Los materiales celulósicos procedentes de cascarilla de arroz y café se incorporaron a películas de almidón termoplástico (TPS), obtenidas mediante mezclado en fundido y moldeo por compresión. El módulo elástico aumentó un 186 y 121% cuando se incorporó a la matriz un 1% (p/p) de CNC de cascarilla de arroz y café, respectivamente. Del mismo modo, las CF se añadieron a las películas de TPS al 1, 5 y 10 pt%. Ambas CF aumentaron la rigidez y redujeron la extensibilidad de los films, aunque las CF de cascarilla de café

mantuvieron mejor la ductilidad al 1 y 5% (p/p). La permeabilidad al vapor de agua de las películas de TPS no se redujo en los materiales compuestos, aunque la permeabilidad al oxígeno se redujo en aproximadamente un 17%. Al incorporar extractos activos a los films de almidón, mejoraron sus propiedades de tracción; el módulo elástico aumentó un 350%, a la vez que se hicieron menos extensibles. Las fibras de celulosa de ambos residuos fueron más efectivas como agentes de refuerzo en los films con extractos sólidos que en los de almidón solo.

Se estudiaron también mezclas de almidón-PLA utilizando como compatibilizador policaprolactona funcionalizada con anhídrido maléico y/o glicidil metacrilato (PCL_{MG} o PCL_G). Se analizó el efecto de la proporción de PLA en la mezcla (20 y 40% respecto al almidón), y la de ambos compatibilizadores (2,5 y 5%), en las propiedades de los films. Los análisis de la microestructura, el comportamiento térmico y las propiedades funcionales (mecánicas, ópticas y de barrera) de los films, demostraron que sustituir el 20% del almidón por PLA e incorporar el 5% de PCL_G podría ser una buena estrategia para obtener materiales adecuados para envasado de alimentos. Además, se estudió el efecto de la adición de rellenos celulósicos (CF y CNC) y del extracto antioxidante de cascarilla de café en la mezcla de almidón-PLA compatibilizada seleccionada. Las propiedades antioxidantes de los films se probaron a través de su eficacia para preservar al aceite de girasol de la oxidación. Se observaron diferencias significativas en las propiedades funcionales de los films cuando los CNC se incorporaron mediante dos métodos diferentes. El efecto de refuerzo de los materiales celulósicos en mezclas de S-PLA fue menos notable que en las películas de almidón, probablemente debido a la superposición del efecto de refuerzo de PLA. El extracto antioxidante no mejoró el comportamiento mecánico en la mezcla, pero le confirió capacidad antioxidante, adecuada para aplicaciones en el envasado de alimentos.

RESUM

L'ús massiu de plàstics sintètics, especialment en l'àrea d'envassos, ha provocat seriosos problemes ambientals que, junt l'inconvenient associat als seu orígen no renovables, requereix de diferents estratègies per a minimitzar el seu ús. Un dels enfocaments més interessants per a reduir aquest problema, és el desenvolupament de materials biodegradables (preferentment renovables) per a reemplaçar els plàstics convencionals. El midó i l'àcid polí làctic (PLA) són polímers biodegradables obtinguts de recursos naturals, els quals poden utilitzar-se per a l'envasat d'aliments degut a la seua capacitat per a formar materials plàstics aptes per al contacte en aliments, a un preu competitiu. No obstant, algunes de les seues propietats funcionals tals com la sensibilitat a l'aigua (midó), la baixa capacitat barrera a l'oxigen (PLA) o les limitades propietats mecàniques, deuen adaptar-se als requeriments d'envasat. En este sentit, els residus lignocel·lulòsics són una font de agents de reforç (fibres de cel.lulosa/nano cristalls de cel.lulosa) i composts actius (antioxidants/ antimicrobians), que poden utilitzar-se per a millorar les propietats funcionals de plàstics biodegradables.

La present Tesi Doctoral s'ha centrat en l'aïllament i caracterització de materials cel.lulòsics i extractes actius, procedents de pellorfa d'arròs i café, i la seua incorporació a pel·lícules de midó i mescles compatibilitzades de midò-PLA, per a millorar les seues propietats funcionals com materials per al envasat d'aliments.

Les fibres de cel.lulosa (CF) s'obtingueren mitjançant tractament alcalí i de blanqueig, amb un rendiment de 41 i 53 g fibres/100g pellorfa, respectivament per a pellorfa d'arròs i cafè. Els nanocristalls de cel·lulosa (CNC) es van aïllar de les fibres de cel·lulosa per mig d'hidròlosi àcida, amb un rendiment del 5% respecte a les fibres; en tots dos casos, amb alta cristal·línitat (90-92%), resistència tèrmica i relació d'aspecte (L/d: 20-40). Els composts actius s'obtingueren mitjançant l'extracció hidrotèrmica (180 ^{o}C; 9,5 bars), amb un rendiment del 17-18 g/100 g de pellorfa. Aquests composts exhibiren capacitat antioxidant (EC_{50}: 5,37-5,29 mg extracte solit/ mg DPPH) i antimicrobiana, (quantificada en termes de concentració mínima inhibitòria: CMC) enfront a *L. innocua* (MIC: 48-52 mg pols/mL) i *E. coli* (MIC: 50-66 mg pols/ mL).

Els materials cel·lulòsics procedents de pellorfa d'arròs i cafè es van incorporar a pel·lícules de midó termoplàstic (TPS), obtingudes mitjançant mesclat en fos i modelatge per compressió. El mòdul elàstic va augmentar un 186 i 121% quan es va incorporar a la matriu un 1 pt% CNC de pellorfa d'arròs i café, respectivament. De la mateixa manera, les CF es van afegir a les pel·lícules de TPS al 1, 5 i 10 pt%. Ambdues CF va augmentar la rigidesa de les pel·lícules i es va reduir la seua capacitat d'estirament. No obstant, les CF de pellorfa de cafè

mantingueren millor la ductilitat al 1 i 5%. La permeabilitat al vapor d'aigua de les pel·lícules de TPS no es va reduir en els materials compostos, encara que la permeabilitat a l'oxigen es va reduir en aproximadament un 17%. A l'incorporar extractes actius a les pel·lícules de midó, milloraren les propietats de tracció de les pel·lícules ; el mòdul elàstic va augmentar un 350%, mentre que les pel·lícules es feren menys extensibles. Les CF dels dos residus foren més efectives com agents de reforç en pel·lícules que contenien extractes actius, que en pel·lícules de midó pur.

També es van estudiar mescles de midò-PLA utilitzant com a compatibilitzador policaprolactona funcionalitzada amb anhídrid maleic i/o glicidil metacrilat (PCL_{MG} o PCL_G). Es va analitzar l'efecte de la proporció de PLA en la mescla (20 i 40% respecte al midó), i de la tots dues compatibilitzadors (2,5 i 5%), en les propietats de les pel·lícules. Els anàlisis de la microestructura, el comportament tèrmic i les propietats funcionals (mecàniques, óptiques i de barrera) de les pel·lícules, demostraren que substituir el 20% del midó per PLA i incorporar el 5% de PCL_G podria ser una bona estratègia per a obtindré pel·lícules adequades per a l'envasat d'aliments. A demés, es va estudiar l'efecte de l'addició de reforçaments cel·lulòsics (CF i CNC) i extracte antioxidant de pellorfa de cafè, en mescles de midó-PLA compatibilitzades. Les propietats antioxidants de les pel·lícules s'analitzaren a través de la seua eficàcia per a preservar de l'oxidació l'oli de gira-sol. S'observaren diferències significatives en les propietats funcionals de les pel·lícules quan els CNC s'incorporaren mitjançant dos mètodes diferents. L'efecte de reforç dels materials cel·lulòsics en mescles de S-PLA va ser menys notable que en les pel·lícules de midó, provablement degut a la superposició de l'efecte de reforç del PLA. L'extracte antioxidant no va millorar el comportament mecànic en les mescles, però li va conferir la capacitat antioxidant adequada per a aplicacions a l'envasat d'aliments.

PREFACE

DISSERTATION OUTLINE

The Doctoral Thesis has been structured in five sections, as described in Figure 1: Introduction, Objectives, Chapters, General Discussion and Conclusions.

The **Introduction** section discusses the state of the art concerning the potential use of reinforcing agents of differing natures and sizes in biopolymer materials that are potentially useful for food packaging, analysing their effect on the mechanical and barrier properties, and on the thermal resistance of the material. The surface properties and biodegradation behaviour were also analysed in different kinds of composites. This corresponds to a published Book Chapter entitled "*Properties of micro- and nano-reinforced biopolymers for food applications*". A specific discussion on the use of lignocellulosic wastes to obtain cellulosic reinforcing agents, at micro- and nano-scale, and active compounds was also included. Likewise, previous studies into the effect of their incorporation on pure starch or polylactic acid matrices, and their blends, were discussed. Afterwards, the **Objective** section presents the general and specific objectives of the Doctoral Thesis.

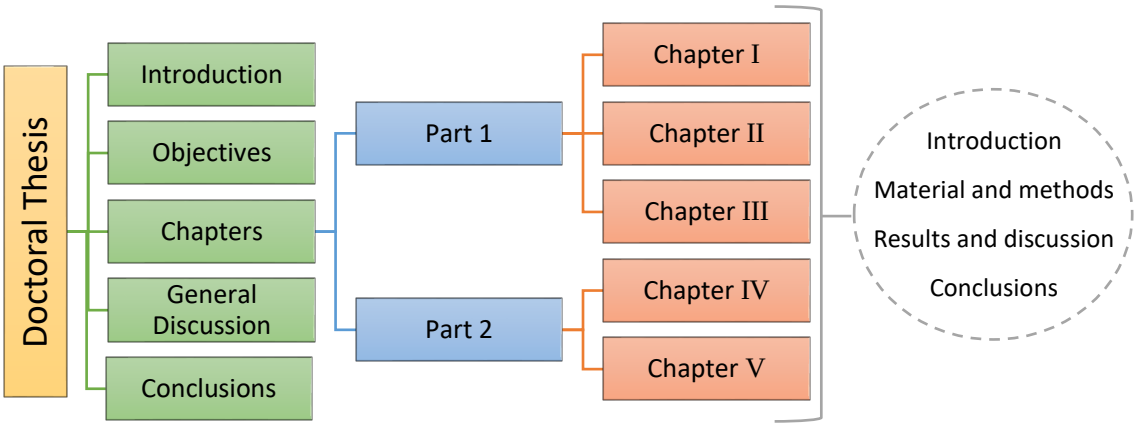

Figure 1. Structure of the present Doctoral Thesis.

The obtained results are organized in two main parts, which are divided into five **Chapters** as a collection of scientific publications with the usual sections: Introduction, Materials and Methods, Results and Discussion and Conclusions (Figure 1). Part 1 deals with the isolation and characterisation of cellulosic fractions and active compounds from lignocellulosic biomass, such as rice and coffee husk, and their effectiveness at improving the functional properties of the thermoplastic starch matrices. Thus, **Chapter I**, entitled "*Isolation and*

characterisation of microcrystalline cellulose and cellulose nanocrystals from coffee husk and comparative study with rice husk", analyses the ability of coffee husk to provide cellulosic fibres and cellulose nanocrystals as reinforcing agents. This study was made in parallel with rice husk, previously studied, for comparison purposes. These fillers have been exhaustively characterised, and the reinforcing capacity of the isolated cellulose fibres and nanocrystals, from both coffee and rice husks, have been analysed in corn starch films through their effect on tensile behaviour. In line with the good reinforcing capacity observed, a more in-depth study was carried out in order to analyse the best polymer-fibre ratio in thermoplastic starch composites. Thus, **Chapter II**, entitled "*Reinforcement of thermoplastic starch films with cellulose fibres obtained from rice and coffee husks*," analyses the changes induced by different ratios of micro-fibres from both rice and coffee husks in the microstructure, tensile, barrier and optical properties, as well as the thermal stability, of the starch film composites. Additionally to the cellulosic fractions, the active compounds from these polyphenol-rich residues were extracted by using a hydrothermal method. The extracts were characterised as to their antioxidant and antibacterial properties and also incorporated into thermoplastic starch matrices to obtain materials able to extend the food shelf life. So, **Chapter III**, entitled "*Improving properties of thermoplastic starch films by incorporating active extracts and cellulose fibres isolated from rice or coffee husk*", describes the improvement of the functional properties of thermoplastic starch films by incorporating the active aqueous extracts at different ratios. Cellulose fibres, coming from these by-products, were also incorporated as reinforcing agents into the optimal formulation with active compounds. The effect of the incorporation of both active extracts and reinforcing agents into thermoplastic starch matrices was analysed.

Part 2 includes the development of compatibilised starch-polylactic acid (PLA) blends and the addition of cellulosic materials and active extracts to these matrices. For this purpose, **Chapter IV**, entitled "*Using grafted poly(ε-caprolactone) for the compatibilisation of starch-polylactic acid blends*", analyses the effectiveness of functionalised PCL, by grafting with maleic anhydride and/or glycidyl methacrylate, at improving the properties of blend films based on corn starch and PLA, obtained by melt blending and compression moulding. The microstructure and functional properties of blend films with different ratios of PLA and compatibilisers were analysed in order to select the best formulation for food packaging applications. Finally, **Chapter V**, entitled "*Using lignocellulosic fractions of coffee husk to improve properties of compatibilised starch-PLA blend films*", concluded the chapter section. This chapter includes the incorporation of cellulosic reinforcing agents (cellulose fibres and cellulose nanocrystals) and antioxidant aqueous extract from coffee husk to improve the functional properties of compatibilised starch-PLA blend films. The effect of the incorporation method of cellulose nanocrystals into the blend films is analysed, as well as the antioxidant properties of the films through their efficacy at preserving sunflower oil from oxidation.

The most relevant results obtained in the different chapters are analysed from a global perspective, in the **General Discussion** section. Finally, in the last section the most relevant **conclusions** are presented.

DISSEMINATION OF RESULTS

INTERNATIONAL JOURNALS JCR

Published

"Antifungal starch-based edible films containing *Aloe vera*". Rodrigo Ortega-Toro; Sofía Collazo-Bigliardi; Josefa Roselló; Pilar Santamarina; Amparo Chiralt. *Food Hydrocolloids* (2017), 72, 1-10.

"Isolation and characterisation of microcrystalline cellulose and cellulose nanocrystals from coffee husk and comparative study with rice husk". Sofía Collazo-Bigliardi; Rodrigo Ortega-Toro; Amparo Chiralt. *Carbohydrate Polymers* (2018), 191, 205-215.

"Reinforcement of thermoplastic starch films with cellulose fibres obtained from rice and coffee husks". Sofía Collazo-Bigliardi; Rodrigo Ortega-Toro; Amparo Chiralt. *Journal of Renewable Materials* (2018), 6, 599-610.

Chapter. "Properties of Micro- and nano-reinforced biopolymers for food applications". Sofía Collazo-Bigliardi; Rodrigo Ortega-Toro; Amparo Chiralt. In: Gutiérrez, T. (Ed.*). Polymers for food applications*. Springer (2018), pp. 61-99.

Submitted

"Improving properties of thermoplastic starch films by incorporating active extracts and cellulose fibres isolated from rice or coffee husk". Sofía Collazo-Bigliardi; Rodrigo Ortega-Toro; Amparo Chiralt*. Food Packaging and Shelf Life.*

"Using grafted poly(ε-caprolactone) for the compatibilization of starch-polylactic acid blends". Sofía Collazo-Bigliardi; Rodrigo Ortega-Toro; Amparo Chiralt. *Reactive and Functional Polymers.*

"Using lignocellulosic fractions of coffee husk to improve properties of compatibilized starch-PLA blend films". Sofía Collazo-Bigliardi, Rodrigo Ortega-Toro, Amparo Chiralt*. Food Packaging and Shelf Life.*

Chapter. "Use of by-products in edible coatings and biodegradable packaging materials". Chelo González-Martínez; Sofía Collazo-Bigliardi; Carolin Menzel; Eva Hernández García; Amparo Chiralt. *Sustainability of the Food System: Sovereignty, Waste, and Nutrients Bioavailability*. Ed Elsevier.

COMMUNICATIONS IN INTERNATIONAL CONGRESSES

Poster: **"Coffee wastes to obtain useful compounds for biodegradable packaging material"**. Sofía Collazo-Bigliardi; Rodrigo Ortega-Toro; Amparo Chiralt. International XXI IUPAC Chermin conference: Solid urban waste management. Roma, Italy (2016).

Poster: **"Obtaining cellulose nanocrystals from lignocellulosic biomass from coffee husk"**. Sofía Collazo-Bigliardi; Rodrigo Ortega-Toro; Amparo Chiralt. International Conferences in Food Innovation. Food Innova 2017. Cesena, Italy (2017).

Poster: **"Reinforcement of thermoplastic starch films with cellulosic material obtained from rice and coffee huks"**. Sofía Collazo-Bigliardi; Rodrigo Ortega-Toro; Amparo Chiralt 6th International Conference on Biobased and Biodegradable Polymers. BIOPOL 2017. Mons, Belgium (2017).

Poster: **"Rice husk: from wastes to useful compounds for biodegradables food packaging"**. Sofía Collazo-Bigliardi; Rodrigo Ortega-Toro; Amparo Chiralt. 3rd International & 4th National Student Congress of Food Science and Technology (AVECTA 2017). Burjassot, Spain (2017).

Poster: **"Micro- and nano-cellulosic fillers from rice and coffee husks to improve properties of thermoplastics starch films"**. 4th International & 5th National Student Congress of Food Science and Technology (AVECTA 2018). Burjassot, Spain (2018).

COMMUNICATION IN SCIENTIFIC EVENTS

Oral communication: "**Aprovechamiento de residuos lignocelulósicos para la obtención de materiales activos de envasado a base de almidón y ácido poliláctico**". Sofía Collazo-Bigliardi; Rodrigo Ortega-Toro; Amparo Chiralt. "V encuentro de estudiantes de doctorado en la UPV", en Valencia, Spain (2018).

PREDOCTORAL STAYS AT FOREIGN INSTITUTIONS

Engineering Department, Process Engineering and Chemical/Food Products Research Group, Universidad Jorge Tadeo Lozano (Bogotá, Colombia). From 5th February 2017 to 6th August 2107, under the supervision of Professor Rodrigo Ortega-Toro and Professor Yineth Piñeros-Castro.

TABLE OF CONTENTS

NOMENCLATURE

A: Active extract

AE: Antioxidant extract

AFM: Atomic Force Microscopy

Ag-NPs: Ag nanoparticles

ATBC: Acetyltributyl citrate

BCNW: Bacterial cellulose nanowhiskers

C: Coffee

C_{ab}*: Chroma

ChNC: Chitin nanocrystals

CMC: Carboxymethyl cellulose

CNC: Cellulose nanocrystals

CNF: Cellulose nanofibrils

Da: Dalton

DPPH: 2,2-Diphenyl-1-pikryl-hydrazyl

DSC: Differential Scanning Calorimetry

DTGA: Thermal weight loss derivate

EC_{50}: Half maximal effective concentration

EM: Elastic Modulus

ε: Elongation at break point

F: Cellulose fibres

FESEM: Field Emission Scanning Electron Microscopy

FTIR: Fourier Transform Infrared Spectroscopy

G: Glycidyl methacrylate

GAE: Gallic acid equivalent

Gly: Glycerol

GTA: Glycerol triacetate

h_{ab}*: Hue

HPMC: (Hidroxypropil)metil cellulose

L*: Luminosity

LDPE: Low Density Polyethylene

M: Maleic Anhydride

MC: Methylcellulose

MCC: Microcrystalline cellulose

MIC: Minimum Inhibitory Concentration

MMT: Montmorillonite

NCC: Nano-crystalline cellulose

OP: Oxygen Permeability

PBS: Poly(butylene succinate)

PBTA: Poly(butylene adipate co-terephthalate)

PCL: Polycaprolactone

PE: Polyethylene

PEG: Polyethylen glycol

PET: Polyethylene terephthalate

PHA: Polyhydroxyalcanoates

PHB: Polyhydroxybutyrate

PHBV: Polyhydroxyl-3-butyrate-co23-valerate

PHBV12: Polyhydroxybutyrate with 12 mol% of valerate and containing 10 wt% of the plasticizer citric ester

PLA: Poly(lactic) acid

PLLA: Poly(l-lactide)

PP: Polypropylene

PS: Polystyrene

PV: Peroxide Value

PVA: Poly(vinyl alcohol)

R: Rice

S: Starch

SEM: Scanning Electron Microscopy

TE: Trolox equivalent antioxidant capacity

T_g: Glass transition temperature

TGA: Thermogravimetric Analysis

Ti: Internal transmittance

T_{Onset}: Onset Temperature from TGA

TPCS: Thermoplastic corn starch

T_{Peak}: Peak Temperature from TGA

TPS: Thermoplastic starch

TS: Tensile Strength

UV: UltraViolet

UV-VIS: UltraViolet-Visible Spectroscopy

WSNC: Waxy starch nanocrystals

WVP: Water Vapour Permeability

INTRODUCTION

1. Properties of micro- and nano-reinforced biopolymers for food applications

Polymers for food applications. Sofía Collazo-Bigliardi; Rodrigo Ortega-Toro; Amparo Chiralt. Springer (2018), pp. 61-99.

Of all the materials available for food packaging, plastics have increased exponentially over the past two decades, with an annual growth of approximately 5%. It is estimated that worldwide annual plastic production exceeds 300 million tonnes, and was about 59 million tonnes in Europe in 2014. In fact, nowadays, plastics represent almost 40% of the European packaging market (Muller et al. 2017a). Of the plastic materials, petroleum-based plastics, such as polyethylene (PE), polypropylene (PP), polyamide (PA), are widely used as packaging materials due to their ready availability at relatively low cost, good mechanical and barrier properties, thermo-processing ability and chemical characteristics, which make them suitable for food packaging. However, despite their good properties, their use and accumulation imply serious environmental problems and a dependence on fossil fuels. 63% of the current plastic waste comes from packaging applications, and it is estimated that less than 14% is recyclable. Taking this scenario into account, and bearing in mind the growing environmental awareness, research has focused on the development of alternative bio-packaging materials, derived from renewable sources, which are biodegradable or compostable.

Biopolymers can be used for food packaging applications or food coating purposes, reducing the environmental impact and oil-dependence (Rivero et al. 2017; Emadian et al. 2017). They can be divided into three main categories, based on their origin and biodegradable nature. Together with the conventional, non-biodegradable, oil-based plastics, there are biobased-non-degradable bioplastics (e.g polyethylene terephthalate: PET), biobased-biodegradable bioplastics (e.g. polylactic acid: PLA, starch and other polysaccharides, or proteins) or fossil-based biodegradable bioplastics (e.g. polycaprolactone: PCL, polyvinyl alcohol. PVA or polybutylene succinate: PBS). So, biopolymers are biodegradable, biobased or both and can be classified as those directly obtained from biomass (polysaccharides and proteins), synthetic biopolymers from biomass or petrochemicals (e.g. PLA, PCL) or those obtained by microbial fermentation (polyhydroxyalcanoates: PHA and bacterial cellulose) (Nair et al. 2017). The former are directly extracted from biological and natural resources and they are hydrophilic and somewhat crystalline in nature, making an excellent gas barrier. Biodegradable polyesters (synthetic or biosynthesized) are more hydrophobic and constitute better barriers to water vapour. In general, the functional properties of biopolymer-based materials in terms of their mechanical and barrier properties need to be adapted to food requirements by using different strategies, such as physical or chemical modifications (crosslinking), blending with other components, fillers, plasticizers or compatibilizers (Ortega-Toro et al. 2017).

The industrial uses of biopolymers have been restricted because of their usually poor mechanical, barrier or thermal properties, and high price. The incorporation of micro- and nano-reinforcing agents into the matrix for the purposes of obtaining composites has been

seen to improve their functional properties and so their competitiveness in the plastics market. Composites are made up of a continuous polymer matrix in which the filler particles are dispersed, thus contributing to a modification of the functional characteristics of the material (Azeredo et al. 2009). Fillers differing in size, shape, amount, distribution and chemical nature have been used. Lignocellulosic or cellulosic materials obtained from agro-waste have been widely studied as organic micro-fillers. Fibres from cotton (Ludueña et al. 2013), garlic straw (Kallel et al. 2016), rice husk (Johar et al. 2012), wheat straw (Berthet et al. 2015) or coffee silverskin (Sung et al. 2017), have been used as reinforcing agents in different biopolymer films. Micro-particles significantly improved the elastic modulus of composites while providing great thermal resistance to the matrices due to the presence of hydroxyl groups interacting with the biopolymer network (Ludueña et al. 2013; Berthet et al. 2015). Different organic nano-fillers can be obtained, mainly from cellulose (cellulose nanocrystals or nanofibres), chitin/chitosan nanocrystals from crustacean waste or starch nanoparticles. These nano-reinforcing agents improve the tensile strength and elastic modulus when they have a proper distribution, chemical affinity with the polymer and high aspect ratio. The crystalline structure of nano-fillers enhances the tortuosity factor for the mass transport of gas molecules into the biopolymer matrix, contributing to the formation of a hydrogen-bonded network (Ng et al. 2015; Azeredo et al. 2009; Azeredo et al. 2017). On the other hand, inorganic particles are relevant as filling agents in food packaging materials due to the enhancement of the mechanical and barrier properties (MgO, silicon carbide or nano-clays) Some of them also exhibited antimicrobial activity, such as Ag, TiO_2 and ZnO nanoparticles (Gutiérrez et al. 2017; Azeredo et al. 2009).

It is remarkable that biodegradation behaviour is a crucial factor in the development of composites. The biodegradation process takes place in aerobic conditions by the action of a microorganism, which identifies the polymer as a source of energy to produce organic residues from the packaging material. The incorporation of nano-fillers can affect the biodegradability of composites. In this sense, cellulose nanocrystals (CNC) promoted the material's water intake due to their hydrophilic nature, contributing to an acceleration of the biodegradation process (Ludueña et al. 2012; Luzi et al. 2016). Some inorganic nano-fillers could also affect the disintegration processes, such as what occurs with Ag nanoparticles (Ramos et al. 2014; Cano et al. 2016), or nano-clays, whose hydroxyl groups react with the chains of the polymer matrices (montmorillonite and fluorohectorite, Fukushima et al. 2013).

1.1. Bioplastics for food packaging

Over the last decade, several bioplastics, bio-based, biodegradable, or both, have been available as a suitable alternative to conventional plastics for food packaging applications (Fabra et al. 2014; Ortega-Toro et al. 2017). At least 90% of natural or synthetic biodegradable

polymers decompose in less than 180 days (ASTM 2003). Fig. 2 shows the main polymers of potential use in food packaging. Of the natural polymers, different polysaccharides and proteins and microbially-produced biopolymers have been extensively studied for food packaging applications.

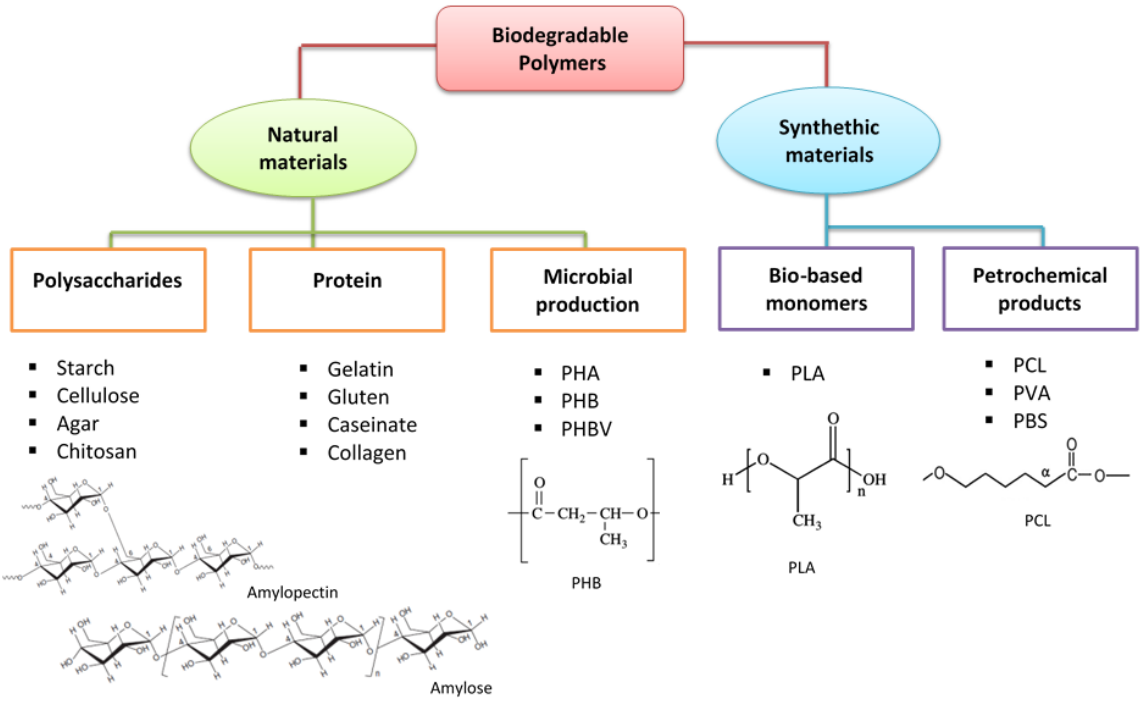

Figure 2. Main biopolymers with potential application in food packaging. Some molecular structures are included.

Starch is a promising polymer, suitable for processing by means of different techniques, such as the casting method (Moreno et al. 2017), compression moulding (Muller et al. 2017b), extrusion (González-Seligra et al. 2017) or injection moulding (López et al. 2015). Starch is naturally highly abundant, low cost and renewable. Cellulose, constituted by glucose units via β-1,4-glycosidic bonds, is the most naturally abundant carbohydrate (Xiao 2014). This polymer is usually used as micro-filler or nano-filler (Shankar and Rhim 2016) in the composite formulation. These could be processed by compression moulding and injection moulding (Graupner et al. 2016) to obtain semi-rigid packaging (trays). On the other hand, agar is a fibrous polysaccharide obtained from marine algae, such as *Gelidium* sp. and *Gracilaria* sp., consisting of a mixture of agarose and agaropectin, which is slightly branched and sulphated. This is thermoplastic polysaccharide, biodegradable and biocompatible, which exhibits great mechanical strength with moderate water resistance (Giménez et al. 2013). Chitosan, the

second most naturally abundant polysaccharide, has non-toxic, biodegradable, and antimicrobial characteristics, which are of great interest for packaging purposes (Leceta et al. 2013). Chitin, the precursor of chitosan, is a linear polymer of mainly β-(1→4)-2-acetamido-2-deoxy-d-glucopyranose units and low amounts of β-(1→ 4)-2-amino-2-deoxy-d-glucopyranose residues (Van den Broek et al. 2015). Others relevant natural polymers are proteins, such as gelatin or collagen, gluten proteins and dairy proteins. Gelatin is an animal protein obtained by the hydrolysis of the fibrous insoluble collagen from skins and bones of different animals. It is well known for its film-forming properties. It is abundantly available, low cost and easily biodegradable and biocompatible (Kanmani and Rhim 2014). On the other hand, wheat gluten (constituted by gliadins and glutenin proteins) is an inexpensive protein from the milling process, which allows the production of membranes that are semipermeable to water vapour, oxygen and carbon dioxide molecules. This polymer can be applied as a food coating or edible film on different foods (Rocca-Smith et al. 2016), or processed by compression moulding (Zubeldía et al. 2015) and extrusion (Rombouts et al. 2013) for the purposes of developing flexible or semi-rigid packaging. Caseinates have been proposed as raw materials for food packaging development, since this protein exhibited good film-forming ability with good mechanical properties (Fabra et al. 2012; Arrieta et al. 2014a; Jiménez et al. 2013). The use of caseinates could be considered an alternative means of obtaining a high degree of protection from oxygen in modified atmosphere packaging (Arrieta et al. 2014a). Biopolymers obtained from several microorganisms, such as poly-hydroxyalkanoates -PHA-, poly-hydroxybutyrate -PHB-, or poly- hydroxybutyrate-co-hydroxyvalerate -PHBV-, are a family of biodegradable thermoplastic polymers. The polymer is produced in the microbial cells through a fermentation process and then collected by solvents, like chloroform. More than 100 PHA are identified, of which PHB is the most common (Peelman et al. 2013). PHB is a biopolymer produced from renewable sources and fermentation by certain microorganisms, like *Halomonas hydrothermalis* and *Burkholderia* sp. and *Chelatococcus daeguensis*, inter alia (Bera et al. 2015). In addition to being biodegradable, PHB exhibits some properties similar to some synthetic polymers, especially polypropylene (PP) (Heitmann et al. 2016). PHBV is a copolymer of 3-hydroxybutanoic acid and 3-hydroxypentanoic acid produced directly by microorganisms. This polymer is less brittle and more stretchable than PHB (Requena et al. 2017).

Other biodegradable polymers are obtained by synthesis from biobased monomers (e.g. PLA) and non-biobased monomers (e.g. PCL, PVA or PBS). PLA is the most common synthetic polymer obtained from biobased monomers. The synthetic routes to obtain PLA are through the ring-opening polymerisation of the esters of the acid and the direct condensation of the free acid (Cheng et al. 2009). PLA is of great potential to the packaging industry because of its mechanical, barrier and optical properties. It can be processed using readily available production technologies, and exhibits good thermal behaviour and water vapour barrier properties, although it is brittle and only a moderate gas barrier (Bonilla et al. 2013).

In the category of biodegradable synthetic petroleum-based polymers, PCL, PVA and PBS are the most representative. PCL is a linear, semicrystalline hydrophobic polyester, highly flexible, tough and thermally stable (Correa et al. 2017). In contrast, PVA is a synthetic, water soluble polymer which forms translucent films with good tensile strength, elongation at break and barrier properties (Dominguez-Martinez et al. 2017). PVA has been used in polymeric blends, with glycerol as a proper plasticiser because of its chemical affinity. PBS is another biodegradable thermoplastic polymer which has desirable melt processability and good mechanical properties, which are closely comparable to those of widely-used polyethylene (PE) or polypropylene (PP) (Mizuno et al. 2015).

1.2. Micro- and nano-reinforcing agents

An alternative means of improving the properties of biopolymers for food packaging applications, and reducing some of their drawbacks, is by the incorporation of micro- or nano-fillers to the matrix for the purposes of obtaining micro- and nano-composites. Composites have immiscible phases constituted by the polymer continuous network in which the filler particles are dispersed, thus generating new structures with different properties to those of the original polymer matrix. The filler can positively modify the functional characteristics of the material, depending on the filler polymer network interactions. Different kinds of fillers have been used, which modify the material characteristics as a function of the filler-matrix interactions. The size, shape, amount, distribution and chemical nature of the fillers are crucial factors in the final properties of the composite.

Many studies reported the use of different kinds of fillers. As is shown in Table 1, cellulose has been frequently used as a reinforcing agent in different forms, such as cellulosic fibres (Martino et al. 2015; Moustafa et al. 2016; Ludueña et al. 2012), bacterial cellulose (Fabra et al. 2016), nano-cellulosic fibres (Abdul Khalil et al. 2016) or cellulose nanocrystals (El-Hadi 2017; Fortunati et al. 2013a; Follain et al. 2013). In the polymer matrices, the incorporation of cellulosic fillers directly affects the mechanical and barrier properties depending on the particle size (micro or nano), which is a significant factor. As has been observed by various authors, particle size has differing effects on the mechanical properties. Cho et al. (2006) studied the effect of the particle size on the mechanical properties of polymeric composites with spherical micro (0.5 mm) and nano (15 nm) particles. They observed that, at nano-scale, Young's modulus and tensile strength increased as the particle size decreased. As regards the barrier properties, it is expected that nano-scale and a homogeneous distribution increase the tortuosity factor for the migration of molecules through the composite, decreasing the permeability of both water vapour and gases. On the other hand, the amount of filler included significantly affects the composite properties.

Table 1. Main inorganic and organic reinforcing agents used as fillers in biopolymer matrices and main provoked changes in the matrix.

Micro- and Nano-fillers	Filler information	Polymer matrix	Main provoked changes	Applications	Reference
Organic fillers					
Lignocellulosic fibres	Natural Lignocellulosic material	PHBV/ wheat straw	-Decrease cost -Increase EM -Decrease deformation	-Food Packaging	Martino et al. 2015
	Natural by-product	PBAT/coffee ground	-Compatibiliser not necessary -Improve mechanical properties	-Food packaging	Moustafa et al. 2016
Cellulosic fibres	Natural Previously alkali treated agro-waste	PCL/cotton	-Improve mechanical properties and biodegradation in soil	-Food packaging	Ludueña et al. 2012
Bacterial cellulose	Obtained from bacterial strain *Gluconacetobacter xylinus* 7351	TPS, PHB	-Improve mechanical and barrier properties	-Food packaging	Fabra et al. 2016
Nanocellulosic fibres	Natural Glucose units (beta-1,4 glycosidic linkages) $(C_6H_{10}O_5)n$	TPS, PLA	-Improve mechanical, thermal and barrier properties	-Food packaging -Pharmaceutical and industrial packaging -Medical application	Abdul Khalil et al. 2016
Cellulose nanocrystal	Natural Obtained from agro-wastes	PHB and PLA	-Reduce Tg, Tc and Tm -Improve mechanical properties	-Food packaging	El-Hadi 2017
		PVA	-Increase tensile strength	-Food packaging	Fortunati, et al. 2013a
		PCL	- Decrease WVP	-Food packaging	Follain et al. 2013
Chitin nanocrystals	Powder from crustacean waste	PLA	-Improve mechanical properties and transparency	- Packaging and food packaging	Herrera et al. 2016
Starch nanocrystals	Amadumbe corms. Botanical sources: normal maize, waxy maize, amylomaize, potato, rice, oat, peas or beans.	TPS PLA, PVA, PBS, natural rubber, pullulan, carboximethyl chitosan	-Increase barrier properties -Improve mechanical properties -Increase the biodegradability	- Food packaging - Water treatment - Adhesive applications - Medical application	Mukurubira et al. 2017 Le Corre and Angellier-Coussy 2014

Table 1. (Continued)

Micro- and Nano-fillers	Filler information	Polymer matrix	Main provoked changes	Applications	Reference
Inorganic fillers					
Ag nanoparticles	Metal	-Cellulose -HPMC -Pullulan -TPS -Alginate	- Provide antimicrobial and antiviral properties	- Fresh food packaging: meat, fruit and dairy products. -Food packaging -Agricultural	Carbone et al. 2016. Gutiérrez et al. 2017
		-Agar	-Decrease WVP	-Food packaging	Rhim, et al. 2014
TiO_2 nanoparticles	Oxide	Several polymers TPS	- Provide antimicrobial properties -Change colour	-Food packaging: active and intelligent packaging -Food packaging -Agricultural	He et al. 2015 Gutiérrez et al. 2017
ZnO nanoparticles	Oxide	TPS	- Provide antimicrobial properties	-Food packaging -Agricultural	Gutiérrez et al. 2017
MgO nanoparticles	Oxide	Chitosan	-Increase tensile strength and deformation -Decrease water solubility	-Food packaging	Sanuja et al. 2014
Silicon carbide	SiC Melting point: 2730 °C Molar mass: 40,11 g/mol	Starch	-Decrease OP	-Food packaging -Industrial packaging	Dash and Swain 2013
Nano-clays	Phyllosilicates $Al_2Si_2O_5(OH)_4$ Specific gravity: 2-2.65	Pectin/PEG/hallosyte	-Decrease water uptake capacity -Increase EM	-Industrial packaging	Cavallaro et al. 2013
	$M_x(Al_4\text{-}xMg_x)Si_8O_{20}(OH)_4$	Several polymers/MMT	-Increase barrier properties -Improve mechanical properties	-Food Packaging -Industrial packaging	Majeed et al. 2013
		Alginate	-Reduced water solubility -Decrease elongation and increase tensile strength -Decrease WVP	-Food Packaging	Abdollahi et al. 2013

At high concentrations, the polymer matrix could lose cohesiveness and continuity which could lead to a loss in functional properties (mechanical and barrier). In this sense, Maqsood et al. (2016) studied the reinforcing capacity of enzyme-hydrolysed longer jute micro-crystals in polylactic acid matrices. The elastic modulus and tensile strength increased by 40% and 28% respectively, once the filler loading rose to 5% with respect to neat PLA. However, a filler loading of 10% led to a decrease of 32% in the elastic modulus and 33% in tensile strength with respect to materials containing 5% of fillers. Other organic fillers are chitin nanocrystals (Herrera et al. 2016) from crustacean waste that improve the mechanical properties and transparency of neat PLA. Also, starch nanocrystals are frequently added to several biopolymers, improving the mechanical and barrier properties and decreasing the biodegradation time (Mukurubira et al. 2017; Le Corre and Angellier-Cousy 2014).

Some inorganic particles have been extensively studied as fillers in food packaging materials. Some of these, such as MgO, (Sanuja et al. 2014); silicon carbide, (Dash and Swain 2013) and nano-clays (Cavallaro et al. 2013; Majeed et al. 2013; Abdollahi et al. 2013), enhanced the mechanical and barrier properties of the films. Additionally, other ones can provide antimicrobial activity to the material, as occurs with Ag nanoparticles (Carbone et al. 2016; Gutiérrez et al. 2017), TiO_2 nanoparticles (He et al. 2015; Gutiérrez et al. 2017) and ZnO nanoparticles (Gutiérrez et al. 2017).

1.3. The effect of reinforcing agents on the functional properties of biopolymers

In the following sections, the effect that micro- and nano-fillers have on the tensile behaviour, barrier properties, thermal resistance and biodegradability of biopolymer matrices is discussed, taking the processing method into account.

1.3.1. Processing method

In general, thermomechanical processes (melt compounding, extrusion and compression moulding) with high shearing forces, temperature and adequate time are necessary to guarantee the convenient dispersion of the filler in the polymer matrix. However, the casting of polymer-filler dispersions is an alternative method to obtain nano-composites, due to the high aggregation tendency of nanoparticles, which are better maintained in liquid dispersions. Table 2 shows some recent studies on composite materials, including micro- or nano- fillers of differing characteristics, using different processing methods.

Table 2. Recent studies on composite materials including micro- or nano- fillers of different nature, applying different processing methods.

Composite material	Filler content	Processing method	Effect of filler	Possible application	Reference
Polymer/micro-filler					
PHBV/wheat straw fibres	10, 20 and 30 wt% filler with different preparation process	Extrusion and compression moulding	-Increased the water vapour transmission -Decrease ultimate tensile strength	-Food packaging to fresh products	Berthet et al. 2015
PHBV/keratin	0.5, 1, 3, 5, 10, 25 and 50 wt% filler	Melt compounding	-Reduction WVP and OP -Improve mechanical properties	-Packaging	Pardo-Ibáñez et al. 2014
PBAT/roasted coffee ground	10, 20 and 30 wt% filler with roating process at 250°C and 270°C	Extrusion	-Increase hydrophobicity -Increase thermal stability -Compatibiliser is not necessary	-Food packaging	Moustafa et al. 2016
Polymer/nano-filler					
PCL-MC/NCC	2 wt% NCC	Casting and compression moulding	- Increased the tightly of the matrix - Increased stability of active components - Increased the rough and density of the matrix	- Vegetable packages	Boumail et al. 2013
PLA/CNC from MCC and Ag-NPs	1 and 5 wt% CNC with/without surfactant and 1 wt% Ag nanoparticles	Casting	- Increase barrier effect - Antimicrobial effect	- Food active packaging	Fortunati et al. 2013b
Agar/Ag-NPs	20, 40 and 80mg Ag-NPs	Casting	-Increase thermal stability. -Barrier properties to water vapour increase slightly -Antimicrobial activity against Listeria monocytogenes and Escherichia coli O157:H7	-Food packaging	Rhim, et al. 2014
Alginate/Nano-clays MMT and CNC from MCC	1, 3 and 5wt% fillers	Casting	-Decrease water solubility -Increase surface hydrophobicity with CNC and decrease of this parameter with nanoclays addition -Reduction in WVP -Tensile properties improved	-Food packaging	Abdollahi et al. 2013
Chitosan/MgO	0.1g MgO/g chitosan	Casting	-Improve mechanical proper -Decrease swelling, permeability and solubility -Antimicrobial properties	- Food active packaging	Sanuja et al. 2014
Starch/Silicon carbide	1, 2, 5, 8, 10 wt% filler	Casting	-Increase thermal stability -Reduce OP	-Adhesive application -Protecting applications -Food packaging	Dash and Swain 2013
Pectin-PEG/Halloysite nanotubes	5, 10, 15, 20, 30 and 50 wt% filler	Casting	-Decrease wettability -Improve mechanical properties	-Coatings for food conservation	Cavallaro et al. 2013

Berthet et al. (2015) studied the properties of PHBV composites containing wheat straw micro-fibres (10, 20 and 30 wt%). Compounding was carried out with a lab-scale twin-screw extruder, using a temperature profile from the polymer feeding to the die of 180°C to 160°C. Composite films were obtained by compression moulding at 170°C. The mechanical and barrier properties of composites were poorer than those of neat PHVB, although the authors point that the obtained materials could be applied as packaging for respiring fresh products. Melt compounding using a Plastograph mixer (16 cm3) for 4 min at 160 °C was also applied to obtain PHBV composites with micro-particles of keratin at 0.5, 1, 3, 5, 10, 25 and 50 wt%. The composites exhibited improved mechanical and water vapour and oxygen barrier properties with only 1 wt% of micro-filler (Pardo-Ibañez et al. 2014). Moustafa et al. (2016) studied the use of roasted coffee grounds as micro-reinforcing agent to produce high-quality biodegradable Polybutylene adipate co-terephthalate (PBAT) composites for food packaging applications. The composites were extruded at 160 to 165°C with a screw speed of 100 rpm for 5 min mixing. The films were obtained by a special die attached to the mixing chamber. The authors observed an increase in the hydrophobicity and thermal stability compared to the control films without fillers. A compatibiliser was not necessary to obtain a filler-polymer matrix with suitable interfacial adhesion, especially at low filler content (< 30%), which was attributed to the good grindability of roasted coffee, which improved compatibility and filler dispersion during processing.

As concerns the incorporation of nano-fillers in composites, casting is the most commonly used method due to the better dispersion (more limited aggregation) of nano-particles in a liquid medium. Casting is suitable for the obtaining of coatings, mulch films and flexible films. In some cases, this technique has been used as a preliminary test to study the filler effect before thermomechanical processing with actual industrial applications. Boumail et al. (2013) characterized trilayer antimicrobial films based on methylcellulose and PCL composites with 2% of cellulose nanocrystals (CNC). These were prepared under stirring before sonication at room temperature for 30 min and the subsequent casting of the PCL-CNC dispersion. The trilayer films were obtained by compression moulding at 120 °C. An increase in the matrix toughness and greater stability of active components was found by the filler addition. Fortunati et al. (2013b) incorporated the CNCs and Ag-NPs PLA films obtained by casting, leading to improved barrier properties and antimicrobial activity in the composites. Ag-NPs (20, 40 and 80 mg Ag-NPs) have also been included in other polymers, such as agar matrices; although a significant increase in the thermal stability of the material was obtained, with improved water vapour barrier properties and antimicrobial activity against Listeria monocytogenes and Escherichia coli O157:H7, the mechanical strength and stiffness of the composites slightly decreased with respect to filler-free polymers (Rhim et al. 2014). Chitosan composites with MgO nano-filler, obtained by casting, also exhibited antimicrobial properties. In addition, the metallic oxide improved the mechanical properties and reduced the water

swelling capacity and solubility and water vapour permeability of the films, which became less transparent.

Other nanocomposites with organic (CNC) or inorganic nano-clays:MMT) obtained by casting, using an alginate matrix, exhibited improved functional properties with respect to the net polymer matrix (Abdollahi et al. 2013). The addition of both nano-fillers improved the tensile properties of the material and promoted a decrease in water solubility and water vapour permeability, whereas the surface hydrophobicity increased with the use of CNC but decreased with nano-clays. In the same way, nanoparticles of silicon carbide increased the thermal stability and reduced the oxygen permeability in starch composites (Dash and Swain 2013). This material could be used as adhesive and coating in food applications. Halloysite nanotubes promoted a decrease in film wettability and improved the mechanical properties in composites of pectin and polyethylene glycol blends (Cavallaro et al. 2013).

1.3.2. The effect on tensile properties

In this section, the changes in the tensile properties of some biopolymers caused by incorporating nano- and micro-fillers of differing characteristics are analysed, as summarized in Table 3. The main mechanical properties characterized in plastic packaging materials are elastic modulus (EM) and the tensile strength (TS) and elongation (ε) at break, which provide information about the rigidity and resistance to deformation and break of the material, respectively.

The changes in the polymer's functional properties caused by filler addition are strongly associated with surface properties and polymer-filler interfacial interactions. In this sense, the effects caused by fillers on the mechanical properties of polymer are not always positive. The main reason is the interruption of the polymer matrix continuity, but this effect could be diminished if the polymer and fillers have chemical affinity or an interfacial agent is added into the composite formulation. As previously mentioned, Berthet et al. (2015) found a deterioration in the tensile properties of neat PHBV when wheat straw fibres were added to the matrix. Strain and stress at break decreased by 61% and 63%, respectively, with 30 wt% filler in the composite. However, Young's modulus increased by 13% with 20 wt% filler. Moustafa et al. (2016) found different trends in the tensile strength with the variation in filler content, using differently roasted coffee ground (CG) in PBAT matrices. As compared with neat PHBV, the best tensile behaviour was obtained with 10% of filler roasted at the highest temperature (270 °C), while the worst behaviour was observed for 30% of non-roasted CG powder. As the authors mentioned in their study, roasted CG showed a better affinity with PBAT compared to untreated CG when obtaining green composites without the need for a compatibiliser.

Table 3. Changes in tensile properties of some biopolymers by incorporating micro- or nano-fillers of different nature. Data show the range in the values of each property reported for the different formulations.

Composite material	Filler content	Plasticizer/ equilibrium RH	Thickness (µm)	TS (MPa)	EM (MPa)	ε (%)	Reference
Polymer/micro-filler							
PHBV/wheat straw fibres	10, 20 and 30 wt.% filler with different preparation process	---	---	2.2 - 3.13	14.4-39.2	0.89 -*2.3	Berthet et al. 2015
PBAT/roasted coffee ground	10,20 and 30 wt.% filler with roasting process at 250°C and 270°C	/50%	300-400	6.8 - 18.2	---	98 - *1545	Moustafa et al. 2016
PHBV /keratin	0.5, 1, 3, 5, 10, 25 and 50 wt.% filler	---	100	---	540 - 600	2.9 - *5.5	Pardo-Ibáñez et al. 2014
Polymer/nano-filler							
PCL-MC/NCC	7.7 wt% NCC	Glycerol/	225-280	*20.3 - 24.0	175.2 - *218.3	---	Boumail et al. 2013
PLA/CNC and ChNC	1 wt % nanocrystals	Triethyl citrate/	100	*15.8 - 24.2	*300 - 1200	16 - 309	Herrera et al. 2016
Corn Starch-Gelatin/CNC from eucalyptus wood pulp	0.44, 1.5, 2.56; 3% CNC and 20 % plasticizer	Glycerol/50%	50-140	11 - 49	---	1.24 - 38	Alves et al. 2015
Alginate/Nano-clays MMT and CNC from MCC	1, 3 and 5wt% fillers	Glycerol/53%	---	CNC: *18 - 23	*150 - 270	9 - *12	Abdollahi et al. 2013
				MMT: 17 - 19	*150 - 210	8 - *12	
Pectin-PEG/Halloysite nanotubes	5, 10, 15, 20, 30 and 50 wt% filler	/53%	60	25 -26	*2.6 - 4.1	0.9 - *1.5	Cavallaro et al 2013
Chitosan/MgO	0.1g MgO/g chitosan	---	220-470	*30 - 60	---	*7.5 - 15	Sanuja et al. 2014
Agar/Ag-NPs	20, 40 and 80mg Ag-NPs	Glycerol/50%	62.2-65.8	45.2 - *49.6	1290 - 1460	19.0 - *23.6	Rhim et al. 2014

TS: tensile strength; EM: young's modulus; ε: elongation at break. *Identifies the value for the control sample (without filler), when it is in the edge of the range.

This is important because the greater chemical affinity among the components led to stronger structures and better tensile properties of the composites. The values of the strain at break were lower than in the net polymer films for every composite. Pardo-Ibañez et al. (2014) also found a decrease in the elongation at break of PHBV composites in line with differing quantities of keratin microparticles, but the elastic modulus at low loading was significantly improved. The content of filler greatly affected the tensile behaviour of composites and, in general, low filler contents improved both tensile strength and elastic modulus.

As regards nano-fillers, different studies have shown the improvement in tensile strength and elastic modulus when nanoparticles are incorporated into the polymer matrices. This effect is enhanced by a good particle distribution, a chemical affinity between filler and polymer and a high aspect ratio of the particles and filler-polymer contact area (more interactions). However, the processing conditions and the filler-polymer ratio must be taken into account to optimize the composite properties. Excessively high filler content results in the polymer matrix interruption and formation of micro- nano-cracks. Herrera et al. (2016) studied the effect of the incorporation of CNCs and chitosan nano-crystals (ChNC) into PLA films obtained by extrusion and compression moulding using fast and slow cooling rates. The tensile properties of composites were affected by both the chemical nature of the filler and processing conditions. Strength at break was improved by CNC incorporation, both at fast and slow cooling rates, but ChNC only improved the film strength when processing at a slow cooling rate. Young's modulus increased and elongation at break decreased after the addition of both nanoparticles at both processing cooling rates. Alves et al. (2015) studied the effect of CNC and gelatin on corn starch plasticised films. Nanocrystals were added at 0.44, 1.5, 2.56 and 3% with respect to the polymers. They found a significant increase in the film resistance when the CNC ratio rose, with a slight fall in the elongation values. Similar results were obtained in nanocomposites based on pectin/polyethylene glycol blends containing halloysite nanotubes (Cavallaro et al. 2013). The incorporation of nanotubes led to significantly more rigid films, but reduced the elongation capacity of the material. Metallic oxide nanoparticles have been used as a suitable option to improve the mechanical properties of biopolymers. Sanuja et al. (2014) reported a significant increase in both the tensile strength and elongation at break of chitosan composites with 10% magnesium oxide, obtained by casting. Abdollahi et al. (2013) compared fillers of differing chemical characteristics (MMT and CNC) added to alginate matrices at 1, 3 and 5%. The tensile strength values exhibited a constant growth as the CNC content increased but this parameter decreased when the content of MMT was higher than 1%. Young´s modulus also behaved differently, depending on the filler. The composite stiffness was higher as the CNC content increased from 0 to 5%, but decreased when the MMT content rose from 3 to 5%. However, the elongation values exhibited the same trend for both kinds of nanocomposites; decreasing when both CNC and MMT contents increased.

1.3.3. The effect on barrier properties

Some biodegradable materials need to improve the gas and water vapour permeability because it is a fundamental property in packaging (Ng et al. 2015). The incorporation of micro- and nano-fillers, of organic or inorganic nature, to biodegradable polymer matrices can modify the barrier properties (oxygen permeability: OP and water vapour permeability: WVP). The barrier properties of polymers containing fillers depend on their chemical nature, the particle size and shape of the particles, as well as other factors such as polarity, hydrogen bonding capacity and polydispersity (González et al. 2015; Pardo-Ibañez et al. 2014). Table 4 summarizes the different effects several fillers were observed to have on the barrier properties of some biopolymer matrices. In every case, the addition of fillers can improve the oxygen permeability and the values of the control samples (without filler) were in the range of the corresponding composites or at the high end, especially when CNC fillers were used. Fabra et al. (2016) studied the incorporation of bacterial cellulose nanowhiskers (BCNW) into thermoplastic corn starch matrices (TPCS) and a 95% decrease in OP was obtained with 15% of filler with respect to the TPCS sample. The reinforced TPCS was assembled in multilayer PHB films to obtain more hydrophobic matrices and to improve the film performance. The best functional properties of multilayers were obtained with 15% BCNW-TPCS composite inner layer and PHB outer layers. Luzi et al. (2016) observed a reduction of 47% in OP with the incorporation of 3 wt% CNC from Carmagnola carded hemp fibres and a commercial surfactant into a PLA-PBS matrix. The addition of a surfactant could contribute to a better dispersion of the CNCs and PBS. They observed that the CNCs were well dispersed in the polymer matrices, through the Atomic Force Microscopy (AFM) analysis of surface roughness.

As regards values, analyses of WVP in composites provide similar tendencies to those OP values. In most cases, WVP was reduced after the incorporation of fillers, especially nano-size ones. Table 4 shows the different effect of micro- and nano-fillers on this barrier property for several biopolymer matrices. Raw lignocellulosic fibres (Berthet el al. 2015) or cellulose fibres obtained after chemical treatments (Ludueña et al., 2012) only slightly decreased, or did not affect, the WVP of some composites due to their hydrophilic nature. However, Pardo-Ibáñez et al. (2014) observed a 59% reduction in WPV of the PHVB matrices with 1 wt% of keratin micro-filler, while no significant differences were obtained with a filler load higher than 5 wt%. They detected a homogenous particle distribution in the matrix at 1 wt% filler, where the micro-particles are not aggregated, causing an increase in the tortuosity factor for the diffusion of gas molecules, which reduced the permeability values. On the other hand, the incorporation of nano-filler into different polymer matrices, especially CNCs, improved the WVP values. The crystalline structure of nanocrystals makes it difficult for certain molecules (O_2, CO_2, H_2O) to diffuse into the biopolymer matrix because of the formation of a hydrogen-bonded network (Brinchi et al. 2013; Ng et al. 2015), which favours the development of a percolation network, as reported by Miranda et al. (2015).

Table 4. Changes in barrier properties (oxygen and water vapour permeability) of some biopolymers by incorporating micro- or nano-fillers of different nature. Data show the range in the values of each property reported for the different formulations. *Identifies the value of the control sample (without filler) when it is in the edge of the range.

Composite material	Filler content	Processing method	Plasticizer/ equilibrium RH	OP ($m^3.m/m^2.Pa.s$)	WVP ($Kg.m/Pa.s.m^2$)	RH (%)	T (°C)	Thickness (µm)	Reference
Polymer/micro-filler									
PHBV/wheat straw	10, 20 and 30 wt% filler with different preparation process	Extrusion and compression moulding	---	---	*1.26 (10^{-7}) - 1.27 (10^{-6}) ($Kg/m^2.s$)	100	20		Berthet et al. 2015
PHBV/keratin from poultry feathers	0.5, 1, 3, 5, 10, 25 and 50 wt% filler	Brabender Plastograph mixer and compression moulding	---	1.0 (10^{-18}) - 3.2 (10^{-18})	3.1 (10^{-15}) - 62.0 (10^{-15})	40	24	100	Pardo-Ibáñez et al. 2014
PCL/Cellulose fibres from cotton	5 and 15 wt% filler	Brabender Plastograph mixer and compression moulding	---	---	*1.6 (10^{-14}) - 1.7 (10^{-14})	68	---	---	Ludueña et al. 2012
Polymer/nano-filler									
Corn Starch-Gelatin/CNC from eucalyptus wood pulp	0.44, 1.5, 2.56; 3% CNC	Casting	Glycerol/50%	---	5.21 (10^{-14}) - *6.99 (10^{-14})	50	37.8	90-140	Alves et al. 2015
Pea starch-PVA/CNC from MCC	1, 3 and 5 wt% CNC	Casting	/53 %	---	2.32 (10^{-11}) - 2.43 (10^{-11})	100	25	1000	Cano et al. 2015
TPS/CNC from gravata fibres	0.5, 1, 2 and 3 wt% CNC	Casting	Glycerol and lignin/	---	1.27 (10^{-13}) - *2.67 (10^{-13})	100	25	---	Miranda et al. 2015
Starch-CMC/CNC from sugarcane bagasse	0.5, 2.5 and 5 wt% CNC	Casting	Glycerol/	---	9.72 (10^{-14}) - *3.75 (10^{-13})	50	32	---	El Miri et al. 2015

Table 4. (Continued)

Composite material	Filler content	Processing method	Plasticizer/ equilibrium RH	OP ($m^3.m/m^2.Pa.s$)	WVP ($Kg.m/Pa.s.m^2$)	RH (%)	T (°C)	Thickness (µm)	Reference
Polymer/nano-filler									
TPS/WSNC	1, 2.5 and 5 wt% WSNC	Casting	Glycerol/	8.79 (10^{-16}) - 3.07 (10^{-15})	57.3 (10^{10}) - 66.7 (10^{10}) ($Kg/m^2.s.Pa$)	50	23	---	González et al. 2015
TPCS-PHB/BCNW	2, 5, 10, 15, 20 and 25 wt% CNC	Brabender Plastograph internal Mixer, compression moulding and Electrospinning	Glycerol/0%	2.03 (10^{18}) - *41 ± 2.3 (10^{18}) (80% HR)	6.42 (10^{13}) - *15.52 (10^{13})	0-100	25	---	Fabra et al. 2016
Chitosan/Commercial CNC	1, 3 and 5 wt% CNC	Casting	---	---	2.62 (10^{-7}) - *4.20 (10^{-7}) ($Kg.d.m/m^2.Pa$)	75	25	50	Corsello et al. 2017
Wheat gluten/CNC and CNF from sunflower stalks	1 and 3 wt% CNC or CNF	Casting	/53%	CNC 1 (10^7) - *1.21 (10^7)	CNC 1.40 (10^{-11}) - 1.55 (10^{-12})	53	25	---	Fortunati et al. 2016
				CNF 1.08 (10^7) - 1.37 (10^7)	CNF 1.39 (10^{-12}) 1.55 (10^{-12})				
PLA-PBS/CNC from *Carmagnola* carded hemp fibres	1 and 3 wt% CNC with/without surfactant	Casting	---	1.05 (10^{-6}) - *1.98 (10^{-6})	1.52 (10^{-14}) - 2.41 (10^{-14})	53	25	---	Luzi et al. 2016
PVA/CNC from potato peel waste	1 and 2 wt% CNC	Casting	Glycerol/50%	---	1.25 (10^{-5}) - 1.33 (10^{-5}) ($Kg/m^2.s$)	50	23	150	Chen et al. 2012
Alginate/Nano-clays MMT and CNC from MCC	1, 3 and 5wt% fillers	Casting	Glycerol/53%	---	1.6 (10^{-13}) – *1.99(10^{-13})	20	1.5	---	Abdollahi et al. 2013
Agar/Ag-NPs	20, 40 and 80mg Ag-NPs	Casting	Glycerol/50%	---	1.38(10^{-12}) - *1.52 (10^{-12})	---	---	---	Rhim, et al. 2014

OP: Oxygen permeability; WVP: water vapour permeability; RH: equilibrium relative humidity of samples; T: temperature of the analysed samples

The incorporation of 1 wt% of CNC from gravata fibres into thermoplastic corn starch matrices, provoked a 30% decrease in WVP. The addition of 2.5 wt% of CNC from sugarcane bagasse into matrices made up of corn starch and CMC decreased WVP by 50% due to the impermeable crystalline structure of CNC and a good dispersion of CNCs, creating a highly tortuous path for water vapour transfer (El Miri et al. 2015).

The use of inorganic fillers had similar effects on barrier properties to those of organic nano-fillers. The improvement in the barrier properties is due to the increased tortuosity factor for the gas molecule mass transport in the matrix and the impermeable nature of fillers, as reported by Abdollahi et al. (2013) in alginate films with 5% of MMT nano-clays, where WVP decreased by about 20%. Studying agar films reinforced with Ag-NPs, Rhim et al. (2014) observed that the dispersed phase of Ag-NPs in the polymer impeded the mobility of its chains, inducing an improvement in WVP of the composites.

1.3.4. The effect on thermal properties

The effects of micro- and nano-fillers of differing characteristics on the thermal properties of some biopolymers have been studied by several authors. Table 5 shows the main calorimetric parameters obtained from Differential Scanning Calorimetry (DSC) and the thermal stability of different materials obtained by Thermogravimetric Analysis (TGA) for different biopolymers and composites. Information about glass transition temperature (Tg), crystallisation temperature (Tc), melting temperature (Tm), melting enthalpy (ΔHm), onset temperature (T_{Onset}) and peak temperature (T_{Peak}) of thermodegradation are given in the Table 5.

In general, the addition of micro- or nano-fillers can modify the Tg and crystallization/melting properties (Tc, Tm, ΔHm) of polymer in line with the established interactions between particles and polymer chains. As expected, the addition of plasticizers to the filler-biopolymer blends decreases both the Tg and melting point (Tm). In this sense, Martino et al. (2015) analysed the effect of different plasticisers, such as ATBC (acetyltributyl citrate), GTA (glycerol triacetate) and PEG (polyethylen glycol) in PHVB films with 20 wt% of wheat straw fibres. Blends with ATBC showed the strongest Tg reduction due to its non-polar nature and great affinity with the polymer. Similar effects were observed in both polymer and composites. Cano et al. (2015) observed a ~5 °C reduction in Tg of pea starch-PVA (1:1) matrices after the addition of 3 wt% of CNC from MCC. This was related to the partial inhibition of the PVA crystallisation and to the lower mean molecular weight of the amorphous PVA fraction.

As regards the thermal degradation of materials, the addition of fillers generally improves the thermal stability of composites for both micro- or nano-fillers.

Table 5. Changes in thermal behaviour (calorimetric parameters and thermal degradation,) of some biopolymers by incorporating micro- or nano-fillers of different nature. Data show the range in the values of each property reported for the different formulations. *Identifies the value of the control sample (without filler) when it is in the edge of the range.

Composite material	Filler content	Processing method	Plasticizer/ equilibrium RH	Calorimetric parameters				Thermal degradation		Reference
				T_g (°C)	T_c (°C)	T_m (°C)	ΔHm (J/g)	T_{Peak} (°C)	T_{Onset} (°C)	
Polymer/micro-filler										
PHBV/Wheat straw fibres	10, 20 and 30 wt% filler with different preparation process	Extrusion and compression moulding	---	---	---	---	---	273 - *315	227 *276	Berthet et al. 2015
PHBV/Wheat straw fibres	20 wt % fibres	Extrusion and compression moulding	ATBC, GTA and PEG/	-14 - *3	---	161 - *170	70 - 95	---	---	Martino et al. 2015
PHBV/Keratin from poultry feathers	0.5, 1, 3, 5, 10, 25 and 50 wt% filler	Brabender Plastograph blending and compression moulding	---	---	101.9 - 103.3	147.1 - 148.3	35 - 49.9	---	---	Pardo-Ibáñez et al. 2014
PBAT/Coffee ground	10,20 and 30 wt% filler with roasting process at 250°C and 270°C	Extrusion with die attached with the mixing chamber	---	---	80.7-88.1	95.8-115.1	6.3 - 6.7	334.7 - *404.8	278.5 - *353.3	Moustafa et al. 2016
Mater Bi – KE/Cotton, kenaf, and hemps fibres	10% (w/w) fibres	Extrusion and compression moulding	---	---	*41.85 - 46.65	*62.85 - 67.95	*61.1 - 68.8	*335 - 356	*319 - 334	Moriana et al. 2011
PCL/Cellulose fibres from cotton	5 and 15 wt% filler	Brabender Plastograph blending and compression moulding	---	---	---	---	---	354 - *417	---	Ludueña et al. 2012

Table 5. (Continued)

Composite material	Filler content	Processing method	Plasticizer/ equilibrium RH	Calorimetric parameters				Thermal degradation		Reference
				T_g (°C)	T_c (°C)	T_m (°C)	ΔHm (J/g)	T_{Peak} (°C)	T_{Onset} (°C)	
Polymer/nano-filler										
Corn starch-gelatin/CNC from eucalyptus wood pulp	0.44, 1.5, 2.56 and 3% CNC	Casting	Glycerol/	---	---	---	---	296.39 - *298.47	248.34 - 304.13	Alves et al. 2015
Pea starch-PVA/CNC from MCC	1, 3 and 5 wt% CNC	Casting	Glycerol/53%	73.9 - *78.6	*200.7 - 202.3	225.6 - *227.04	61 - *108	*419 - 431.9	---	Cano et al. 2015
PLA-PHB/CNC from MCC	5% CNC	Extrusion and compression moulding	-	55.3 - 62.5		148.6 - 150.2	*17.7 - 28.6	267 - *357	*278-280	Arrieta et al. 2014b
PLA-PHB/CNC from MCC	1 wt% and 5 wt% CNC 15 wt% plasticizer	Electrospinning Extrusion and compression moulding	ATBC/	27.1 *51	80.7 - *107.6	147.5 - *155	35 - *48	332 - 340	*76 - 141.1	Arrieta et al. 2015
PLA-PBS/CNC from *Carmagnola* carded hemp fibres	1 and 3 wt% CNC with/without surfactant	Casting	-	46.9 - 54.6	---	138.6 - *138.6	21.5 - 30.3	344 - *364	---	Luzi et al. 2016
PLA/CNC from *Posidonia oceanica* plant waste	1 and 3 wt % CNC	Casting	-	40.6 - 54.3	91.5 - *118.6	157.2 - 164.1	*37.4 - 40.4	313 - 332	240 - *270	Fortunati et al. 2015

Table 5. (Continued)

Composite material	Filler content	Processing method	Plasticizer/ equilibrium RH	Calorimetric parameters				Thermal degradation		Reference
				T_g (°C)	T_c (°C)	T_m (°C)	ΔHm (J/g)	T_{Peak} (°C)	T_{Onset} (°C)	
Polymer/nano-filler										
PLA/CNC from *Phormium tenax* leaves	1 and 3 wt% CNC with or without 20 wt% plasticizer	Extrusion and compression moulding	Limonene/	31.6 - 59.6	92.6 - *112.6	143.2 - *147.9	*29.1 - 44.0	352 - *357	---	Fortunati et al. 2014
PLLA/CNC from eucalyptus wood pulp	10 wt% CNC	Casting	-	*59	98 - *100	160 - *162	*41 - 48	---	---	De Paula et al. 2016
PLA/CNC from MCC	1 and 3 wt% CNC-g-PLLA	Grafting Extrusion and compression moulding	-	57.7 - *60.4	96.2 - *100.5	166. - 168.8	42.4 - 47.9	300-310	---	Lizundia et al. 2016
Poly(butylene/triethylene succinate)/CNC from MCC	1 and 5 wt% CNC with surfactant	Extrusion and compression moulding	-	-40 – -33	50 - *89	84 - *114	27 - 63	402 - 407	---	Fortunati et al. 2017

T_g: glass transition temperature; T_c: crystallisation temperature; T_m: melting temperature; ΔHm: melting enthalpy; T_{peak}: peak temperature in DGTA; T_{onset}: onset temperature in DTGA.

The network of the matrices becomes more resistant to heat based on the inherently high heat resistance of organic and inorganic fillers. Lignocellulosic fillers, such as wheat straw fibres (Berthet et al. 2015; Martino et al. 2015), kenaf fibres (Moriana et al. 2011), garlic straw (Kallel et al. 2016), rice husk (Johar et al. 2012), sisal fibres (Santos et al. 2015), pineapple leaf fibres (Shih et al. 2014), soy hull (Flauzino-Neto et al. 2013), rice straw (Boonterm et al. 2015), coconut husk fibres (Rosa et al. 2010) or banana peel waste (Hossain et al. 2016) decompose in the temperature range of 150-500 °C. Specifically, hemicellulose decomposes mainly from 150 to 350 °C, cellulose at between 275 and 350 °C and lignin undergoes gradual decomposition in the range of 250-500 °C. This high/wide range of decomposition temperatures promotes the greater thermal resistance of composites. Moriana et al. (2011), found a Tpeak increase of 6% when natural micro-fibres (cotton, kenaf and hemp fibres) were incorporated into starch-based composites. The greatest increase was obtained with kenaf fibres, probably due to the better compatibility between this filler and the starch matrix. This was associated with the higher content of hemicellulose, which promotes the hydrogen bonding between the fibres and the matrix, improving the interfacial adhesion and thermal stability. However, with other biopolymer matrices, the addition of micro-fibres did not affect the thermal stability as described by Berthet et al. (2015) for PHBV-wheat straw micro-fibres blends. The presence of lignocellulosic micro-fibres could contribute to a reduction in the mean polymer molecular weight of the blend, reducing the overall thermal stability, as was also observed by Ludueña et al. (2012) in PCL-cotton micro-fibre films.

The particle size reduction from micro- to nano-scale of fibres (e.g. by means of alkali and bleaching treatments of lignocellulosic material and acid hydrolysis to obtain pure cellulose nanocrystals (Brinchi et al. 2013; Jonoobi et al. 2015; Zhou et al. 2016), implies a high yield in thermal resistance, as well as in the previously mentioned barrier and mechanical properties. The incorporation of CNCs into biopolymer composites improved their thermal stability due to the crystalline structure and compact chains present in the nanocrystals, which are not easily dissociated by heating, increasing the thermal stability (Ng et al. 2015). Arrieta et al. (2014 and 2015) reported greater thermal stability in PLA-PHB blends reinforced with 1 wt% or 5 wt% of CNC, from commercial MCC, obtained by electrospinning or extrusion processes. Similar behaviour was observed by Cano et al. (2015) in PVA-starch matrices with 1, 3 and 5 wt% of the same reinforcing agent.

As concerns the influence of inorganic nano-fillers on the thermal properties of composites, they also enhanced the thermal stability of biopolymer matrices. Rhim et al. (2014) studied the use of Ag nanoparticles in glycerol plasticised agar matrices obtained by casting. The thermogravimetric analysis exhibited a high residual mass of the composite films due to the inclusion of the more thermically stable metallic nanoparticles. Cavallaro et al. (2013) obtained pectin-PEG blends with nano-clays, specifically hallosyte nanotubes, at 5, 10, 15, 20, 30 and 50 wt% by casting. The thermal degradation analyses reflected the fact that nano-

composites had a high degree of thermal resistance in comparison with the control sample, which was attributed to the fact that the nano-clay lumen can encapsulate the pectin degradation products delaying the process. Moreover, the good dispersion of the nano-filler inside the polymer matrix improved the thermal stabilization of the biopolymer.

1.4. The surface properties of micro- and nano-reinforced polymers for food applications

In this section, recent studies into the effect of the addition of micro- and nano-fillers of differing characteristics on the surface properties of some biopolymers are analysed, and summarised in Table 6. The main changes in biopolymer functional properties caused by the addition of a filler are strongly associated with surface properties and the interfacial interactions between biopolymer and filler. Several methods have been used to characterise the morphology and the surface composition/structure of biomaterials, such as contact angle, electron spectroscopy for chemical analysis (ESCA) or X-ray photoelectron spectroscopy (XPS), secondary ion mass spectrometry (SIMS), scanning electron microscopy (SEM), atomic force microscopy (AFM) (Gutiérrez et al. 2018). The surface properties of the composites can directly impact on the macroscopic observation of the material gloss, which can have notable influence on their practical applications. In this section, recent studies into the effect of different fillers on the surface hydrophobicity (contact angle), topographic analysis (AFM) or sample gloss are discussed and summarised in Table 6.

The contact angle (θ) of a liquid in contact with a solid material mainly depends on the balance between the adhesive liquid-solid forces and the cohesive forces of the liquid (Gutiérrez et al. 2018). Aqueous or organic solvents can be used on a determined material in order to characterise the relative affinity of the material for polar or non-polar systems, thus obtaining information about its respective wettability properties according to the hydrophobic-hydrophilic nature of the surface. The θ values vary according to the type of biopolymer and nature of the filler (organic/inorganic). The inorganic fillers, such as nano-clays, could negatively affect the surface hydrophobicity of matrices due to their great water affinity, as reported by Abdollahi et al. (2013) for matrices of alginate-montmorillonite (MMT) nano-clays at 1, 3 and 5 wt%. The film's surface was more hydrophilic than the control sample mainly due to the hydrophilic nature of the MMT also present at surface level. However, the same authors observed an 87.5% increase in hydrophobicity when they used CNC from commercial MCC in the same matrices. Films with 5 wt% CNC exhibited the highest degree of hydrophobicity, which was associated with the high ratio of CNCs at surface level and their crystalline nature, with lower water affinity than the alginate matrix. Similar results are reported by Slavutsky and Bertuzzi (2014) for thermoplastic starch (TPS) matrices reinforced with CNCs from sugarcane bagasse.

Table 6. Effect of fillers on surface properties of different composite films.

Composite material	Formulation	Processing method	Surface analysis	Effect on polymer matrix	Reference
Polymer/micro-filler					
PHBV/Wheat straw fibres (WSF)	20 wt % fibres 10 wt% plasticizer (ATBC, GTA or PEG)	Extrusion and compression moulding	-Surface hydrophobicity (Contact angle reference liquids: distilled water, diiodomethane ethylene glycol and glycerol)	Contact angle values of the plasticized composite with WSFs were lower than that of the PHBV matrix.	Martino et al. 2015
Polymer/nano-filler					
Alginate/Nano-clays MMT and CNC from MCC	1, 3 and 5wt% fillers	Casting	-Surface hydrophobicity (contact angle)	Composites with MMT had more hydrophilic surface Composites with CNC had more hydrophobic surface due to their highly crystalline nature.	Abdollahi et al. 2013
Pea starch-PVA/CNC from MCC	1, 3 and 5 wt% CNC	Casting	-Gloss	The incorporation of filler do not affect gloss in composites.	Cano et al. 2015
TPS/CNC from sugarcane bagasse	Appropriate amount of CNC suspension and glycerol as plasticizer	Casting	- Surface hydrophobicity (contact angle)	Contact angle increased with CNC addition. Strong interactions between starch chains and CNC, which reduced the water affinity of the film surface.	Slavutsky and Bertutuzzi 2014

Table 6. (Continued).

Composite material	Formulation	Processing method	Surface analysis	Effect on polymer matrix	Reference
Polymer/nano-filler					
Wheat gluten/CNC and CNF from sunflower stalks	1 and 3 wt% CNC or CNF	Casting	-Gloss - AFM topographic analysis	Good distribution of CNC into the matrix and some regions with aggregated CNF. CNC promoted gloss a function of filler content CNF decreased gloss as a function of filler content.	Fortunati et al. 2016
Poly(butylene/triethylene succinate)/CNC from MCC	1 and 5 wt% CNC, with surfactant	Extrusion and compression moulding	-Gloss - Surface hydrophobicity (contact angle)	Decreased the gloss value as the amount of CNC increased. Higher contact angle values for 1% filler	Fortunati et al. 2017
PLA-PHB/CNC from MCC	1 wt% and 5 wt% CNC 15 wt% plasticizer	Extrusion and compression moulding	- Topographic analysis by AFM	Presence of aggregated and individualized CNC. The surfactant allowed for the polymer chain penetration between the cellulose structures.	Arrieta et al. 2014b

The water contact angle increased (rise in the surface hydrophobicity) when CNCs were incorporated into TPS, while strong interactions and the formation of hydrogen bonds between the starch chains and CNCs are expected. These strong internal bonds could also reduce the surface interactions between water molecules and the material. Cao et al. (2008) obtained nanocomposites with TPS and CNCs from hemp fibres and they also observed an increase in the water contact angle or surface hydrophobicity of the matrices. On the contrary, the incorporation of CNCs into hydrophobic polymer matrices, such as PBS, enhanced the water wettability of the films (decrease in contact angle). This could be expected from the surface presence of the cellulose hydroxyl groups, which favour water affinity at the surface (Fortunati et al. 2017).

From the AFM analyses, the presence of nanoparticles on the composite surface and their aggregation/isolation state can be assessed, while their effect on the surface roughness can be verified. Arrieta et al. (2014b) studied the surface properties of PLA-PHB matrices containing CNCs from MCC. The AFM analysis showed the presence of some agglomerated and individualised CNCs in matrices. The aggregation of nanoparticles was reduced by the use of surfactants, which allowed for a better polymer chain interaction with the cellulose nanostructure. Nevertheless, an opposite effect was deduced by Fortunati et al. (2016) from the AFM images for CNCs in wheat gluten matrices, probably due to the different kinds of interactions between cellulose and the amphiphilic protein chains. The tendency of nanocrystals to aggregate has been widely found in numerous studies (Brinchi et al. 2013; Ng et al. 2015; Zhou et al. 2016) due to the spontaneous tendency to reduce the interfacial free energy of the system, accumulated at the contact surface area. The aggregated nanocrystals can be successfully dispersed and homogenised by strong mechanical shearing effects into a homogeneous suspension (Ng et al. 2015) or with the incorporation of surfactants to achieve a good dispersion in the matrices (Hu et al. 2015; Kaboorani and Riedl 2015); all of this is dependent on the nature of the polymer and filler and the processing conditions.

The influence of fillers on the material gloss is related with the surface topography achieved in the composite. Materials with aggregated fillers exhibit greater surface roughness so that they are less bright than other homogeneous material with a smoother surface. Fortunati et al. (2016) studied the homogeneity of CNC and cellulose nano-fibril (CNF) dispersion in wheat gluten composites and observed changes in the material gloss as a function of the filler. In the case of bionanocomposites that are reinforced with CNC, the values of gloss increase as a function of the filler percentage while the opposite behavior was observed in the CNF-reinforced materials. This could be related with the presence of CNF aggregates on the composite surface, evidenced by optical microscopy, whereas in CNC nanocomposites, nanoparticles were homogeneously distributed in the matrix. Cano et al. (2015) observed that the addition of CNCs to pea starch-PVA matrices did not affect the gloss values, as compared

with the control samples, which was attributed to the good CNC dispersion in the biopolymer blends, with strong adhesion forces between the filler and the matrix.

1.5. The effect of reinforcing agents on the material biodegradability

The disintegration and biodegradation behavior of the materials is analyzed through their composting under controlled aerobic processes, designed to produce organic residues from the biodegradable parts of the material, by the action of microorganisms. In this sense, ISO standards establish methodologies, where specific disposal pathways, specific time frames and criteria are indicated in order to unify a proper composting analysis (Cano et al. 2016). The biodegradation behavior is a crucial factor for the purposes of developing environmentally-friendly packaging materials. Biodegradable polymers are able to decompose in the medium by the enzymatic action of microorganisms in a defined period (Nair et al. 2017). In the disintegration and biodegradation processes produced by the action of microorganisms (bacteria, fungi and algae), these identify the polymer as a source of energy to produce organic residues from the biodegradable materials. These chemically react under the microbial enzymatic action and the polymer chains are fragmented (Cano et al. 2016; Nair et al. 2017).

Table 7 shows the effect of some reinforcing agents on the composite disintegration or biodegradation, using different composting conditions. The degradation rate of the materials varies according to the type of polymer and reinforcing agent. Ludueña et al. (2012) analysed the biodegradation behavior of PCL composites containing cotton fibres and CNC from cotton fibres at 20 °C and 40% relative humidity (RH), using compost material with the natural microflora present in soil (Pinocha type). The analysis was carried out throughout 6 months by controlling the average weight loss of the samples. They observed that the biodegradability of the reinforced material was enhanced with the addition of both kinds of fillers, which was attributed to the high hydrophilicity of the natural fibres, which promoted water transport and provided a rougher support for microbial growth. PCL is semicrystalline polyester and the reduction in the degree of crystallinity benefits the biodegradation process, since the amorphous regions are more quickly attacked by microorganisms. Similar conclusions were reported by Luzi et al. (2016), for PLA-PBS composites reinforced with CNC from *Carmagnola* carded hemp fibres submitted to composting in sawdust, rabbit food, compost inoculum, starch, sugar, oil and urea, at 58°C and 50% HR throughout 90 days. The authors evaluated the degree of disintegration (D) and the physical changes and observed that the presence of CNC in the matrices benefited the biodegradation process. Likewise, the use of a hydrophilic surfactant improved the dispersion of cellulosic nano-fillers in the matrices and the D parameter. The biodegradation in blends with PBS was retarded due to the more hydrophobic and semicrystalline nature of PBS.

Table 7. Effect of reinforcing agents on the material biodegradability.

Composite material	Formulation	Processing method	Biodegradation test	Control method	Effect of filler on biodegradation of polymer matrix	Reference
Polymer/micro-filler						
PCL/cellulose fibres from cotton	5 and 15 wt% filler	Brabender Plastograph blending and compression moulding	-Samples: 10 mm x 20 mm x 0.3–0.5 mm. -Compost material: Natural microflora present in soil (Pinocha type). -Incubation: 20°C, 40%HR under aerobic conditions. -Time tested: 6 months.	-Average weight loss (%WL).	The high hydrophilicity of the natural fibres promoted the water intake and provides a rougher support for microbial growth.	Ludueña et al. 2012
Polymer/nano-filler						
PCL/CNC from cotton	5 and 15 wt% filler	Brabender Plastograph mixer and compression moulding	-Samples: 10 mm x 20 mm x 0.3–0.5 mm. -Compost material: Natural microflora present in soil (Pinocha type). -Incubation: 20°C, 40%HR under aerobic conditions. -Time tested: 6 months.	-Average weight loss (%WL).	The crystalline structure of CNC promoted the water intake.	Ludueña et al. 2012
PLA-PHB/CNC from MCC	1 wt% and 5 wt% CNC 15 wt% ATBC as plasticizer	Electrospinning	-Sample: 15 mm × 15 mm. -Compost materials: 10% compost, 30% rabbit food, 10% starch, 5% sugar, 1% urea, 4% corn oil, 40% sawdust and 50 wt% of water content. -Incubation: 58 °C, under aerobic conditions. -Time tested: 28 days.	-Photographs of physical changes -SEM analysis	The presence of nano-filler speeded up the disintegration process. Matrices became breakable after 10 days of composting.	Arrieta et al. 2015
PLA/PVAc/CNC from Whatmann paper	3 wt% CNC and 10 wt% Glycidyl methacrylate resect to PVAc	Extrusion	-Samples: -- -Compost material: sawdust, rabbit food, starch, sugar, oil and urea. -Incubation: 58 °C, 50% humidity under aerobic conditions. Time tested: 60 days.	-Disintegration value	Variation in terms of mass loss was limited because the water attack starts on the more susceptible component with hydroxyl groups available on the surface.	Haque et al. 2017

Table 7. (Continued)

Composite material	Formulation	Processing method	Biodegradation test	Control method	Effect of filler on biodegradation of polymer matrix	Reference
Polymer/nano-filler						
PLA/CNC from *Phormium tenax l*eaves	1 and 3 wt% CNC with or without 20 wt% limonene as plasticizer	Extrusion and compression moulding	-Samples: 15 mm x15 mm x 0.05 mm. -Compost material: compost inoculum, sawdust, rabbit food, starch, sugar, oil, urea and 50 wt% water of content. -Incubation: 58 °C, under aerobic conditions. Time tested: 14 days.	-Photographs of physical changes -FESEM -FTIR -Disintegration value	The CNCs increased the crystallinity and inhibited water diffusion into the material, causing a lower disintegration rate.	Fortunati et al. 2014
PLA-PBS/CNC from *Carmagnola* carded hemp fibres	1 and 3 wt% CNC with/without surfactant	Casting	-Samples: 15 mm × 15 mm × 0.03 mm. -Compost material: sawdust, rabbit food, compost inoculum, starch, sugar, oil and urea. -Incubation: 58°C, 50%HR under aerobic conditions. Time tested: 90 days	-Photographs of physical changes -Degree of disintegration (*D*)	CNCs benefited disintegration process due to their hydrophilic nature. Hydrophilic surfactant improved the CNC dispersion in the matrices and the *D* parameter.	Luzi et al. 2016
PLA/Ag-NPs	1 wt% CNC and 2 ratio of antioxidant	Extrusion and compression moulding	-Samples: 15 x 5 x 2 mm3. - Compost material: sawdust, rabbit food, starch, oil and urea. -Incubation: 58°C, under aerobic conditions. Time tested: 35 days.	-DSC -FTIR -FESEM -Disintegration test	Ag-NPs and thymol (plasticizer) accelerated the PLA hydrolysis process. Ag atoms could catalyse the disintegration process.	Ramos et al. 2014
Starch-PVA/Ag-NPs	0.6, 6, 16 and 32% respect to starch ratio	Casting	- Compost material: organic fraction of solid municipal waste and vermiculite. -Incubation: 58°C, under aerobic conditions. Time tested: 45 days.	- CO_2 produced - Disintegration test	Ag-NPs enhanced film disintegration due to the incorporation of structural discontinuities in the composite network. Low Ag-NPs concentrations are recommended to avoid alterations in the bio-degradation process.	Cano et al. 2016

Table 7. (Continued)

Composite material	Formulation	Processing method	Biodegradation test	Control method	Effect of filler on biodegradation of polymer matrix	Reference
Polymer/nano-filler						
PLA/Montmorillonite and Fluoro-hectorite nano-clays	5 and 10 wt% filler	Extrusion and compression moulding	-Samples: 75 mm x 0.5 mm. -Compost material: pruning residues. -Incubation: 40 °C, 50-70%RH under aerobics conditions. - Time tested: 35 days.	-Photographs of physical changes. -DSC -Tensile properties	The hydroxyl groups of silicate layers and/or of their organic modifiers promoted biodegradation of the PLA matrix.	Fukushima et al. 2013
Methyl cellulose/Montmorillonite	1, 2, 3, 5 and 10 wt% filler	Casting	-Samples: 5g of fragmented samples. -Compost material: 70% topsoil and 30% composted manure. 80-100% moisture content. -Incubations: 25°C in dark cabinet. Time tested: 42 days.	-CO_2 produced	The filler improved the composite barrier properties, restricting the segmental movement at the interface. The silicate layers on the film surface could hide part of the polymer chains, making biodegradation more difficult.	Rimdusit et al. 2008
Alginate/Chitin whiskers	0.1 and 2 wt% filler	Extrusion	- Medium: Tris-HCl buffer solution (pH =7.4) or buffer solution containing 0.4 mg/mL of lysozyme (pH = 7.4). - Incubation: Shaking incubator at 37°C. - Time tested: 5 days.	-SEM -Mechanical integrity	Biodegradation process was improved by lysozyme: Surface of the samples was smoother and weight loss was higher.	Watthanaphanit et al. 2008
Poly(butylene/triethylene succinate)/CNC from MCC	1 and 5 wt% CNC, with surfactant	Extrusion and compression moulding	-Samples: 20 x 30 mm and ~35 mg of weight. - Compost material: 22.08% organic carbon, 13.44% humic and fulvic carbon. - Incubation: 58°C. - Time tested: 30 days.	-Residual mass -Visual observations -SEM	The surface hydrophilicity increased when the CNC content rose. This provoked higher resistance to water uptake and diffusion, delaying disintegration process.	Fortunati et al. 2017

However, Fortunati et al. (2014) observed CNC from *Phormium tenax* leaves had the opposite effect on PLA composites. The presence of CNCs increased the crystallinity of the composites, limiting the water transport through the PLA matrices. When limonene was incorporated as plasticiser in the PLA composites, an increase in the biodegradation rate was observed due to an improvement in the chain mobility, which favoured the polymer erosion. Nevertheless, each sample was 90% disintegrated after 14 days of composting, which is within the limit defined by the ISO 20200. In PBS composites containing CNC from MCC, similar behavior was observed, but the hydrophobic nature of PBS and the degree of crystallinity slowed down the biodegradation process (Fortunati et al. 2017).

The addition of inorganic nano-fillers provoked similar effects to those brought about by organic fillers in the biodegradation process of composites. Ramos et al. (2014) studied the effect of Ag nanoparticles on the disintegrability of PLA composites at 58 °C, using a compost media made from sawdust, rabbit food, starch, oil and urea, throughout 35 days. They assumed that Ag atoms could catalyse the disintegration process and the synergies between the Ag-NPs and thymol could accelerate the hydrolysis process. The presence of homogeneously dispersed thymol in the PLA matrix could promote the polymer chain mobility and thus, diffuse the water molecules through the PLA structure. Cano et al. (2017) also observed an increase in the film disintegration rate when different ratios of Ag-NPs were incorporated in starch-PVA composites. Nevertheless, the generation of CO_2 as the result of total carbon conversion was notably reduced when the Ag ratio increased, probably due to its antimicrobial effect on the microorganisms responsible for the biodegradation process. Fukushima et al. (2013) also observed an increase in the disintegration rate of PLA composites with montmorillonite and fluorohectorite nano-clays at 5 and 10 wt%. The biodegradation of PLA matrices was enhanced by the catalytic effect of the hydroxyl groups of silicate layers.

It is remarkable that many factors can affect the degradation rate of composites. The environmental conditions have a significant impact on microbial growth and parameters, such as humidity, temperature, pH, salinity, oxygen pressure, and microbial nutrients, have a great influence on the microbial degradation of polymers. The biodegradation process also depends on the chemical and physical characteristics of the biopolymer. Nair et al. (2017) report that the enzymatic degradation implies the binding of the enzyme to the bioplastic surface, followed by hydrolytic split; biopolymers are degraded into low-molecular-weight oligomers, dimers, monomers and finally mineralised to CO_2 and H_2O. For instance, the biodegradation of PLA starts with the hydrolysis of the polymer chains promoted by the water diffusion in the matrices. When the molecular weight reaches about 10,000-20,000 g mol^{-1}, microorganisms, such as fungi and bacteria, can metabolise the macromolecules, converting them into carbon dioxide, water and humus (Luzi et al. 2016; Fortunati et al. 2014; Fukushima et al. 2013). Several microorganisms are able to decompose biomaterials, such as *Tritirachium album*, *Amycolatopsis* strain 41, *Amycolatopsis* sp. strain 3118, *Kibdelosporangium aridum* for PLA,

Penicillium sp. strain 26-1 (ATCC 36507), *Aspergillus* sp. strain ST-01, *Clostridium* sp. for PCL or *Pseudomonas* sp., *Bacillus* sp., *Streptomyces* sp., *Aspergillus* sp. for PHB (Nair et al. 2017).

1.6. Finals remarks

The incorporation of reinforcing agents of different natures (organic or inorganic) and size (micro or nano-sized) represents a good strategy for the purposes of improving the functional properties of biopolymers. In general, improved barrier and mechanical properties can be achieved when compatible micro or nano-particles are adequately dispersed in the polymer matrix. Nano-particles are generally more effective, but their natural tendency towards aggregation makes the dispersion process difficult, requiring carefully designed dispersion techniques. To a great extent, the surface interactions of the filler with the polymer matrix define the effectiveness of the reinforcement and the promotion of barrier properties. Therefore, if materials with optimal functionality are to be obtained, it is of relevance to make an adequate selection of both the filler for a determined polymer matrix and the processing conditions necessary to ensure high dispersion levels of the particles. Composite biodegradability is generally enhanced by the presence of the filler dispersed particles. However, the total conversion of carbon to CO_2 through the action of microorganisms could be limited when the filler exhibits antimicrobial action.

2. Lignocellulosic residues as a source of reinforcing agents and active compounds useful for food packaging applications

Lignocellulosic biomass represents a natural source of renewable and biodegradable polymers and compounds for multiple applications. It is mainly composed of different proportions of hemicellulose, cellulose and lignin (structural components) and other non-structural components, such as waxes, pectin, pigments, inorganic salts and nitrogenous salts, in lower quantities. Siqueira et al. (2010) and Ng et al. (2015) described the lignocellulosic materials as lignocellulosic fibres formed by rigid cellulose microfibrils embedded in a cementing matrix of polysaccharides and glycoproteins, like lignin, hemicellulose and pectin (Figure 3). An assembly of helically cellulose microfibrils, embedded in cementing material, is formed from long-chain cellulose molecules.

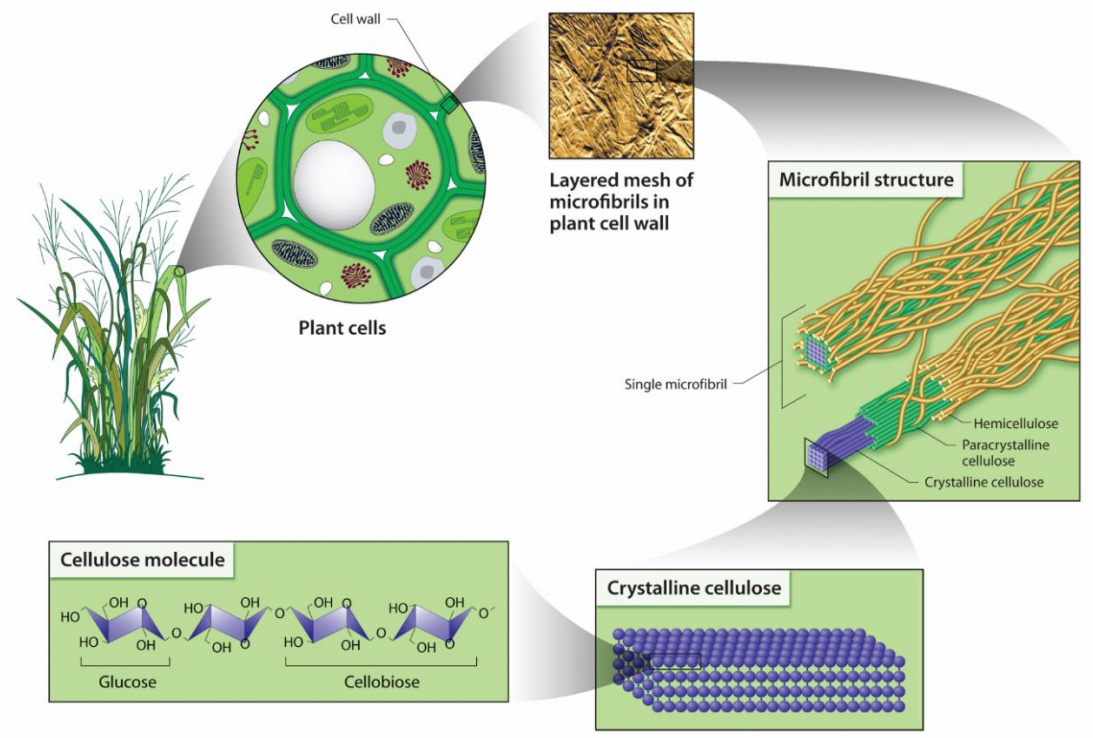

Figure 3. Scheme of lignocellulosic fibres structure (Siqueira et al. 2010).

Cellulose is a hydrophilic polysaccharide that consists of a linear homopolysaccharide composed of β-D-glucopyranose units linked together by β-(1-4)glycosidic bonds (Siqueira et al. 2010). Each glucopyranose unit has three hydroxyl groups, and their presence facilitates the formation of hydrogen bonds, which play a key role in directing the crystalline packing, while governing the physical properties of cellulose. The hydrogen bonding within and between cellulose chains is responsible for its particular mechanical properties, crystallinity, durability and biocompatibility (Wei and McDonald, 2016). The formation of inter-chain hydrogen bonds gives rise to a complex network where the cellulose chains are ordered through crystalline packing. The cellulose chains without hydroxyl groups that could not be stabilized laterally through hydrogen bonding, form disordered amorphous holocellulose segments bonded with cellulose crystals. These chains are more separated, with lower density than crystalline regions and more readily available for hydrogen bonding with other molecules, such as water. The amorphous regions can be hydrolysed through a strong acid treatment leaving highly crystalline zones. The crystalline cellulose segments are known as cellulose nanocrystals (CNC) (Figure 4).

Hemicellulose is the supportive matrix for cellulose microfibrils and the amount of hemicellulose present in the material could be estimated from the difference between the holocellulose content and α-cellulose content. Its thermal degradation temperature is low due to the presence of acetyl groups (Ng et al. 2015).

Lignin is a complex hydrocarbon polymer with both aliphatic and aromatic constituents, amorphous and hydrophobic in nature, which acts as cementing agent that links individual fibre cells together, giving rigidity to the plants (Patel et al. 2017). Lignin is thermally stable but susceptible to UV degradation.

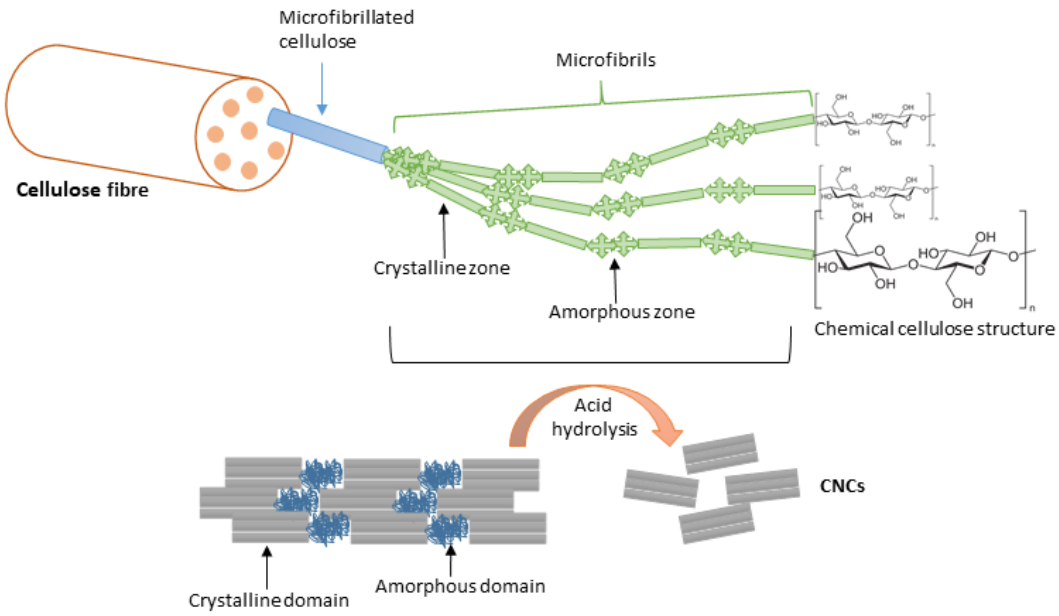

Figure 4. From cellulose fibres to cellulose nanocrystals structure. Adapted from Ng et al. (2015).

In the field of plant biomass valorisation, the biorefinery approach for the production of useful products including chemicals, energy and materials is of great interest due to the potential generation of multiple products in a cascade manner, aiming for a near-complete utilization of the inherent biomass components (Abraham et al. 2016).

Micro-cellulose fibres or cellulose nanocrystals can be isolated from lignocellulosic materials through different processes, which involve mechanical and washing pre-treatments and the use of some chemical reagents to carry out alkali and bleaching treatments and acid hydrolysis (Ng et al. 2015; Mondal et al. 2017). For this purpose, it is necessary to remove the cementing materials around the cellulose fibril bundles to obtain purified cellulose fibres and, subsequently, to extract the CNC. CNC are considered as one of the most attractive renewable reinforcements for biodegradable polymers due to their promising properties and broad range of applications in several fields (Ferreira et al. 2018). These reinforcing compounds are of particular interest due to their abundant hydroxyl groups, which allow different derivative materials with adequate compatibility to be obtained, their high degree of crystallinity,

excellent mechanical properties, large specific surface area, high aspect ratio and great thermal stability (Patel et al. 2017).

Another potential use of this kind of agro- waste is the extraction of active compounds, such as polyphenols with antioxidant and antimicrobial capacity. These substances can be extracted by high-pressure hot water treatments or via different chemical solvents. Antioxidants are substances used to reduce the oxidative reactions of foods and can be incorporated directly or into the packaging material. Usually, synthetic antioxidants have been used in packaging materials. However, their potential toxicity when the migration of these compounds to the food matrices occurs, has led to the search for alternative compounds from natural sources (Bonilla and Sobral, 2016). Lignocellulosic residues contain a great variety of phenolic compounds, such as cinnaminic acid, benzoic acid, tannins, ferulic acid, gallic acid, syringic acid, vanillinic acid, syringaldehyde or flavonoids (Piñeros-Castro and Otálvaro, 2014), some of which exhibit antimicrobial and/or antioxidant capacity.

2.1. Isolation of cellulosic reinforcing agents from lignocellulosic agro-waste

Several studies describe the potential use of lignocellulosic materials to obtain cellulosic reinforcing agents for thermoplastic biopolymers (Haque et al. 2017; Sanjay et al. 2018). The use of residual biomass can give added value to the waste product, while also offering new renewable materials. In this sense, different agro-wastes, such as rice husk, coffee husk (Collazo-Bigliardi et al. 2018), garlic straw (Kallel et al. 2016), red algae waste (El Achaby et al. 2018), hemp fibres (Luzi et al. 2016), sunflower stalks (Fortunati et al., 2016) or bamboo pulp (Borkotoky et al. 2018) among others, have been evaluated. The composition of this raw material varies according to the resource used, as shown in Table 8.

Natural cellulose obtained from biomass can be transformed into micro- and nano-scale materials with adequate properties as reinforcing agents for composites (Azeredo et al. 2017). The isolated cellulose fibres submitted to different treatments yield different crystalline fractions, such as CNC. The final yield of the isolation process depends on the type of initial raw material and process conditions.

Micro-cellulose fibres or cellulose nanocrystals have been isolated from lignocellulosic materials through different processes, which involve mechanical and washing pre-treatments, alkali treatment with subsequent bleaching process and acid hydrolysis, as shown in Figure 5. It is necessary to remove the cementing materials around the cellulose fibril bundles to obtain purified cellulose fibres for the subsequent CNC extraction. The presence of hemicellulose and lignin reduces the crystallinity ratio, mechanical performance and thermal stability of cellulose fibres (Mondal et al. 2017).

Table 8. Composition of some lignocellulosic materials.

Resource	Hemicellulose (%)	Cellulose (%)	Lignin (%)	Reference
Rice husk	17.1	33.8	21.5	Collazo-Bigliardi et al. (2018)
Coffee husk	18.2	35.4	23.2	
Oat husk	25.1	40.1	26.1	Oliveira et al. (2017)
Pineapple leaf	12.3	81.3	3.5	Cherian et al. (2011)
Wood chips	26.3	39.8	26.3	Moriana et al. (2016)
Branches	21.3	30.9	31.0	
Pine needles	23.5	16.0	33.0	
Sugarcane bagasse	23.9	46.5	22.1	Rani et al. (2016)
Garlic straw	18.0	41.0	6.3	Kallel et al. (2016)
Eucalyptus	13.1	49.5	27.7	Wei and McDonald (2016)
Bamboo	20.5	34.5	26.0	
Kenaf	21.0	53.5	17.0	
Jute	16.0	67.0	9.0	
Soy hulls	12.5	56.4	18.0	Jonoobi et al (2015)
Wheat straw	34.1	43.2	22.0	
Cotton	6.0	90.0	-	Siqueira et al. (2010)
Corn cob	-	70.0	20.0	Brinchi et al. (2013)
Coir fibres	-	43.0	45.0	

Prior to chemical treatments, it is necessary to condition the raw material. Washing with distilled water in continuous agitation is usually required to eliminate undesirable residues and to favour the contact with the reagents. A mechanical process (milling/grinding/cutting) is required to reduce the particle size in every case. The particle size must be as uniform as possible to increase the surface area of contact between the chemicals and the matrix and to increase the reaction rate (Ng et al. 2015; Patel et al. 2017). Alkaline treatment consists of submitting lignocellulosic fibres to the action of a strong base solution (usually aqueous KOH or NaOH solution) to remove the alkali-soluble substances, partially exposing the short-length crystallites. Through this treatment, the disruption of -OH bonding in the fibre network structure occurs, by ionizing these groups to alkoxides (Ng et al. 2015). This stage is essential to eliminate hemicellulose, a part of the lignin, pectins, waxes and other impurities present on the external surface of the cell wall fibres (Mondal et al. 2017). Moreover, the aspect ratio increases due to the reduction of fibre diameter, which leads to a growth of the surface area. Finer fibrillary structures with new reactive sites can be formed by the removal of these inert materials along with -OH groups of fibres (Mishra et al. 2019). After alkali treatment, the lignin must be eliminated through the bleaching process, also called delignification. The fibres previously treated with alkali solution are bleached by boiling them with sodium chlorite under the acidic conditions promoted by the acetate buffer solution. In acidic conditions, sodium chlorite would break down into chlorine dioxide, which oxidizes lignin by attacking its aromatic ring. Usually, this treatment is repeated as many times as necessary until the sample becomes completely white, which is an indication that the lignin has been removed. The

insufficient removal of lignin would lead to the subsequent acid hydrolysis being of limited efficiency due to the fact that a significant amount of lignin could prevent the acid from imparting any major morphological changes on the cellulose fibrils (Ng et al. 2015).

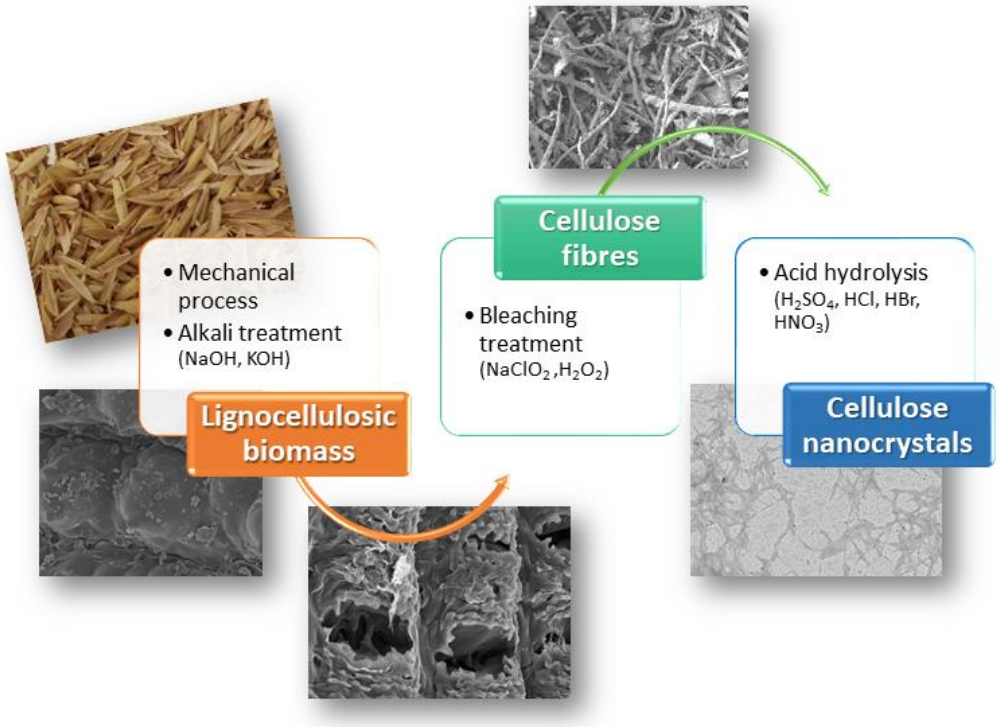

Figure 5. Isolation process of cellulose fibres and cellulose nanocrystals.

Finally, to obtain the cellulose nanocrystals, acid hydrolysis must be carried out on the bleached fibres. The amorphous zones are attacked by acid, while the crystalline zones are acid-insoluble. The acids have the capacity to release hydronium ions to hydrolyse the glycosidic bonds of the cellulose chains within the amorphous regions, breaking down the hierarchical structure of nanofibril bundles into nanocrystals (Jonoobi et al. 2015). The most commonly used acids are sulfuric acid, hydrochloric acid, hydrobromic acid and nitric acid. This treatment could also hydrolyse the residual hemicellulose and pectin by breaking down the polysaccharides into simple sugars (Ng et al. 2015). According to Brinchi et al. (2013), the production of CNC consists of (1) the strong acid hydrolysis of cellulose fibres under controlled temperature, time, acid concentration and fibre:acid ratio; (2) dilution with water to stop the reaction and washing by centrifugation; (3) dialysis with distilled water to remove free acid molecules; (4) sonication to obtain a stable suspension of CNC and, finally, (5) drying the suspension to obtain CNC powder, as an optional stage.

Table 9. Properties of micro- and nano- cellulosic materials for different sources.

Source	Pre-treatment	Bleaching treatment	Acid hydrolysis	Aspect ratio	Crystallinity index	Reference
Garlic husk	2 wt% NaOH	Acetate buffer $NaClO_2$ Distilled water	64 wt% H_2SO_4 45°C, 40 min	80	CF: 47% CNC: 69%	Kallel et al. (2016)
1Rice husk [2]Coffee husk	4 wt% NaOH	Acetate buffer 1.7 wt% $NaClO_2$ Distilled water	64 wt% H_2SO_4 50°C, 40 min	10-40	CF: [1]50, [2]52% CNC: [1]90, [2]92%	Collazo-Bigliardi et al. (2018)
Red algae waste	4 wt% NaOH	Acetate buffer 1.7 wt% $NaClO_2$ Distilled water	64 wt% H_2SO_4 45°C, 30, 40 and 80min	35-57	CF: 66% CNC: 81-87%	El Achaby et al. (2018)
Spruce bark	Acetone 100°C	Acetate buffer 1 wt% $NaClO_2$ Distilled water	60 wt% H_2SO_4 50°C, 60 min	63	CF: 78% CNC: 84%	Le Normand et al. (2014)
Oat husk	4 wt% NaOH	Acetate buffer 1.7 wt% $NaClO_2$ Distilled water	-	-	CF: 64%	Oliveira et al. (2017)

Table 9. (Continued)

Source	Pre-treatment	Bleaching treatment	Acid hydrolysis	Aspect ratio	Crystallinity index	Reference
[1]Woody chips [2]Branches [3]Pine needles	4.5 wt% NaOH	Acetate buffer 1.7 wt% $NaClO_2$ Distilled water	65 wt% H_2SO_4 45°C, 40 min	[1]26-82 [2]39-112 [3]30-73	CF: [1]74, [2]76, [3]80% CNC: [1]86, [2]84, [3]93%	Moriana et al. (2016)
Sugarcane bagasse	2 wt% NaOH	8 wt% H_2O_2	10 wt% HCl	-	CNC: 80%	Rani et al. (2016)
Pineapple crown waste	5 wt% NaOH	16 wt% H_2O_2 5 wt% NaOH	60 wt% H_2SO_4 45°C, 60 min	6.3	CNC: 73%	Prado and Spinacé (2019)
Pueraria root residue	Water HCl	NaClO	80 wt% H_3PO_4 50°C, 7 h	40	CF: 48% CNC: 60%	Wang et al. (2018)
Walnut shell	NaOH	Acetate buffer 1.7 wt% $NaClO_2$ Distilled water	64 wt% H_2SO_4	-	CNC: 60%	Hemmati et al. (2018)
Pistachio shell	4 wt% NaOH	3 wt% H_2O_2 Acetic acid	H_2SO_4 50°C, 90 min	16	CNC: 67%	Marett et al. (2017)

Aspect ratio (L/d; L: length, d: diameter) of CNC. CF: cellulose fibres; CNC: cellulose nanocrystals.

Table 9 summarizes the process conditions applied to obtain micro and nano cellulosic materials, obtained from different sources, as well as their relevant properties, such as crystallinity and aspect ratio. Differences in temperature and time of reaction, the fibre-chemical agent ratio and the characteristics of raw material affect the final properties of the cellulosic material, such as the particle dimensions, aspect ratio (L/d) and crystallinity index (Xc), as shown in Table 9.

In the case of CNC, their final form (water suspension or dry powder) is crucial for their final application in composites. Melt blending techniques are commonly used to process the polymers in the production of packaging materials. The direct incorporation of CNC as water suspension is inconvenient due to the foam formation or overpressure in line with water evaporation, as well as the water incompatibility with some polymers, such as polyesters or polyamides (Ng et al. 2015). Therefore, the incorporation method of CNC into the polymer blends must be optimized. The strong hydrogen bonds between water and cellulose particles enable the system to remain stable against particle aggregation in aqueous suspension form (Zhou et al. 2016). Nevertheless, the CNC suspension can be dried, maintaining the inherent nano-scale dimensions, through effective methods, such as oven drying, freeze drying, spray dry and supercritical drying (Ng et al, 2015). In this case, the obtained yield of CNC should be high. On the other hand, they are difficult to handle in dry form due to their electrostatic forces and there is a risk of agglomeration (Khalil et al. 2016).

2.2. Isolation of active compounds from lignocellulosic agro-waste

The development of an antioxidant and antimicrobial packaging materials is an adequate strategy for extending the shelf life of food products. Oxidative reactions and microbiological alteration are the main processes that cause undesirable changes in the quality and safety attributes of foodstuffs (Talón et al. 2017). Active compounds may migrate from the packaging to the food product (or the surrounding headspace) to improve its safety and quality properties and to extend its shelf life (Bonilla and Sobral, 2016; Majid et al. 2016; Piñeros-Hernández et al. 2017).

The use of natural active compounds as an alternative to synthetic preservatives has greater acceptance by consumers. In this sense, lignocellulosic agro-wastes are a promising source of antioxidants and antimicrobials, since they are rich in polyphenols linked to the hemicellulose or lignin fractions, which exhibit active properties for controlling microbial or oxidative processes (Aguiar et al. 2016; Wanyo et al. 2014).

Table 10. Antioxidant and antimicrobial behaviour of some lignocellulosic waste.

Source	Extraction method	Antioxidant character		Antimicrobial character		Reference
		Method	Antioxidant activity	Antimicrobial Test	MIC	
Leaves of boldo Leaves of rosemary	Ethanolic extracts Solvent:powder 1:8 (w/v) 25°C, 4 h	DPPH	EC_{50}: 25 µL/mL	-	-	Bonilla and Sobral (2016)
Coffee silverskin	*in vitro* gastrointestinal digestion	[1]ABTS [2]FRAP	[1]558 [2]654 (µmol TE/g dry matter)	Microtiter plate-based assay	S. *aureus*: 2.3 OTEV E. *coli*: 0.9 OTEV	Jiménez-Zamora (2015)
Garlic husk	Methanol extraction 25°C, 45 min	DPPH	EC_{50}: 0.64 (mg/mL)	Disk diffusion assay	S. *aureus*: 2 mg/mL E. *coli*: 10 mg/mL	Kallel et al. (2014)
Thyme leaves	Water extraction 100°C, 30 min	DPPH	EC_{50}: 0.26 (kg/mol)	-	-	Talón et al. (2017)
Coconut husk	-	-	-	-	S. *aureus*: 0.2 mg/mL	Guil-Guerrero et al (2016)
Sugarcane bagasse	-	-	-	-	S. *aureus*: 0.6 mg/mL	
Rice hull	[1]Ethanol [2]H_2SO_4 [3]NaOH extraction	DPPH	[1]26 [2]76 [3]79 (% inhibition)	-	-	Vadivel and Brindha (2015)
Coffee silverskin	[1]Water extraction (80°C) [2]0.1M HCl extraction (80°C) [3]0.1M NaOH extraction (80°C)	DPPH	[1]75 [2]71 [3]63 (µmol TE/g extract)	-	-	Narita and Inouye (2012)
Cardoon leaf	-	-	-	Inhibition halo	S. *aureus*: 1 cm width of inhibition zone	Scavo et al. (2019)
Flax fibres	-	-	-	-	S. *aureus*: 17% reduction	Fillat et al. (2012)
Vine shoots	Ethyl acetate extraction 200°	[1]DPPH [2]ABTS [3]FRAP	[1]0.82 [2]3.56 [3]1.99 (g TE/100 g shoots)	Microdilution assay	S. *aureus*: 5 mg/mL E. *coli*: 15 mg/mL	Gullón et al. (2017)

DPPH: (1,1-diphenyl-2-picrylhydrazyl) radical method; ABTS: 2,2'-azino-bis(3-ethylbenzothiazoline-6-sulfonic acid)radical method; FRAP: Ferric reducing antioxidant power; TE: trolox equivalent; OTV: OxyTetracyclin Equivalent Value, expressed as mg oxytetracyclin/l, against S. *aureus* and E. *coli*; MTT (3-[4,5-dimethylthiazol-2-yl]-2,3-diphenyl tetrazolium bromide) assay.

Different kinds of polyphenols, such as lignans, stilbenes, flavonoids or phenolic acids have been classified based on their structure or phenol units. The antioxidant character of polyphenols is associated with their ability to act as free radical scavengers, to inhibit lipoxygenase enzyme activity and to chelate metals (Talón et al. 2017). They are naturally biosynthesised by plants and have been isolated from different plant products, such as spices or aromatic herbs, plant-food by-products and agro-wastes (Cong-Cong et al. 2017; Shavandi et al. 2018). Phenolic compounds have been successfully extracted from guarana seeds, boldo leaves, cinnamon barks, rosemary leaves (Bonilla and Sobral, 2016), thyme (Talón et al. 2017), rice hulls, almond hulls, buckwheat hulls, oat hulls (Balasundram et al. 2006) or garlic waste (Kallel et al. 2014). Different extraction methods have been described for several plant products, while the extracts have been characterised as to their antioxidant or antimicrobial capacity against different microorganisms. Table 10 summarizes some studies carried out in this field.

The antimicrobial nature of polyphenols is related with their ability to inhibit extracellular microbial enzymes, to destabilise the cytoplasmic membrane and to provoke a deficit of the substrates required for microbial growth (Guil-Guerrero et al. 2016). In phenolic acids, the protonated form spreads across the membrane, which produces the acidification of the cytoplasm and, usually, cell death. Another group of phenols are flavonoids, which possess the capacity to form complexes with both extracellular and soluble proteins as well as bacterial cell walls, although high-lipophilic flavonoids can disrupt microbial membranes (Cong-Cong et al. 2017; Guil-Guerrero et al. 2016). Plant extracts have been tested against Gram-positive and Gram-negative bacteria, yeast, fungi and moulds. Guil-Guerrero et al. (2016) exhaustively reviewed the antimicrobial behaviour of several polyphenols (simple phenolic acids, flavonoids, tannins) extracted from plant by-products, and reported effective antibacterial action against pathogens, such as *E. coli, Lactobacillus* spp., *Staphylococcus aureus, P. aeruginosa*, and *Listeria* spp. strains, among others. Table 10 also summarizes some studies into the antimicrobial action of plant by-product extracts.

The extraction procedure of polyphenols plays a key role in their efficacy as active agents and different studies have focused on the extraction and analysis of polyphenols from plant materials (Cong-Cong et al. 2017). Many conventional methods have been used for the extraction purposes, such as solid-liquid extraction or reflux extraction, while more advanced methods, such as ultrasound-assisted extraction, microwave-assisted extraction, supercritical fluid extraction, accelerated solvent extraction, or high hydrostatic pressure extraction have also been applied. Solid-liquid extraction process involves the direct extraction of fresh or freeze-dried raw materials with different solvents, such as methanol, ethanol, acetone, water or solvent mixtures. Piñeros-Castro and Otálvaro (2014) used hot-water at high-pressure as extraction solvent, obtaining a better-preserved fraction of hemicellulose and linked phenols, while a part of the lignin is degraded providing a great variety of phenolic compounds.

2.3. Incorporation of cellulosic fillers and/or active extracts in biopolymer matrices for food packaging

Different groups of biodegradable polymers have been studied, such as those obtained from biomass (polysaccharides) or by synthesis from bio-based monomers (polylactic acid: PLA) (Brigham, 2018). Nowadays, starch and PLA are some of the most competitive biodegradable polymers, which, in turn, exhibit complementary barrier properties.

Starch is the most widely-studied polysaccharide for food packaging applications, and it can be transformed into thermoplastic material (TPS) by thermo-mechanical treatment, in combination with plasticizers (Ortega-Toro et al. 2016). Despite its highly hydrophilic nature and water sensitivity, limited mechanical properties and instability during storage, it is an interesting material for food packaging because it is food compatible and has the ability to form homogeneous and transparent films with high barrier capacity against oxygen and lipids. Likewise, the presence of abundant hydroxyl groups in the starch chains provides several modification possibilities (Koch, 2018).

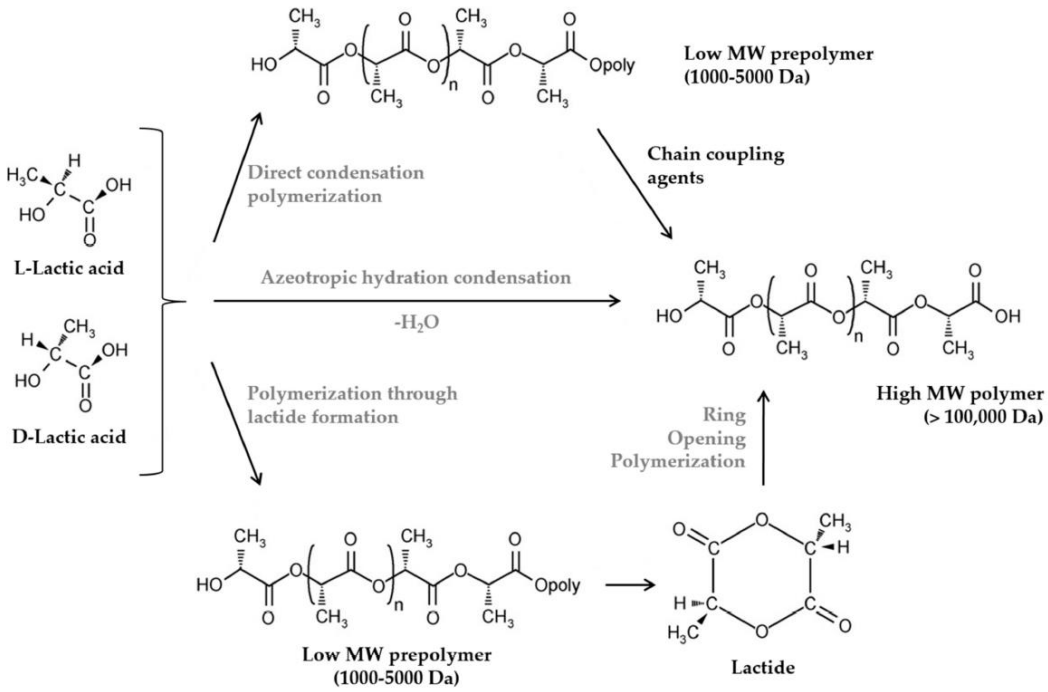

Figure 6. Production of PLA through different process (Muller et al. 2017a).

PLA is a linear aliphatic biodegradable polyester derived from lactic acid, which is obtained from the fermentation of renewable sources, such as corn or rice starch, and raw materials with high sugar content. Its production is based on the chemical conversion of these

carbohydrate sources into dextrose. The dextrose is fermented to lactic acid followed by the polycondensation of lactic acid monomers (Balaji et al. 2017). It is commonly produced by the ring-opening polymerization (ROP) of lactide monomers formed from lactic acid (Figure 6; Muller et al. 2017a). PLA has attracted considerable attention over the last 20 years because of its good processability and properties, comparable with other traditional petrochemical-based polymers (polystyrene: PS or polyethylene terephthalate: PET) (Hamad et al., 2018). The main characteristics of PLA are its transparency and excellent water vapour barrier capacity (Murariu & Dubois, 2016). Likewise, the production technologies developed permit a competitive market price of PLA (Hamad et al., 2018). However, it has certain limitations, such as its low oxygen barrier capacity and brittleness (less than 10% extensibility), despite it being highly resistant to traction (Muller et al., 2017b).

TPS-PLA combinations by blending (Akrami et al. 2016; Davachi et al. 2017; Debiagi et al. 2017; Koh et al. 2018; Müller et al. 2016) or multilayer assemblies (Muller et al., 2017a and 2017b; Requena et al. 2018; Sanyang et al. 2016) have been studied to counteract the respective disadvantages of the pure polymers. However, they are thermodynamically immiscible due to the lack of chemical affinity and their blends exhibit phase separation and a heterogeneous structure, which affects the functional properties of the materials (Muller et al. 2017a). To obtain TPS-PLA blends with better functionality, the polymer interfacial adhesion must be improved through the addition of compatibilizers (Hamad et al. 2018). In this sense, Muller et al (2017a) reviewed the different compatibilizers used in TPS-PLA blends, such as citric acid (wheat flour-PLA), methylene diphenyl diisocytane (wheat starch-PLA), stearic acid (corn starch-PLA), maleic anhydride (potato starch-PLA). Dicumyl peorxyde/maleic anhydride (corn starch-PLA), adipate or citrate esters (cassava starch-PLA), formamide (corn starch-PLA), maleic anhydride or epoxidized soybean oil (corn starch-PLA). Ortega-Toro et al. (2016) used grafted poly(ε-caprolactone), as described by Laurienzo et al. (2006), to compatibilize starch-PCL blends, obtaining improved films with a more homogenous structure and good mechanical barrier properties. To this end, PCL was chemically modified with the reactive polar groups, epoxide (from glycidyl methacrylate) or anhydride (from maleic anhydride), as shown in Figure 7. These grafted PCL compounds could also be used as a coupling agent between PLA and TPS, improving their compatibility.

On the other hand, the incorporation of reinforcing agents, such as micro- and nano- cellulose fibres, for the purposes of improving the performance of biodegradable materials in terms of their mechanical and barrier properties is an interesting option, mainly when fillers come from renewable sources. Likewise, the addition of active compounds, such as antioxidants or antimicrobials, provides added value to the packaging material. In the following points, previous studies focused on improving the starch or PLA properties by incorporating cellulose reinforcing agents or active compounds are discussed.

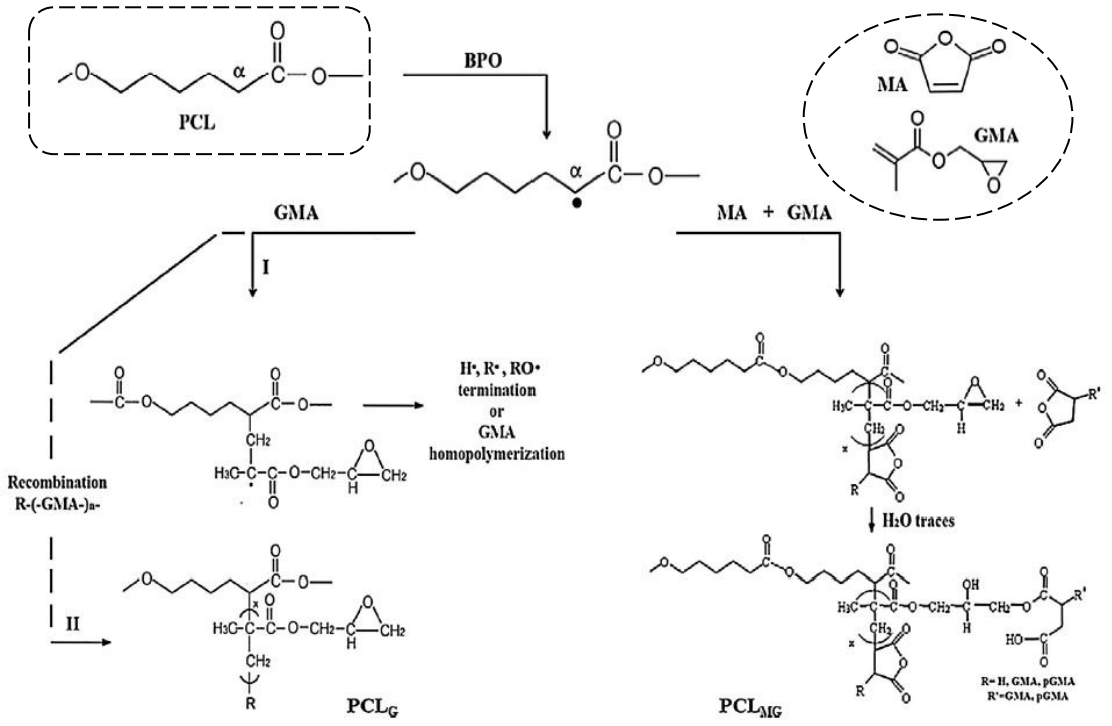

Figure 7. Chemical modification of poly(ε-caprolactone) (PCL) with glycidyl methacrylate (GMA; PCL_G) and maleic anhydride + glycydyl methacrylate (MA+GMA; PCL_{MG}) (Ortega-Toro et al. 2016).

Karimi et al. (2016) studied the effect of the incorporation of CNC from kenaf bast in order to reinforce glycerol-plasticized TPS matrices varying the filler contents (0–10 wt%) by casting. The elastic modulus increased as the filler content grew (up to 343%), while the elongation at break was reduced. Savadekar et al. (2012) incorporated different contents of CNC from cotton fibres (from 0.1 to 1 wt%) into TPS. Nanocomposite films exhibited higher tensile strength and reduced elongation at break and improved water vapour and oxygen transmission rate with respect to neat TPS. Yang et al. (2014), report an increase of 6% in tensile index, 9% in tear index, 23% in folding endurance and 4% in burst index, with respect to the net starch films, for a TPS-cellulose blend with 0.3 wt% of cotton fibre CNC. Kargardazeh et al. (2018) reviewed several studies into nanocellulose-reinforced starch composites, focusing on the loading levels of nanocellulose, the processing methods and the effects of mechanical reinforcement.

Sung et al. (2017) developed bio-nanocomposite films based on a PLA matrix reinforced with cellulose nanocrystals at 1, 3 and 5 wt%, by using a twin-screw extruder. The tensile strength and elastic modulus increased with 1% and 3% of filler, while the barrier properties gradually decreased as the CNC content rose. This was also observed by Gazzoti et al. (2017) when CNC (at 0.5, 2, 2.5, 3, and 5 wt%) from cotton was incorporated into PLA films. Murariu & Dubois (2016) reviewed different studies into the incorporation of cellulose fibres from lignocellulosic

agro-waste (flax, kenaf, wood) into PLA matrices. They report that the incorporation of these kinds of fillers promoted the stiffness of PLA and the impact resistance, while enhancing the crystallization rate, storage modulus and thermal properties. Hamad et al. (2018) reported that kenaf, jute, flax, coir, and bamboo fibres have been extensively used for enhancing the mechanical properties of PLA films. The effect of the chemical modification of the fibres and process conditions on the mechanical, rheological and thermomechanical properties of the PLA composites was analysed.

The improvement in the functional properties of the polymer films brought about by the addition of cellulosic reinforcing agents has been mainly attributed to the synergistic effect of the increased crystallinity of the polymer matrix, due to the nucleation ability of CNC and the CNC reinforcing effect. The enhanced mechanical response of the composite can be related to the addition of a hard phase (reinforcing agent) which absorbs part of the external stress, due to its high elastic modulus, and dissipates this external stress by particle-particle and particle-polymer friction. The barrier properties were enhanced because the fillers act as blocking agents within the polymeric matrix, promoting a tortuous path to the permeation of the water and gas molecules. Usually, CNC incorporation leads to an increase in the polymer melting temperature (Tm), which can be related to the presence of thicker polymer crystalline lamellae, and to the fact that CNC can act as a nucleating agent. Cellulosic reinforcing agents also promoted the biodegradation of composites due to their hydrophilic nature which favours water sorption and thus polymer depolymerization (Ferreira et al. 2018).

The functional properties of compatibilized TPS-PLA blends could also be improved by the incorporation of reinforcing agents. In fact, micro- or nano-fillers from different sources have been studied as a means of improving the functional properties of blend films. Macedo et al. (2019) demonstrated that the natural cotton fibre agricultural residue incorporated at 10 wt% in PLA with the addition of TPS (3 wt %), promoted an increase in the mechanical modulus. De Oliveira et al. (2019) developed composites of PLA with starch (0, 3 and 5 wt%) reinforced with natural cotton fibres at 0%, 10 and 20 wt% without additives. They focused on the eco-efficiency of producing these kinds of composites, and concluded that composites with natural cotton fibres exhibited a reduced environmental impact in comparison to neat PLA or PLA/TPS based materials.

As regards the addition of active compounds to these matrices, Piñeros-Hernandez et al. (2017) incorporated polyphenol-rich rosemary extracts into cassava starch films in order to produce active food packaging with antioxidant properties. The films exhibited an increase in their antioxidant activity and better barrier properties against UV light as the polyphenol content rose. The polyphenol migration was analysed in water and 95% ethanol, as food simulants, revealing that the total polyphenol content migrated after seven contact days of the film with the aqueous food simulant. Talón et al. (2017) studied films based on starch-

chitosan with active compounds from thyme extract. This extract provided the films with remarkable antioxidant activity. The polyphenols interacted with the polymer chains, acting as cross-linkers and enhancing the tensile behaviour of chitosan films. However, this effect was not observed for the starch matrix.

References

Abdollahi M, Alboofetileh M, Rezaei M et al (2013) Comparing physico-mechanical and thermal properties of alginate nanocomposite films reinforced with organic and/or inorganic nanofillers. Food Hydrocoll 32:416-424

Abdul Khalil H P, Davoudpour Y, Saurabh C et al (2016) A review on nanocellulosic fibres as new material for sustainable packaging: Process and applications. Renew Sustain Energy Rev 64:823-836

Abraham, A, Mathew, A. K, Sindhu, R, Pandey, A, Binod, P (2016) Potential of rice straw for bio-refining: an overview. Bior Technol 215:29-36.

Aguiar, J, Estevinho, B. N, Santos, L (2016) Microencapsulation of natural antioxidants for food application - The specific case of coffee antioxidants - A review. Trends in Food Sci Tech 58:21-39

Akrami, M, Ghasemi, I, Azizi, H, Karrabi, M, Seyedabadi, M (2016) A new approach in compatibilization of the poly(lactic acid)/thermoplastic starch (PLA/TPS) blends. Carbohydr Polym 144:254-262

Alves J S, dos Reis K C, Menezes E G T et al (2015) Effect of cellulose nanocrystals and gelatin in corn starch plasticized films. Carbohydr Polym 115:215-222.

Arrieta M, Peltzer M, López, J et al (2014a) Functional properties of sodium and calcium caseinate antimicrobial active films containing carvacrol. J Food Eng 121:94-101

Arrieta M P, Fortunati E, Dominici F et al (2014b) Multifunctional PLA–PHB/cellulose nanocrystal films: Processing, structural and thermal properties. Carbohydr Polym 107:16-24

Arrieta M P, López J, Kenny J M et al (2015) Biodegradable electrospun bionanocomposite fibers based on plasticized PLA–PHB blends reinforced with cellulose nanocrystals. Ind Crop Prod 96:290-301

ASTM (2003) Standard Test Method for Determining Aerobic Biodegradation of Plastic Materials Under Controlled Composting Conditions, Incorporating Thermophilic Temperatures. Standards designations: D5338. In Annual book of ASTM standards. Philadelphia, PA: American Society for Testing and Materials

Azeredo H M C (2009) Nanocomposites for food packaging applications. Food Res Int 42:1240-1253

Azeredo H M C, Rosa M F, Mattoso L H C (2017) Nanocellulose in bio-based food packaging applications. Ind Crop Prod 97:664-671

Balaji, A. B, Pakalapati, H, Khalid, M, Walvekar, R, Siddiqui, H (2017) Natural and synthetic biocompatible and biodegradable polymers. In: Gopal Shimpi, N (ed.). Biodegradable and biocompatible polymer composites. Woodhead Publishing, pp. 3–32

Balasundram, N, Sundram, K, Samman, S (2006) Phenolic compounds in plants and agri-industrial by-products: Antioxidant activity, occurrence, and potential use. Food Chem 99:191-203

Bera A, Dubey S, Bhayani, K et al (2015) Microbial synthesis of polyhydroxyalkanoate using seaweed-derived crude levulinic acid as co-nutrient. Int J Biol Macromol 72:487-494

Berthet M A, Angellier-Coussy H, Chea V et al (2015) Sustainable food packaging: valorising wheat straw fibres for tuning PHBV-based composites properties. Compos Part A: Appl Sci Manuf 72:139-147

Bonilla J, Fortunati E, Vargas M (2013) Effects of chitosan on the physicochemical and antimicrobial properties of PLA films. J Food Eng 119(2):236-243

Bonilla, J, Sobral, J. A (2016) Investigation of the physicochemical, antimicrobial and antioxidant properties of gelatin-chitosan edible film mixed with plant ethanolic extracts. Food Biosci 16:17-25

Boonterm M, Sunyadeth S, Dedpakdee S et al (2015) Characterization and comparison of cellulose fiber extraction from rice straw by chemical treatment and thermal stem explosion. J Clean Prod 134:592-599

Borkotoky, S. S, Dhar, P, Katiyar, V (2018) Biodegradable poly (lactic acid)/Cellulose nanocrystals (CNCs)composite microcellular foam: Effect of nanofillers on foam cellular morphology, thermal and wettability behaviour. Inter J Biolog Macromol 106:433–446

Boumail A, Salmieri S, Klimas E et al (2013) Characterization of trilayer antimicrobial diffusion films (ADFs) based on methylcellulose−polycaprolactone composites. J Agric Food Chem 61:811-821

Brigham, C (2018) Biopolymers: Biodegradable alternatives to traditional plastics. In: Török, B, Dransfield, T (eds.). Green chemistry. Elsevier Inc., pp. 753–770

Brinchi L, Cotana F, Fortunati E et al (2013) Production of nanocrystalline cellulose from lignocellulosic biomass: Technology and applications. Carbohydr Polym 94:154-169

Cano A, Fortunati E, Cháfer M et al (2015) Effect of cellulose nanocrystals on the properties of pea starch–poly(vinyl alcohol) blend films. J Mater Sci 50:6979-6992

Cano A, Cháfer M, Chiralt A et al (2016) Biodegradation behaviour of starch-PVA films as affected by the incorporation of different antimicrobials. Polym Degrad Stab 132:11-20

Cao X, Chen Y, Chang P R et al (2008) Green composites reinforced with hemp nanocrystals in plasticized starch. J Appl Polym Sci 109(6):3804-3810

Carbone M, Donia D M, Sabbatella G et al (2016) Silver nanoparticles in polymeric matrices for fresh food packaging. J King Saud Univ Sci 28:273–279

Cavallaro G, Lazzara G, Milioto S (2013) Sustainable nanocomposites based on halloysite nanotubes and pectin/polyethylene glycol blend. Polym Degrad Stab 98:2529-2536

Chen D, Lawton D, Thompson M R et al (2012) Biocomposites reinforced with cellulose nanocrystals derived from potato peel waste. Carbohydr Polym 90:709-716

Cheng Y, Deng S, Chen P et al (2009) Polylactic acid (PLA) synthesis and modifications: a review. Front Chem China 4(3):259-264

Cherian, B. M, Leâo, A. L, de Souza, S. F, Costa, L. M. M, de Olyveira, G. M, Kottaisamy, M, et al (2011) Cellulose nanocomposites with nanofibres isolated from pineapple leaf fibers for medical applications. Carbohydr Polym 86:1790–1798

Cho J, Joshi M S, Sun, C T (2006). Effect of inclusion size on mechanical properties of polymeric composites with micro and nano particles. Compos Sci Technol 66(13):1941-1952

Collazo-Bigliardi, S, Ortega-Toro, R, Chiralt, A (2018a) Isolation and characterisation of microcrystalline cellulose and cellulose nanocrystals from coffee husk and comparative study with rice husk. Carbohydr Polym 191:205-215.

Cong-Cong, X, Bing, W, Yi-Qiong, P, Jian-Sheng, T, Tong, Z (2017) Advances in extraction and analysis of phenolic compounds from plant materials. Chinese J Nat Med 15(10):721-731

Correa J P, Molina V, Sanchez M et al (2017) Improving ham shelf life with a polyhydroxybutyrate/polycaprolactone biodegradable film activated with nisin. Food Packag Shelf Life 11:31-39

Corsello F A, Bolla P A, Anbinder P S et al (2017) Morphology and properties of neutralized chitosan-cellulose nanocrystals biocomposite films. Carbohydr Polym 156:452-459

Dash S, Swain S K (2013) Synthesis of thermal and chemical resistant oxygen barrier starch with reinforcement of nano silicon carbide. Carbohydr Polym 97:758-76

Davachi, S. M, Heidari, B. S, Hejazi, I, Seyfi, J, Oliaei, E, Farzaneh, A, Rashedi, H (2017) Interface modified polylactic acid/starch/poly ε-caprolactone antibacterial nanocomposite blends for medical applications. Carbohydr Polym 155:336-344

Debiagi, F, Mello, L. R, Mali, S (2017) Thermoplastics starch-based blends: processing, structural, and final properties. Starch-Based Materials in Food Packaging, In: Villar, M. A, Barbosa, S. E, López, O (eds.) Academic Press, pp 153-186

De Oliveira, J. P, Bruni, G. P, Lima, K, El Halal, S. L, da Rosa, G, Dias, A, Zavareze, E (2017). Cellulose fibers extracted from rice and oat husks and their application in hydrogel. Food Chem 221:153-160

De Oliveira, S. A, De Macedo, J. R, Rosa, D (2019) Eco-efficiency of Poly (lactic acid)-Starch-Cotton composite with high natural cotton fiber content: environmental and functional value. J Clean Prod 217:32-41

De Paula E L, Roig F, Mas A et al (2016) Effect of surface-grafted cellulose nanocrystals on the thermal and mechanical properties of PLLA based nanocomposites. Eur Polym J 84:173-187

Dominguez-Martinez B, Martínez-Flores H, Berrios J et al (2017) Physical characterization of biodegradable films based on chitosan, polyvinyl alcohol and opuntia mucilage. J Polym Environ 25(3):683-691

El Achaby, M, Kassab, Z, Aboulkas, A, Gaillard, C, Barakat, A (2018) Reuse of red algae waste for the production of cellulose nanocrystalsand its application in polymer nanocomposites. Int J Biolog Macromol 106:681–691

El-Hadi A (2017) Increase the elongation at break of poly (lactic acid) composites for use in food packaging films. Sci Rep. doi: 10.1038/srep46767

El Miri N, Abdelouahdi K, Barakar, A et al (2015) Bio-nanocomposite films reinforced with cellulose nanocrystals: Rheology of film-forming solutions, transparency, water vapor barrier and tensile properties of films. Carbohydr Polym 129:156-167

Emadian S M, Onay T T, Demirel B (2017) Biodegradation of bioplastics in natural environments. Waste Manag 59:526-536

Fabra M J, Talens P, Gavara R et al (2012) Barrier properties of sodium caseinate films as affected by lipid composition and moisture content. J Food Eng 109(3):372-379

Fabra M J, López-Rubio A, Lagaron J M (2014) Biopolymers for food packaging applications. In: Aguilar de Armas M R, Román J S (eds). Smart Polymers and their Applications. Elsevier, p 476-509

Fabra M J, López-Rubio A, Ambrosio-Martín J et al (2016) Improving the barrier properties of thermoplastic corn starch-based films containing bacterial cellulose nanowhiskers by means of PHA electrospun coatings of interest in food packaging. Food Hydrocoll 621:261-268

Ferreira, F. V, Dufresne, A, Pinheiro, I. F, Souza, D. H. S, Gouveia, R. F, Mei, L. H. I, Lona, L. M. F (2018) How do cellulose nanocrystals affect the overall properties of biodegradable polymer nanocomposites: A comprehensive review. Eur Polym J 108: 274-285

Fillat A, Gallardo O, Vidal T, Pastor F. I. J, Díaz P, Roncero M. B (2012) Enzymatic grafting of natural phenols to flax fibres: Development of antimicrobial properties. Carbohydr Polym 87(1):146-152

Flauzino Neto W P, Silvério H A, Dantas N O et al (2013) Extraction and characterization of cellulose nanocrystals from agro-industrial residue soy hulls. Ind Crop Prod 42:480-488

Follain N G, Belbekhouche S, Bras J et al (2013) Water transport properties of bionanocomposites reinforced by Luffa cylindrica cellulose nanocrystals. J Membr Sci 427: 218-229

Fortunati E, Puglia D, Luzi F et al (2013a) Binary PVA bio-nanocomposites containing cellulose nanocrystals extracted from different natural sources: part I. Carbohydr Polym 97:825-836

Fortunati E, Pelltzer M, Armentano I et al (2013b) Combined effects of cellulose nanocrystals and silver nanoparticles on the barrier and migration properties of PLA nano-biocomposites. J Food Eng 118:117-124

Fortunati E, Luzi F, Puglia D et al (2014) Investigation of thermo-mechanical, chemical and degradative properties of PLA-limonene films reinforced with cellulose nanocrystals extracted from Phormium tenax leaves. Eur Polym J 56:77-91

Fortunati E, Luzi F, Puglia D et al (2015) Processing of PLA nanocomposites with cellulose nanocrystals extracted from *Posidonia oceanica* waste: Innovative reuse of coastal plant. Ind Crop Prod 67:439-447

Fortunati E, Luzi F, Jiménez, A et al (2016) Revalorization of sunflower stalks as novel sources of cellulose nanofibrils and nanocrystals and their effect on wheat gluten bionanocomposite properties. Carbohydr Polym 149:357-368

Fortunati E, Gigli M, Luzi F et al (2017) Processing and characterization of nanocomposite based on poly(butylene/triethylene succinate) copolymers and cellulose nanocrystals. Carbohydr Polym 165:51-60

Fukushima K, Tabuani D, Arena M et al (2013) Effect of clay type and loading on thermal, mechanical properties and biodegradation of poly(lactic acid) nanocomposites. React Funct Polym 73:540-549

Gazzoti, S, Farina, H, Lesma, G, Rampazzo, R, Piergiovanni, L, Ortenzi, M. A, Silvani, A (2017) Macromolecular nanotechnology polylactide/cellulose nanocrystals: the *in situ* polymerization approach to improved nanocomposites. Eur Polym J 94:173-184

Giménez B, López de Lacey A, Pérez-Santín E et al (2013) Release of active compounds from agar and agar–gelatin films with green tea extract. Food Hydrocoll 30:264-271

González K, Retegi A, González A et al (2015) Starch and cellulose nanocrystals together into thermoplastic starch bionanocomposites. Carbohydr Polym 117:83-90

González-Seligra P, Guz L, Ochoa-Yepes O et al (2017) Influence of extrusion process conditions on starch film morphology. LWT - Food Sci Technol 84:520-528

Graupner N, Ziegmann G, Wilde F et al (2016) Procedural influences on compression and injection moulded cellulose fibre-reinforced polylactide (PLA) composites: Influence of fibre loading, fibre length, fibre orientation and voids. Compos Part A: Appl Sci Manuf 81:158-171

Gullón B, Eibes G, Moreira M. T, Dávila I, Labidi J, Gullón P (2017) Antioxidant and antimicrobial activities of extracts obtained from the refining of autohydrolysis liquors of vine shoots. Ind Crop Prod 107:105-113

Guil-Guerrero, J. L, Ramos, L, Moreno, C, Zúñiga-Paredes, J. C, Carsama-Yepez, M, Ruales, P (2016) Antimicrobial activity of plant-food by-products: A review focusing on the tropics. Livestock Sci 189:32-49

Gutiérrez TJ (2017) Chitosan applications for the food industry. In: Ahmed S, Ikram S (eds) Chitosan: derivatives, composites and applications. Wiley-Scrivener, Beverly, MA, pp 183–232. EE.UU. ISBN: 978-1-119-36350-7.

Gutiérrez TJ, Alvarez VA (2017) Cellulosic materials as natural fillers in starch-containing matrix-based films: a review. Polym Bull 74(6):2401–2430.

Gutiérrez T, González P, Medina C et al (2017) Effect of filler properties on the antioxidant response of thermoplastic starch composites. In: Thakur V, Thakur M, Kessler M (eds) Handbook of composites from renewable materials, Wiley, New York, p337-369

Gutiérrez TJ (2018) Biodegradability and compostability of food nanopackaging materials. In: Cirillo G, Kozlowski MA, Spizzirri UG (eds) Composite materials for food packaging. Wiley-Scrivener, Beverly, MA, pp 263–289 EE.UU. ISBN: 978-1-119-16020-5.

Gutiérrez TJ, Alvarez VA (2018) Bionanocomposite films developed from corn starch and natural and modified nano-clays with or without added blueberry extract. Food Hydrocoll 77:407–420.

Gutiérrez T J, Ollier R, Alvarez V A (2018) Surface Properties of Thermoplastic Starch Materials Reinforced with Natural Fillers. In: Thakur V, Thakur M (eds) Functional Biopolymers. Springer Series on Polymer and Composite Materials. Springer, Cham. p 131-158

Hamad, K, Kaseem, M, Ayyoob, M, Joo, J, Deri, F (2018) Polylactic acid blends: The future of green, light and tough. Progr Polym Sci 85:83-127

Haque M M, Puglia D, Fortunati E et al (2017) Effect of reactive functionalization on properties and degradability of poly(lactic acid)/poly(vinyl acetate) nanocomposites with cellulose nanocrystals. React Funct Polym 110:1-9

He J, Chong Yap R, Wong S et al (2015) Polymer composites for intelligent food packaging. J Mol Eng Mater 3(1):1-12

Hemmati F, Jafari S, Kashninejad M, Motalh, M (2018) Synthesis and characterization of cellulose nanocrystals derived from walnut shell agricultural residues. Inter J Biolog Macromol 120:1216:1224

Heitmann A, Patrício P, Coura I et al (2016) Nanostructured niobium oxyhydroxide dispersed Poly (3-hydroxybutyrate) (PHB) films: Highly efficient photocatalysts for degradation methylene blue dye. Appl Catal B: Environ 189:141-150

Herrera N, Salaberria A M, Mathe A et al (2016) Plasticized polylactic acid nanocomposite films with cellulose and chitin nanocrystals prepared using extrusion and compression molding with two cooling rates: Effects on mechanical, thermal and optical properties. Compos: Part A 83:89-97

Hossain A B M S, Ibrahim N, AlEissa M S (2016) Nano-cellulose derived bioplastic biomaterial data for vehicle bio-bumper from banana peel waste biomass. Data in Brief 8:286-294

Hu Z, Ballinger S, Pelton R et al (2015) Surfactant-enhanced cellulose nanocrystal pickering emulsions. J of Coll Interface Sci 439:139-138

Jiménez A, Fabra M J, Talens P et al (2013) Physical properties and antioxidant capacity of starch–sodium caseinate films containing lipids. J Food Eng 116(3):695-702

Jiménez-Zamora A, Pastoriza S, Rufián-Henares J (2015) Revalorization of coffee by-products. Prebiotic, antimicrobial and antioxidant properties. LWT – Food Sci Technol 61:12-18

Johar N, Ahmad I, Dufresne A (2012) Extraction, preparation and characterization of cellulose fibres and nanocrystals from rice husk. Ind Crop Prod 37:93-99

Jonoobi M, Oladi R, Davaoudpour, Y et al (2015) Different preparation methods and properties of nanostructured cellulose from various natural resources and residues: a review. Cellul 22:935-969

Kaboorani A, Riedl B (2015) Surface modification of cellulose nanocrystals (CNC) by a cationic surfactant. Ind Crop Prod 65:45-55

Kallel, F, Driss, D, Chaari, F, Belghith, L, Bouaziz, F, Ghorbel, R, Chaabouni, S. E (2014) Garlic (Allium sativum L.) husk waste as a potential source of phenolic compounds: Influence of extracting solvents on its antimicrobial and antioxidant properties. Ind Crops Prod 62:34-41

Kallel F, Bettaieb F, Khiari R et al (2016) Isolation and structural characterization of cellulose nanocrystals extracted from garlic straw. Ind Crop Prod 87:287-296

Kanmani P, Rhim J W (2014) Physicochemical properties of gelatin/silver nanoparticle antimicrobial composite films. Food Chem 148:162-169

Karimi S, Abdulkhami A Tahir P, Karimi A, Dufresne A (2014) Effect of cellulosic fiber scale on linear and non-linear mechanical performance of starch-based composites. Inter J Biolg Macromol 91:1040-1044

Kargarzadeh, H, Huang, J, Lin, N, Ahmad, I, Mariano, M, Dufresne, A, Thomas, S, Galeski, A (2018) Recent developments in nanocellulose-based biodegradable polymers, thermoplastic polymers, and porous nanocomposites. Prog Polym Sci 87:197-227

Koch, K (2018) Starch-based film. In: Sjöö, M & Nilsson, L (eds), Starch in food Woodhead Publishing, pp. 747-767

Laurienzo, P, Malinconico, M, Mattia, G, Romano, G (2006) Synthesis and characterization of functionalized crosslinkable poly(ε-caprolactone). Macromol Chemi Phy 207:1861-1869

Le Corre D, Angellier-Coussy H (2014) Preparation and application of starch nanoparticles for nanocomposites: A review. React Funct Polym 85:97-120

Leceta I, Guerrero P, de la Caba K (2013) Functional properties of chitosan-based films. Carbohydr Polymers 93(1):339-346

Le Normand, M, Moriana, R, Ek, M (2014) Isolation and characterization of cellulose nanocrystals from spruce bark in a biorefinery perspective. Carbohydr Polym 111:979–987

Lizundia E, Fortunati E, Dominici F et al (2016) PLLA-grafted cellulose nanocrystals: Role of the CNC content and grafting on the PLA bionanocomposite film properties. Carbohydr Polym 142:105-113

López O V, Ninago M D, Soledad Lencina M M et al (2015) Thermoplastic starch plasticized with alginate–glycerol mixtures: Melt-processing evaluation and film properties. Carbohydr Polym 126:83-90

Ludueña L, Vázquez A, Alvarez V (2012) Effect of lignocellulosic filler type and content on the behavior of polycaprolactone based eco-composites for packaging applications. Carbohydr Polym 87:411-421

Luzi F, Fortunati E, Jiménez A (2016) Production and characterization of PLA PBS biodegradable blends reinforced with cellulose nanocrystals extracted from hemp fibres. Ind Crop Prod 93:276-289

Macedo, J. R, dos Santos, D. J, Rosa, D (2019) Poly(lactic acid)–thermoplastic starch–cotton composites: Starch-compatibilizing effects and composite biodegradability. J Appl Polym Sci 47490:1-10.

Majeed K, Jawaid M, Hassan A et al (2013) Potential materials for food packaging from nanoclay/natural fibres filled hybrid composites. Mater Des 46:391-410

Majid I, Nayik G, Dar S, Nanda V (2016) Novel food packaging technologies: innovations and future prospective. J Saudi Soc Agric Sci 17(4):454-462

Maqsood H S, Baheti V, Wiener J et al (2016) Reinforcement of enzyme hydrolyzed longer jute micro crystals in polylactic acid. Polym Compos. doi:10.1002/pc.24036.

Marett J, Aning A, Foster E. J (2017) The isolation of cellulose nanocrystals from pistachio shells via acid hydrolysis. Ind Crop Prod 109:869-874

Martino L, Berthet M A, Angellier-Coussy H et al (2015) Understanding external plasticization of melt extruded PHBV–wheat straw fibers biodegradable composites for food packaging. J Appl Polym Sci 41611:2-11

Miranda C S, Ferreira M S, Magalhães M T, Santos W J et al (2015) Mechanical, thermal and barrier properties of starch-based films plasticized with glycerol and lignin and reinforced with cellulose nanocrystals. Mater Today: Proc 2:63-69

Mizuno S, Maeda T, Kanemura C et al (2015) Biodegradability, reprocessability, and mechanical properties of polybutylene succinate (PBS) photografted by hydrophilic or hydrophobic membranes. Polym Degrad Stab 117:58-65

Mondal, S (2017) Preparation, properties and applications of nanocellulosic materials. Carbohydr Polym 163:301–316

Moreno O, Gil A, Atarés L et al (2017) Active starch-gelatin films for shelf-life extension of marinated salmon. LWT - Food Sci Technol 84:189-195

Moriana R, Vilaplana F, Karlsson S et al (2011) Improved thermo-mechanical properties by the addition of natural fibres in starch-based sustainable biocomposites. Compos: Part A 42:30-40

Moriana, R, Vilaplana, F. Ek, M (2016) Cellulose nanocrystals from forest residues as reinforcing agents for composites: A study from macro- to nano-dimensions. Carbohydr Polym 139:139–149

Moustafa H, Guizani C, Dupont C et al (2016) Utilization of Torrefied Coffee Grounds as Reinforcing Agent To Produce High-Quality Biodegradable PBAT Composites for Food Packaging Applications. ACS Sustain Chem Eng 5(2):1906–1916

Mukurubira A R, Mellem J M, Amonsou E O (2017) Effects of amadumbe starch nanocrystals on the physicochemical properties of starch biocomposite films. Carbohydr Polym 165:142-148

Müller, P, Bere, J, Fekete, R, Móczó, J, Nagy, B, Kállay, M, Gyarmati, B, Pukánszky, B (2016) Interactions, structure and properties in PLA/plasticized starch blends. Polym 103:9-18

Muller J, González-Martínez C, Chiralt A (2017a) Combination of poly(lactic) acid and starch for biodegradable food packaging. Mater. doi: 10.3390/ma10080952

Muller J, González-Martínez C, Chiralt A (2017b) Poly(lactic) acid (PLA) and starch bilayer films, containing cinnamaldehyde, obtained by compression moulding. Eur Polym J 95:56-70

Murariu, M, Dubois, P (2016) PLA composites: From production to properties. Adv Drug Deliver Rev 107:17-46

Nair N R, Sekhar V C, Nampoothir, K M et al (2017) Biodegradation of biopolymers. In: Pandey A, Negi S, Soccol C R (eds) Current Developments in biotechnology and Bioengineering. Elsevier, p 739-755

Narita, Y, Inouye, K (2012) High antioxidant activity of coffee silverskin extracts obtained by the treatment of coffe silverskin with subcritical water. Food Chem 135:943-949

Ng H M, Sin L T, Tee T T et al (2015) Extraction of cellulose nanocrystals from plant sources for application as reinforcing agent in polymers. Compos Part B 75:176-200

Ortega-Toro, R, Santagata, G, Gomez d'Ayala, G, Cerruti, P, Talens, P, Chiralt, A, Malinconico, M (2016). Enhancement of interfacial adhesion between starch and grafted poly(ε-caprolactone). Carbohydr Polym 147:16-27

Ortega-Toro R, Bonilla J, Talens P et al (2017) Future of starch-based materials in food packaging. In: Vilar M (ed) Starch-based materials in food packaging: Processing, characterization and application. Academic Press, p 257-312

Pardo-Ibáñez P, López-Rubio A, Martínez-Sanz M et al (2014) Keratin–Polyhydroxyalkanoate melt-compounded composites with improved barrier properties of interest in food packaging applications. J Appl Polym Sci 39947:1-10

Patel, J. P, Parsania, P. H (2018) Characterization, testing, and reinforcing materials of biodegradable composites. In: Shimpi N. G (ed.) Biodegradable and biocompatible polymer composites. Woodhead Publishing, pp. 55–79

Peelman N, Ragaert P, Meulenaer B et al (2013) Application of bioplastics for food packaging. Trends in Food Sci Technol 32(2):128-141

Piñeros-Castro, Y, Otálvaro, A. M (2014) Use of lignocellulosic biomass, some research in Colombia. In: Piñeros-Castro, Y, Melo, J (eds.). Antioxidant activity in liquids from pre-treatments with hot water carried out on rice husk. Bogotá, pp. 237-254. ISBN: 978-958-725-152-4

Piñeros-Hernandez, D, Medina-Jaramillo, C, López-Córdoba, A, Goyanes, S (2017) Edible cassava starch films carrying rosemary antioxidant extracts for potential use as active food packaging. Food Hydrocoll 63:488-495

Prado, K, Spinacé, M. A. S (2019) Isolation and characterisation of cellulose nanocrystals from pineapple crown waste and their potential uses. Inter J Biolog Macromol 122:410-416

Ramos M, Fortunati E, Peltzer M et al (2014) Influence of thymol and silver nanoparticles on the degradation of poly(lactic acid) based nanocomposites: Thermal and morphological properties. Polym Degrad Stab 108:158-165

Rani, A, Monga, S, Bansal, M, Sharma, A (2016) Bionanocomposites reinforced with cellulose nanofibers derived from sugarcane bagasse. Polym Compos 39(S1):55-64

Requena R, Vargas M, Chiralt A (2017) Release kinetics of carvacrol and eugenol from poly(hydroxybutyrate-co-hydroxyvalerate) (PHBV) films for food packaging applications. Eur Polym J 92:185-193

Rhim J W, Wang L F, Lee Y et al (2014) Preparation and characterization of bio-nanocomposite films of agar and silver nanoparticles: laser ablation method. Carbohydr Polym 103:456-465

Rimdusit S, Jingjid S, Damrongsakkul S et al (2008) Biodegradability and property characterizations of Methyl Cellulose: Effect of nanocompositing and chemical crosslinking. Carbohydr Polym 72:444-455

Rivero C P, Hu Y, Kwan T H et al (2017) Bioplastics from solid waste. In: Wong J W C, Tyagi R D, Pandey A R (eds) Current Developments in biotechnology and Bioengineering. Elsevier, p 1-26

Rocca-Smith J, Marcuzzo E, Karbowiak T et al (2016) Effect of lipid incorporation on functional properties of wheat gluten based edible films. J Cereal Sci 69:275-282

Rombouts I, Lagrain B, Delcour J et al (2013) Crosslinks in wheat gluten films with hexagonal close-packed protein structures. Ind Crop Prod 51:229-235

Rosa M F, Medeiros E S, Malmonge J A et al (2010) Cellulose nanowhiskers from coconut husk fibers: effect of preparation conditions on their thermal and morphological behavior. Carbohydr Polym 81:83-92

Santos R P O, Rodrigues B V M, Ramires E C et al (2015) Bio-based materials from the electrospinning of lignocellulosic sisal fibers and recycled PET. Ind Crop Prod 72:69-76

Sanuja S, Agalya A, Umapathy M J (2014) Studies on magnesium oxide reinforced chitosan bionanocomposite incorporated with clove oil for active food packaging application. Int J Polym Mater Polym Biomater 63:733-740

Sanjay, M. R, Madhu, P, Jawaid, M, Senthamaraikannan, P, Senthil, S, Pradeep, S (2018) Characterization and properties of natural fiber polymer composites: A comprehensive review. J Clean Produc 172:566–581.

Sanyang, M. L, Sapuan, S. M, Jawaid, M, Ishak, M. R, Sahari, J (2016) Development and characterization of sugar palm starch and poly (lactic acid) bilayer films. Carbohydr Polym 146:36-45

Savadekar, N. M, Mhaske, S. T (2012) Synthesis of nano cellulose fibers and effect on thermoplastics starch based films. Carbohydr Polym 89:146–151

Scavo A, Pandino G, Restuccia C, Parafati L, Cirvilleri G, Mauromicale G (2019) Antimicrobial activity of cultivated cardoon (*Cynara cardunculus* L. var. *altilis* DC.) leaf extracts against bacterial species of agricultural and food interest. Ind Crop Prod 129:206-211

Shankar S, Rhim J W (2016) Preparation of nanocellulose from micro-crystalline cellulose: The effect on the performance and properties of agar-based composite films. Carbohydr Polym 135:18-26

Shavandi, A, Bekhit, A. E. A, Saeedi, P, Izadifar, Z, Bekhit, A. A, Khademhosseini, A (2018) Polyphenol uses in biomaterials engineering. Biomater 167.91-106

Shih Y F, Chang W C, Liu W C et al (2014) Pineapple leaf/recycled disposable chopstick hybrid fiber-reinforced biodegradable composites. J Taiwan Inst Chem Eng 45(4):2039-2046

Siqueira G, Bras J, Dufresne, A (2010) Cellulosic bionanocomposites: A review of preparation properties and applications. Polym 2:728–765

Slavutsky A M, Bertuzzi M A (2014) Water barrier properties of starch films reinforced with cellulose nanocrystals obtained from sugarcane bagasse. Carbohydr Polym 110:53-61

Sung S H, Chang Y, Han J (2017) Development of polylactic acid nanocomposite films reinforced with cellulose nanocrystals derived from coffee silverskin. Carbohydr Polym 169:495-503

Talón, E, Trifkovic, K. T, Nedovic, V. A, Bugarski, B. M, Vargas, M, Chiralt, A, González-Martínez, C (2017a). Antioxidant edible films based on chitosan and starch containing polyphenols from thyme extracts. Carbohydr Polym 157:1153-1161.

Vadivel V, Brindha P (2015) Antioxidant property of solvent extract and acid/alkali hydrolysates from rice hulls. Food Biosci 11:85-91

Van den Broek L, Knoop R, Kappen F et al (2015) Chitosan films and blends for packaging material. Carbohydr Polym 116:237-242

Wang Z, Yao Z, Zhou,J, He M, Jiang W, Li S, Ma Y, Liu M, Luo S (2018) Isolation and characterization of cellulose nanocrystals from pueraria root residue. Inter J Biolog Macromol. In press.

Wanyo P, Meeso N, Siriamornpun S (2014) Effects of different treatments on the antioxidant properties and phenolic compounds of rice brand and rice husk. Food Chem 157:457-463

Watthanaphanit A, Supaphol P, Tamura H et al (2008) Fabrication, structure, and properties of chitin whisker-reinforced alginate nanocomposite fibers. J Appl Polym Sci 110:890-899

Wei, L, Mc Donald, G (2016) A review on grafting biofibers for biocomposites. Mater 9:303-326

Xiao S, Liu B, Wang Y et al (2014) Efficient conversion of cellulose into biofuel precursor 5-hydroxymethylfurfural in dimethyl sulfoxide–ionic liquid mixtures. Bioresour Technol 151:361-366

Zhou Y, Fan M, Chen L (2016) Interface and bonding mechanisms of plant fibre composites: An overview. Compos Part B 101:41-45

Zubeldía F, Ansorena M, Marcovich N (2015) Wheat gluten films obtained by compression molding. Polym Test 43:68-77

OBJECTIVES

General objective

The **general objective** of this Doctoral Thesis is the isolation and characterization of cellulosic materials and active extracts from rice and coffee husks, and their incorporation into starch films and starch-PLA compatibilized blend films in order to improve their functional properties as food packaging materials.

Specific objectives

1. To isolate and characterise the cellulose fibres and cellulose nanocrystals from coffee and rice husks and to analyse their reinforcing capacity in corn starch films, through their effect on the film tensile behaviour.

2. To analyse the reinforcement properties of cellulose fibres from coffee and rice husks, when incorporated into corn starch matrices at different ratios, through the characterization of the changes induced in the film microstructure, tensile, barrier and optical properties and thermal stability.

3. To improve the properties of thermoplastic starch films by incorporating active extracts (with antioxidant and antimicrobial capacity) and cellulose fibres from rice and coffee husks. The effect of these agents on the mechanical, thermal, barrier, optical and microstructural properties of thermoplastic corn starch matrices will be analysed.

4. To analyse the effectiveness of PCL, functionalised by grafting with maleic anhydride and/or glycidyl methacrylate, at improving the properties of blend films based on corn starch and PLA, obtained by melt blending and compression moulding. The microstructure, thermal behaviour and functional properties (mechanical, optical and barrier) of blend films with different ratios of PLA and compatibilisers will be analysed in order to select the best formulation for food packaging applications.

5. To analyse the effectiveness of the incorporation of cellulosic reinforcing agents (cellulose fibres and cellulose nanocrystals) and antioxidant aqueous extract from coffee husk at improving the functional properties of compatibilised starch-PLA blend films. The effect of the incorporation method of cellulose nanocrystals into the blend films will be analysed, as well as the antioxidant properties of the films through their efficacy at preserving sunflower oil from oxidation.

CHAPTERS

PART 1

Incorporation of cellulosic fillers and active compounds from agro-wastes into starch matrices

Chapter I. Isolation and characterisation of microcrystalline cellulose and cellulose nanocrystals from coffee husk and comparative study with rice husk.

Chapter II. Reinforcement of thermoplastics starch films with cellulose fibres obtained from rice and coffee husks.

Chapter III. Improving properties of thermoplastic starch films by incorporating active extracts and cellulose fibres isolated from rice or coffee husk.

PART 2

Development of starch-PLA compatibilised matrices and addition of cellulosic materials and antioxidant extract from coffee agro-waste

Chapter IV. Using grafted poly(ε-caprolactone) for the compatibilization of starch-polylactic acid blends.

Chapter V. Using lignocellulosic fractions of coffee husk to improve properties of compatibilized starch-PLA blend films.

Chapter I

Isolation and characterisation of microcrystalline cellulose and cellulose nanocrystals from coffee husk and comparative study with rice husk

[1]**Sofía Collazo-Bigliardi;** [2]Rodrigo Ortega-Toro; [1]Amparo Chiralt

Carbohydrate Polymers, 191, 205-215 (2018)

[1]Institute of Food Engineering for Development, Universitat Politècnica de València. Valencia, Spain

[2]Food Engineering Program, Faculty of Engineering, Universidad de Cartagena. Cartagena de Indias, Colombia

socol@doctor.upv.es

ABSTRACT

Cellulosic material from coffee husk has not been previously studied despite being a potential source of reinforcing agents for different applications. This material has been extracted and characterised from coffee husk, in parallel with previously studied rice husk. Samples have been analysed as to their ability to obtain cellulosic fibres and cellulose nanocrystals (CNC) by applying alkali and bleaching treatments and final sulphuric acid hydrolysis. Microstructural changes were analysed after treatments, and the size and aspect ratio of CNCs were determined. Crystallinity and thermal stability of both materials progressed in line with the enrichment in cellulosic compounds. The CNC aspect ratio was higher than 10, which confers good reinforcing properties. These were tested in thermoplastic starch films, whose elastic modulus increased by 186 and 121% when 1 wt% of CNCs from rice and coffee husks, respectively, was incorporated into the matrix. Coffee husk represents an interesting source of cellulosic reinforcing materials.

Keywords: Agro-wastes; Cellulose fibres; Cellulose nanocrystals; Biocomposite; Tensile properties.

1. INTRODUCTION

A growing concern for environmental conservation has encouraged research into the development of new types of green bio-based and biodegradable materials from natural sources for different engineering applications (Balaji, Pakalapati, Khalid, Walvekar, & Siddiqui, 2017; Bassas-Galia, Follonier, Pusnik, & Zinn, 2017; Jiang & Zhang, 2017; Brigham, 2018; Ng et al., 2015), such as biodegradable packaging materials for the food industry (Fabra, López-Rubio, & Lagarón, 2014; Talegaonkar, Sharma, Pandey, Mishra, & Wimmer, 2017). Many studies have focused on the use of agro-wastes to obtain more valuable materials in a sustainable and environmentally-friendly way, which can be applied in different industrial applications, as an alternative to conventional petroleum-derived plastics (Mondal, 2017; Reis et al., 2015). The use of residual biomass can give added value to a waste product while also offering new renewable materials. This way, lignocellulosic materials are one of the most important natural sources of renewable polymers, which are attractive because of their biodegradability, low density and excellent mechanical properties, such as great stiffness and strength (Hake, Mondal, Khan, Usmani, Bhat, & Gazal, 2017; Patel & Parsania, 2018). Several authors have studied the potential use of lignocellulosic materials as sources of reinforcing fillers for thermoplastic biopolymers. In this sense, different agro wastes, such as sunflower stalks (Fortunati et al., 2016), hemp fibres (Luzi et al., 2016), bamboo pulp (Borkotoky, Dhar, & Katiyar, 2018), cotton (Ludueña, Vázquez, & Alvarez, 2012), spruce bark (Le Normand, Moriana, & Ek, 2014), sisal fibres (Santos, Rodrigues, Ramires, Ruvolo-Filho, & Frollini, 2015), pineapple leaf fibres (Shih et al., 2014), garlic skin (Reddy & Rhim, 2014), soy hull (Flauzino Neto, Silvério, Dantas, & Pasquini, 2013), rice straw (Boonterm et al., 2015; Kargarzadeh, Johar, & Ahmad, 2017), coconut husk fibres (Rosa et al., 2010), mango seeds (Henrique, Silvério, Neto, & Pasquini, 2013), red algae waste (El Achaby, Kassab, Aboulkas, Gaillard, & Barakat, 2018) or banana peel waste (Hossain, Ibrahim, & AlEissa, 2016) have been evaluated, although no previous studies into the extraction and characterization of cellulosic materials from coffee husk have been reported. However, coffee husks, obtained after de-hulling the coffee cherries during dry processing, also constitute a source of lignocellulosic materials, containing ~57% of cellulosic and ~22% lignin components (Moreno-Contreras, Serrano-Rico, & Palacios-Restrepo, 2009). Likewise, the coffee (*Coffea sp.*) crop generates a significant amount of waste, which could be used as a source of different valuable products (Alves, Rodrigues, Nunes, Vinha, & Oliveira, 2017), with a positive impact on the economy of producing countries, such as Brazil, Vietnam, Indonesia, Colombia, Ethiopia, India or Mexico (Oliveira & Franca, 2015).

On the other hand, rice husk, with a similar composition in lignocellulosic compounds to coffee husk (~55% cellulose and ~35% lignin, Brinchi, Cotana, Fortunati, & Kenny, 2013), has been previously studied as a source of these materials. The previously described methods to obtain and characterize cellulose fibres from rice husk (Johar, Ahmad, & Dufresne, 2012;

Kargarzadeh et al., 2017) could be applied to evaluate the coffee husk's potential as a source of cellulosic fractions, useful as filling compounds in composite materials.

Natural cellulose obtained from these kinds of biomasses can be transformed into micro- and nano-scale materials, yielding products, such as microcrystalline cellulose, microfibrillar cellulose or cellulose nanocrystals (CNC) (Azeredo, Rosa, & Mattoso, 2017; Brinchi et al., 2013; Sanjay et al., 2018) with very good properties as reinforces, at the same time that the this allows for a better exploitation of lignocellulosic residues. The isolated cellulose fibres submitted to different treatments yield different crystalline fractions such as CNCs. These are a good option as reinforcing agent due to their abundant hydroxyl groups, which allows for obtaining different derivative materials with adequate compatibility, high degree of crystallinity, excellent mechanical properties, large specific surface area, high aspect ratio, and high thermal stability (Azeredo et al., 2017; Ng et al., 2015). The final yield of the isolation process depends on the type of initial raw material and process conditions.

The aim of this study was to isolate and characterise the cellulose fibres and cellulose nanocrystals from coffee husks, in parallel with rice husk, for comparison purposes. Likewise, the reinforcing capacity of the isolated cellulose fibres and CNCs, from both coffee and rice husk, have been analysed in corn starch films through their effect on tensile behaviour of the films.

2. MATERIALS AND METHODS

2.1. Materials

Rice husk was obtained from Dacsa (Almàssera, Valencia, Spain) and coffee husk was provided by Centro Surcolombiano de Investigaciones en Café de la Universidad Surcolombiana (Neiva, Colombia). Corn starch was purchased from Roquette (Roquette Laisa, Benifaió, Spain). Glycerol and sodium hydroxide was purchased from Panreac Química, S.A (Castellar del Vallès, Barcelona, Spain). Sodium chlorite and acetate buffer for bleaching treatment and sulphuric acid (purity 98%) used for acid hydrolysis were provided by Sigma Aldrich Química S.L (Madrid, Spain). For sample conditioning, phosphorus pentoxide (P_2O_5) and magnesium nitrate-6-hydrate ($Mg(NO_3)_2$) were supplied by Panreac Química, S.A. (Castellar del Vallès, Barcelona, Spain). All other chemicals used were reagent grade and underwent no further purification.

2.2. Extraction/purification process applied to rice and coffee husks

The same process conditions for both raw materials were applied, adapted from Johar et al. (2012). Ground rice or coffee husks, with a mean particle size of 2-3 mm, were alkali treated and afterwards submitted to bleaching treatment and acid hydrolysis.

2.2.1. Alkali treatment

Alkali treatment was carried out with a 4 wt% NaOH solution, with a solid solution mass ratio of 1:20, at reflux temperature for 3 h, under continuous stirring. Then, the solid was filtered and washed with distilled water several times until the alkali solution was removed. This treatment was repeated twice.

2.2.2. Bleaching treatment

For bleaching treatment, equal parts of acetate buffer solution, sodium chlorite (1.7 wt%) and water were mixed with the alkali treated solid (1:20 mass ratio) and submitted at reflux temperature for 4 h. This process was repeated as many times as necessary (4 in rice samples and 6 in coffee samples) until the samples were completely white. After that, the samples were filtered and washed with distilled water several times until the solution was removed.

2.2.3. Acid hydrolysis

Cellulose nanocrystals were prepared by acid hydrolysis of the obtained bleached fibres as described Johar et al. (2012) and Cano et al. (2015). Fibre treatment with sulphuric acid, (64%, wt/wt) at 50 °C for 40 min, was carried out under continuous stirring, using 7.5 wt% of fibre content. The hydrolysed cellulose sample was washed several times with distilled water by centrifugation at 14.000 rpm for 30 min to concentrate cellulose material and to remove acid excess. The suspension was then dialysed against distilled water until a constant pH was reached and then neutralised with 10 wt% ion resin (Dowex Marathon MR-3) for 24 h. The resin was separated by vacuum filtration through a Whatman 541 filter, and the filtrate CNC suspension was sonicated for 30 min, using a tip sonicator (Vibra-Cell™ VCX 750, Sonics & Materials, Inc., Newton, USA) in an ice bath and kept refrigerated for further analyses.

2.3. Structural characterization of fibres and cellulose nanocrystals (CNC)

2.3.1. Thermal properties

The thermal stability of the different samples was analysed using a Thermogravimetric Analyzer TGA 1 Star^e System analyser (Mettler-Toledo, Inc., Switzerland) under nitrogen atmosphere (gas flow: 10 mL min^{-1}). Samples (about 8 mg) were heated from 25 to 900 °C at 10 °C/min (Johar et al., 2012). At least two replicates for each sample were obtained. Initial degradation temperature (Onset) and peak temperature (Peak) were registered from the first derivative of the resulting weight loss curves using the STAR^e Evaluation Software (Mettler-Toledo, Inc., Switzerland).

2.3.2. X-ray diffraction

A Diffractometer (XRD, Bruker AXS/D8 Advance) was used to obtain X-Ray diffraction patterns of the different samples conditioned at 25 °C and 53% RH, between 2ϑ: 5° and 40° using Kα Cu radiation (λ: 1.542 Å), 40 kV and 40 mA with a step size of 0.05°. For this analysis, the samples were milled and spread until covering the sample holder. The degree of crystallinity (X_c) of the samples was estimated from the ratio of crystalline peak areas and the integrated area of XRD diffractograms, using OriginPro 8.5 software, assuming Gaussian profiles for crystalline and amorphous peaks, as described by Ortega-Toro et al. (2016a).

2.3.3. Optical microscopy

Light microscopy (Optika Microscopes B-350 connected to an Optikam B2 camera, Italy) was used to measure the length range of the fibres after alkali and bleaching treatments. A drop (30 μL of the 1% solid dispersions was spread over the porta and observed at 10X magnification level. The bleached fibres were stained with gentian violet to obtain the adequate contrast.

2.3.4. Scanning Electron Microscopy (SEM)

A Scanning Electron Microscope (JEOL JSM-5410, Japan) was used to analyse the microstructure of the material after different treatments: untreated (C), alkali treated (At) and bleached (Bt) fibres. The fibres were maintained in desiccators with P_2O_5 for 2 weeks at 25 °C and the SEM observations were carried out in duplicate for each material. Samples were gold coated and observed, using an accelerating voltage of 15 kV.

2.3.5. Morphological analysis in CNCs

The particle size distribution of rice and coffee cellulose nanocrystals was analysed by using 2 mL of CNC suspensions in Zetasizer equipment (Zetasizer Nano ZS, Malvern Instruments, U.K). Five measurements were taken for each sample.

Transmission Electron Microscopy (JEOL JEM-1010, Japan) was also used to analyse morphology and the size of the CNCs. A drop of diluted CNC dispersion was deposited on the carbon film supported by the copper grid. TEM analysis was performed at an accelerating voltage of 80 kV. The aspect ratio (Ar) (L/*d*, L mean length and *d* mean diameter) was measured in 100 individualised crystals of each sample, from the digital images recorded with an AMT V600 camera, using the ImageJ software.

2.3.6. Chemical composition

The contents of cellulose, hemicellulose, lignin and ashes of the rice and coffee husk samples submitted to the different treatments were determined according to the NREL standard method for biomass (NREL/TP-510-42618, 2011), applying sulphuric acid hydrolysis to the samples and determining the cellulose and hemicellulose content from the glucose, xylose and arabinose amounts determined by HPLC (Hitachi LaChrom, Japan) in the sample hydrolysate. The Biorad Aminex HPX-87H column and an IR detector (Agilent 1200 series RID) were used. The injection volume of all samples was 60 µL, and 5 mM sulphuric acid has been used as mobile phase at 0.5 mL/min flow rate and 65 °C. Data acquisition was carried out by using Galaxie Chromatography Data System. Raw husk powders were first water extracted, according to the method recommendation (NREL/TP-510-42619, 2008) to avoid interferences in the HPLC analysis. Lignin and ashes were also determined from the acid insoluble fraction by filtration, desiccation and incineration. Total ashes were analysed in the whole sample by sample incineration at 575 °C for 24 h.

2.3.7. Reinforcing capacity of the cellulose fibres and CNCs

The reinforcing capacity of 1 wt% of cellulose fibres and CNCs was evaluated in corn starch films containing 30% glycerol, obtained by melt blending (using Model LRM-M-100, Labtech Engineering, Thailand roller) and compression moulding (using Model LP20, Labtech Engineering, Thailand press). Pellets of thermoplastic starch (with or without filler) were obtained at 160 °C in the roller-mill using a prepared dispersion of the starch-glycerol-filler-water (1:0.3:0.01:0.5). The pellets conditioned at 53% relative humidity (RH) were compressed at 130 bars and 160 °C for 8 min, and cooled down to 50 °C for 3 min.

The obtained films were conditioned at 53% RH and 25 °C for 1 week and analysed as to the tensile behaviour (ASTM standard method D882; ASTM, 2001), using a universal test machine (TA.XTplus model, Stable Micro Systems, Haslemere, England). Rectangular film samples (2.5 x 10 cm) were submitted to the tensile test at 50 mm/min till break. Tensile strength-Henky strain curves were obtained and elastic modulus, tensile strength and deformation at break were determined for each sample. Ten replicates were carried out for each film sample.

2.4. Statistical analysis

Statgraphics Plus for Windows 5.1 (Manugistics Corp., Rockville, MD) was used for statistical analyses of data through analysis of variance (ANOVA). Fisher's least significant difference (LSD) was used at the 95% confidence level.

3. RESULTS AND DISCUSSION

3.1. Morphological changes and yield in alkali and bleaching treatments of rice and coffee husk

The effect of the different treatments on the appearance of the raw material can be observed in Fig. 1a, 1b and 1c. Alkali treatment provoked a colour change in both rice and coffee husk samples, the former turning more brownish whereas the latter became brownish-orange, which could be associated with the different pigmentation of the lignin fraction remaining in the material. This treatment was effective at purifying the cellulose fibres, removing non-cellulosic components, such as a part of the lignin fraction, hemicellulose, pectin and wax (Kallel et al., 2016). After the bleaching treatment, the sample colour change was more evident and the samples exhibited the characteristic whiteness of cellulose fibres, where extensive extraction of cementing compounds, such as lignin, occurred. Table 1 shows the sample composition of the products submitted to the different treatments, where the contents in lignin, hemicellulose, cellulose and ashes are shown. The progressive enrichment in cellulose of the husk products can be observed after the successive treatments. Cellulosic fibres obtained after bleaching still contained a fraction of hemicellulose in both rice and coffee products and the cellulose enrichment of the rice sample was slightly lower than the 96% reported by Johar et al. (2012), applying similar treatments to rice husks.

The cellulose and lignin content of the husk samples ranged between 34-35% and 22-23 %, respectively, showing lower values than those previously reported by other authors. Brinchi et al. (2013) reported about 55% and 36% for cellulose and lignin content in rice husk, respectively, while Moreno-Contreras et al. (2009) quantified about 57% cellulose and 22% lignin in coffee husk. Both coffee and rice husks contained a similar amount of cellulosic compounds, which agrees with the similar solid yield obtained for both products after the alkali and bleaching processes.

Table 1. Chemical composition (wt. percentage) of the rice (R) and Coffee (C) husk samples at the different treatment step (untreated: C, alkali treated: At, bleaching treated: Bt).

Samples	Water extractables (%)	Cellulose (%)	Hemicellulose (%)	Lignin (%)	Ashes (%)
R-C	14.5 ± 0.9	33.8 ± 0.5	17.1 ± 0.2	21.5 ± 0.3	16.5 ± 0.4
R-At	-	55.9 ± 0.3	15.8 ± 0.4	19.9 ± 0.8	0.59 ± 0.05
R-Bt	-	73.8 ± 0.3	19.2 ± 0.7	1.6 ± 0.5	0.14 ± 0.03
C-C	17.8 ±1.4	35.4 ± 0.9	18.2 ± 1.3	23.2 ± 0.5	1.4 ± 0.3
C-At	-	52.6 ± 1.1	19.0 ± 0.2	20.4 ± 0.6	0.74 ± 0.15
C-Bt	-	61.8 ± 2.6	27.2 ± 0.9	2.6 ± 0.4	0.49 ± 0.19

Alkali treatment yielded 86 and 88% with respect to the initial dry powder of rice and coffee husks, respectively, while this yield was 48 and 60%, respectively, for the bleaching treatment, which produced a cellulose-rich sample (41 and 53%, respectively with respect to the initial mass). Moreover, taking the final cellulose content of each bleached product into account, a better purification of the rice husk cellulosic fraction than that of the coffee husk was reached. The cellulose content found in different lignocellulosic wastes varies between 40-80%. Jonoobi, Ahmad & Dufresne (2015) reported cellulose and lignin contents of different raw materials, such as kenaf stem (~58%, ~17.5%), wheat straw (~43%, ~22%), pineapple leaf (~81%, ~3.5%) and banana rachis (~48%, ~12%).

After treatments, the particle size of the ground raw materials (2-3 mm) was drastically reduced, as reflected in the light microscopy images (Fig. 1c and 1e), in which the fibre length ranges are shown after the alkali and bleaching treatments.

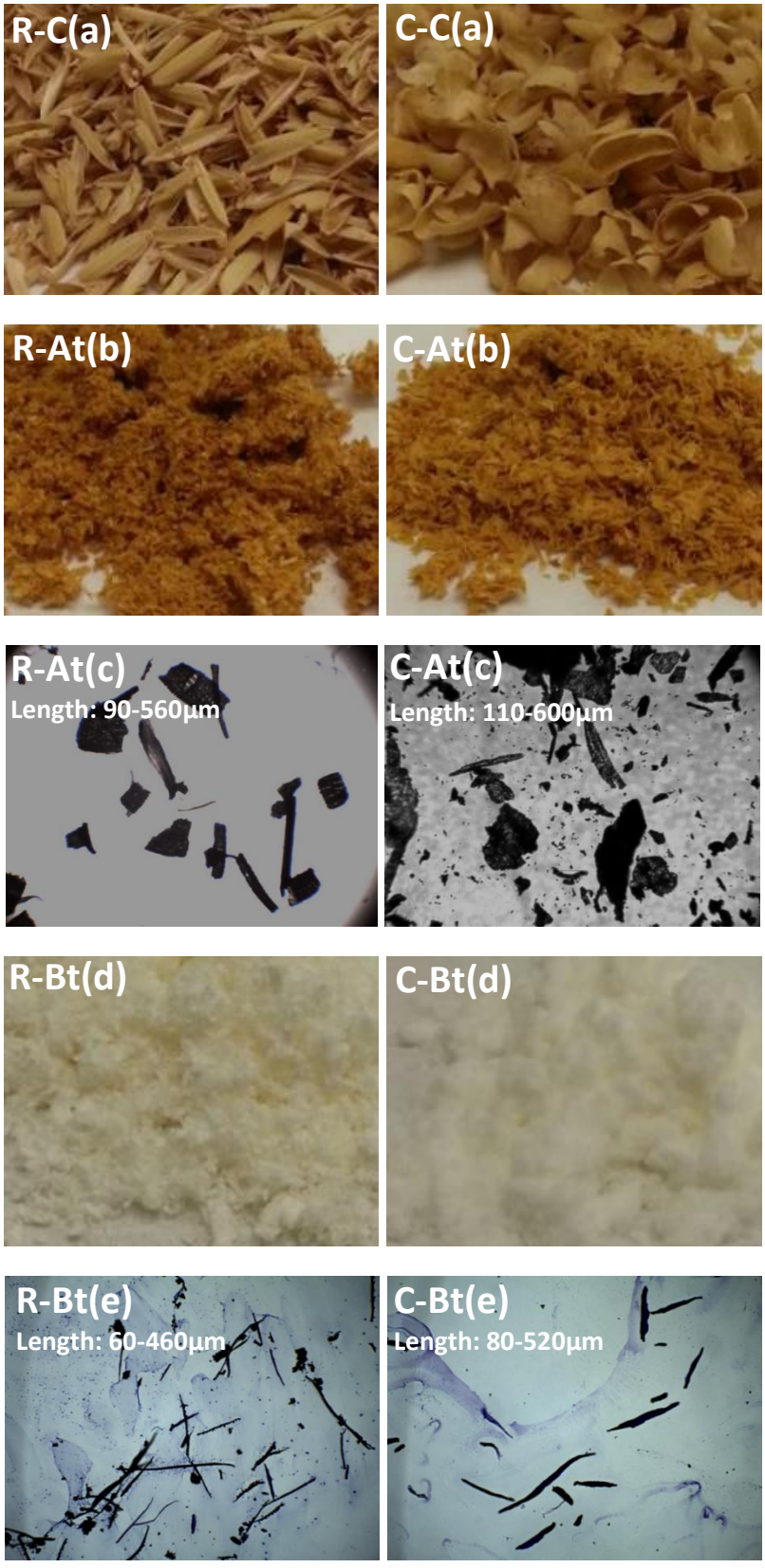

Fig. 1. Appearance of rice (R) and coffee (C) husk samples after each treatment: untreated sample (control: C-a), alkali treatment (At-b), bleaching treatment (Bt-d). Light micrographs of rice and coffee husk fibres after alkali (At-c) and bleaching treatment (Bt-e).

Particle size reduction provoked by bleaching treatment was similar for both husk materials and reflects the effective attack of the chemical agents disrupting the internal structure of the material while removing the non-cellulosic components. Other authors reported different fibre sizes depending on the raw material. As examples, bleached water hyacinth fibre was 25–50 µm in size (Sundari & Ramesh, 2012); bleached garlic straw filaments were about 14-17 µm length (Kallel et al., 2016) and pineapple leaf fibres were in the range of 50-12 µm (Cherian et al., 2011). The main difference between cellulosic rice and coffee fibres are the trend to aggregate in the water dispersion. Whereas coffee fibres appear as scattered elements, rice fibres are flocculated in the aqueous medium (Fig. 1, R-Atc). This suggests the action of more attractive forces between particles despite the similarity in size and composition, which could be associated to different surface bonded molecules.

3.2. Micro- and Nano-structural analysis

Fig. 2 shows SEM micrographs of the rice and coffee fibres, either untreated or submitted to the different treatments, where the structural changes produced by the successive processes can be observed. In the raw material, an ordered and homogeneous organisation could be distinguished evidencing the natural arrangement of the constituents. In both samples, the fibres are arranged in parallel and an ordered assembly can be observed, while pectin and intercellular junctional material fill the cell unions. Wax crystals covering the sample surface can also be seen, mainly in rice husk, which showed a rougher appearance. After the alkali treatment, the fibre surface becomes rougher due to the losses in the outer non-cellulosic compounds (hemicellulose, lignin, pectin and wax). This change was more appreciable in rice husk.

Both wax and pectin are known to surround the surface of natural fibres as a protective layer. In both cases, fibre bundles remain after alkali treatment, which indicates the retention of the cementing lignin material, which acts as a binder in the fibre components and preserves the bundle shape during the alkali treatment. Nevertheless, a great part of the pectin and hemicellulose content was removed from the fibres during this treatment, according to previous studies (Batra, 1981; Johar et al., 2012). The appearance of coffee husk samples reveals a less aggressive effect of the alkali treatment, which can be explained by its different composition. In fact, the product yield in the alkali treatment was higher in coffee than in rice husk, which could be due to a lower extraction of components in this product, as reflected in sample composition (Table 1).

The alkali process is more effective when the biomass has low lignin content and the process yield depends on the raw material and treatment conditions.

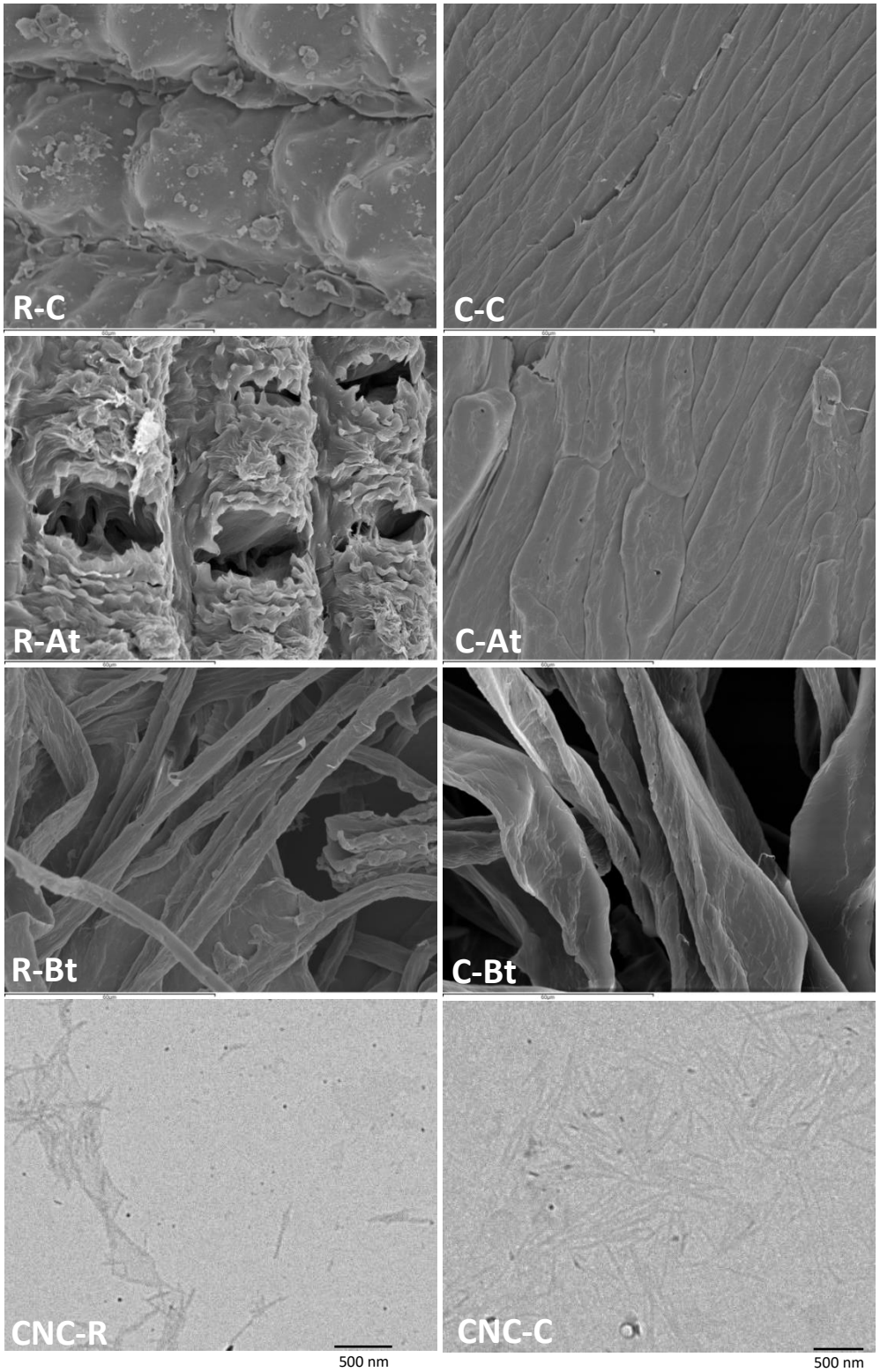

Fig. 2. SEM micrographs of the rice and coffee husks untreated (R-C or C-C) and after the alkali (R-At or C-At) and bleaching treatments (R-Bt or C-Bt). TEM micrographs of nanocrystals obtained from rice (CNC-R) and coffee (CNC-C) bleached fibres are also shown.

Treatment with sodium hydroxide decreases the degree of polymerization and crystallinity in the material, disrupts the lignin structure and increases the internal surface of cellulose fibres (Singh, Shukla, Tiwari, & Srivastava, 2014). All of this favours the penetration of the bleaching agents into the structure (Kallel et al., 2016). In both husk materials, the subsequent bleaching treatment was very effective at separating isolated fibres, as observed in Fig. 2 (R-Bt and C-Bt). The rice and coffee husk fibre bundles separate into very thin individual fibres with different diameters, thus indicating the great efficacy of the treatment to eliminate the non-cellulosic components, as previously reported (Chen et al., 2011; Espino et al., 2014; Savadekar & Mhaske, 2012). In the treatment, sodium chlorite becomes chlorine dioxide in acetate buffer solution, provoking the oxidation of the lignin aromatic ring (Ng et al., 2015; Ni, Kubes, & Van Helnlngen, 1993; Zainuddin, Ahmad, Kargarzadeh, Abdullah, & Dufresne, 2013). Coffee fibres were flatter and mainly helically folded, while rice fibres were similar to those previously reported by Johar et al. (2012), more cylindrical of less than 10 µm in diameter. The fibres diameters were in the range of previously reported for other plant wastes such as bleached garlic straw (Kallel et al., 2016). The obtained cellulose fibres showed a very high aspect ratio (L/d, L being the length and d the diameter), which provides them with adequate properties as reinforcing materials for composite applications.

The Van der Waals forces and hydrogen bonds that act in the crystalline zones of the cellulose provide high resistance to acid attack, while the amorphous regions are disordered and prone to sulfuric acid hydrolysis (Khalil et al., 2016; Qiao, Chen, Zhang, & Yao, 2016). Thus, the sulphuric acid treatment removes the cellulose fibres of the amorphous zones and reduces the fibre size to nanometric scale (Azizi Samir, Alloin, & Dufresne, 2005). Therefore, observations of the isolated CNCs were carried out by TEM at higher magnification. Fig. 2 also shows micrographs of the CNCs with a short, rod-like structure and many aggregates. These aggregates emerged in the drying step for sample preparation due to strong intermolecular hydrogen bonds between the particles (Sung et al., 2017). Likewise, the particle morphology and aggregation is highly affected by the TEM sample preparation (Chauve, Fraschini, & Jean, 2013; Kaushik, Fraschini, Chauve, Putaux, & Moores, 2015). However, some specimens remained isolated, which allows for the characterisation of their length and diameter and so, their aspect ratio, from digital images recorded with the camera and the use of the image analysis software. Fig. 3a and 3b show the distribution of diameter and aspect ratio of CNCs extracted from rice and coffee husk fibres. Length (L) and width (d) of rice CNC were 310 ± 160 and 39 ± 13 nm, and similar values were obtained for coffee CNC (310 ± 160 and 20 ± 4 nm, respectively), the latter being slightly thinner. Most of the CNCs exhibited an aspect ratio (L/d) in the range of 10-20 for both husk materials.

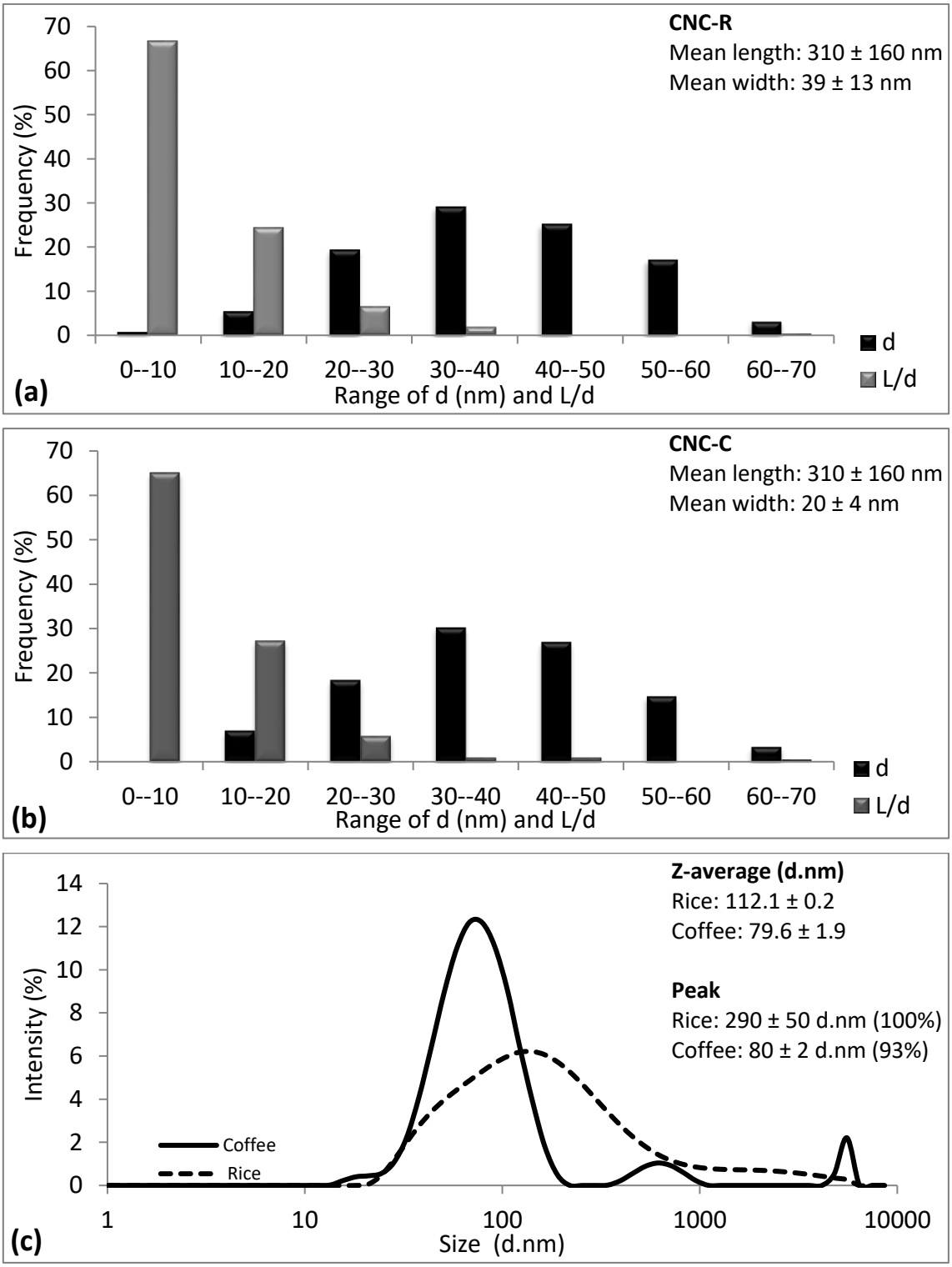

Fig. 3. Diameter distribution and aspect ratio of the CNC extracted from rice (a) and coffee (b) bleached fibres. Particle size distribution from dynamic light scattering of the CNC aqueous dispersion from rice and coffee samples (c).

These were similar both to those obtained by Johar et al. (2012) for rice husk and to the values reported for different lignocellulosic materials, such as ramie fibres (Habibi & Dufresne, 2008), bagasse pulp (Bras et al., 2010), sugarcane bagasse (Hassan M.L, Mathew, Hassan E. A, El-Wakil, & Oksman, 2012), kenaf fibres (Kargarzadeh et al., 2012), banana peel (Khawas & Deka, 2016) or *Alfa tenassissima* (BenMabrouk, Wim, Dufresne, & Boufi, 2009). Kallel et al. (2016) report that the aspect ratio of CNC extracted from different materials usually vary from 10 to 70, although the highest values (L/d = 80) were obtained in CNC extracted from garlic straw (Kallel et al., 2016) and tunicate (*Polycarpa aurata*), a sea animal with external cellulosic microfibrils, (L/d = 50-200) (Anglès & Dufresne, 2000). Silvério et al. (2013) reported that CNC could be considered as a good reinforcing material if their aspect ratio exceeds a value of 10. The CNCs dimensions ranges from 2 to 20 nm in diameter and from 100 to 600 nm in length (Moriana, Vilaplana, & Ek, 2016), depending on the nature of the lignocellulosic raw material, purification, mechanical process, pre-treatment and conditions of acid hydrolysis (Chauve et al., 2013).

Fig. 3c also shows the hydrodynamic diameter distribution of the isolated CNCs for water suspensions of CNC from rice and coffee husks obtained from dynamic light scattering analysis. Hydrodynamic diameter corresponds to that of an equivalent spherical specimen that would have the same diffusion coefficient and, for rod-like particles, such as CNCs, are only used for qualitative comparisons. The obtained hydrodynamic diameter distributions were similar to that reported by Kallel et al. (2016) for CNCs obtained from garlic straw. The z-average values and peak values for each sample are also shown in Fig. 3c. This average size, related with the hydrodynamic volume of the crystals, and the wide distribution reflects the aggregation tendency of CNC in the aqueous media. CNC from coffee husk were smaller and with lower tendency to aggregate as revealed by the smaller z-average and narrow distribution. This agrees with the behaviour deduced from the microscopic observations.

Given the crystalline nature of cellulose, contrary to the amorphous nature of hemicellulose and lignin, the crystallinity of the natural fibres rises as the extraction progresses with the different chemical treatments. Indeed, the alkali treatment increases the stiffness of the fibre as it removes different amorphous fractions.

Acid treatment does not affect the crystalline domains, but destroys the amorphous region of the fibre (Fengel & Wegener, 1984). Then, the X-ray diffraction spectra of the different products obtained after each treatment were analysed to control the progressive enrichment in crystalline cellulose.

Fig. 4 shows the X-ray diffraction patterns of the untreated, alkali treated and bleached fibres as well as of the isolated CNC of rice and coffee fibres. In all samples, the typical crystalline peaks of type I cellulose (2θ: 15-16° [110], 22° [200] and 34° [004]) were observed as reported by other authors (Johar et al., 2012; Kallel et al., 2016; Savadekar & Mhaske,

2012). As expected, these peaks become more defined upon each chemical treatment. Likewise, the degree of crystallinity (Xc) in the different samples was estimated from the ratio between the area of the peaks and the total area under spectra which include the amorphous response (Ortega-Toro et al., 2016a). The crystallinity degree increased after each chemical treatment, according to the progressive removal of components of the amorphous fraction (Bettaieb et al., 2015; Le Normand et al., 2014; Sheltami, Abdullah, Ahmad, Dufresne, & Kargarzadeh, 2012). This increase was more noticeable in the last acid treatment when the amorphous regions of cellulose were also eliminated and CNC were purified. During the hydrolysis process, hydronium ions can penetrate the more accessible amorphous regions of cellulose provoking the cleavage of glycosidic bonds, releasing individual crystallites (Lima & Borsali, 2004), which can grow or realign in parallel, thus increasing the cellulose crystallinity (Li et al., 2009).

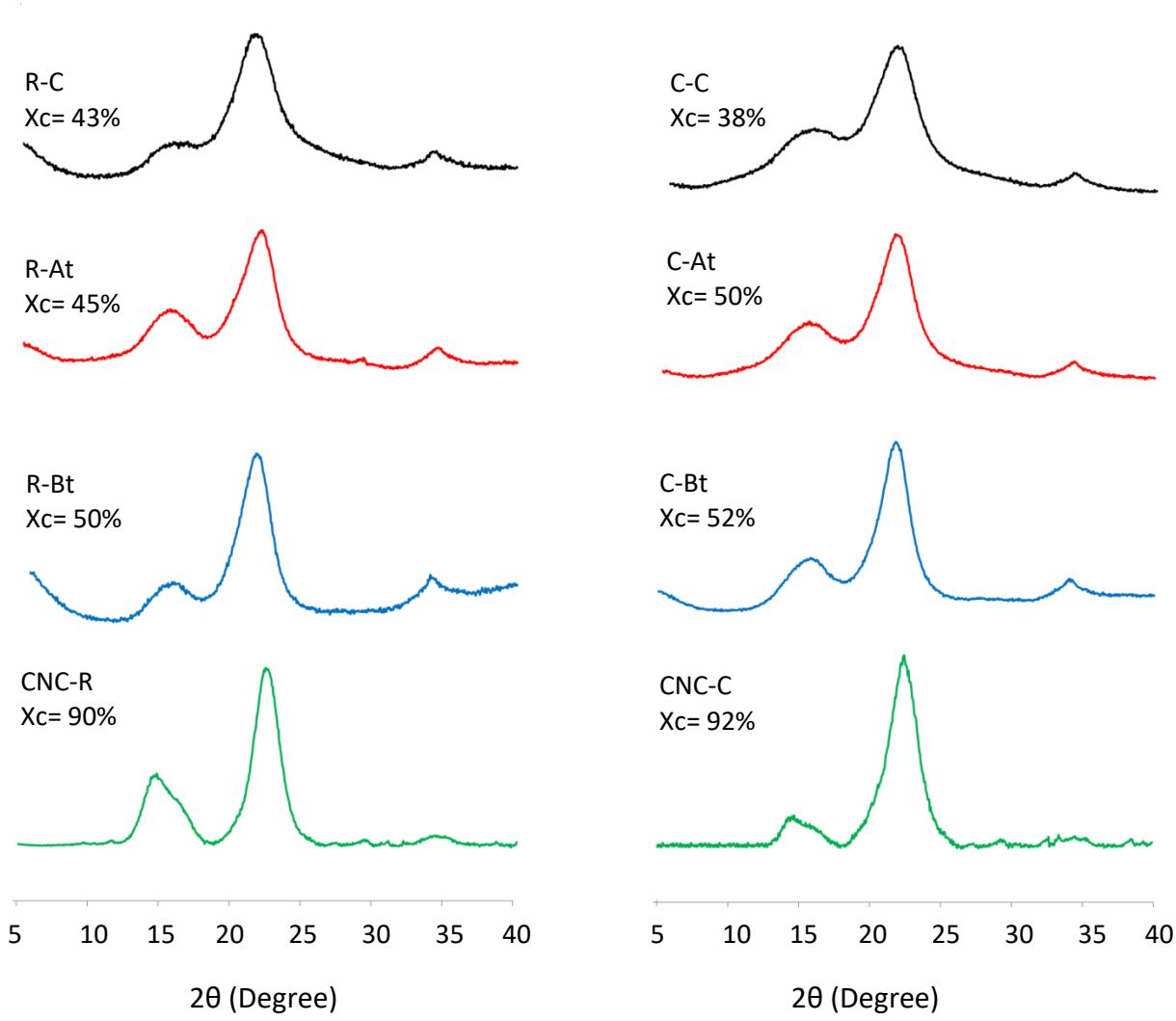

Fig. 4. X-Ray diffraction patterns of rice and coffee husks untreated (C), alkali treated (At), bleaching treated (Bt) and acid hydrolysed (CNC).

CNC exhibited high crystallinity due to the chemical cellulose structure, where each monomer has three hydroxyl groups with the ability to form intra- and inter-molecular hydrogen bonding between cellulose chains giving rise to a highly compact system (Ng et al., 2015; Siqueira, Bras, & Dufresne, 2010). The high degree of crystallinity confers stiffness on the CNC and so a reinforcing capability when included in other polymer materials.

3.3. Thermal analysis

Thermogravimetric analysis allows us to obtain information about how the thermal stability of the material changes in line with the different treatments. The progressive extraction of low molecular weight compounds leads to the enhancement of the thermal stability.

Fig. 5 shows the TGA and DTGA curves of the rice and coffee husk samples, untreated and submitted to the different treatments. The peaks associated with the different weight losses caused by thermal degradation can be observed in DTGA curves. All samples exhibit a small weight loss below 100 °C, which can be attributed to the elimination of physically adsorbed water in the samples. The other peaks are associated with the thermal degradation of the lignocellulosic compounds. Table 2 summarises thermal degradation temperatures (onset and peak) for both rice and coffee samples submitted to the different chemical treatments. The first degradation step in untreated samples, around 271-279 °C, can be attributed to the decomposition of hemicelluloses and a part of the lignin fraction (Shebani, Van Reenen, & Maincken, 2008) and was very similar in both husk samples. In all samples, the peak around 300 °C is attributable to cellulose and lignin decomposition. Mensaray & Ghaly (1998) reported that lignocellulosic materials decompose in the temperature range of 150-500 °C. Specifically, hemicellulose decomposes mainly from 150 to 350 °C, cellulose at between 275 and 350 °C and lignin undergoes gradual decomposition in the range of 250-500 °C. As shown in Table 2, the rice and coffee samples exhibited similar thermal behaviour, similarly affected by chemical treatments.

Two decomposition peaks were observed in both untreated material associated to the successive degradation of the different lignocellulosic fractions. However, only one peak appeared after alkali treatment in both cases, which can be attributed to the loosening of the low molecular weight lignin fragments, which degrade at lower temperatures (Johar et al., 2012). After the bleaching treatment, a significant increase in degradation temperature was observed due to the removal of hemicellulose and lignin fractions and the higher content of cellulose.

The residual mass at temperature around 400–700 °C in raw rice husks fibre were remarkably high (more than 30%), which is due to the high content of ash and lignin (Fahma,

Iwamoto, Hori, Iwata, & Takemura, 2011) as well as to the high silica content of the rice husk, all of these contributing to the high char content for raw fibres. Similar thermogram patterns have also been reported on raw rice husk fibres (Johar et al., 2012). For coffee husk no remarkable differences on the mass resides were observed for untreated and treated fibres, all these being lower than 30%, according to the lower ash content of the material. The isolated, more crystalline cellulose fraction from the acid treatment had a lower degradation temperature in both husk products, which has been attributed to the surface sulphation resulting from the sulphuric acid treatment (Johar et al., 2012) by the replacement of hydroxyl groups of the cellulose structure by sulphate groups throughout the hydrolysis process (Jonoobi et al., 2015; Siqueira et al., 2010).

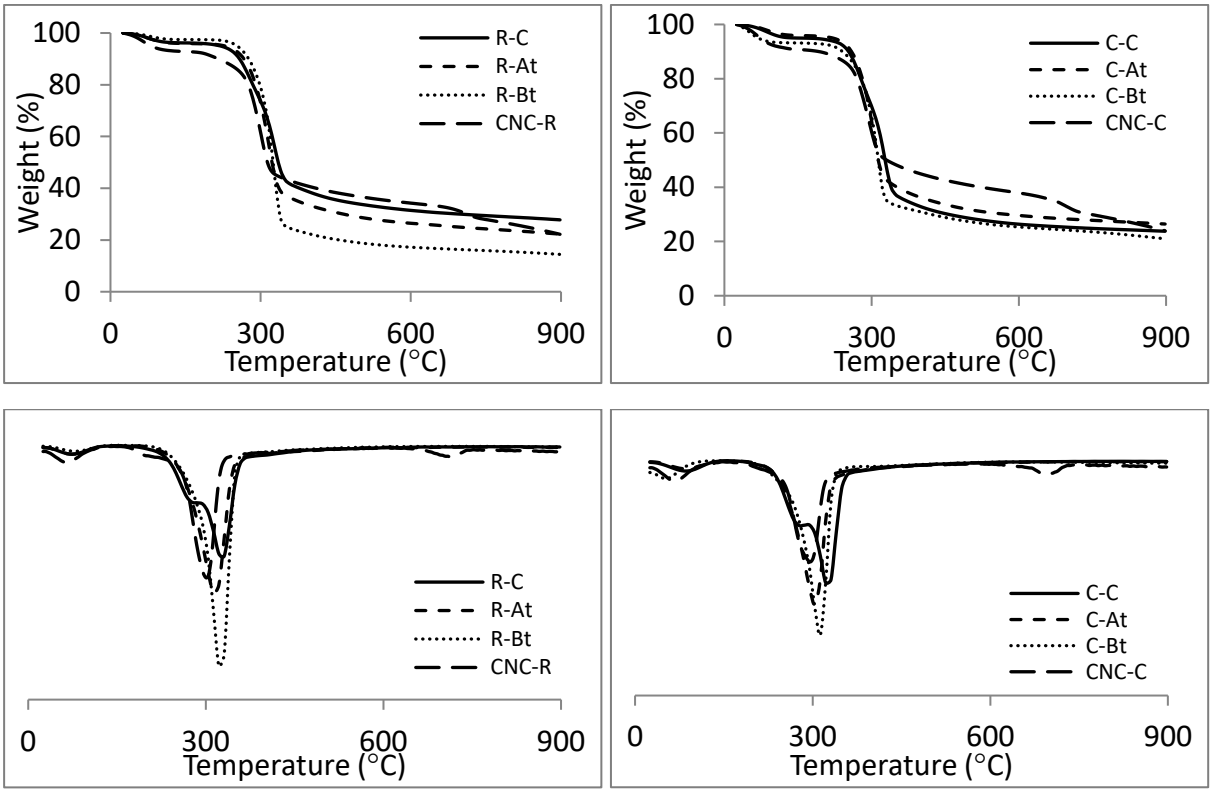

Fig. 5. TGA and DTGA curves of rice and coffee husks untreated (C), alkali treated (At), bleaching treated (Bt) and acid hydrolysed (CNC).

Moreover, this treatment induces an increase in the char fraction compared to the bleached fibres, also due to the introduction of sulphated groups which act as flame retardants (Roman & Winter, 2004). However, at about 700 °C, a final mass loss step was observed in both acid hydrolysates, reflecting the action of a final degradation mechanism, which led to

a similar residual mass to the bleached fibres and which was not observed in previous studies on rice husk cellulosic materials (Johar et al., 2012).

The small differences in the thermal behaviour of rice and coffee husk can be explained by the compositional differences, since thermal degradation of cellulose-based fibres is significantly influenced by their structure and composition.

Table 2. Mean values and standard deviation of onset and peak temperatures for thermal degradation of rice and coffee husks of each stage of treatment (untreated: C, alkali treated: At, bleaching treated: Bt).

	[245-280]°C		[248-330]°C	
Samples	**Onset (°C)**	**Peak (°C)**	**Onset (°C)**	**Peak (°C)**
R-C	247.6 ± 0.5^{b}	271.1 ± 0.7^{a}	301.8 ± 0.2^{f}	329.8 ± 0.7^{f}
R-At	-	-	263 ± 4^{c}	317.3 ± 1.4^{d}
R-Bt	-	-	292.4 ± 0.6^{e}	326.8 ± 0.2^{e}
CNC-R			261.8 ± 0.4^{c}	301.2 ± 0.3^{b}
C-C	245.0 ± 0.4^{a}	279.16 ± 1.12^{b}	302.6 ± 1.2^{f}	327.8 ± 0.7^{ef}
C-At	-	-	254.1 ± 0.4^{b}	304.8 ± 1.2^{c}
C-Bt	-	-	280 ± 3^{d}	315.6 ± 2^{d}
CNC-C			248.9 ± 0.4^{a}	295.6 ± 1.1^{a}

Different superscript letters within the same column indicate significant differences among formulations ($p < 0.05$).

3.4. Reinforcing capacity of the cellulose fibres and CNCs

Starch is one of the most widely studied thermoplastic biopolymers because it is an abundant material, cheap, renewable and biodegradable (Ortega-Toro, Collazo-Bigliardi, Talens, & Chiralt, 2016b). Thermoplastic starch (TPS) film matrices exhibit high barrier properties to oxygen, carbon dioxide and lipids (Ghanbarzadeh, Almasi, & Entezami, 2011), although they have limited mechanical properties and are highly water sensitive. Different studies revealed the improvement in mechanical properties of starch films by the incorporation of cellulosic materials, especially CNCs from different sources (Kargarzadeh et al. 2017; Zainuddin et al, 2013). Likewise, CNCs also increased the film hydrophobicity, reducing the water vapour permeability (Slavutsky & Bertuzzi, 2014) and water uptake capacity (Kargarzadeh et al., 2017). In this sense, cellulosic materials (isolated fibres and CNCs) obtained from rice or coffee husks were incorporated into TPS films in order to analyse their reinforcing ability in this biopolymer matrix.

Fig. 6 shows the tensile behaviour of corn starch films containing, or not, cellulosic reinforcing agents, where the values of the elastic modulus (EM), tensile strength (TS) and percentage deformation (E) at break are also shown. Both cellulosic fibres and CNCs enhanced the elastic modulus of the films, reflecting the reinforcing capacity of both cellulosic fractions. Nanocrystals provoked a higher increase in the film elastic modulus than fibres, while rice husk crystals were more effective at reinforcing the TPS network (186 and 121% higher elastic modulus, respectively for rice and coffee husk CNCs).

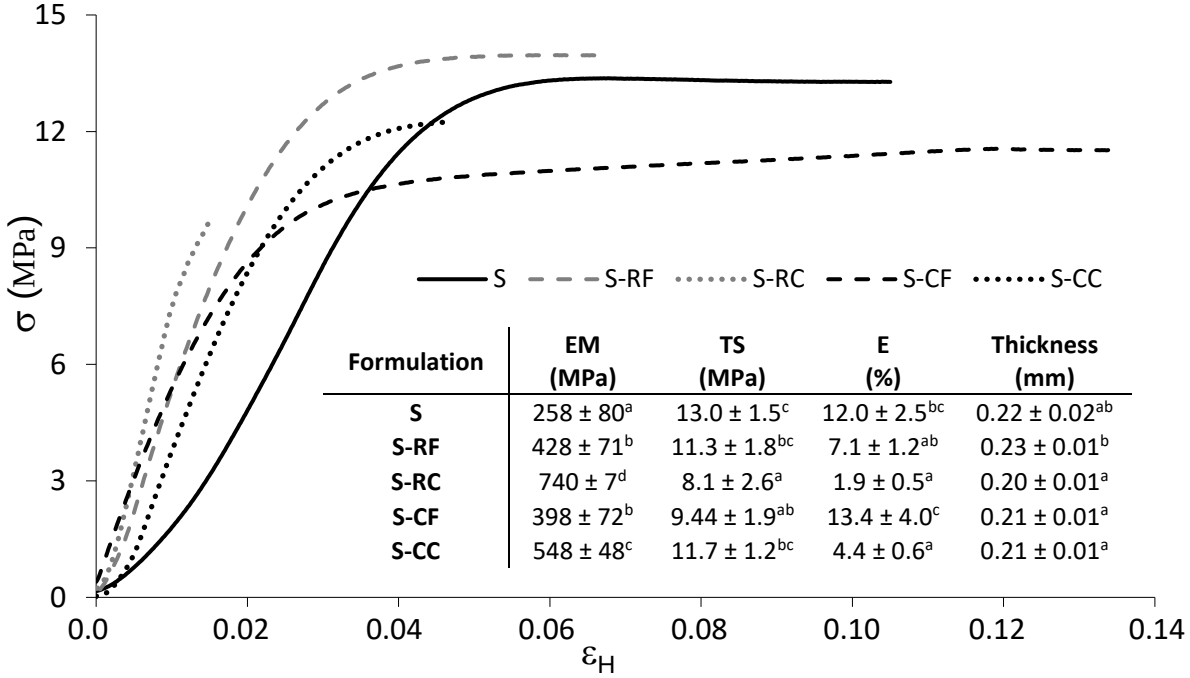

Formulation	EM (MPa)	TS (MPa)	E (%)	Thickness (mm)
S	258 ± 80^{a}	13.0 ± 1.5^{c}	12.0 ± 2.5^{bc}	0.22 ± 0.02^{ab}
S-RF	428 ± 71^{b}	11.3 ± 1.8^{bc}	7.1 ± 1.2^{ab}	0.23 ± 0.01^{b}
S-RC	740 ± 7^{d}	8.1 ± 2.6^{a}	1.9 ± 0.5^{a}	0.20 ± 0.01^{a}
S-CF	398 ± 72^{b}	9.44 ± 1.9^{ab}	13.4 ± 4.0^{c}	0.21 ± 0.01^{a}
S-CC	548 ± 48^{c}	11.7 ± 1.2^{bc}	4.4 ± 0.6^{a}	0.21 ± 0.01^{a}

Fig. 6. Tensile behaviour of corn starch films without (S) and with 1 wt% cellulose fillers (S-CF: with coffee husk fibres, S-RF: with rice husk fibres) and CNCs (S-CC: with CNCs from coffee husk, S-RC: with CNCs from rice husk).

However, no significant differences were observed for the effect of cellulosic fibres, which increased the elastic modulus of TPS films by 60%. Other authors also observed better reinforcing properties for nanocrystals than for fibres, by incorporating multiscale kenaf fibres (Zainuddin et al., 2013) or rice husk (Kargarzadeh et al. 2017) fibres in cassava starch films, due to the higher surface area and aspect ratio of the nanocrystals. As previously reported, the mechanical impact of CNCs on TPS films can be, in part, explained by the formation of a percolating network within the polymer matrix, where the stress is assumed to be transferred through crystal-crystal interactions and crystal-polymer matrix interactions (Fortunati et al., 2013). According to the statistical percolation theory for cylindrically shaped particles (Favier, Cavaille, Canova, & Shrivastavas, 1997), the critical percolation volume fraction (percolation threshold: X_P) can be estimated from the particle aspect ratio (Ar) as

0.7/Ar. For the composite films with CNCs, X_P could be estimated as 0.09 and 0.045, respectively for rice and coffee crystals, considering the respective Ar values (7.9 and 15.6). So, the percolation threshold was reached in the nanocomposites and percolation network formation can explain the enhancement of the mechanical behaviour of the films containing CNCs.

As concerns resistance and elongation at break, all cellulosic materials provoked a decrease in the film extensibility, except coffee husk fibres which did not significantly affect the stretchability and resistance of the TPS films. Reduction of the elongation capacity at break implied slightly lower values of the corresponding resistance. Other authors also observed the reinforcing effect of starch films by CNCs, through the enhancement of the elastic modulus, although the film stretchability became more limited (González K, Retegi, González A, Eceiza, & Gabilondo, 2015). This was attributed to the stronger affinity between glycerol and the nanocrystal phase, as deduced from the dynamic mechanical analyses (DMA), which show an increase in the relaxation temperature of the material with the addition of nanocrystals (González et al. 2015).

4. CONCLUSIONS

The cellulose contents of rice and coffee husks were similar in the range of 34-35%, which make them a good source of cellulosic material for different industrial uses. Purification of cellulose, using the classical alkali and bleaching treatments was effective at removing hemicellulose and lignin, providing white fibres with about 50% crystallinity degree and 60-500 μm length, with good thermal stability (thermo-degradation T peak: 315-327 °C). Coffee fibres were flatter and more helically folded than rice fibres. Acid hydrolysis of both fibres gave rise to CNCs, with small morphological differences. CNCs from coffee husk were slightly thinner (20 against 39 nm, in average diameter), but with similar aspect ratio (higher than 10). The CNCs exhibited slightly lower thermal stability than the cellulose fibres (thermo-degradation T peak: 249-362 °C). The properties of cellulosic fractions from rice and coffee husk make them very adequate as reinforcing materials in biopolymer composites, especially nano-sized reinforcement (CNCs from rice and coffee husks) which increased the elastic modulus of TPS films by 186% and 121%, respectively. So, coffee husk represents an interesting source of cellulosic reinforcing material, whose use in different applications, such as packaging materials, could boost the value of this waste.

Acknowledgements

The authors thank the Ministerio de Economía y Competitividad (Spain) for the financial support provided through Project AGL2016-76699-R. Authors also thank the Electron Microscopy Service of the UPV for their technical assistance.

REFERENCES

Alves, R. C., Rodrigues, F., Nunes, M. A., Vinha, A. F., & Oliveira M. B. P. P. (2017). State of the art in coffee processing by-products. In: C. M. Galanakis (Ed.), *Handbook of Coffee Processing By-Products* (pp. 1-26). Cambridge: Academic Press.

Anglès, M. N., & Dufresne, A. (2000). Plasticized starch/tunicin whiskers nanocomposites. 1. Structural analysis. *Macromolecules*, 33, 8344-8353.

ASTM. (2001). Standard test method for tensile properties of thin plastic sheeting. Standard Designations: D882. *In Annual book of ASTM standards*. Philadelphia, PA: American Society for Testing and Materials.

Azeredo, H. M. C., Rosa, M. F., & Mattoso, L. E. C. (2017). Nanocellulose in bio-based food packaging applications. *Industrial Crops and Products*, 97, 664-671.

Azizi Samir, M. A. S., Alloin, F., & Dufresne, A. (2005). Review of recent research into cellulosic whiskers, their properties and their applications in nanocomposite field. *Biomacromolecules*, 6, 612-626.

Balaji, A.B., Pakalapati, H., Khalid, M., Walvekar, R., & Siddiqui, H. (2017). Natural and synthetic biocompatible and biodegradable polymers. In: N. Gopal Shimpi (Ed.), *Biodegradable and Biocompatible Polymer Composites* (pp. 3-32). United Kingdom: Woodhead Publishing.

Bassas-Galia, M., Follonier, S., Pusnik, M., & Zinn, M. (2017). Natural polymers: a source of inspiration. In: G. Perale, & J. Hilborn (Eds.), *Bioresorbable Polymers for Biomedical Applications* (pp. 31-64). United Kingdom: Woodhead Publishing.

Batra, S.K. (1981). Other long vegetables fibres. In: M. Lewin, E. M. Pearce (Eds.), *Handbook of Fiber Science and Technology*. New York: Marcel Dekker Inc.

BenMabrouk, A., Wim, T., Dufresne, A., & Boufi, S. (2009). Preparation of Poly(styrene-*co*-hexylacrylate)/cellulose whiskers nanocomposites via miniemulsion polymerization. *Journal of Applied Polymer Science*, 114, 2946-2955.

Bettaieb, F., Khiari, R., Hassa, M.L., Belgacem, M.N., Bras, J., Dufresne, A., & Mhenni, M.F. (2015). Preparation and characterization of new cellulose nanocrystals from marine biomass *Posidonia oceanica*. *Industrial Crops Products*, 72, 175-182.

Boonterm, M., Sunyadeth, S., Dedpakdee, S., Athichalinthorn, P., Patcharaphun, S., Mungkung, R., & Techapiesancharoenkij, R. (2015). Characterization and comparison of cellulose fiber extraction from rice straw by chemical treatment and thermal stem explosion. *Journal of Cleaner Production*, 134, 592-599.

Borkotoky, S. S., Dhar, P., & Katiyar, V. (2018). Biodegradable poly (lactic acid)/Cellulose nanocrystals (CNCs)composite microcellular foam: Effect of nanofillers on foam cellularmorphology, thermal and wettability behaviour. *International Journal of Biological Macromolecules*, 106, 433-446.

Bras, J., Hassan, M.L., Bruzesse, C., Hassan, E.A., El-Wakil, N.A., & Dufresne, A. (2010). Mechanical barrier and biodegradability properties of bagasse cellulose whiskers reinforced natural rubber nanocomposites. *Industrial Crops Products*, 32, 627-633.

Brigham, C. (2018). Biopolymers: biodegradable alternatives to traditional plastics. In: B. Török, & T. Dransfield (Eds.), *Green Chemistry* (pp. 753-770). Amsterdam: Elsevier Inc.

Brinchi, L., Cotana, F., Fortunati, E., & Kenny, J.M. (2013). Production of nanocrystalline cellulose from lignocellulosic biomass: Technology and applications. *Carbohydrate Polymers*, 94, 154-169.

Cano, A., Fortunati, E., Cháfer, M., González-Martínez, C., Chiralt, A., & Kenny, J. M. (2015). Effect of cellulose nanocrystals on the properties of pea starch-poly(vinyl alcohol) blend films. *Journal of Materials Science*, 50, 6979-6992.

Chauve, G., Fraschini, C., & Jean, B. (2013). Separation of cellulose nanocrystals. In K. Oksman, A. P. Mathew, A. Bismark, O. Rojas, & M. Sain (Eds), *Handbook of Green Materials: Processing Technologies, Properties and Applications* (pp. 73-87). World Scientific Publishing Co.

Chen, W. S., Yu, H. P., Liu, Y. X., Chen, P., Zhang, M. X., & Hai, Y. F. (2011). Individualization of cellulose nanofibers from wood using high-intensity ultrasonication combined with chemical pretreatments. *Carbohydrate Polymers*, 83(4), 1804-1811.

Cherian, B. M., Leâo, A. L., de Souza, S. F., Costa, L. M. M., de Olyveira, G. M., Kottaisamy, M., Negarajan, E. R., & Thomas, S. (2011). Cellulose nanocomposites with nanofibres isolated from pineapple leaf fibers for medical applications. *Carbohydrate Polymers*, 86, 1790-1798.

El Achaby, M., Kassab, Z., Aboulkas, A., Gaillard, C., & Barakat, A. (2018). Reuse of red algae waste for the production of cellulose nanocrystalsand its application in polymer nanocomposites. *International Journal of Biological Macromolecules*, 106, 681-691.

Espino, E., Cakir, M., Domenek, S., Román-Gutiérrez, A. D., Belgacem, N., & Bras, J. (2014). Isolation and characterization of cellulose nanocrystals from industrial by-products of Agave tequilana and barley. *Industrial Crops Products,* 62, 552-559.

Fabra, M. J., López-Rubio, A., & Lagarón, J. M. (2014). Biopolymers for food packaging applications. In M.R. Aguilar De Armas, & J.S. Román (Eds.), *Smart Polymers and their Applications* (pp. 476-509). United Kingdom: Woodhead Publishing.

Fahma, F., Iwamoto, S., Hori, N., Iwata, T., & Takemura, A. (2011). Effect of pre –acid-hydrolysis treatment on morphology and properties of cellulose nanowhiskers from coconut husk. *Cellulose*, 18, 443–450.

FAO. (2016). Food and Agriculture Organization of the United Nations (FAO). Rice Market Monitor, vol 11, No. 2. http://www.fao.org/ economic/est/publications/ rice-publications/rice-market-monitor-rmm/en/. (Accessed 27.04.2017).

Favier, V., Cavaille, J. Y., Canova, G. R., & Shrivastavas, S. C. (1997). Mechanical percolation in cellulose whisker nanocomposites. *Polymer Engineering and Science*, 37(10), 1732-1739.

Fengel, D., & Wegener, G. (1984). *Wood Chemistry, Ultrastructure, Reactions*. (1th ed.). New York: Walter de Gruyter, (Chapter 3).

Flauzino Neto, W. P., Silvério, H. A., Dantas, N. O., & Pasquini, D. (2013). Extraction and characterization of cellulose nanocrystals from agro-industrial residue soy hulls. *Industrial Crops Products*, 42, 480-488.

Fortunati, E., Puglia, D., Luzi, F., Santulli, C., Kenny, J. M., & Torre, L. (2013). Binary PVA bio-nanocomposites containing cellulose nanocrystals extracted from different natural sources: part I. *Carbohydrate Polymers*, 97, 825-836.

Fortunati, E., Luzi, F., Jiménez, A., Gopakumar, D. A., Puglia, D., Thomas, S., Kenny, J. M., Chiralt, A., & Torre, L. (2016). Revalorization of sunflowers stalks as novel sources of

cellulose nanofibrils and nanocrystals and their effect on wheat gluten. *Carbohydrate Polymers*, 149, 357-368.

Ghanbarzadeh, B., Almasi, H., & Entezami, A. A. (2011). Improving the barrier and mechanical properties of corn starch-based edible films: Effect of citric acid and carboxymethyl cellulose. *Industrial Crops Products*, 33(1), 229-235.

González, K., Retegi, A., González, A., Eceiza, A. & Gabilondo, N. (2015). Starch and cellulose nanocrystals together into thermoplastic starch bionanocomposites. *Carbohydrate Polymers*, 117, 83-90.

Habibi, Y., & Dufresne, A. (2008). Highly filled bionanocomposites from functionalized polysaccharide nanocrystals. *Biomacromolecules*, 9, 1974-1980.

Hake, A., Mondal, D., Khan, I., Usmani, M. A., Bhat, A. H., & Gazal, U. (2017). Fabrication of composites reinforced with lignocellulosic materials from agricultural biomass. In: M. Jawaid, P. M. Tahir, & N. Saba (Eds.), *Lignocellulosic fibre and biomass-based composite materials* (pp. 179-191). United Kingdom: Woodhead Publishing.

Hassan, M. L., Mathew, A. P., Hassan, E. A., El-Wakil, N. A., & Oksman, K. (2012). Nanofibers from bagasse and rice straw: process optimization and properties. *Wood Science and Technology,* 46, 193-205.

Henrique, M. A., Silvério, H. A., Neto, W. P. F., & Pasquini, D. (2013). Valorization of an agro-industrial waste, mango seed, by the extraction and characterization of its cellulose nanocrystals. *Journal of Environmental Management*, 121, 202-209.

Hossain, A. B. M. S., Ibrahim, N. A., & AlEissa, M. S. (2016). Nano-cellulose derived bioplastic biomaterial data for vehicle bio-bumper from banana peel waste biomass. *Data in Brief, 8*, 286-294.

Jiang, L., & Zhang, J. (2017). Biodegradable and biobased polymers. In: M. Kutz (Ed.), *Applied Plastics Engineering Handbook* (pp. 127-143). New York: William Andrew.

Johar, N., Ahmad, I., & Dufresne, A. (2012). Extraction, preparation and characterization of cellulose fibres and nanocrystals from rice husk. *Industrial Crops Products,* 37, 93-99.

Jonoobi, M., Oladi, R., Davaoudpour, Y., Oksman, K., Dufresne, A., Hamzeh, Y., & Davoodi, R. (2015). Different preparation methods and properties of nanostructured cellulose from various natural resources and residues: a review. *Cellulose*, 22, 935-969.

Kallel, F., Bettaieb, F., Khiari, R., García, A., Bras, J., & Ellouz Chaabouni, S. (2016). Isolation and structural characterization of cellulose nanocrystals extracted from garlic straw. *Industrial Crops and Products,* 87, 287-296.

Kargarzadeh, H., Ahmad, I., Abdullah, I., Dufresne, A., Zainudin, S. Y., & Sheltami, R. M. (2012). Effects of hydrolysis conditions on the morphology, crystallinity, and thermal stability of cellulose nanocrystals extracted from kenaf bast fibers. *Cellulose*, 19, 855-866.

Kargarzadeh, H., Johar, N., & Ahmad, I. (2017). Starch biocomposite film reinforced by multiscale rice husk fiber. *Composite Science and Technology*, 15, 147-155.

Kaushik, M., Fraschini, C., Chauve, G., Putaux, J. L., & Moores, A. (2015). Transmission electron microscopy for the characterization of cellulose nanocrystals. In K. Maaz (Ed.), *The Transmission Electron Microscope - Theory and Applications* (pp. 129-163). InTech.

Khalil, H. P. S. A., Davoudpour, Y., Saurabh, C. K., Hossain, Md. S., Adnan, A. S., Dungani, R., Paridah, M. T., Sarker, Md. Z. I., Fazita, M. R. N., Syakir, M. I., & Haafiz, M. K. M. (2016). A review on nanocellulosic fibres as new material for sustainable packaging: Process and applications. *Renewable and Sustainable Energy Reviews,* 64, 823-836.

Khawas, P., & Deka, S. C. (2016). Isolation and characterization of cellulose nanofibers from culinary banana peel using high-intensity ultrasonication combined with chemical treatment. *Carbohydrate Polymers*, 137, 608-616.

Le Normand, M., Moriana, R., & Ek, M. (2014). Isolation and characterization of cellulose nanocrystals from spruce bark in a biorefinery perspective. *Carbohydrate Polymers*, 111, 979-987.

Li, R., Fei, J., Cai, Y., Li, Y., Feng, J., & Yao, J. (2009). Cellulose whiskers extracted from mulberry: a novel biomass production. *Carbohydrate Polymers*, 76, 94–99.

Lima, M. M. S., & Borsali, R. (2004). Rod-like cellulose microcrystal: structure, properties, and applications. *Macromolecular Rapid Communication*, 25, 771–787.

Ludueña, L., Vázquez, A., & Alvarez, V. (2012). Effect of lignocellulosic filler type and content on the behavior of polycaprolactone based eco-composites for packaging applications. *Carbohydrate Polymers*, 87, 411-421.

Luzi, F., Fortunati, E., Jiménez, A., Puglia, D., Pezzolla, D., Gigliotti, G., Kenny, J. M., Chiralt, A., & Torre, L. (2016). Production and characterization of PLA_PBS biodegradable blends

reinforced with nanocrystals extracted from hemp fibres. *Industrial Crops and Products*, 93, 276-289.

Mansaray, K. G., & Ghaly, A. E. (1998). Thermal degradation of rice husks in nitrogen atmosphere. *Bioresource Technology*, 65, 13-20.

Mondal, S. (2017). Preparation, properties and applications of nanocellulosic materials. *Carbohydrate Polymers*, 163, 301-316.

Moreno-Contreras, G. G., Serrano-Rico, J. C., & Palacios-Restrepo, J. A. (2009). Industrial waste combustion performance in a bubbling fluidized bed reactor. *Ingeniería Universidad de Bogotá*, 13, 251-266.

Moriana, R., Vilaplana, F., & Ek, M. (2016). Cellulose nanocrystals from forest residues as reinforcing agents for composites: a study from macro- to nano-dimensions. *Carbohydrate Polymers*, 139, 139-149.

National Renewable Energy Laboratory, NREL/TP-510-42618., 2011. Determination of structural carbohydrates and lignin in biomass. Colorado.

National Renewable Energy Laboratory, NREL/TP-510-42619., 2008. Determination of extractives in biomass. Colorado.

Ng, H. M., Sin, L. T., Tee T. T., Bee S. T., Hui, D., Low, C. Y., & Rahmat, A. R. (2015). Extraction of cellulose nanocrystals from plant sources for application as reinforcing agent in polymers. *Composites Part B*, 75, 176-200.

Ni, Y., Kubes, G. J., & Van Helnlngen, A. R. P. (1993). Mechanism of chlorate formation during bleaching of kraft pulp with chlorine dioxide. *Pulp Paper Science,* 19, 1-5.

Oliveira, L. S., Franca, A. S. (2016). An overview of the potential uses for coffee husks. *Coffee in Health Disease and Prevention*, 31, 283-291.

Ortega-Toro, R., Santagata, G., Gomez D'Ayala, G., Cerruti, P., Talens Oliag, P., Chiralt Boix, M.A., & Malinconico, M. (2016a). Enhancement of interfacial adhesion between starch and grafted poly(-caprolactone). *Carbohydrate Polymers*, 147, 16-27.

Ortega-Toro, R., Collazo-Bigliardi, S., Talens, P., & Chiralt, A. (2016b). Thermoplastic starch: improving their barrier properties. *Agronomía Colombiana*, 34, 73-75.

Patel, J. P., & Parsania, P. H. (2018). Characterization, testing, and reinforcing materials of biodegradable composites. In: N. G. Shimpi (Ed.), *Biodegradable and Biocompatible Polymer Composites* (pp. 55-79). United Kingdom: Woodhead Publishing.

Qiao, C., Chen, G., Zhang, J., & Yao, J. (2016). Structure and rheological properties of cellulose nanocrystals suspension. *Food Hydrocolloids*, 55, 19-25.

Reddy, J. P., & Rhim, J. W. (2014). Isolation and characterization of cellulose nanocrystals from garlic skin. *Materials Letters*, 129, 20-23

Reis, K. C., Pereira, L., Nogueira Alves Melo, I. C., Marconcini, J. M., Trugilho, P. F., & Denzin Tonoli, G. H. (2015). Particles of coffee wastes as reinforcement in polyhydroxybutyrate (PHB) based composites. *Materials Research*, 18 (3), 546-552.

Roman, M., & Winter, W. T. (2004). Effect of sulfate groups from sulfuric acid hydrolysis on the thermal degradation behavior of bacterial cellulose. *Biomacromolecules*, 5, 1671–1677.

Rosa, M. F., Medeiros, E. S., Malmonge, J. A., Gregorski, K. S., Wood, D. F., & Mattoso, L. H. C. (2010). Cellulose nanowhiskers from coconut husk fibers: effect of preparation conditions on their thermal and morphological behavior. *Carbohydrate Polymers*, 81, 83-92.

Sanjay, M. R., Madhu, P., Jawaid, M., Senthamaraikannan, P., Senthil, S., & Pradeep, S. (2018). Characterization and properties of natural fiber polymer composites: A comprehensive review. *Journal of Cleaner Production*, 172, 566-581.

Santos, R. P. O., Rodrigues, B. V. M., Ramires, E. C., Ruvolo-Filho, A. C., & Frollini, E. (2015). Bio-based materials from the electrospinning of lignocellulosic sisal fibers and recycled PET. *Industrial Crops and Products*, 72, 69-76.

Savadekar, N. M., & Mhaske, S. T. (2012). Synthesis of nano cellulose fibers and effect on thermoplastics starch based films. *Carbohydrate Polymers*, 89, 146-151.

Shebani, A. N., van Reenen, A. J., & Meincken, M. (2008). The effect of wood extractives on the thermal stability of different wood species. *Thermochimica Acta*, 471, 43-50.

Sheltami, R. M., Abdullah, I., Ahmad, I., Dufresne, A., & Kargarzadeh, H. (2012). Extraction of cellulose nanocrystals from Mengkuang leaves (Pandanus tectorius). *Carbohydrate Polymers*, 88, 772-779.

Shih, Y. F., Chang, W. C., Liu, W.C., Lee, C. C., Kuan, C. S., & Yu, Y. H. (2014). Pineapple leaf/recycled disposable chopstick hybrid fiber-reinforced biodegradable composites. *Journal of Taiwan Institute of Chemical Engineering*, 45(4), 2039-2046.

Slavustky, A. M., & Bertuzzi, M. A. (2014). Water barrier properties of starch films reinforced with cellulose nanocrystals obtained from sugarcane bagasse. *Carbohydrate Polymers*, 110, 53-61.

Silvério, H. A., Neto, W. P. F., Dantas, N. O., & Pasquini, D. (2013). Extraction and characterization of cellulose nanocrystals from corncob for application as reinforcing agent in nanocomposites. *Industrial Crops and Products*, 44, 427-436.

Singh, R., Shukla, A., Tiwari, S., & Srivastava, M. (2014). A review on delignification of lignocellulosic biomass for enhancement of ethanol production potential. *Renewable and Sustainable Energy Reviews*, 32, 713-728.

Siqueira, G., Bras, J., & Dufresne, A. (2010). Cellulosic bionanocomposites: a review of preparation, properties and applications. *Polymer*, 2, 728-765.

Sundari, M. T., & Ramesh, A. (2012). Isolation and characterization of cellulose nanofibers from the aquatic weed water hyacinth—*Eichhornia crassipes. Carbohydrate Polymers*, 87, 1701-1705.

Talegaonkar, S., Sharma, H., Pandey, S., Mishra, P. K., & Wimmer, R. (2017). Bionanocomposites: smart biodegradable packaging material for food preservation. In: A. M. Grumezescu (Ed.), *Food Packaging* (pp. 79-110). Cambridge: Academic Press.

Zainuddin, S. Y. Z., Ahmad, I., Kargarzadeh, H., Abdullah, I., & Dufresne, A. (2013). Potential of using multiscale kenaf fibers as reinforcing filler in cassava starch- kenaf biocomposites. *Carbohydrate Polymer*, 92, 2299-2305.

Chapter II

Reinforcement of thermoplastics starch films with cellulose fibres obtained from rice and coffee husks

[1]**Sofía Collazo-Bigliardi;** [2]Rodrigo Ortega-Toro; [1]Amparo Chiralt

Journal of Renewable Materials, 6, 599-610 (2018)

[1]Institute of Food Engineering for Development, Universitat Politècnica de València. Valencia, Spain

[2]Food Engineering Program, Faculty of Engineering, Universidad de Cartagena. Cartagena de Indias, Colombia

socol@doctor.upv.es

ABSTRACT

Cellulosic fibres from coffee (CF) and rice (RF) husks have been obtained applying chemical treatments and characterized as to their microstructure and thermal behaviour. These materials have been incorporated into glycerol plasticised thermoplastic starch (TPS) films obtained by melt blending and compression moulding at 1 wt%, 5 wt% and 10 wt%. Microstructure, thermal behaviour and optical, tensile and barrier properties of the composites were analysed. Both kinds of micro-fibres improve the film stiffness while reduced the film stretchability. However, CF better maintained the film ductility at 1 and 5 wt%. A network of fine oriented fibres was observed on the surface of the films, while internal fibres exhibited a good adherence to the polymer network. The water vapour permeability of TPS films was not reduced in composites, although oxygen permeability was lowered by about 17%. Film transparency decreased by fibre addition in the UV-VIS range. Thermal stability of composites was slightly higher than net TPS films.

Keywords: Cellulose fibres; coffee husk; reinforcing properties; rice husk; starch composites.

1. INTRODUCTION

The increasing concern about the environmental preservation points to the replacement of most common non-biodegradable petroleum-derived plastics, causing high environmental problems, by more environmental-friendly materials which are biodegradable materials and, boarding a more sustainable approach, which are bio-based [1]. Food packaging involves a high consumption of plastics, which in many cases are non-recyclable due to the load of organic compounds. One of the most important groups of biodegradable and bio-based plastic materials is polysaccharides obtained from renewable resources. These biopolymers are directly extracted from biomass and, depending on their origin, different types of starch, cellulose, chitosan, gums or alginates can be found [2] [3].

Starch is the most widely studied thermoplastic sustainable biopolymer for food packaging applications because it is abundant, low cost and able for food contact purposes. It is composed of different ratios of amylose and amylopectin, depending on the plant source (cassava, corn, potato, rice, etc.). Native starch can be transformed in thermoplastic starch through the gelatinization process induced by temperature and plasticisers (mainly water or glycerol). Thermoplastic starch exhibit very good filmogenic capacity, forming homogenous and transparent polymeric matrices with barrier properties to high oxygen, carbon dioxide or lipids [4] although they are water sensitive, present low barrier properties to water vapour and exhibits relatively poor and unstable mechanical resistance and extensibility; all of this due to its hydrophilic nature and to its natural tendency to retrogradation [5]. In order to enhance their limited properties as packaging materials, different strategies has been developed, such as the addition of plasticisers which reduce the intermolecular forces in the native starch increasing the flexibility or stretchability [6] [7], incorporation of cross-linking agents, such as citric acid [8], blending with other polymers [9], or incorporation of inorganic [10] [11] [12] and organic fillers [13] [14] [15] [16]. Many studies analysed the behaviour of different organics fillers as reinforcing agents of TPS matrices. Micro- and nano-fillers derived from lignocellulosic wastes have been used in different studies to develop enhanced starch biocomposites, including eucalyptus wood pulp [17], sugarcane bagasse [18], wood [19], cotton, hemp or kenaf fibres [20]. In this sense, the use of agro-waste to obtain micro or nano-fillers able to reinforce packaging films represents a good alternative to, additionally, valorise the waste product.

Lignocellulosic residues are attractive materials because of their biodegradability, excellent mechanical properties, such as great stiffness and strength, and low density [21]. The manufacture of soluble coffee is the main industry of different countries like Brazil, Vietnam, Indonesia, Colombia, Ethiopia, India or Mexico [22] which generates a significant amount of waste that is usually burned causing great environmental contamination. Coffee husk (endocarp of coffee beans) is the residue obtained after de-hulling operation in coffee dry

processing, being rich in cellulosic (~57%) and lignin (~22%) components [23]. Studies of the extraction and characterization of cellulosic materials from coffee husk have not been previously reported at the best of our knowledge. Sung et al. [24] studied the incorporation of other similar coffee agro-waste such as cellulose nanocrystals from coffee silverskin (tegument of green coffee beans liberated as the primary by-product during the coffee roasting process) into polyester matrix. On the other hand, rice husk is one of the main renewable by-products of rice milling operations with similar composition in lignocellulose content of coffee husk (~55% cellulose and ~35% lignin; [25]). The high cellulose content makes these residues interesting materials to obtain cellulosic materials for different uses. Johar et al. [26] applied the traditional alkali and bleaching treatments to obtain and characterise cellulose fibres from rice husk. But no previous studies were carried out for coffee husk. Cellulose fractions obtained from these kinds of biomasses can be transformed into micro-scale materials to be incorporated into starch matrices in order to improve their functional properties as packaging materials.

In this study, cellulose fibres from coffee and rice husks have been obtained by alkali and bleaching treatment and analysed as to their reinforcement properties into starch matrices. The changes induced in the film microstructure and tensile, barrier and optical properties of the films containing different ratios of micro-fibres have been analysed, as well as their effect in the thermal stability of the composites.

2. MATERIALS AND METHODS

2.1. Materials

Rice husk was provided from Dacsa (Almàssera, Valencia, Spain) and coffee husk was obtained by Centro Surcolombiano de Investigaciones en Café from Universidad Surcolombiana (Neiva, Colombia). Corn starch was purchased from Roquette (Roquette Laisa, Benifaió, Spain). Glycerol and sodium hydroxide, for alkali treatment, were obtained from Panreac Química, S.A. (Castellar del Vallès, Barcelona, Spain). Sodium chlorite and acetate buffer for bleaching treatment were provided by Sigma Aldrich Química S.L (Madrid, Spain). For conditioning samples, Phosphorus pentoxide (P_2O_5) and magnesium nitrate-6-hydrate ($Mg(NO_3)_2$) were obtained from Panreac Química, S.A. (Castellar del Vallès, Barcelona, Spain).

2.2. Extraction of cellulose fibres from coffee and rice husks

The extraction process of cellulose fibres (CeF) from coffee and rice husk was carried out according to the method reported by Johar et al. [26] with some modifications. Rice or coffee husk, previously ground (mean particle size about 2-3mm), were alkali treated to purify the fibres by removing hemicelluloses, pectin, waxes, part of lignin and other impurities. For this purpose, the samples were treated with 4 wt% of NaOH at 80 °C for 3h, at a 1:15 solid-liquid ratio, with mechanical stirring. Then, the solid was filtered and washed with distilled water several times, with the subsequent filtration, until the alkali solution (brown) was removed (colourless filtrate).

Bleaching process was performed to remove the lignin content. Equal parts of acetate buffer solution, sodium chlorite (1.7 wt%) and distilled water were mixed with the alkali treated solid (at 1:15 solid: liquid ratio) and submitted to reflux temperature (about 100°C) for 4h. This process was repeated as many times as necessary until the samples were completely white, as an indicator of the lignin removing. Then, the samples were filtered and washed with distilled water several times, with the subsequent filtration, until the solution was removed and dried in a desiccator containing P_2O_5 and grounded in a Moulinex grinder DJ200031 350W. The fibres were characterised as to their thermal properties (Thermogravimetric Analyzer TGA 1 Stare System analyser, Mettler-Toledo, Inc., Switzerland) and microstructure (Scanning Electron Microscope, JEOL JSM-5410, Japan).

2.3. Preparation of TPS composite films

Cellulose fibres from coffee or rice husk, glycerol (as plasticiser) and native corn starch were dispersed in water and hand-blended till a homogenous blend was obtained. Starch:glycerol:water ratio (w/w) was 1:0.3:0.5, according to previous studies [6] [8] and fibres were incorporated at 1, 5, and 10 wt% respect the starch. Seven formulations were prepared identified as S (starch-glycerol), S-CF or S-RF (starch with fibres from coffee or rice husk) and 1, 5 or 10, referred to percentage of fibre contents. In Table 1 the mass fraction of each component in the dry blends and their identification codes are reported.

Each formulation was melt blended in a two-roll mill (Model LRM-M-100, Labtech Engineering, Thailand) at 160 °C and 8 rpm for 30 min until a homogeneous paste sheet of TPS was obtained. The TPS sheets were cut as pellets and conditioned at 25 °C and 53% relative humidity (RH) for one week before the film performance. The films were obtained by compression moulding using a hot plate press (Model LP20, Labtech Engineering, Thailand). Four grams of the conditioned pellets were put onto Teflon sheets and preheated on the heating unit for 5 min. Films were obtained by compressing at 160 °C for 2 min at 30 bars, followed by 6 min at 130 bars; thereafter a cooling cycle was applied for 3 min [6]. The obtained films were conditioned at 25 °C and 53% RH for 1 week before their characterization.

Table 1. Mass fraction of the different components (Starch: S, Glycerol: Gly and Cellulose: C) in the TPS film (S) and composites with 1%, 5% or 10 % of coffee fibres (CF) or rice fibres (RF).

Formulations	X_S	X_{Gly}	X_C
S	0.77	0.23	---
S-CF1	0.76	0.23	0.01
S-CF5	0.73	0.22	0.05
S-CF10	0.69	0.21	0.10
S-RF1	0.76	0.23	0.01
S-RF5	0.73	0.22	0.05
S-RF10	0.69	0.21	0.10

2.4. Characterization of fibres and composites

2.4.1. Optical properties

The internal transmittance of the films was determined through their transmittance in the UV-VIS range using a UV-VIS spectrophotometer (Perkin Elmer Instruments, Lambda 35, Waltham, USA), within 300-950 nm wavelength range. The film gloss was determined at an incidence angle of 60°, according to the ASTM standard D523 method [27] using a flat surface gloss meter (Multi.Gloss 268, Minolta, Germany). All results are expressed as gloss units (GU), relative to a highly polished surface of black glass standard with a value near to 100 GU.

2.4.2. Microstructure analysis

Light microscopy (Optika Microscopes B-350 connected to an Optikam B2 camera, Italy) was used to measure the length range of the cellulose fibres. A drop (20 µL) of the 1.5% solid dispersions was spread over the slide and observed at 10X magnification level. Fibre length range was estimated by measuring more than 100 fibres elements in at least 10 different microscopic observations for each sample (Optika Vison Lite 2.1). A Scanning Electron Microscope (JEOL JSM-5410, Japan) was used to analyse the microstructure of cellulose fibres, previously conditioned in P_2O_5 for 2 weeks at 25 °C. Samples were gold coated and observed, using an accelerating voltage of 15 kV. Field Emission Scanning Electron Microscopy (FESEM Ultra 55, Zeiss, Oxford Instruments, UK) was used to analyse the surface and cross-sections microstructure of the films, previously conditioned at the same condition as fibres. Film samples were adequately mounted on support stubs and platinum coated. Observations were carried out at 1.5 kV.

2.4.3. Film thickness and equilibrium moisture content

The film thickness of conditioned films was measured using a Palmer digital micrometer at six random positions around the film. The water content of conditioned film at 53% RH and 25 °C was determined, in triplicate, gravimetrically, by drying for 24h at 60 °C using a convection oven (J.P. Selecta, S.A. Barcelona, Spain) and subsequent conditioning in a desiccator at 25 °C with P_2O_5 (a_w=0) for 2 weeks.

2.4.4. Water vapour permeability and oxygen permeability

The ASTM E96-9532 [28] gravimetric method was used to determine the Water Vapour Permeability (WVP) of the films, considering the modification proposed by McHugh et al. [29]. Distilled water was placed in Payne permeability cups (3.5 cm diameter, Elcometer SPRL, Hermelle/s Argenteau, Belgium) to expose the film to 100% RH on one side. Each cup was placed in a cabinet equilibrated at 25 °C and 53% RH, with a fan placed on the top of the cup in order to reduce the resistance to water vapour transport, thus avoiding the stagnant layer effect in this exposed side of the film. The relative humidity of the cabinet (53%) was held constant using $Mg(NO_3)_2$ oversaturated solutions. The cups were weighed periodically (0.0001 g) and the water vapour transmission rate (WVTR) was determined from the slope obtained from the regression analysis of weight loss data versus time. From this data, WVP was obtained according to Ortega-Toro et al. [6] [8].

The oxygen permeability (OP) was determined using an OX-TRAN Model 2/21 ML (Mocon Lippke, Neuwied, Germany), in samples conditioned at 53% RH and 25°C. The oxygen transmission values were determined every 20 min until equilibrium was reached. The film area used in the tests was 50 cm^2. From these values OP was obtained, considering the measured film thickness. All barrier properties were determined in triplicate for each film sample.

2.4.5. Tensile properties

A universal test machine (TA.XTplus model, Stable Micro Systems, Haslemere, England) was used to determine the tensile properties of films. The tensile strength (TS), the elastic modulus (EM), and the elongation at break (ε) of the films were determined from the stress-strain curves, estimated from force-distance data obtained for different films (2.5 cm width; 10 cm length), according to the ASTM standard method D882 [30]. Equilibrated samples were mounted in the film-extension grips (with 5 cm of separation) of the testing machine and stretched at 50 mm/min until breaking. Tests were carried out at 25 °C and 53% RH. Ten

replicates were performed for each film formulation. The measures were carried out at initial time (1 week conditioned films) and final time (28 weeks conditioned films).

2.4.6. Thermal analysis

The thermal stability of the different samples (fibres and films) was analysed using a Thermogravimetric Analyzer TGA 1 Star^e System analyser (Mettler-Toledo, Inc., Switzerland) under nitrogen atmosphere (gas flow: 10 mL min^{-1}). Samples (about 4-5 mg) were heated from 25 to 600 °C at 20 °C/min. At least two replicates for each sample were obtained. Initial degradation temperature (T_{Onset}) and peak temperature (T_{Peak}) corresponding to the maximum degradation rate, were obtained from the first derivative of the resulting weight loss curves using the STAR^e Evaluation Software (Mettler-Toledo, Inc., Switzerland).

2.5. Statistical analysis

Statgraphics Plus for Windows 5.1 (Manugistics Corp., Rockville, MD) was used for carrying out statistical analyses of data through analysis of variance (ANOVA). Fisher's least significant difference (LSD) was used at the 95% confidence level.

3. RESULTS AND DISCUSSION

3.1. Microstructure and thermal behaviour of cellulose fibres

Figure 1 shows the appearance of both cellulose fibres after the chemical treatments. The sample colour drastically changed from brownish in raw material to the characteristic whiteness of cellulose (Figure 1a) thus indicating the high removing degree of lignin compounds [26]. The particle size of the ground raw materials (2-3 mm) was highly reduced, as observed in the light microscopy images Figure 1b. The estimated fibre length from the image analyses ranged between 70-570 µm for coffee husk and 60-490 µm for rice husk. Particle size reduction provoked by bleaching treatment was similar for both samples where the effective attacks of the chemical agents disrupted the internal structure of the material, removing the non-cellulosic components. Bleaching treatment with the sodium chlorite solution, which becomes chlorine dioxide in acetate buffer solution, provokes the oxidation of the lignin aromatic ring [31] [1], releasing purified cellulose materials.

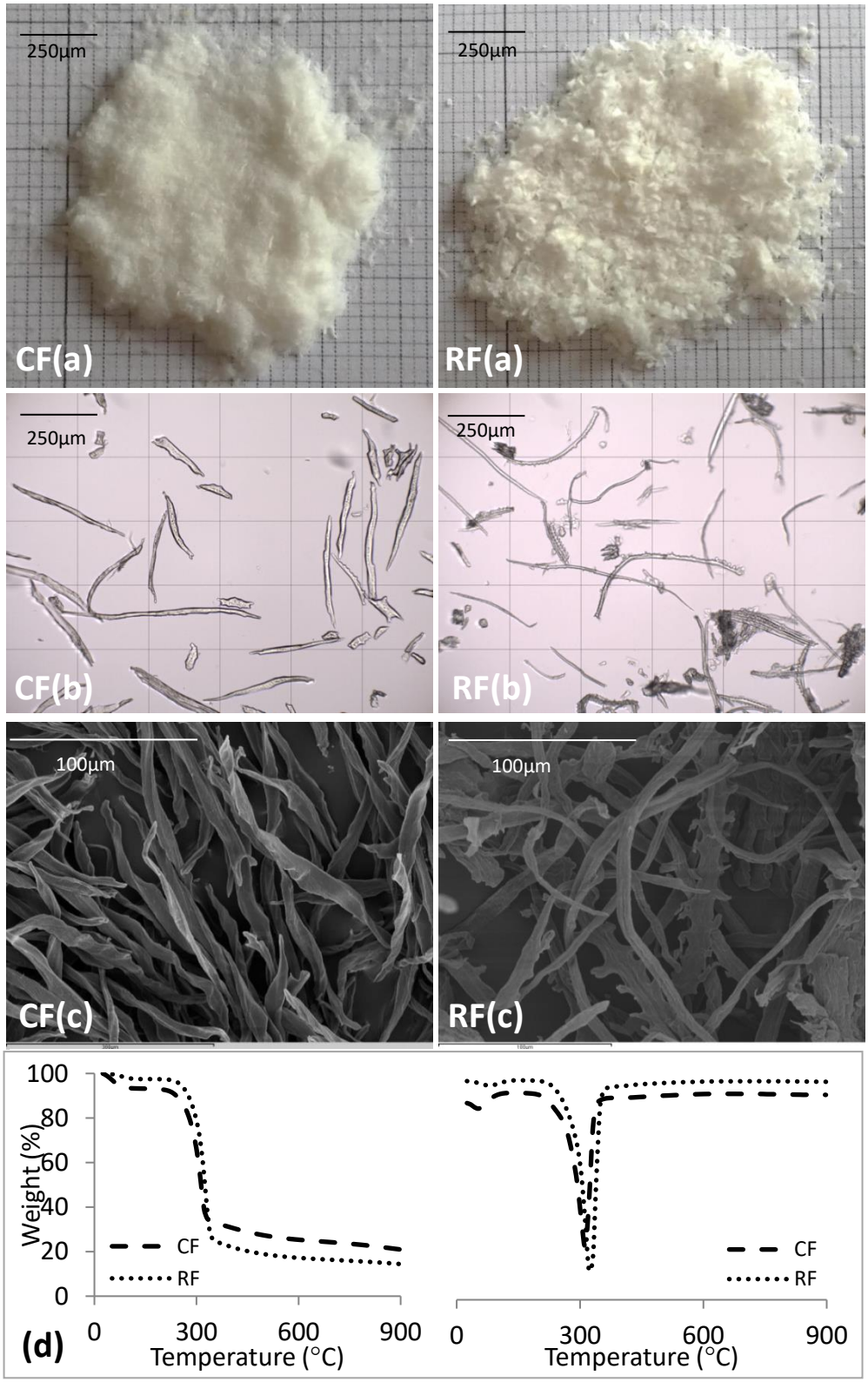

Figure 1. (a) Appearance of coffee (CF) and rice (RF) fibres after bleaching treatment, (b) light micrographs of fibre water dispersions (grid: 250 µm) (c). SEM micrographs of isolated fibres and (d) TGA and DTGA curves of the fibres.

SEM images (Figure 1c) revealed the different shape of both fibres; coffee fibres were flatter and helically folded, whereas rice fibres were more cylindrical with less than 10 µm in diameter as previously reported by Johar et al. [26]. The obtained cellulose fibres showed a good aspect ratio (relationship between the length and the diameter). The length range was 60-570 µm with very small diameters, as can be observed in Figure 1a and 1b. This provides adequate properties as reinforcing materials for composite applications [1].

Thermal analysis of cellulose fibres (Figure 1d) shows the characteristic peaks for these materials. A small weight loss was observed in all cases in the range of 100°C, attributable to the evaporation of bonded water in the films. The temperatures of the onset and main peak, around 270 and 300 °C, respectively, are typical of cellulose decomposition, as reported by several authors for cellulosic materials such as cotton (T_{peak} 349 °C [32]), bleached garlic straw (T_{peak} ~290 °C [33]), cellulose recycled office paper (T_{peak} 361 °C [34]) or bleached rice husk (T_{peak} ~305 °C [26]). Mensaray and Ghaly [35] reported that lignocellulosic materials decompose in the temperature range of 150-500 °C; depending on the initial raw material. Very similar behaviour was observed for both kinds of fibres, although a higher residual mass was noted for the coffee material, thus indicating a greater content of ashes or thermostable degradation products. Nevertheless, the observed thermal stability of these materials allows for their effective use for obtaining composite polymer films applying the usual thermoprocessing (extrusion, melt blending and injection moulding) of the plastics industries.

3.2. Properties of composite films

3.2.1. Optical properties

Figure 2 shows the internal transmittance (Ti) of the films in the wavelength range of 300-950 nm as an indicator of the film transparency to both near UV and VIS radiation. Gloss values are also indicated in Figure 2 for each film sample. The low transparency of the starch and composite films in the low wavelength range is remarkable, as observed by other authors [7] [36]. This aspect can be considered positive since this implies potential protection ability in food applications, to reduce UV-induced oxidation reactions [13]. Incorporation of fibres reduced the films transparency in the whole wavelength range, according to the introduction of a dispersed phase in the polymer matrix with the subsequent anisotropy in the refractive index and light dispersion effects. The higher fibre ratio, the greater the film opacity. This effect was also remarkable in the UV region, reinforcing for the mentioned protective function. At low fibre ratio (1 wt%) the transparency reduction of coffee fibres was significantly lower than that promoted by rice fibres, which could be related with the different particle size or aggregation or orientation in

the films. At higher ratios, the differences were mitigated probably due to the fact that from a determined concentration of dispersed phase, the high light interferences masked the possible structural differences between the composites with the different fibres, which would affect the light dispersion behaviour.

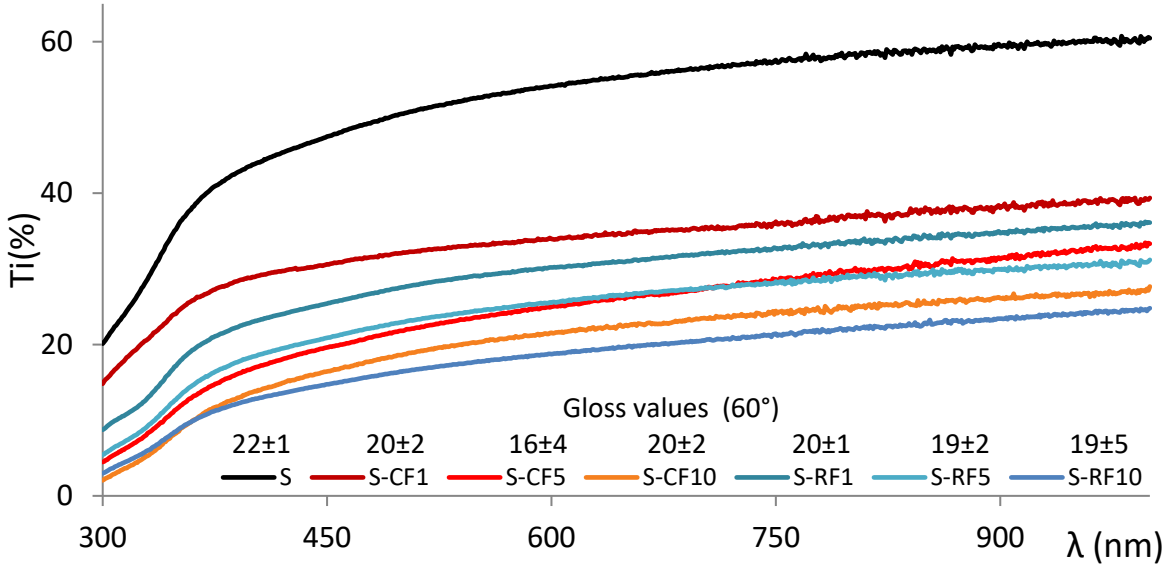

Figure 2. UV-VIS Transmittance spectra of the corn starch films containing different ratios of cellulose fibres from coffee (CF) or rice (RF) husks. Gloss values are also indicated for each sample.

The gloss of the films is mainly associated to their surface roughness, which can be also affected by the film processing method [8]. Figure 2 shows the obtained values for the different films. In general, the composite films exhibited low gloss compared with neat starch films. Their values ranged between 16-20 GU for coffee fibres and 19-20 GU for rice fibres, with high variability, and without clear tendencies as a function of filler content. The addition of fillers induced irregularities at the films surface where fibre fragments will be present, which contributes to light dispersion, giving a matt appearance to the composites, as previously observed by other authors when micro- and nano-fillers were incorporated into the polymer matrices [15] [37] [20] [38].

3.2.2. Tensile properties

Reinforcing materials, such as cellulosic fibres can contribute to improve mechanical properties of starch films which possess poor mechanical properties not enough adequate

for food handling [39]. Figure 3 shows the typical tensile curves of corn starch films containing different ratios of the isolated cellulosic fillers from coffee or rice husks, in comparison to the film control sample (S), every one conditioned at 53% RH and 25 °C for 1 week.

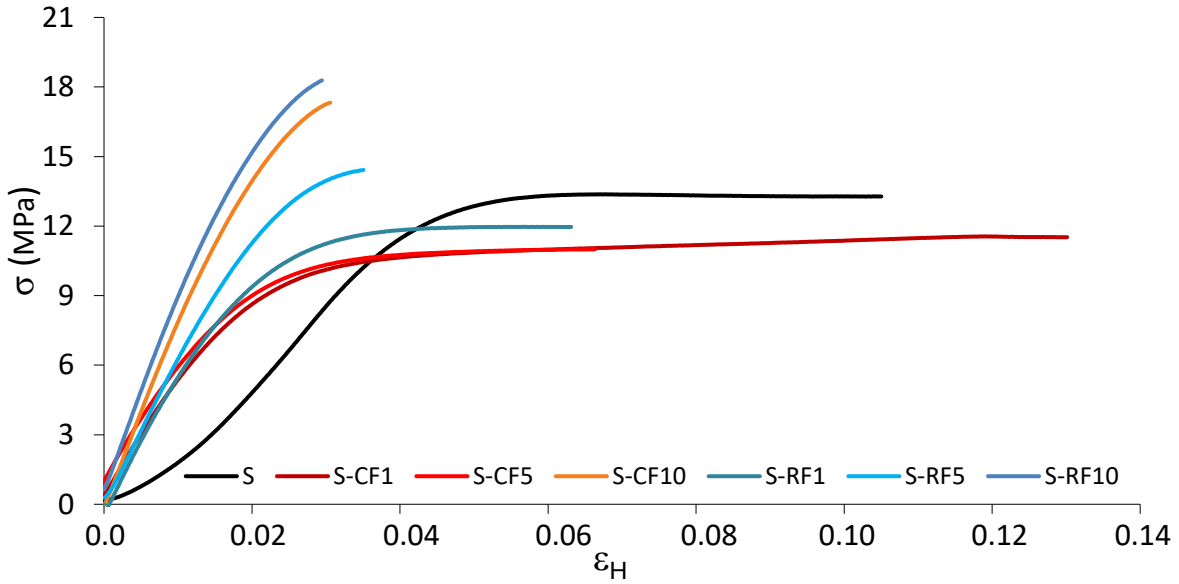

Figure 3. Typical stress-Hencky strain curves for starch films with 1 wt%, 5 wt% and 10 wt% of cellulose fibres from coffee (CF) and rice (RF) husk.

A clear tendency of increasing stiffness of the samples was observed for all of the composites with increasing the fibre content, such as also observed Kargarzadeh et al. [40]. On the other hand, fibre inclusion provoked a marked decrease in the film extensibility, except in composites with 1 wt% of coffee fibres, which did not significantly affect the stretching capacity and resistance to break of the TPS films. Composites with 10 wt% of both fillers and 5 wt% of rice fibres were considerably less extensible than TPS films. Table 2 shows the tensile parameters (Elastic modulus: EM, tensile strength: TS and percentage deformation E% at break), for both 1week conditioned films and 28 weeks stored films under the same ambient conditions, to also observe the effect of fillers on the starch ageing in the films. The obtained EM values reflect the above commented reinforcing effect of both cellulosic fillers, since a considerable increase in EM was observed when the filler content rose. Composites with only 1 wt% of filler improved the elastic modulus of films in about 60% regardless of the fibre source, whereas more than 100% and 200% increase was observed for 5 and 10 wt% of fibre content, respectively. The increase in the film stiffness was higher than that observed by Kargarzadeh et al. [40], for cassava starch matrix incorporated with 10 wt% of rice husk cellulose (only 55%). Taking into account the

variability in the values, no significant differences in the EM enhancement were detected for both kinds of fibres. This high improvement in EM could due to the purity degree of cellulose in the obtained fibres (62 and 74% respectively for coffee and rice fibres, quantified in a previous study), also implying a higher crystallinity degree of the material, which enhanced interaction between the fibres and starch, in line with the chemical affinity between cellulose and starch domains in the film structure [31], avoiding the weakening effect of other components of the lignocellulosic fraction in the starch matrix.

In contrast, notable differences were observed in the film extensibility reduction for both fibres. At 1 wt%, coffee fibres did not significantly reduce the stretching capacity of TPS film, whereas rice fibres provoked a 40% reduction. At 5 wt%, about 40 and 75% extensibility reduction were respectively produced by coffee and rice fibres, while 75% was observed with 10 wt% of both fillers. These results suggest a better performance of coffee fibres in the corn TPS films in terms of reinforcement effect, since films become harder with lower increase in brittleness.

Table 2. Mean values and standard deviation of tensile properties of TPS and composite films conditioned (1 week) and stored (28 weeks), at 53% RH and 25 °C. (Elastic modulus: EM; Tensile strength: TS; Percentage deformation E% at break).

Formulation	EM (MPa)	TS (MPa)	E (%)	EM (MPa)	TS (MPa)	E (%)	Thickness (mm)
	Initial time (1 week)			Final time (28 weeks)			
S	260 ± 80^{a}	13.0 ± 1.5^{b}	12 ± 7^{b}	126 ± 4^{a}	7.0 ± 2.0^{a}	22 ± 12^{b}	0.22 ± 0.02^{ab}
S-CF1	399 ± 106^{b}	9.0 ± 2.0^{a}	13 ± 4^{b}	181 ± 74^{a}	8.3 ± 2.1^{ab}	18 ± 4^{b}	0.21 ± 0.01^{a}
S-CF5	563 ± 75^{c}	12.2 ± 1.4^{ab}	7 ± 3^{a}	330 ± 20^{bc}	9.8 ± 1.0^{b}	23 ± 1^{b}	0.26 ± 0.01^{c}
S-CF10	822 ± 38^{d}	19.0 ± 1.0^{c}	3 ± 1^{a}	401 ± 35^{c}	8.7 ± 0.7^{ab}	14 ± 1^{a}	0.22 ± 0.01^{ab}
S-RF1	430 ± 70^{b}	11.3 ± 1.8^{ab}	7 ± 1^{a}	268 ± 34^{b}	7.4 ± 0.9^{a}	33 ± 3^{b}	0.23 ± 0.01^{b}
S-RF5	671 ± 105^{c}	16.5 ± 2.7^{c}	4 ± 1^{a}	339 ± 31^{bc}	7.9 ± 2.7^{ab}	14 ± 2^{a}	0.21 ± 0.01^{a}
S-RF10	863 ± 2^{d}	17.0 ± 3.0^{c}	3 ± 1^{a}	387 ± 60^{c}	8.1 ± 0.6^{ab}	16 ± 5^{a}	0.24 ± 0.02^{b}

Different superscript letters within the same column indicate significant differences among formulations ($p < 0.05$).

As concerns the development of the mechanical behaviour of the films after 28 weeks storage time, a sharp decrease in the elastic modulus was observed for all formulations (40-55% depending on the film sample), but in composites with 5 and 10 wt% of filler, still remained higher than in TPS films conditioned for 1 week. Comparison of EM values of composites with that of TPS films in stored samples revealed similar improvement

percentages to those non stored films. As concerns elongation at break all films became much more extensible after storage, this effect being more marked when the fibre content increase. As compared with the stored TPS films, the brittleness effect induced by fibres, observed in one week conditioned samples, especially at higher fibre concentration, was notably mitigated and, even in for composites with 1 and 5 wt% coffee fibres and 1 wt% of rice fibres there were not significant differences in the film elongation at break respect TPS film. These changes in tensile behaviour of the films during the relatively long storage time could be attribute to a progressive water sorption in the films in the relatively wet storage ambient (53% RH), which could cause the polymer-glycerol-fibres rearrangement in the matrix, leading to a higher ductility, or even to a partial degradation of the starch matrix under these conditions. Nevertheless, even taking these changes into account, reinforcing materials exerted beneficial effects at maintaining mechanical resistance of the films.

3.2.3. Barrier properties

Table 3 shows the moisture content and barrier properties of the conditioned films. The moisture content did not show significant differences among film formulations with different content or type of fillers. This agrees with the similar hygroscopic nature of starch and cellulose, which led to similar water sorption capacity in the composites, as compared with TPS films.

Table 3. Mean values and standard deviation of moisture content, water vapor permeability (WVP) and oxygen permeability (OP) of TPS and composite films conditioned at 53% RH and 25 °C.

Formulation	Moisture content (g water/g dried film)	WVP ($g \cdot mm \cdot kPa^{-1} \cdot h^{-1} \cdot m^{-2}$)	OP x10^{14} ($cm^3 \cdot m^{-1} \cdot s^{-1} \cdot Pa^{-1}$)
S	0.093 ± 0.002^{a}	11.1 ± 0.4^{ab}	4.8 ± 0.7^{b}
S-CF1	0.086 ± 0.004^{a}	12.5 ± 1.7^{b}	4.9 ± 0.1^{b}
S-CF5	0.094 ± 0.016^{a}	12.7 ± 1.3^{b}	4.8 ± 0.2^{b}
S-CF10	0.082 ± 0.003^{a}	10.7 ± 1.0^{a}	3.9 ± 0.2^{a}
S-RF1	0.087 ± 0.003^{a}	10.4 ± 0.5^{a}	4.0 ± 0.2^{a}
S-RF5	0.093 ± 0.020^{a}	11.5 ± 1.1^{ab}	4.3 ± 0.4^{ab}
S-RF10	0.086 ± 0.004^{a}	10.6 ± 0.2^{a}	4.3 ± 0.5^{ab}

Different superscript letters within the same column indicate significant differences among formulations ($p < 0.05$).

Likewise, WVP of the TPS films was not affected by the fibre incorporation (different type or content) (Table 3). Although an increase in the tortuosity factor in the matrix could be expected by fibre dispersion, the high water affinity of cellulose did not imply a limitation for the transport of water molecules in composites. However, Wattanakornsiri et al. [34] found a 63% reduction in WVP of cassava starch films incorporating 8 wt% of cellulose fibres from recycled paper. Differences in the amylose:amylopectin ratio (which is higher in corn starch) could play a key role in the composite nanostructure, provoking a different effect of fillers on the WVP of the films. Table 3 also shows the values of oxygen permeability of the different composites and TPS film. The presence of cellulose fibres in starch matrices slightly improved the oxygen barrier (about 17% reduction in OP) especially for rice fibres at any ratio and coffee fibres at the highest ratio. Formation of a more tortuous pathway for transport of the oxygen molecules explains the OP reduction in the starch matrix already in itself with great resistance to oxygen transport [39]. Similar results were obtained by López et al. [41] in starch films containing inorganic filler (talc). The improvement of barrier properties by fillers depends on many factors such as the structure of the matrix, crystallinity, polarity and type of reinforcement agent [39].

3.3. Microstructure of the composites

The interaction and dispersion degree of the fibres into starch matrix was studied by FESEM analysis. Figure 4 and 5 shows the surface and cross section of TPS films and composites. In contrast with the smooth surface of TPS film a rougher surface can be appreciated in composites, evidencing the fibre presence at surface level. Individualised fibres uncoated or infiltrated in the starch matrix can be observed in all composites, resulting in surface irregularities, which explain the lower observed gloss of composites, compared to TPS films. Kargarzadeh et al. [40] also studied the incorporation of multiscale rice husk into cassava starch and observed that the reduction in particle size of the fibres after alkali and bleaching treatments allowed starchy materials to infiltrate inside the fibre bundles. A similar fibre distribution at surface level was observed for all composites, regardless the fibre ratio, whereas the internal fibre dispersion clearly reflected the different amount incorporated in the films, which exhibited a different fibre density as a function of total concentration (Figure 5). This fact indicates the particular tendency of fibres to adsorb at the film surface, especially the finest ones, reaching an oriented distribution (quasi-parallel) on the film surface. This fibre arrangement explains the increase in the film stiffness, in line with the formation of an oriented fibrous tissue with offers greater resistance to deformation, even at low fibre ratio. The addition of higher amount of fibres will also lead to a weakening effect in the starch matrix due to the interruption of the polymer network.

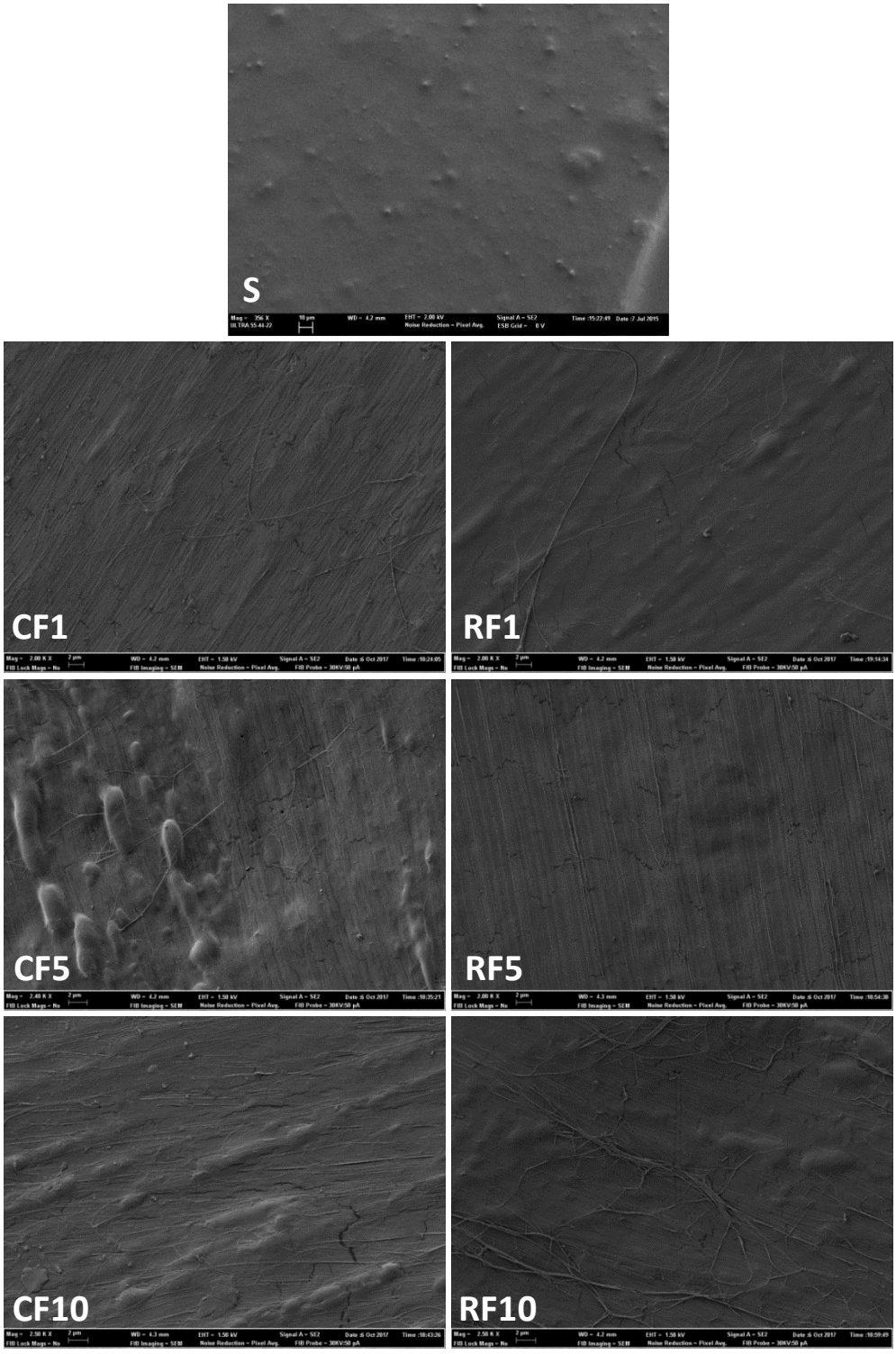

Figure 4. FESEM micrographs of the surface of TPS and composite films with different ratios of cellulose fibres.

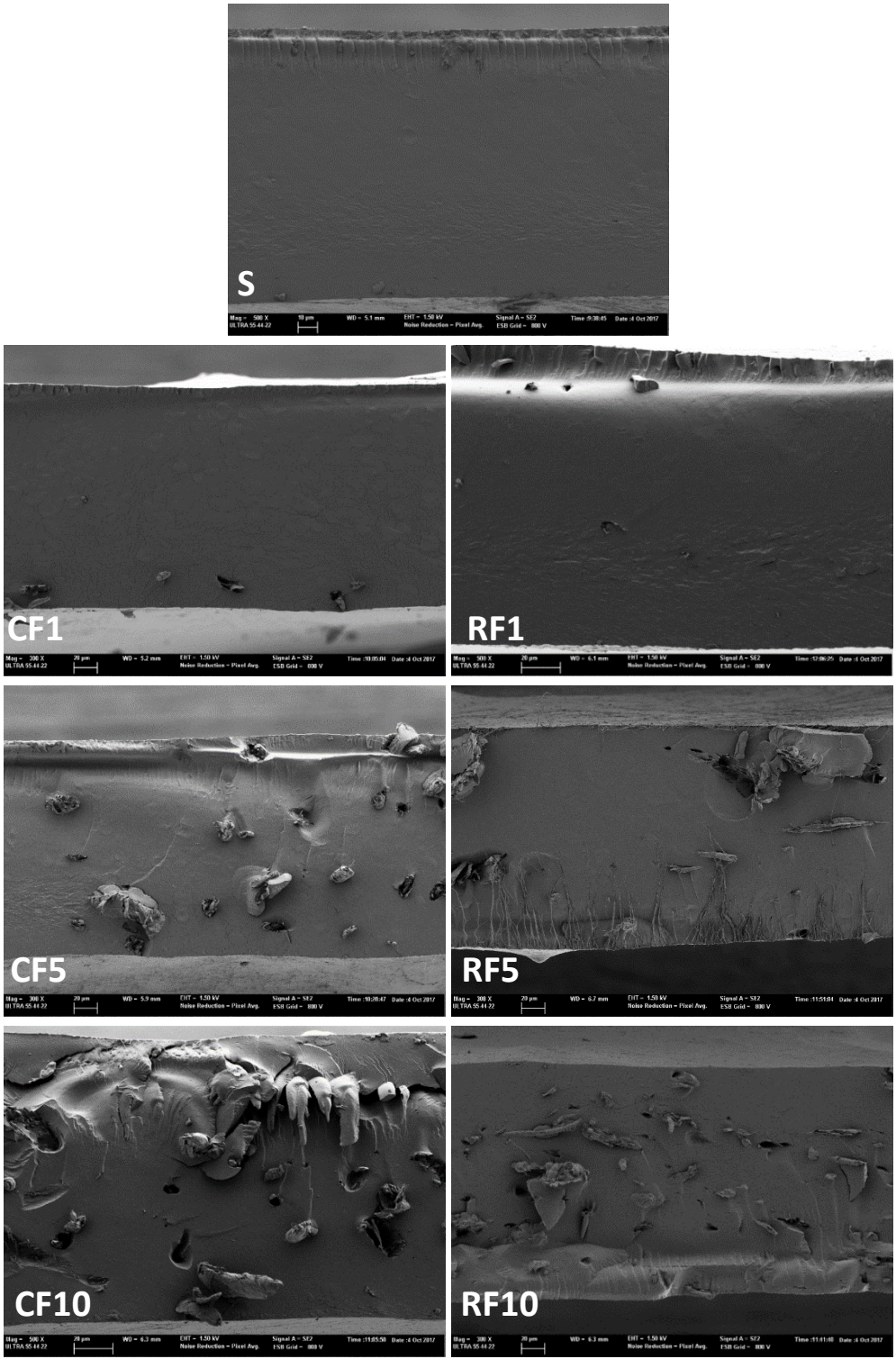

Figure 5. FESEM micrographs of the cross-section of TPS and composite films with different ratios of cellulose fibres.

Figure 6 shows the FESEM images at higher magnification, where the above commented arrangement are more clearly observed. It is remarkable that in the fractured cross section of the films the fibre bundles break practically at the same level than then the polymer matrix, which suggests high interaction forces between fibres and polymeric matrix. The elimination of more hydrophobic compounds (hemicelluloses and lignin) provided a notable adhesion capacity to the fibre with starch chains, as be observed in the micrographs. Similar results were obtained by Zainudin et al. [31] using of multiscale kenaf fibres as reinforcing filler in cassava starch matrices. Likewise, the fibre distribution observed in the film cross section is quite homogeneous, mainly exhibiting the bundle arrangement, in contrast with the more individualized form present at the film surface. A similar behaviour was observed by Chen et al. [36] with the incorporation of pea hull micro-fibres into pea starch; some cracks, holes and fibres aggregates appeared in the cross sections of films.

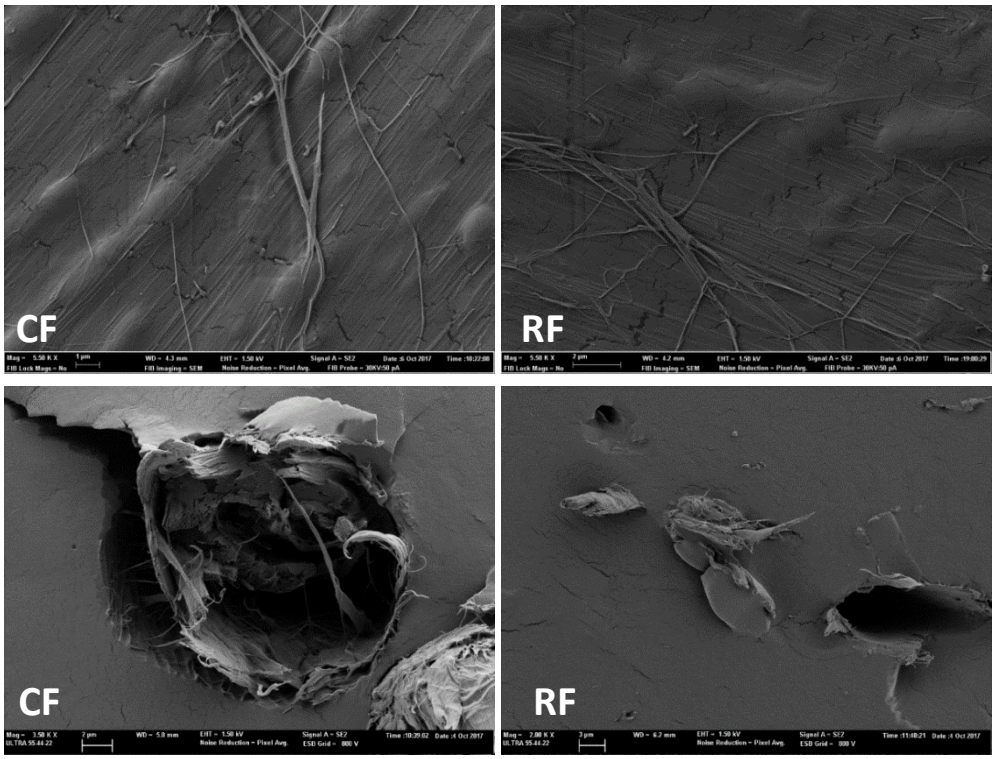

Figure 6. FESEM micrographs at higher magnification of fibres into the starch matrices, on the surface (top) and inside the film (bottom).

3.4. Thermal behaviour

The thermogravimetric analysis (TGA) was carried out to investigate the influence of fibres on thermal stability of the starch matrix. Figure 7 shows the TGA and DTGA curves of starch

films with 0, 1, 5 and 10 wt% of cellulose fibres from coffee or rice husk. DTGA curves shows the different peaks related to weight losses caused by thermal degradation. All samples exhibit a weight loss between 95-104 °C, which corresponds to the loss of bonded water in the materials. The main peak is associated with the thermal degradation of the cellulosic compounds and starch matrix. Table 4 summarises thermal degradation temperatures, T_{onset} and T_{peak}, for TPS and composite films. Corn starch film exhibited the peak degradation around 295 °C, in the range reported by Zainudin et al. [31] for degradation of cassava starch (275 °C), associated with the scission of the main chains (1,4-β-D-glucopyranose). The thermal stability of starch matrices increased between 1 and 3% with the incorporation of the cellulosic fillers, especially with 1 wt% of rice husk cellulose fibres. Composites showed a degradation temperature range between 299-304 °C without notable differences among them, in contrast with the lower interval (280-295 °C) of TPS. Similar observations were described by Kargarzadeh et al. [40] when 6% of bleached rice husk fibres were incorporated into cassava starch. Niranjana Prabhu and Prashantha [39] reviewed the properties of TPS composites for food packaging applications, and also reported a greater thermal resistance of composites containing different lignocellulose fibres.

Table 4. Mean values and standard deviation of onset and peak temperatures for thermal degradation of TPS and composite films conditioned at 53% RH and 25 °C.

Samples	[41-104]°C		[265-305]°C	
	Onset (°C)	**Peak (°C)**	**Onset (°C)**	**Peak (°C)**
S	46.3 ± 2.1^{cd}	94.8 ± 0.2^{a}	280 ± 1^{d}	295.0 ± 0.5^{a}
S-CF1	45.6 ± 1.8^{cd}	94.8 ± 0.2^{a}	271.5 ± 0.2^{b}	300.3 ± 0.5^{b}
S-CF5	41.8 ± 0.7^{a}	95.0 ± 0.1^{a}	270 ± 3^{ab}	300 ± 2^{b}
S-CF10	48.7 ± 1.4^{d}	95.0 ± 0.2^{a}	265.5 ± 0.2^{a}	299 ± 2^{b}
S-RF1	45.9 ± 0.3^{cd}	96.8 ± 0.2^{a}	276.5 ± 1.4^{cd}	305 ± 1^{c}
S-RF5	45.1 ± 0.7^{b}	95.0 ± 0.1^{a}	274 ± 4^{bc}	299 ± 0.4^{b}
S-RF10	48.0 ± 1.4^{cd}	104.8 ± 0.2^{b}	272 ± 1^{b}	300 ± 1^{b}

Different superscript letters within the same column indicate significant differences among formulations ($p < 0.05$).

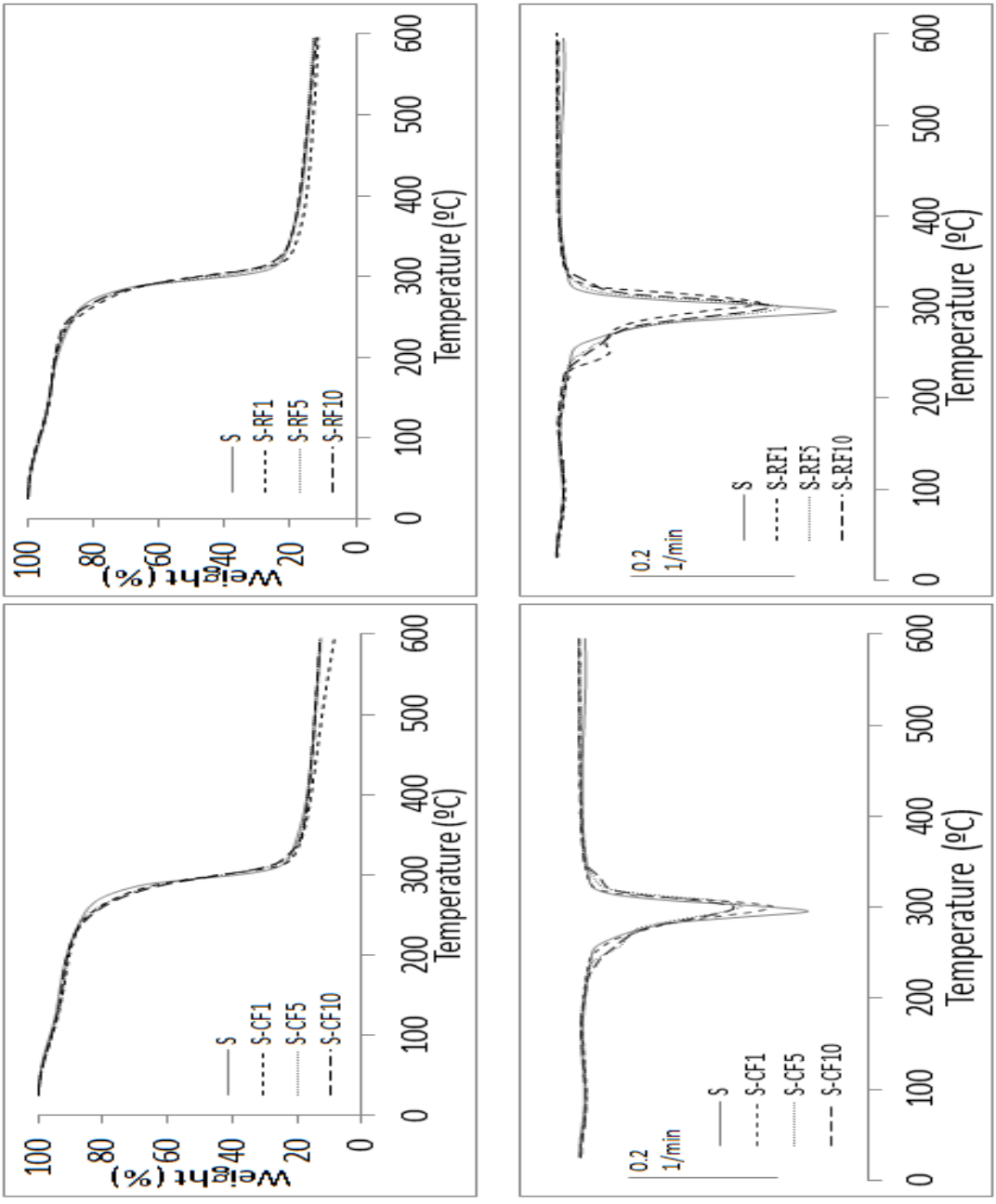

Figure 7. TGA and DTGA curves of TPS films with different contents of coffee (CF) and rice (RF) fibres.

4. CONCLUSIONS

Coffee and rice husk cellulosic fibres provoked a relevant reinforcing effect on glycerol plasticised TPS films, this being higher (more than 200%) when the fibre content increased till 10 wt%, while reduced the film stretchability. However, CF better maintained the film ductility than RF at 1 and 5 wt%. This reinforcing effect was maintained during film storage (28 weeks). A network of fine oriented fibres was observed in the surface of the films, which could contribute greatly to the increase in the resistance to deformation of the films. The fibres distributed in the internal part of the matrix exhibited a good adherence to the polymer network as revealed by the FESEM analysis of the film cross-section. WVP of TPS films was not reduced in composites, although oxygen permeability was lowered by about 17%. Film transparency decreased by fibre addition in the UV-VIS range, which could be interesting to preserve foods from light-induced oxidation reactions. Thermal stability of composites was slightly higher than net TPS films. These results indicate the excellent capacity of fibres from coffee and rice husks to improve functional properties of TPS films while representing a good alternative to give added value to these agricultural wastes.

Acknowledgements

The authors thank the Ministerio de Economía y Competitividad (Spain) for the financial support provided through Project AGL2016-76699-R. Authors also thank the Electron Microscopy Service of the UPV for their technical assistance.

REFERENCES

[1] H.M. Ng, L.T. Sin, T.T. Tee, S.T. Bee, D. Hui, C.Y. Low, and A.R. Rahmat. Extraction of cellulose nanocrystals from plant sources for application as reinforcing agent in polymers. *Compos. Part B* **75**, 176-200 (2015).

[2] M.J. Fabra, A. López-Rubio, and J.M. Lagarón, Biopolymers for food packaging applications, In *Smart Polymers and their Applications*, M.R. Aguilar, J. San Román, (Eds), pp. 476-50, Elservier (2014).

[3] Z. Zhang, O. Ortiz, R. Goyal, and J. Khon. Biodegradable polymers. *Handb. Polym. Appl.Med. Méd. Devices*, 303-335 (2014).

[4] B. Ghanbarzadeh, H. Almasi, and A.A. Entezami. Improving the barrier and mechanical properties of corn starch-based edible films: Effect of citric acid and carboxymethyl cellulose. *Ind. Crop. Prod*. **33**(1): 229-235 (2011).

[5] R. Ortega-Toro, S. Collazo-Bigliardi, P. Talens, and A. Chiralt, A. Thermoplastic starch: improving their barrier properties. *Agronom. Colomb.* **34**, 73-75 (2016).

[6] R. Ortega-Toro, J. Contreras, P. Talens, and A. Chiralt. Physical and structural properties and thermal behaviour of starch-poly(e-caprolactone) blend films for food packaging. *Food Packag. Shelf Life* **5**, 10-20 (2015).

[7] N.R. Savadekar, and S.T. Mhaske. Synthesis of nano cellulose fibers and effect on thermoplastics starch based films. *Carbohydr. Polym*. **89**, 146-151 (2012).

[8] R. Ortega-Toro, S. Collazo-Bigliardi, P. Talens, and A. Chiralt, A. Influence of citric acid on the properties and stability of starch-polycaprolactone based films. *J. Appl. Polym. Sci.* **42220**, 1-16 (2016).

[9] A.K. Shrestha, and P.J. Halley. Starch modification to develop novel starch biopolymer blends: state of art and perspectives. *Starch Polym.* 105-143 (2014).

[10] M. Carbone, D.M. Donia, G. Sabbatella, and R. Antiochia. Silver nanoparticles in polymeric matrices for fresh food packaging. *J. King Saud Univ. Sci*. **28**, 273-279 (2016).

[11] T. Gutiérrez, P. González, C. Medina, L. Famá, and S. Goyanes. Effect of filler properties on the antioxidant response of thermoplastic starch composites. In *Handbook of composites from renewable materials*, V. Thakur, M. Thakur, M. Kessler, (Eds),Wiley-Scrivener Publishing, New York, USA (2017).

[12] A.S. Abreu, M. Oliveira, A. de Sá, R.M. Rodrigues, M.A Cerqueira, A.A Vicente, and A.V Machado. Antimicrobial nanostructured starch based films for packaging. *Carbohydr. Polym.* **129**, 127-134 (2015).

[13] A. Cano, E. Fortunati, M. Cháfer, C. González-Martínez, A. Chiralt, and J.M Kenny. Effect of cellulose nanocrystals on the properties of pea starch poly(vinyl alcohol) blend films. *J. Mater. Sci*. **50**, 6979-6992 (2015).

[14] C.S. Miranda, M.S. Ferreira, M.T. Magalhães, W.J. Santos, J.C. Oliveira, J.B. Silva, and N.M José. Mechanical, thermal and barrier properties of starch-based films plasticized with glycerol and lignin and reinforced with cellulose nanocrystals. *Mater. Today: Proc*. **2**, 63-69 (2015).

[15] K. González, A. Retegi, A. González, A. Eceiza, and N. Gabilondo. Starch and cellulose nanocrystals together into thermoplastic starch bionanocomposites. *Carbohydr. Polym*. **117**, 83-90 (2015).

[16] M.J. Fabra, A. López-Rubio, J. Ambrosio-Martín, and J.M. Lagarón. Improving the barrier properties of thermoplastic corn starch-based films containing bacterial cellulose nanowhiskers by means of PHA electrospun coatings of interest in food packaging. *Food Hydrocoll*. **61**, 261-268 (2016).

[17] J.S. Alves, K.C. dos Reis, E.G.T. Menezes, F.V. Pereira, and J.Pereira. Effect of cellulose nanocrystals and gelatin in corn starch plasticized films. *Carbohydr. Polym.* **115**, 215-222 (2015).

[18] N. El Miri, K. Abdelouahdi, A. Barakar, M. Zahouily, A. Fihri, A. Solhy, and M. El Achaby. Bio-nanocomposite films reinforced with cellulose nanocrystals: Rheology of film-forming solutions, transparency, water vapor barrier and tensile properties of films. *Carbohydr. Polym.* **129**, 156-167 (2015).

[19] P. Müller, K. Renner, J. Móczó, E. Fekete, and B. Pukánszky. Thermoplastic starch/wood composites: Interfacial interactions and functional properties. *Carbohydr. Polym*. **102**, 821-829 (2014).

[20] R. Moriana, F. Vilaplana, S. Karlsson and A. Ribes-Greus. Improved thermos mechanical properties by the addition of natural fibres in starch-based sustainable biocomposites. *Compos.: Part A* **42**, 30-40 (2011).

[21]L. Yusriah, S.M. Sapuan, E.S Zainudin, and M. Mariatti. Underutilized malaysian agro-wastes fiber as reinforcement in polymer composites: potential and challenges. *J. Polym. Mater*. **29**, 21-36 (2012).

[22] L.S. Oliveira, and A.S. Franca. An overview of the potential uses for coffee husks. *Coffee Health Dis. Prev*. **31**, 283-291 (2016).

[23] G.G. Moreno-Contreras, J.C. Serrano-Rico, and J.A. Palacios-Restrepo, J.A. Industrial waste combustion performance in a bubbling fluidized bed reactor. *Ing. Univ. Bogotá* **13**, 251-266 (2009).

[24] S.H. Sung, Y. Chang, and J. Han. Development of polylactic acid nanocomposite films reinforced with cellulose nanocrystals derived from coffee silverskin. *Carbohydr. Polym.* **169**, 495-503 (2017).

[25] L. Brinch, F. Cotana, E. Fortunati, and J.M. Kenny. Production of nanocrystalline cellulose from lignocellulosic biomass: Technology and applications. *Carbohydr. Polym*. **94**, 154-169 (2013).

[26] N. Johar, I. Ahmad, and A. Dufresne. Extraction, preparation and characterization of cellulose fibres and nanocrystals from rice husk. *Ind. Crop. Prod*. **37**, 93-99 (2012).

[27] Standard test method for specular gloss. ASTM D523 (1999).

[28] Standard test methods for water vapor transmission of materials. ASTM E96-9532 (1995).

[29] T.H. McHugh, R. Avena-Bustillos, and J.M Krochta. Hydrophobic edible films: Modified procedure for water vapour permeability and explanation of thickness effects. *J. Food Sci.* **58**(4), 899–903 (1993).

[30] Standard test method for tensile properties of thin plastic sheeting. ASTM D882 (2001).

[31] S.Y.Z. Zainuddin, I. Ahmad, H. Kargarzadeh, I. Abdullah, and A. Dufresne. Potential of using multiscale kenaf fibers as reinforcing filler in cassava starch- kenaf biocomposites. *Carbohydr. Polym*. **92**, 2299-2305 (2013).

[32] L. Ludueña, A. Vázquez, and V. Alvarez. Effect of lignocellulosic filler type and content on the behavior of polycaprolactone based eco-composites for packaging applications. *Carbohydr. Polym*. **87**, 411-421 (2012).

[33] F. Kallel, F. Bettaieb, R. Khiari, A. García, J. Bras, and S. Ellouz Chaabouni. Isolation and structural characterization of cellulose nanocrystals extracted from garlic straw. *Ind. Crop. Prod*. **87**, 287-296 (2016).

[34] A. Wattanakornsiri, K. Pachana, S. Kaewpirom, M. Traina, and C. Migliaresi. Preparation and properties of green composites based on tapioca starch and differently recycled paper cellulose fibers. *J. Polym. Environ.* **20**, 801-809 (2012).

[35] K.G. Mansaray, and A.E. Ghaly, A.E. Thermal degradation of rice husks in nitrogen atmosphere. *Bioresour. Technol*. **65**, 13-20 (1998).

[36] Y. Chen, L. Changhua, P.R. Chang, D.P. Anderson, and M.A. Huneault. Pea starch-based composite films with pea hull fibers and pea hull fiber-derived nanowhiskers. *Polym. Eng. Sci*. **49** (2), 369-378 (2009).

[37] E. Fortunati, F. Luzi, A. Jiménez, D.A. Gopakumar, D. Puglia, S. Thomas, J.M Kenny, A. Chiralt, and L. Torre. Revalorization of sunflower stalks as novel sources of cellulose nanofibrils and nanocrystals and their effect on wheat gluten bionanocomposite properties. *Carbohydr. Polym*. **149,** 357-368 (2016).

[38] M.P. Arrieta, E. Fortunati, F. Dominici, E. Rayón, J. López, and J.M. Kenny. Multifunctional PLA–PHB/cellulose nanocrystal films: Processing, structural and thermal properties. *Carbohydr. Polym*. **107**, 16-24 (2014).

[39] T. Niranjana Prabhu, and K. Prashantha, K. A review on present status and future challenges of starch based polymer films and their composites in food packaging applications. *Polym. Compos*., 1-24 (2016).

[40] H. Kargarzadeh, N. Johar, and I. Ahmad. Starch biocomposite film reinforced by multiscale rice husk fiber. *Compos. Sci. Technol*. **151**, 147-155 (2017).

[41] O.V. López, L.A. Castillo, M.A. García, M.A. Villar, and S.E. Barbosa. Food packaging bags based on thermoplastic corn starch reinforced with talc nanoparticles. *Food Hydrocoll*. **43**, 18 (2015).

Chapter III

Improving properties of thermoplastic starch films by incorporating active extracts and cellulose fibres isolated from rice or coffee husk

[1]**Sofía Collazo-Bigliardi;** [2]Rodrigo Ortega-Toro; [1]Amparo Chiralt

Food Packaging and Shelf Life. Under Review

[1]Institute of Food Engineering for Development, Universitat Politècnica de València. Valencia, Spain

[2]Food Engineering Program, Faculty of Engineering, Universidad de Cartagena. Cartagena de Indias, Colombia

socol@doctor.upv.es

ABSTRACT

Hydrothermal (60 min, 180 °C) extracts and cellulose fibres from coffee and rice husks were obtained to be incorporated into corn starch films, in order to improve the film functional properties as food packaging material and confer them active properties. Extracts exhibited antioxidant properties (EC_{50}: 5.37-5.29 mg extract solids/ mg DPPH) and antibacterial activity against *Listeria innocua* and *Escheriquia coli* (MIC values: 35-45 and 34-35 mg extract solids/ mL, respectively). The active extracts improved tensile properties of the starch films; elastic modulus increased by about 350% and films become less stretchable. The cellulosic fibres from both residues were more effective as reinforcing agents in films containing extract solids than in net starch films. Extracts also provoked 30% reduction in the WVP of starch films and 50-85% reduction in the oxygen permeability, depending on their amount in the films, but no effect of cellulose fibres was observed on barrier properties.

Keywords: Active compounds; rice husk; coffee husk; cellulose fibres; thermoplastic starch; composites.

1. INTRODUCTION

In food packaging, the development of adequate packaging materials for the purposes of prolonging the shelf life of food represents a challenge. Oxidative reactions and microbiological alteration are the main processes that cause undesirable changes in the quality and safety attributes of foodstuffs (Talón, Trifkovic, Vargas, Chiralt, & González-Martínez, 2017a), and the use of active packaging materials with antimicrobial and/or antioxidant properties can control these deterioration processes, helping to extend the product shelf life.

Lignocellulosic agro-waste, such as rice or coffee husk, is rich in polyphenols linked to the hemicellulose or lignin fractions, which exhibit active properties for controlling microbial or oxidative processes (Aguiar, Estevinho, & Santos, 2016; Balasundram, Sundram, & Samman, 2006; Wanyo, Meeso, & Siriamornpun, 2014). Different kinds of polyphenols, such as lignans, stilbenes, flavonoids or phenolic acids have been classified on the basis of their structure or phenol units (Cong-Cong, Bing, Yi-Qiong, Jian-Sheng, & Tong, 2017; Shavandi et al., 2018). The antioxidant and antimicrobial properties of natural polyphenols have been widely studied. They are biosynthesised naturally by plants, and have been isolated from different plant products, such as spices or aromatic herbs, plant-food by-products and agro-waste (Balasundram et al., 2006; Talón et al., 2017a). Phenolic compounds have been successfully extracted from thyme (Talón et al., 2017a), garlic waste (Kallel et al., 2014), guarana seeds, boldo leaves, cinnamon barks, rosemary leaves (Bonilla & Sobral, 2016), rice hulls, almond hulls, buckwheat hulls or oat hulls (Balasundram et al., 2006), among others. The antioxidant character of polyphenols is associated with their ability to act as free radical scavengers, to inhibit lipoxygenase enzyme activity and to chelate metals (Talón, Trifkovic, Vargas, Chiralt, & González-Martínez, 2017b). The antimicrobial nature of polyphenols is associated with their capacity to inhibit extracellular microbial enzymes, to destabilise the cytoplasmic membrane and to provoke a deficit of the substrates required for microbial growth (Guil-Guerrero et al., 2016). In phenolic acids, the protonated form spreads across the membrane, which produces the acidification of the cytoplasm and, usually, cell death. Guil-Guerrero et al. (2016) reviewed the antimicrobial behaviour of several polyphenols (simple phenolic acids, flavonoids, tannins) extracted from plant-food by-products, and reported effective antibacterial action against pathogens like *E. coli, Lactobacillus* spp., *Staphylococcus aureus, P. aeruginosa*, and *Listeria* spp. strains, among others.

Lignocellulosic wastes, such as rice and coffee husk, are potential sources of active compounds, as well as cellulosic fractions that can be exploited as reinforcing agents (Collazo-Bigliardi, Ortega-Toro, & Chiralt, 2018a). Rice husk is one of the main renewable by-products of rice milling operations, and coffee husk (endocarp of coffee beans) is the residue obtained after de-hulling in coffee dry processing, both of them being rich in cellulosic (~55-

57%) and lignin (~22-35%) components (Collazo-Bigliardi, Ortega-Toro, & Chiralt, 2018b). These kinds of lignocellulosic wastes have been used to extract polyphenols, which have been mostly evaluated as to their antioxidant activity, mainly using organic solvents such as ethanol or methanol (Kallel et al., 2014; Vadivel & Brindha, 2015). Nevertheless, the polyphenol extraction by hydrothermal treatments is a better option because hot-water high-pressure extraction is an environmentally-friendly process, with a low cost, non-toxic solvent. During this treatment, a better preserved fraction of hemicelluloses and linked phenols can be obtained (Piñeros-Castro & Otálvaro, 2014) while a part of the lignin is degraded providing a great variety of phenolic compounds, such as cinnamic, benzoic, ferulic, gallic, syringic or vanillinic acids, tannins, syringaldehyde or flavonoids (Piñeros-Castro & Otálvaro, 2014; She et al., 2012).

Thermoplastic starch (TPS) has been widely studied for food packaging applications because of its biodegradability, low cost, abundance and suitability for food contact. TPS exhibits excellent filmogenic properties with high barrier capacity to oxygen and gases (Collazo-Bigliardi et al., 2018b; Ortega-Toro, Bonilla, Talens, & Chiralt, 2017). However, TPS films have some drawbacks, such as their high water sensitivity, retrogradation phenomena throughout time and low barrier capacity to water vapour. Different strategies have been used to improve these properties (Ortega-Toro et al., 2017), such as the addition of plasticisers the compatibilised blending with other polymers, the incorporation of cross-linking agents (Ortega-Toro, Collazo-Bigliardi, Talens, & Chiralt, 2016) or of different kinds of fillers (Brinchi, Cotana, Fortunati, & Kenny, 2013; Ng et al., 2015). The incorporation of cellulose micro-fillers and active extracts coming from lignocellulosic by-products could improve the starch film properties, while the use of these components allows for the valorisation of these residues in the context of circular economy.

The aim of this work was to improve the properties of thermoplastic starch films by incorporating active fractions, extracted from rice and coffee husk using a hydrothermal method, and cellulose fibres, also coming from these by-products, incorporated as reinforcing agents. The aqueous extracts were characterized as to their antioxidant and antimicrobial properties. The effect of the incorporation of active extracts and reinforcing agents on the mechanical, thermal, barrier, optical and microstructural properties of thermoplastic corn starch matrices was analysed.

2. MATERIALS AND METHODS

2.1. Materials

Rice and coffee husks were provided by the Universidad Jorge Tadeo Lozano (Bogotá, Colombia). Maltodextrin (MD) 18 DE used in spray drying of extracts was from Tecnas S.A., Colombia.

For the characterization of active compounds (±)-6-Hydroxy-2,5,7,8-tetramethylchromane-2-carboxylic acid (Trolox), 2,2-Diphenyl-1-pikryl-hydrazyl (DPPH), Folin-Ciocalteu reagent, gallic acid and methanol was obtained from Sigma-Aldrich (Madrid, Spain). For the antimicrobial activity analysis, stock cultures of *Escherichia coli* (CECT 101) and *Listeria innocua* (CECT 910) were supplied by the Spanish Type Culture Collection (CECT, Burjassot, Spain). Tryptone Soy Broth and agar bacteriological were provided by Scharlab (Barcelona, Spain)

Corn starch was purchased from Roquette (Roquette Laisa, Benifaió, Spain). Glycerol, sodium hydroxide, sodium carbonate, phosphorus pentoxide and magnesium nitrate-6-hydrate were obtained from Panreac Química, S.A. (Castellar del Vallès, Barcelona, Spain). Sodium chlorite and acetate buffer were provided by Sigma Aldrich (Madrid, Spain). All chemicals used were reagent grade and underwent no further purification.

2.2. Extraction of active compounds

Rice and coffee husks were ground in a bladed mill (Model SK100, Retsch, Germany) until 0.75 mm in size to promote the extraction, which was performed in a 5 L pilot scale reactor (A2423 model, Amar Equipment, India) by pressurized hot water. To this end, 750 g (rice husk) or 650 g (coffee husk) and 3 L of distilled water were used and the operation was carried out for 60 min at 180 °C, 9.5 bar, according to previous studies (Piñeros-Castro & Otálvaro, 2014). Then, the extracts were separated from the solid fraction, which was dried for the purposes of subsequently extracting the cellulose fibres. Rice and coffee extracts were concentrated at 90 °C under continuous stirring, obtaining about 6.5 and 7g ss/mL extracts, respectively. To obtain a powdered product, the aqueous extracts were spray dried by using a Vibrasec pilot dryer model Pasalab 1.5 (Universidad Nacional de Colombia, Medellin), operating at 180 °C and 90 °C outlet temperature, with atomizer disk speed of 24,000 rpm. Maltodextrin (18 DE) at 32.1 and 29.8 wt% was added to the rice and coffee extracts, respectively, as drying coadjuvant.

2.2.1. Measurement of antioxidant activity, EC_{50} parameter, total phenolic content and antimicrobial activity

The antioxidant capacity of the extracts was determined by using a 2,2-Diphenyl-1-pikryl-hydrazyl (DPPH) reduction method (Brand-Williams, Cuvelier, & Berset, 1995). To this end, 30µL of water diluted samples (1:5 for the aqueous extract or 1:10 for the powdered samples) were mixed with 1mL of a 0.1 mM DPPH in methanol. The mixture was vortexed

and left to stand at room temperature in darkness (40 min) before reading the absorbance at 517 nm. The results were expressed as mg Trolox equivalents per g of extract solids (mg TE/g extract solids) by using the corresponding calibration curve for Trolox.

Likewise, the EC_{50} parameter corresponding to the amount of sample required to reduce the DPPH concentration by 50%, once the stability of the reaction has been reached (t= 40 min), was determined following the methodology described by Talón et al. (2017a). The water-diluted samples (0.025 to 0.175 mL) were mixed with the 0.1 mM DPPH methanol solution to a final volume of 1mL. The DPPH concentration (mM) in the reaction medium was calculated from the calibration curve, determined by linear regression of DPPH concentration vs Absorbance at 517 nm. The EC_{50} values were obtained by plotting $\%[DPPH]_R$ *versus* the mass ratio of solid extract to DPPH (mg extract solids/mg DPPH), where $\%[DPPH]_R = ([DPPH]_{t=40}/[DPPH]_{t=0})x100$; $[DPPH]_{t=40}$ is the concentration of DPPH when the reaction was stable and $[DPPH]_{t=0}$ is the concentration at the beginning of the reaction.

Total phenolic content was analysed using Folin-Ciocalteu reagent, as described by Singleton & Rossi (1965) with some modifications. For this purpose, 0.05 mL of Folin-Ciocalteu reagent was mixed with 1 mL of Na_2CO_3, 0.5 mL of diluted sample (solids-water ratio was 1:20), at 37 °C. After 50 minutes of incubation in darkness, the absorbance at 765 nm was measured. The total phenolic content was determined applying the equation fitted to the standard curve prepared with gallic acid. The results were expressed as mg of gallic acid equivalents (GAE)/ g extract solids.

To determine the antimicrobial activity of the active powdered extracts against *E. coli* and *L. innocua*, an aliquot of each culture was transferred to a tube with 10mL of TSB and incubated at 37 °C for 24 h. Then, 10 µL aliquots were taken from these cultures and transferred to new 10 mL tubes of TSB, which were incubated at 37 °C for 24 h. In this way, work cultures in exponential growth phase were obtained, which were diluted to a concentration of 10^5 colony forming units (CFU)/mL. From this bacterial suspension, aliquots of 100 µL were deposited in each well of the plate. Then, different concentrations of the active compound diluted in water were added to each well and completed up to 100µL with TSB. The whole plate was incubated at 37 °C for 24 h. After 24 h of incubation, the MTT reagent was reconstituted in PBS (5 mg/mL) and 10µl was incorporated in each well of the plate. The plate was re-incubated for 4 h at 37 °C and the visual colour of the wells was registered. Those wells in which change of colour from yellow to purple is observed, indicate the presence of viable bacteria. In this sense, the MIC (minimum inhibitory concentration) of each active extract was considered as the lowest concentration at which no change in colour in the well was observed.

2.3. Extraction of cellulose fibres

The extraction process of cellulose fibres from rice and coffee husks was carried out according to the methodology reported by Collazo-Bigliardi et al. (2018a). Rice or coffee husks (solid residue from the hydrothermal treatment) was alkali treated with 4 wt% of NaOH at 80 °C for 3 h, at 1:15 solid:liquid ratio under continuous stirring. The samples were washed with distilled water until the alkali solution was removed. Following alkali treatment, the bleaching process was completed by adding equal parts of acetate buffer solution, sodium chlorite (1.7 wt%) and distilled water mixed with the alkali treated solid (at 1:15 solid:liquid ratio) and submitted to reflux temperature (about 100 °C) for 4 h under mechanical stirring. This process was repeated as many times as necessary (3 and 4, respectively for rice and coffee husks) until the samples were completely white. Then, the samples were washed with distilled water several times, dried and ground, in a Moulinex grinder DJ200031 350W, to be incorporated in the films.

2.4. Experimental design and film preparation

Thermoplastic corn starch films were obtained with glycerol as plasticiser (1:0.3 starch:glycerol ratio) by melt blending and compression moulding. To incorporate dry active extracts into the starch films, the total glycerol was partially substituted by the solid extracts in different proportions (glycerol:powdered extract ratios of: 80:20, 70:30 and 60:40), assuming that the extract compounds could also exert a plasticising effect. Then, seven film formulations were initially prepared, identified as S (starch-glycerol) and S-80:20C, S-70:30C, S-60:40C, S-80:20R, S-70:30R, S-60:40R, where C and R specify the origin of the incorporated extract (coffee (C) or rice (R) husks) and the figures reflect the glycerol:extract ratios. Since the films with the 70:30 ratio exhibited the best functional properties, these were selected to incorporate cellulose fibres, at 5% of the total blend, as reinforcing agents, in comparison with the reinforced S formulation. Therefore, four additional film formulations were obtained and identified with the label CF (coffee husk fibre) or RF (rice husk fibre) added to the initial sample code. All materials were hand-blended before the melt blending process. The mass fractions of each component in the different film formulations are reported in Table 1.

The melt blending process was carried out in an internal mixer HAAKE^{TM} PolyLab^{TM} QC, Thermo Fisher Scientific, Germany) at 130 °C, rotor speed 50 rpm, for 12 min. After processing, blends were cut and conditioned at 25 °C and 53% relative humidity (RH) for one week. Four grams of the conditioned pellets were put onto Teflon sheets and preheated for 4 min in a hot plate press (Model LP20, Labtech Engineering, Thailand). Films were obtained by compressing at 160 °C for 2 min at 30 bars, followed by 6 min at 130 bars and a final cooling cycle for 3 min (Ortega-Toro, Contreras, Talens, & Chiralt, 2015). The obtained films were conditioned at 25 °C and 53% RH for 1 week before their characterisation.

Table 1. Mass fraction (Xi, g compound/g dried film) of the different components (Starch: S, Glycerol: Gly, Active extract: A, from coffee (C) or rice (R) husks and cellulose fibres: F, from coffee (CF) or rice husks (RF)) in the different film formulations.

Formulations	X_S	X_{Gly}	X_A	X_F
S	0.7692	0.2308	-	-
S-80:20C	0.7692	0.1846	0.0462	-
S-70:30C	0.7692	0.1615	0.0692	-
S-60:40C	0.7692	0.1385	0.0923	-
S-80:20R	0.7692	0.1846	0.0462	-
S-70:30R	0.7692	0.1615	0.0692	-
S-60:40R	0.7692	0.1385	0.0923	-
S-CF	0.7308	0.2192	-	0.0500
S-70:30C-CF	0.7308	0.1535	0.0658	0.0500
S-RF	0.7308	0.2192	-	0.0500
S-70:30R-RF	0.7308	0.1535	0.0658	0.0500

2.5. Film characterisation

2.5.1. Microstructural properties

The microstructural analysis of the surface and cross-sections (fractured samples) of the films was carried out by using a Field Emission Scanning Electron Microscope (FESEM Ultra 55, Zeiss, Oxford Instruments, U.K). The film samples were maintained in desiccators with P_2O_5 for 2 weeks at 25 °C. Film samples were adequately mounted on support stubs and platinum coated. Observations were carried out at 1.5 kV.

2.5.2. Physico-chemical properties

The mechanical properties were determined using a universal test machine (TA.XTplus model, Stable Micro Systems, Haslemere, England) according to the ASTM standard method D882 (ASTM, 2001). Conditioned samples (2.5 cm x10 cm) were mounted in the film-extension grips of the testing machine and stretched at 50 mm/min until breaking. The

tensile strength (TS), the elastic modulus (EM), and the elongation at break (ε) of the films were determined from the stress-strain curves, estimated from the force-distance data obtained for different films. The conditioned film thickness was measured using a Palmer digital micrometer at six random positions around the film.

The water content of conditioned films at 53% RH and 25 °C was determined gravimetrically by drying for 24 h at 60 °C using a convection oven (J.P. Selecta, S.A. Barcelona, Spain) and their subsequent conditioning in a desiccator at 25 °C with P_2O_5 (a_w=0) for 2 weeks.

The ASTM E96-95 (ASTM, 1995) gravimetric method was used to determine the Water Vapour Permeability (WVP) of the films, with the modification proposed by McHugh, Avena-Bustillos, & Krochta (1993). Payne permeability cups, 3.5 cm in diameter (Elcometer SPRL,Hermelle/s Argenteau, Belgium) were filled with 5mL of distilled water (100% RH). Each cup was placed in a cabinet equilibrated at 25 °C and 53% RH, with a fan placed on the top of the cup in order to reduce the resistance to water vapour transport. The cups were weighed periodically (±0.0001 g), and the water vapour transmission rate (WVTR) was determined from the slope obtained from the regression analysis of weight loss data versus time. From this data, WVP was obtained according to Ortega-Toro et al. (2016).

The oxygen permeability (OP) was determined using an OX-TRAN Model 2/21 ML (Mocon Lippke, Neuwied, Germany), in samples conditioned at 25 °C and 53% RH. The oxygen transmission values were determined every 10 min until equilibrium was reached. The film area used in the tests was 50 cm^2. The film thickness was considered in all cases to obtain the OP values.

The optical properties were determined by the reflection spectra of the samples from 400 to 700 nm using a spectro-colorimeter CM- 3600d (Minolta Co., Tokyo, Japan). The transparency was measured by the internal transmittance (Ti), applying the Kubelka-Munk theory of multiple scattering (Hutchings, 1999), using the film reflection spectra obtained on both black and white backgrounds. The CIEL*a*b* colour coordinates were obtained from the reflectance of an infinitely thick layer of the material by considering illuminant D65 and observer 10°, as reference. The psychometric coordinates, Chroma (C_{ab}*) and hue (h_{ab}*), were also evaluated (Talón et al., 2017a).

The film gloss was determined at an incidence angle of 60° using a flat surface gloss meter (Multi.Gloss 268, Minolta, Germany), according to the ASTM standard D523 method (ASTM, 1999). The results were expressed as gloss units (GU), relative to a highly polished surface of black glass standard with a value near to 100 GU.

2.5.3. Thermal analysis

The thermal stability of the different samples was analysed using a Thermogravimetric Analyser TGA 1 Star^e System analyser (Mettler-Toledo, Inc., Switzerland) under nitrogen atmosphere (gas flow: 10 mL min^{-1}). Samples (about 4-5 mg) were heated from 25 to 600 °C at 20 °C/min. Initial degradation temperature (T_{Onset}) and peak temperature (T_{Peak}) corresponding to the maximum degradation rate, were obtained from the first derivative of the resulting weight loss curves using the STAR^e Evaluation Software (Mettler-Toledo, Inc., Switzerland).

A Differential Scanning Calorimeter (DSC 1 Star^e System, Mettler-Toledo Inc., Switzerland) was used to analyse the phase transitions in the polymer matrices. Samples (8-10 mg) were placed into aluminium pans and sealed. The thermograms were obtained by heating from 25 °C to 160 °C at 10 °C/min; then the samples were cooled until 25 °C, and heated in a second step to 160 °C at the same rate. In the first scan, the bonded water in the film was eliminated and in the second heating scan, the glass transition of starch was analysed.

2.5.4. Antioxidant activity

The antioxidant capacity of the films was determined using a 2,2-Diphenyl-1-pikryl-hydrazyl (DPPH) reduction method, following the methodology described in section 2.2.1. In this case, films (~1.5 g) were dissolved in 100 mL of distilled water under continuous stirring in dark bottles. A final volume of 1 mL was obtained by mixing samples (0.05 to 0.35 mL) with methanol solution of 0.1 mM DPPH. The EC_{50} parameter was determined as described in section 2.2.1.

2.6. Statistical analysis

Statgraphics Plus for Windows 5.1 (Manugistics Corp., Rockville, MD) was used for carrying out statistical analyses of data through analysis of variance (ANOVA). Fisher's least significant difference (LSD) was used at the 95% confidence level.

3. RESULTS AND DISCUSSION

3.1. Properties of coffee and rice husk extracts

Rice and coffee husks were used to extract active compounds with potential antioxidant and antimicrobial activity through the hydrothermal process; the high temperatures and

pressures modify some physical properties of the water that give it particular characteristics as solvent (subcritical water extraction). The aqueous extract, the subsequent concentrate and the powdered form obtained by spray-drying were analysed to know how the process steps affected phenolic content or antioxidant capacity (Table 2). The antioxidant activity was quantified in terms of Trolox equivalent (TE) of the extract solids, as well as the EC_{50} values (amount of extract solids necessary to reduce the initial DPPH concentration by 50%).

Table 2. Mean values and standard deviation of antioxidant activity, in terms of Trolox Equivalent (TE), EC_{50} parameter and polyphenol content of the coffee and rice husk hydrothermal extracts (Extract), after the concentration step (Concentrated) and after spray drying of the concentrates (Powder). Minimum inhibitory concentrations (MIC) of coffee and rice husk spray-dried extracts for *E.coli* and *L. innocua* were also included.

		Antioxidant activity (mg TE/g extract solids)	**EC_{50} (mg extract solids/mg DPPH)**	**EC_{50} (mg powder /mg DPPH)**	**Polyphenol content (mg GAE/ g extract solids)**
Coffee husk	Extract	10.5 ± 0.6^{b}	6.41 ± 0.08^{c}	-	62 ± 9^{ab}
	Concentrated	13.6 ± 0.9^{d}	5.63 ± 0.03^{b}	-	70 ± 2^{b}
	Powder	12.5 ± 0.3^{c}	5.37 ± 0.09^{a}	7.66 ± 0.11^{a}	65 ± 5^{ab}
Rice husk	Extract	9.2 ± 0.5^{a}	6.44 ± 0.02^{c}	-	60 ± 3^{a}
	Concentrated	13.0 ± 0.2^{cd}	6.36 ± 0.04^{c}		67 ± 7^{b}
	Powder	12.4 ± 0.4^{c}	5.29 ± 0.04^{a}	7.76 ± 0.05^{a}	66 ± 5^{ab}
		MIC (mg extract solid/mL)		**MIC (mg powder/mL)**	
		E.coli	***L. innocua***	***E.coli***	***L. innocua***
Extract powder	Coffee	35	34	50	48
	Rice	45	35	66	52

Different superscript letters within the same column indicate significant differences among formulations ($p < 0.05$).

The total phenolic content of rice and coffee husk extracts ranged between 60-67 mg GAE/g extract solids, this being slightly affected by the process steps. After the concentration step, an increase in the quantified phenolic compounds was observed for both samples, whereas a decrease in this content was determined after the spray drying step. The increase after the concentration step could be due to the partial hydrolysis of some linked phenols, which could contribute to the increase in the spectrophotometric response. The reduction in the value of the powder samples, in comparison with the concentrated extract, could be associated with the partial oxidation of some components during the spray-drying process. The obtained contents referred per mass unit of dry husks ranged between 10.7-17.3 mg

GAE/g dry husks and were higher than that reported for other lignocellulosic waste. Kallel et al. (2014) reported 2.97 mg GAE/g dry husk for garlic husk treated with boiling water for 45 min. Other authors (Wanyo et al., 2014) reported that the phenolic content of rice husk was affected by different pre-treatments such as hot air drying at 120 °C for 30 min (1.70 mg GAE/g dry husk), Far-Infrared Radiation at FIR intensity of 2 kW/m^2 (3.14 mg GAE/g dry husk) or enzyme hydrolysis (2.21 mg GAE/g dry husk). The main phenolic acids found in rice husk aqueous extract were gallic, protocatechuic, vanillic and ferulic acids, although chorogenic, caffeic, syringic, p-coumaric and ferulic acids were also found in small quantities (Piñeros-Castro & Otálvaro, 2014; Wanyo et al., 2014). In contrast, caffeic and chlorogenic acids were the main phenolic compounds of coffee husk, and vanillic, gallic, tannic and protocatechuic acids were found in minor proportion (Aguiar et al., 2016; Andrade et al., 2012).

The evaluation of the antioxidant activity by DPPH assay has been widely used. DPPH is a stable free radical compound used to determine the free radical scavenging ability of different kinds of samples, such as pure compounds, plant extracts, fruit, vegetables, cereals, or lignocellulosic agro-waste (Dorta, Lobo, & Gonzalez, 2012; Lapornik, Prosek, & Wondra, 2005; Meneses, Martins, Teixeira, & Mussat, 2013). Coherently with the determined phenol content, the antioxidant activity in terms of TE (Table 2) slightly increased in the concentrated extract (30-40% with respect to the initial extract) and decreased in the dried extract (5-8% with respect to the concentrated extract). In contrast, the EC_{50} parameter revealed a slight increase in the antioxidant capacity (lower EC_{50} values) for both concentrated and dried samples, for both coffee and rice husk extracts. In this sense, it is remarkable that, although the antioxidant activity increases as the amount of phenolic compounds rises, other compounds present in the extracts may also affect this capacity. Thus, γ-oryzanol and tocopherol (Butsat & Siriamornpun, 2010; Wanyo et al., 2014), HMF (hydroxymethylfurfural) resulting from the decomposition of hexoses and pentoses derived from cellulose and hemicellulose (Piñeros-Castro & Otálvaro, 2014), or some proteins and peptides, could be present in the extracts at different concentrations (Narita & Inouye, 2012), affecting the total antioxidant activity.

The values of the EC_{50} parameter expressed in terms of the total solids of powdered extracts (also containing MD) that were used for the film production were 7.66 and 7.76 mg powder/mg DPPH for coffee and rice husk extracts, respectively. Andrade et al. (2012) reported similar antioxidant activity for coffee husk extracts obtained by supercritical fluid extraction with CO_2 and 8% of ethanol (5.25 mg extract solids/mg DPPH), and soxhlet extraction with dichloromethane (5.70 mg extract solids/mg DPPH). Other authors also reported antioxidant activity for the rice husk extracts in terms of the % inhibition of DPPH, with a wide range of values, depending on the extraction method and solvent used. For instance, 74.3-87.7% of DPPH inhibition was reported for rice husk treated with hot air, cellulase and FIR (Wanyo et al., 2014), about 25% for 25:75 water:ethanol extraction, about

78% for alkali extracts with NaOH or about 76% by acid hydrolysis with 2% of H_2SO_4 (Vadivel & Brindha, 2015).

Plant extracts containing polyphenols have been widely studied as to their antimicrobial activity against different Gram-positive and Gram-negative bacteria, yeast, fungi, and moulds (Guil-Guerrero et al., 2016). Some phenolic acids, flavonoids and tannins can destabilise the cytoplasmic membrane of the microorganisms, provoking the inhibition of microbial growth and cell death (de Oliveira et al., 2015; Guil-Guerrero et al., 2016; Sánchez-Maldonado, Mudge, Gänzle, & Schieber, 2014). The use of lignocellulosic waste as a source of potentially antimicrobial extracts is of great interest in order to exploit these kinds of by-products while providing them with potential food applications. This is in response to the growing interest in the use of natural antibacterial products for food preservation. In this sense, Kallel et al. (2014) found antimicrobial activity against *S. aureus* and *B. subtilis* for the 50:50 methanol:water extract from garlic. Likewise, Bonilla & Sobral (2016) found that the boldo leaf extract was effective against *E. coli* and *S. aureus*.

The antibacterial activity of the powdered extracts from coffee and rice husks against *L. innocua* and *E. coli* are shown in Table 2, in terms of their minimal inhibitory concentration (MIC, mg/mL). The coffee sample exhibited the greatest inhibitory effect against *E. coli,* which could be due to the expected presence of caffeic and chlorogenic acids, which are highly effective against this pathogen, as reported by Kallel et al. (2014). This action has been attributed to the diffusion of the undissociated acid through the membrane causing the acidification of the cytoplasm. However, no significant differences were observed in the MIC values of rice and coffee husk extracts against *L. innocua,* both being equally as active against this bacterium, at the same level as coffee husk extract against *E. coli.*

3.2. Properties of starch-based films containing active extracts and cellulosic fibres

This section discusses the effect of the incorporation of different proportions of coffee and rice husk extracts on the properties of the starch films, by substituting a determined fraction of the plasticizing glycerol. Likewise, the effect of adding cellulosic fibres, obtained from coffee or rice husk residue, to the best film formulation containing extract solids was analysed.

3.2.1. Microstructural analysis

This analysis allows for a better understanding of the differences in the physical properties of the films, since the microstructural arrangement of the film components greatly

determine the final physical and functional properties of the material (Talón et al., 2017a). Fig. 1 shows the FESEM micrographs of the surface and cross section of the starch films containing or not extract solids and/or cellulosic fibres from coffee or rice husks.

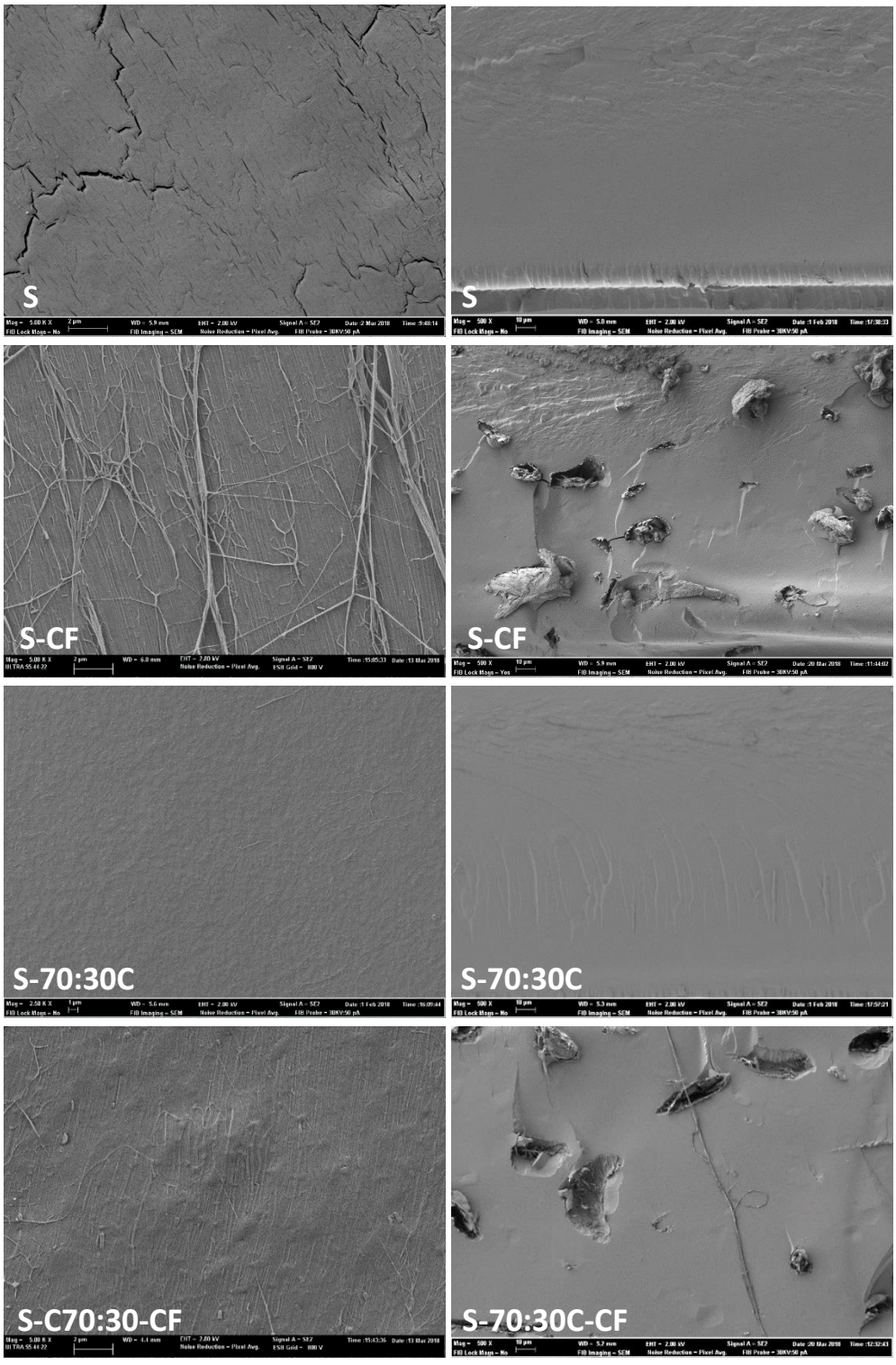

Fig. 1. (Continue).

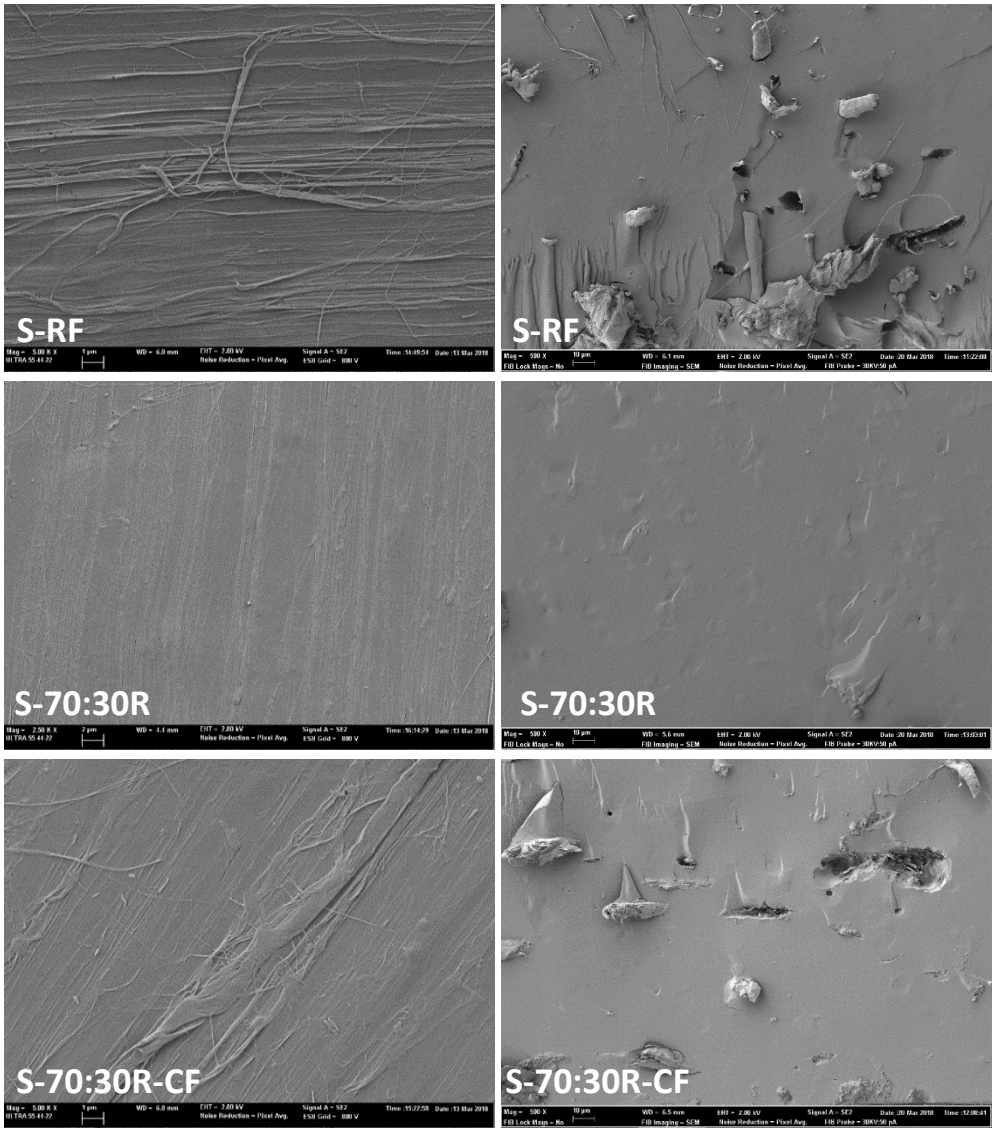

Fig. 1. FESEM micrographs of the surface (left, 5.000X) and cross section (right, 500X) of starch films with extract solids from coffee (S-70:30C) or rice (S-70:30R) husk, cellulose fibres from coffee (S-CF) or rice (S-RF) husk, or both components (S-70:30C-CF; S-70:30R-RF).

The net starch films showed the typical smooth structure, which was not apparently altered when the extract solid was incorporated at different proportions. In fact, the appearance of both the surface and cross section of the films containing extracts was even more homogenous. The ability of these kinds of active compounds to contribute to the formation of a more compact, homogeneous and ordered matrix has previously been observed in other studies (Montero, Rico, Rodriguez-Llamazares, Barral, & Bouza, 2017; Talón et al., 2017a).

The cellulose fibres can be clearly observed at the film surface in all formulations when these were incorporated. In these films, the quasi-parallel distribution of the fibres at surface level is remarkable, mainly in starch films without extract solids. This was also previously observed in these kinds of films (Collazo-Bigliardi et al., 2018b), which indicates a certain tendency of fibres to adsorb at the film surface, principally the finest ones. This was less marked in the films containing extract solids, where a smoother surface was observed, with the fibres better embedded in the matrix. This could be associated with the contribution of the extract compounds to the overall interactions in the matrix, which favoured the fibre integration within the polymer. In the film cross section, individualised uncoated fibres and infiltrated fibres are observed in all cases, but once again the presence of extract solids seems to enhance the fibre integration into the starch matrix. No notable differences at microstructural level could be observed between samples containing components from rice or coffee husks. Kargarzadeh, Johar, & Ahmad (2017) also showed that starchy materials can be infiltrated inside the fibre bundles when cellulose fibres from rice husk were incorporated into cassava starch films.

3.2.2. Tensile properties

Table 3 shows the tensile properties of the films (EM: Elastic Modulus; TS: Tensile Strength and E: Elongation at break point) conditioned at 53% RH and 25 °C for 1 week. The elastic modulus of the films increased as the ratio of extract solids grew. Thus, although the presence of these components in starch matrices allowed more homogeneous and stiffer matrices to be obtained, they were more brittle because the elongation at break was considerably reduced in comparison with the control sample (96 and 92%, respectively, for samples with 60:40 glycerol:extract solid ratio from coffee and rice samples). The larger the amount of glycerol substituted by the extract solids, the greater the enhancement of the film's stiffness and brittleness. This could be caused by the weak plasticizing effect of the different extract solids, but also by the formation of crosslinking effects between the starch hydroxyl groups and phenol or other groups of the extract compounds. The equilibrium moisture content, and thus its plasticising effect, also changed as a consequence of the incorporation of both extracts and fibres, ranging from 9.56 g/100 g dry film in S sample to 7.24-7.28 in samples with the highest amount of extracts, and 7.76-8.22 in samples with extracts and fibres.

The tensile strength at break (film resistance), also increased in proportion with the level of extract solids in the films, but was limited by the increase in the film's brittleness. Thus, films with a glycerol:extract solid ratio of 60:40 were the least resistant due to their very low degree of stretchability. Other authors (Bonilla, Talón, Atarés, Vargas & Chiralt, 2013) also obtained an increase of more than 15% in the EM with the addition of phenols from basil

essential oil in starch-chitosan matrices. However, Talón et al. (2017a) incorporated thyme extract into pure starch films, obtaining a decrease of ~30% in stiffness.

Table 3. Mean values and standard deviation of tensile properties (Elastic modulus: EM, tensile strength: TS and elongation at break: E), water vapour permeability (WVP) and oxygen permeability (OP) of starch films (S) with different ratios of glycerol:extract solids from coffee (C) or rice (R) husks, or cellulose fibres from coffee (CF) or rice (RF) husks, conditioned at 53% RH and 25 °C.

Formulation	EM (MPa)	TS (MPa)	E (%)	WVP ($g \cdot mm \cdot kPa^{-1} \cdot h^{-1} \cdot m^{-2}$)	OP x10^{14} ($cm^3 \cdot m^{-1} \cdot s^{-1} \cdot Pa^{-1}$)
S	77 ± 15^{a1}	5.2 ± 1.6^{a12}	64.9 ± 0.5^{d4}	14.9 ± 0.4^{c34}	10.4 ± 0.1^{e2}
S-80:20C	224 ± 20^{b}	7.0 ± 1.2^{b}	23.5 ± 4.6^{c}	11.3 ± 0.1^{ab}	4.8 ± 0.1^{d}
S-70:30C	344 ± 21^{c3}	9.2 ± 0.4^{cd3}	14.2 ± 1.1^{b1}	11.6 ± 0.4^{b1}	2.4 ± 0.2^{b1}
S-60:40C	516 ± 25^{e}	4.1 ± 1.2^{a}	2.5 ± 1.8^{a}	11.7 ± 1.0^{b}	1.4 ± 0.1^{a}
S-80:20R	234 ± 18^{b}	10.0 ± 1.0^{de}	24.3 ± 4.7^{c}	10.7 ± 0.2^{a}	4.7 ± 0.1^{d}
S-70:30R	348 ± 5^{c3}	12.1 ± 1.1^{e4}	18.3 ± 3.1^{bc2}	10.9 ± 0.4^{ab1}	2.7 ± 0.1^{c1}
S-60:40R	481 ± 22^{d}	7.6 ± 1.4^{bc}	5.4 ± 1.5^{a}	11.1 ± 0.1^{ab}	1.5 ± 0.2^{a}
S-CF	83 ± 6^{12}	4.5 ± 0.2^{1}	30.7 ± 2.7^{3}	14.8 ± 0.9^{34}	11.41 ± 0.3^{2}
S-70:30C-CF	386 ± 25^{4}	11.2 ± 1.2^{4}	12.9 ± 2.6^{1}	13.7 ± 1.7^{23}	2.4 ± 0.2^{1}
S-RF	104 ± 15^{2}	5.8 ± 0.5^{2}	29.7 ± 3.5^{3}	15.6 ± 0.9^{4}	10.5 ± 0.7^{2}
S-70:30R-RF	541 ± 16^{4}	12.1 ± 0.8^{4}	16.4 ± 3.6^{12}	12.2 ± 0.4^{12}	2.1 ± 0.9^{1}

Different superscript letters and numbers within the same column indicate significant differences among formulations ($p < 0.05$).

On the basis of the tensile behaviour of the films with extract solids, the best formulation was selected as that containing a 70:30 glycerol:extract solid ratio, since the films in which a higher of glycerol was substituted were excessively brittle. Then, the reinforcing effect of cellulosic fibre on these films was analysed and compared with its reinforcing effect on the net starch films. The addition of cellulose fibres also increased the EM of the material, mainly when extract solids were present in the films. In this sense, it is remarkable that rice husk fibres have a greater reinforcing capacity than coffee husk fibres in both the net starch matrix and the starch matrix with extract solids. When both components were incorporated, the EM increased, with respect to the control sample (S), by 600% for rice husk solids and

400% for coffee husk solids. Similar behaviour was observed by other authors after the incorporation of cellulose fibres into starch films (Kargarzadeh et al., 2017; Montero et al., 2017; Zainuddin, Ahmad, Kargarzadeh, Abdullah, & Dufresne, 2013). Some authors explain this increase in stiffness as the result of the interaction between the amylopectin chains and the cellulose in the matrix, while others relate it to the crystallinity associated with the hydrogen bonds of the cellulosic fraction (Montero et al., 2017; Zainuddin et al., 2013). The greater reinforcing capacity of both kinds of fibres (CF and RF) in the starch matrix containing extract solids (12 against 8% EM increase for CF and 57 against 35% for RF) revealed the better integration of fibres into the matrix containing extracts, as deduced from the qualitative FESEM observations. On the other hand, fibre (CF and RF) incorporation reduced the film's stretchability by about 50% in the net starch films, as previously reported by Kargarzadeh et al. (2017) for cassava starch films with rice husk cellulose fibres, but did not have a significant effect on this property for matrices containing extracts. In contrast, CF slightly enhanced the film's resistance to break in the matrices containing extracts, whereas there was no significant impact of fibre addition on this parameter for the other cases. Then, the reinforcing of starch matrices containing extracts with cellulosic fibres was more effective than that of net starch matrices, which could be associated with a compatibilizer effect of the extract compounds in the matrix. This supposes additional advantages in the formulation of active films, since better mechanical properties were obtained when cellulosic fibres were added.

3.2.3. Barrier properties

The water vapour permeability and oxygen permeability of the films are shown in Table 3. The addition of extract solids into starch matrices caused a significant decrease in the WVP and in OP. In comparison with the control film (S), the WVP of films containing extracts was reduced by near 30% regardless of the extract and its ratio in the film. In contrast, the reduction in the OP values was dependent on the amount of extract solids, ranging from 50 to 85% respect to the value of the S films, this being similar for both kinds of extracts (C or R). The lower degree of plasticization of the films with extract solids, due to the lower total glycerol content, could also contribute to the improvement in WVP, as well as the previously commented on crosslinking effect in the matrix. The great reduction in the OP values can be associated with the oxygen scavenging effect of the compounds with antioxidant capacity, in addition to the lower degree of plasticization of the films and the increase in the tortuosity factor associated with the crosslinking effect, which hinders mass transport. Similar behaviour (~50% reduction in OP) was found by Bonilla et al. (2013) in starch-chitosan matrices when 11% of α-tocopherol was added as antioxidant.

The incorporation of cellulose fibres did not have a significant effect on the water vapour and oxygen permeabilities. Although an increase in the tortuosity factor in the matrix could be expected from the dispersion of the fibres, the high water affinity of the cellulose could enhance the transport of water molecules through the polymer matrix. However, Wattanakornsiri, Pachana, Kaewpirom, Traina, & Migliaresi (2012) showed a reduction of ~63% in the WVP of cassava starch films after the addition of 8% cellulose fibres from recycled paper. This could be attributed to the differences in the amylose:amylopectin ratio, which could play a key role in the nanostructure of the matrix, producing a different effect of the fillers on the WVP of the films.

Table 4. Lightness (L*), chroma (C*), hue (h*), internal transmittance at 460 nm (Ti) and gloss (60°) values of the films with different ratios of glycerol:extract solids from coffee (C) and rice (R) husks and/or with cellulose fibres from coffee (CF) or rice (RF) husks.

Formulation	L*	C_{ab}*	h_{ab}*	T_i (460nm)	Gloss (60°)
S	73.8 ± 1.8^{f5}	12.7 ± 0.9^{a1}	88.8 ± 1.4^{f45}	0.82 ± 0.01^{f5}	28 ± 2^{e5}
S-80:20C	51.5 ± 0.6^{e}	29.5 ± 0.4^{f}	72.5 ± 0.4^{e}	0.49 ± 0.02^{e}	28 ± 3^{e}
S-70:30C	44.1 ± 0.8^{d3}	27.2 ± 1.0^{e6}	68.1 ± 0.5^{d3}	0.32 ± 0.03^{d3}	22 ± 2^{d34}
S-60:40C	36.3 ± 1.4^{a}	21.9 ± 1.6^{d}	58.0 ± 3.5^{a}	0.13 ± 0.05^{a}	16 ± 2^{bc}
S-80:20R	41.1 ± 1.2^{c}	21.9 ± 1.0^{d}	69.7 ± 1.0^{d}	0.34 ± 0.03^{d}	18 ± 3^{c}
S-70:30R	38.3 ± 3.0^{b2}	19.6 ± 1.9^{c4}	65.0 ± 3.0^{c2}	0.26 ± 0.07^{c2}	15 ± 3^{b2}
S-60:40R	35.1 ± 0.7^{a}	17.0 ± 0.8^{b}	61.6 ± 10^{b}	0.17 ± 0.01^{b}	10 ± 3^{a}
S-CF	70.4 ± 0.6^{4}	12.8 ± 0.3^{1}	89.3 ± 0.5^{5}	0.80 ± 0.01^{45}	24 ± 2^{4}
S-70:30C-CF	39.5 ± 1.0^{2}	22.9 ± 2.0^{5}	65.4 ± 1.4^{2}	0.25 ± 0.02^{2}	16 ± 2^{2}
S-RF	68.9 ± 1.2^{4}	14.9 ± 0.4^{2}	87.4 ± 0.6^{4}	0.78 ± 0.01^{4}	20 ± 3^{3}
S-70:30R-RF	35.2 ± 1.3^{1}	17.4 ± 0.9^{3}	63.0 ± 1.9^{1}	0.17 ± 0.02^{1}	11 ± 2^{1}

Different superscript letters and numbers within the same column indicate significant differences among formulations ($p < 0.05$).

3.2.4. Optical properties

Table 4 presents the values of lightness (L*), chroma (C*), hue (h*) and gloss of the different film formulations, as well as their internal transmittance (Ti) values at 460nm. Likewise, the Ti spectra for the different film formulations are shown in Fig. 2. The lightness value of the matrix decreases when fibres are added, especially after the addition of the extract solids. The presence of immiscible compounds generates heterogeneity in the refractive index in

the samples, which causes greater light dispersion and opacity. The incorporation of coloured components (extract solids) causes the selective absorption of light and the reduction of the transmission at low wavelengths. This also caused changes in the chromatic attributes, chroma and hue. The colour saturation (chroma) increased as with the extracts were incorporated, but decreased when their ratio rose in the films. Likewise, the hue values fell as the extract ratio rose in the formulation. These changes differed depending on whether they were coffee or rice extracts, the latter provoking a greater decrease in hue and less colour saturation, according to the colour difference of the extracts. Films containing rice husk extract also exhibited lower lightness values than those containing coffee husk extract.

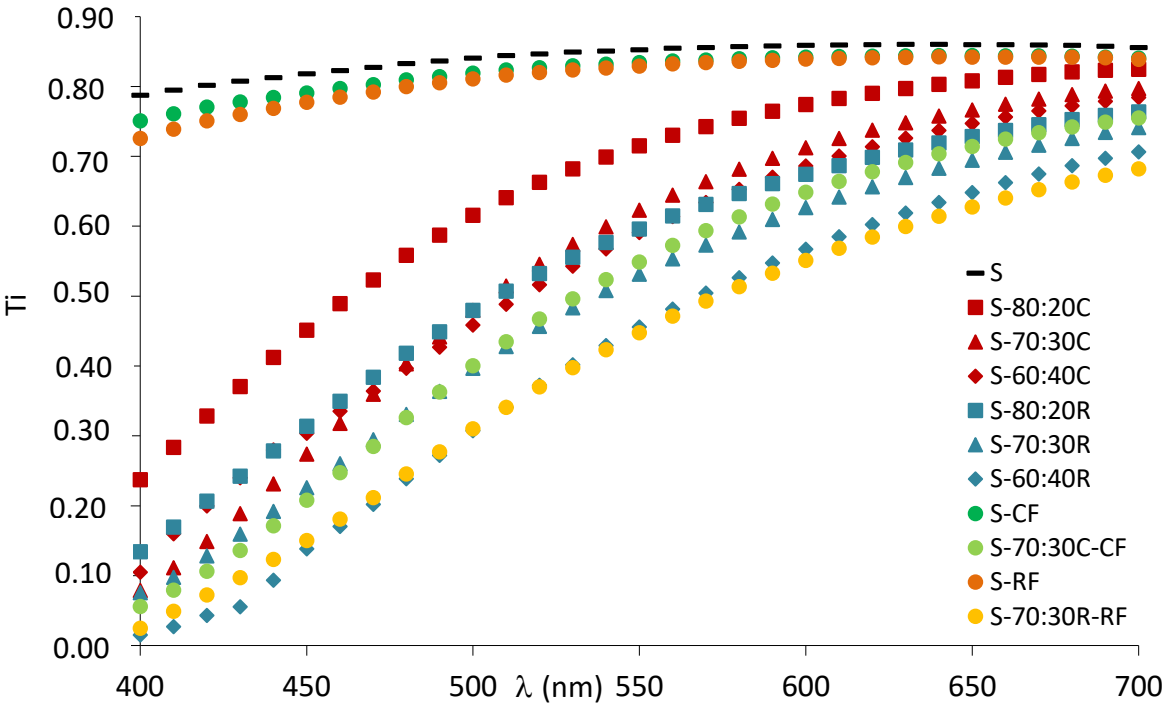

Fig. 2. Internal transmittance of studied formulations.

Fibre addition reduced the film transparency in both films (net starch and those containing extracts) and slightly modified the colour attributes, especially in coloured films with extracts. In general, fibre addition reduced the lightness, chroma and hue of the films, more markedly for films containing extracts due to the overlapped effect of light scattering. Therefore, films containing both solid extracts and fibres exhibited the lowest values of lightness and Ti, while presenting a brown coloration associated with the coloured extracts, with differences between coffee and rice husk extracts. Talón et al. (2017a) observed similar behaviour when thyme extracts were incorporated into starch matrices.

As regards the gloss, a decrease of about 40-60% with respect to the net starch film was observed when fibres and extract solids were incorporated into the films. However, fibre only led to a gloss reduction of about 27% compared to the respective film containing extracts, because extract solids also reduced the film's gloss. This effect can be attributed to the changes in the roughness of the surface of the films because of a heterogeneous distribution of the non-miscible components (Ortega-Toro et al., 2016).

3.2.5. Thermal behaviour

The temperature values of onset thermal degradation (T_{Onset}) and maximum degradation rate (T_{Peak}), obtained from TGA, as well as glass transition temperature (Tg; second heating scan), obtained from DSC analyses, are shown in Table 5. The Tg of starch was about 100 °C, similar to that reported by other authors for glycerol-plasticized corn starch films (Ortega-Toro et al., 2015 and 2016). When extract solids from rice or coffee husk were incorporated in different ratios, the Tg of the starch did not exhibit notable changes, which suggests the extract solids exert a similar plasticizing effect to that of the glycerol, since the latter was partially substituted to a different extent by the extracts in the different formulations. As expected, the addition of cellulose fibres did not provoke any notable changes in the starch Tg either, when compared with the control sample, since they are non-miscible in the polymer. Wattanakornsiri et al. (2012) report that the small variations in the starch Tg in cellulose composites could be attributed to the interaction between fibres and plasticizer, the composites becoming less plasticized than the pure matrix.

As regards the thermogravimetric analysis, Fig. 3 shows DTGA curves of the different formulations. A small weight loss occurred in every case at between about 70-150 °C, which can be attributed to the evaporation of bonded water in the polymer. This peak in the DTGA curves was slightly more marked in films containing fibres, according to the greater water binding capacity of cellulosic material. Likewise, a progressive, slow weight loss was observed until the start of the main degradation peak (mainly associated with the polymer degradation), which can be attributed to the thermal degradation of glycerol (Valencia-Sullca, Vargas, Atarés, & Chiralt, 2018) and/or the extract solids. In this sense, a more marked shoulder was detected at a temperature lower than the onset of the main thermo-degradation step for film formulations containing extract solids, both from coffee and rice husk products. This was reflected in the values registered for the onset temperature of the main peak, which notably decreased with respect to the films without extracts. However, no marked differences were observed for the main peak temperature, due to the addition of extracts or fibres. The main peak occurred at about 300°C and it is associated with the division of the main chains of starch (Zainuddin et al., 2013). The thermal degradation of cellulose fibres occurred at between 290-360 °C (Collazo-Bigliardi et al. 2018a), and the small

shoulder exhibited by the main peak at the higher temperature edge in samples containing fibres can be attributed to their final degradation. No remarkable differences can be observed for the thermal behaviour of coffee or rice husk products; however, coffee husk extracts seemed slightly more unstable than rice husk products (onset of degradation at a lower temperature).

Table 5. Mean values and standard deviation of onset and peak temperatures for thermal degradation of TPS films (conditioned at 53% RH and 25 °C) with different ratios of glycerol: solid extract from coffee (C) and rice (R) husks, with cellulose fibres from coffee (CF) or rice (RF) husks. Mean values and standard deviation of glass transition temperature (Tg) of dry samples were also shown.

	[40-126]°C		[235-340]°C		Second heating scan
Samples	**Onset (°C)**	**Peak (°C)**	**Onset (°C)**	**Peak (°C)**	**Tg (°C)**
S	45 ± 2^{a1}	88 ± 3^{a12}	264 ± 2^{d3}	299 ± 4^{b2}	96 ± 4^{ab1}
S-80:20C	71 ± 7^{b}	104 ± 4^{c}	250 ± 2^{c}	297 ± 2^{b}	91 ± 6^{a}
S-70:30C	101 ± 8^{c2}	119 ± 8^{d3}	237 ± 2^{a1}	285 ± 8^{a1}	94 ± 11^{a}
S-60:40C	95 ± 4^{c}	124 ± 2^{d}	247 ± 7^{bc}	294 ± 2^{b}	95 ± 3^{ab}
S-80:20R	45 ± 1^{a}	93 ± 3^{ab}	247 ± 5^{bc}	295 ± 1^{b}	108 ± 5^{ab}
S-70:30R	44 ± 1^{a1}	92 ± 2^{ab2}	252 ± 2^{c2}	294 ± 1^{b12}	101 ± 5^{ab}
S-60:40R	44 ± 1^{a}	97 ± 1^{bc}	240 ± 2^{a}	294 ± 1^{b}	108 ± 12^{ab}
S-CF	42 ± 1^{1}	87 ± 2^{12}	265 ± 1^{3}	297 ± 1^{2}	111 ± 10^{2}
S-70:30C-CF	48 ± 4^{1}	99 ± 8^{2}	250 ± 2^{2}	295 ± 1^{2}	95 ± 8^{1}
S-RF	42 ± 1^{1}	77 ± 1^{1}	263 ± 2^{3}	300 ± 1^{2}	97 ± 7^{1}
S-70:30R-RF	47 ± 3^{1}	95 ± 8^{2}	244 ± 8^{12}	333 ± 7^{3}	101 ± 4^{12}

Different superscript letters and numbers within the same column indicate significant differences among formulations ($p < 0.05$).

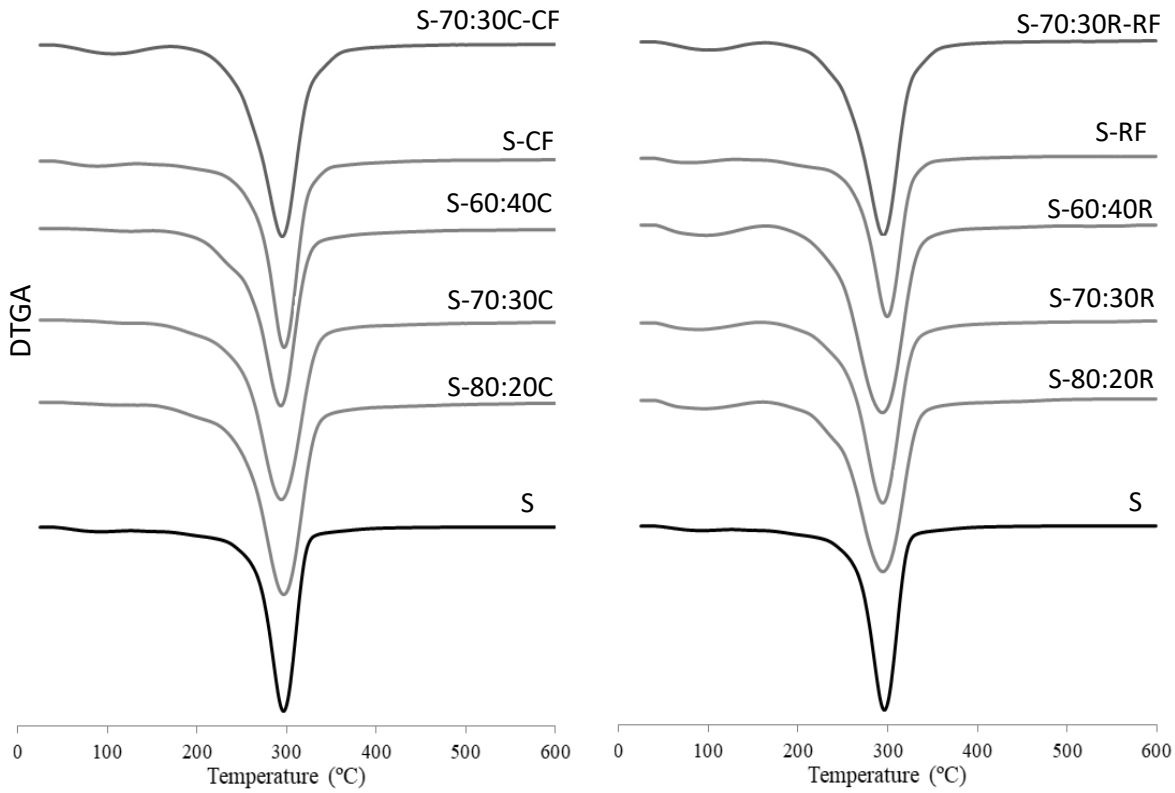

Fig. 3. DTGA curves of TPS films with different ratios of glycerol:extract solids from coffee (C) and rice (R) husks and with cellulose fibres from coffee (CF) or rice (RF) husks.

3.2.6. Antioxidant capacity

The antioxidant activity of the films containing different ratios of glycerol:extract solids, expressed in term of EC_{50} values, are shown in Table 6. As expected, the increase in the amount of active extracts added to the formulations led to films with better antioxidant capacity, associated with lower EC_{50} values. Formulations with coffee husk extracts presented greater antioxidant activity than samples with rice husk extracts, which was more clearly evidenced when the EC_{50} values were referred as mg of extract solids per mg DPPH (Table 6). In this case, a constant value would be expected for films with different extract solid ratios, which was observed for films with rice husk extract, but not for films with coffee husk solids. The decrease in the EC_{50} values, in terms of mg of solids, in line with the increase in the extract solid ratio, reveals that a part of the minor antioxidant compounds could be degraded during the thermal processing of the films. This would exert a milder effect on the total antioxidant capacity when a greater proportion of extract solids was present in the films. Likewise, a greater antioxidant activity was obtained for films with coffee husk extract than that expected from the values obtained for the isolated extract (Table 2). This suggests

changes in the extract composition during the film processing which enhanced the overall antioxidant activity of the extract in the films.

Several authors analysed the antioxidant capacity of starch films incorporating active extracts. Starch-chitosan matrices with thyme extract or tannic acid and thyme extract showed EC_{50} values of 3.5 kg film/mol DPPH and 0.9 kg film/mol DPPH, respectively (Talón et al., 2017a). Cassava starch films with 5, 10 and 20% of rosemary extract exhibited a DPPH inhibition of 28.6, 54.4 and 81.9%, respectively (Piñeros-Hernandez et al., 2017). The antioxidant capacity of the films depended on the kind and content of the different active compounds, since their activity varies widely: e.g. the EC_{50} values of tannic acid, resveratrol, ascorbic acid, gallic acid and caffeic acid were 0.0131, 0.7, 0.27, 0.08 and 0.1 mol/mol DPPH, respectively (Talón et al., 2017a).

Table 6. Antioxidant activity of films containing different ratios of glycerol: extract solids from coffee (C) and rice (R) husks expressed in terms of EC_{50} values.

Formulation	EC_{50} (mg film /mg DPPH)	EC_{50} (mg extract solids /mg DPPH)
S	-	-
S-80:20C	125.1 ± 9.8^{c}	4.7 ± 0.6^{c}
S-70:30C	79.1 ± 6.6^{b}	3.8 ± 0.3^{b}
S-60:40C	48.4 ± 1.3^{a}	3.21 ± 0.09^{a}
S-80:20R	172.5 ± 3.2^{d}	5.7 ± 0.3^{d}
S-70:30R	114.0 ± 0.7^{c}	5.47 ± 0.16^{cd}
S-60:40R	84.8 ± 3.6^{b}	5.3 ± 0.3^{cd}

Different superscript letters within the same column indicate significant differences among formulations ($p < 0.05$).

4. CONCLUSIONS

The incorporation of aqueous extracts and cellulose fibres from rice and coffee husks into thermoplastic starch films leads to improved functional properties as packaging materials, while exploiting these by-products. Both hydrothermal aqueous extracts exhibited antioxidant and antibacterial activity against *L. innocua* and *E. coli*, which provide the films with active properties. The active extracts improved the tensile properties of the starch

films, mainly when they were incorporated by substituting 30% of the plasticizing glycerol. Although the films became less stretchable, a relevant reinforcing effect was observed, with the EM increasing by about 350% for rice and coffee husk extracts. The incorporation of cellulosic fibres from both residues was more effective in films containing extract solids than in net starch films in terms of the reinforcing effect (EM increased by 600% for rice husk solids and 400% for coffee husk solids, respect to net starch films). This can be attributed to a certain compatibilizer effect of the extract compounds that allows for a better integration of the fibres in the starch matrices. Likewise, active extracts led to a 30% reduction in the WVP of starch films and a 50-85% reduction in the oxygen permeability, depending on the amount of extract. However, cellulose fibres at 5% were observed to have no effect on barrier properties. So, the incorporation of extracts and fibres produced films with improved tensile and barrier properties, which, in turn, were less transparent and brown. Then, they could have specific applications in the preservation of foods from light induced oxidation, which may be enhanced by their antioxidant activity. Specific *in vivo* tests would be required to assess their antibacterial action in different food matrices.

Acknowledgements

The authors thank the Ministerio de Economía y Competitividad (Spain) for the financial support provided through Project AGL2016-76699-R. The authors wish to thank Professor Yineth Piñeros-Castro PhD from Universidad Jorge Tadeo Lozano (Bogotá, Colombia) and Professor Misael Cortés PhD from Universidad Nacional de Colombia (Medellín, Colombia) for their assistance in the extraction process and spray drying. Authors also thank the Electron Microscopy Service of the UPV for their technical assistance.

REFERENCES

Aguiar, J., Estevinho, B. N., & Santos, L. (2016). Microencapsulation of natural antioxidants for food application - The specific case of coffee antioxidants - A review. *Trends in Food Science & Technology*, 58, 21-39.

Andrade, K. S., Gonçalvez, R. T., Maraschin, M., Ribeiro-do-Valle, R. M., Martínez, J., & Ferrerira, S. R. S. (2012). Supercritical fluid extraction from spent coffee grounds and coffee husks: Antioxidant activity and effect of operational variables on extract composition. *Talanta*, 88, 544-552.

ASTM. (1995). Standard test methods for water vapor transmission of materials. Standard Designations: E96-95. In Annual books of ASTM. pp. 406–413.Philadelphia: ASTM.

ASTM. (1999). Standard test method for specular gloss. In Designation (D523).annual book of ASTM standards, vol. 06.01. PA: American Society for Testing and Materials Philadelphia.

ASTM. (2001). Standard test method for tensile properties of thin plastic sheeting.In Standard D882. Annual book of American standard testing methods. pp.162–170. PA: American Society for Testing and Materials Philadelphia.

Balasundram, N., Sundram, K., & Samman, S. (2006). Phenolic compounds in plants and agri-industrial by-products: Antioxidant activity, occurrence, and potential use. *Food Chemistry*, 99, 191-203.

Bonilla, J., Talón, E., Atarés, L., Vargas, M., & Chiralt, A. (2013). Effect of the incorporation of antioxidants on physicochemical and antioxidant properties of wheat starch–chitosan films. *Journal of Food Engineering*, 118 (3), 271-278.

Bonilla, J., & Sobral, J. A. (2016). Investigation of the physicochemical, antimicrobial and antioxidant properties of gelatin-chitosan edible film mixed with plant ethanolic extracts. *Food Bioscience*, 16, 17-25.

Brand-Williams, W., Cuvelier, M. E., & Berset, C. L. W. T. (1995). Use of a free radical method to evaluate antioxidant activity. *LWT-Food Science and Technology*, 28(1), 25-30.

Brinch, L., Cotana, F., Fortunati, E., & Kenny, J. M. (2013). Production of nanocrystalline cellulose from lignocellulosic biomass: Technology and applications. *Carbohydrate Polym*ers, 94, 154-169.

Butsat, S., & Siriamornpun, S. (2010). Antioxidant capacities and phenolic compounds of the husk, bran and endosperm of Thai rice. *Food Chemistry*, 119, 606-613.

Collazo-Bigliardi, S., Ortega-Toro, R., & Chiralt, A. (2018a). Isolation and characterisation of microcrystalline cellulose and cellulose nanocrystals from coffee husk and comparative study with rice husk. *Carbohydrate Polymers*, 191, 205-215.

Collazo-Bigliardi, S., Ortega-Toro, R., & Chiralt, A. (2018b). Reinforcement of thermoplastic starch films with cellulose fibres obtained from rice and coffee husks *Journal of Renewable Materials*. In Press.

Cong-Cong, X., Bing, W., Yi-Qiong, P., Jian-Sheng, T., & Tong, Z. (2017). Advances in extraction and analysis of phenolic compounds from plant materials. *Chinese Journal of Natural Medicines*, 15(10), 721-731.

De Oliveira, K. Á. R., de Sousa, J. P., da Costa Medeiros, J. A., de Figueiredo, R. C. B. Q., Magnani, M., de Siqueira Júnior, J. P., & de Souza, E. L. (2015). Synergistic inhibition of bacteria associated with minimally processed vegetables in mixed culture by carvacrol and 1, 8-cineole. *Food Control*, 47, 334-339.

Dorta, E., Lobo, M. G., & Gonzalez, M. (2012). Reutilization of mango by-products: study of the effect of extraction solvent and temperature on their antioxidant properties. *Journal of Food Science*, 77, 80-88.

Guil-Guerrero, J. L., Ramos, L., Moreno, C., Zúñiga-Paredes, J. C., Carsama-Yepez, M., & Ruales, P. (2016). Antimicrobial activity of plant-food by-products: A review focusing on the tropics. *Livestock Science*, 189, 32-49.

Hutchings, J. B. (1999). Food color and appearance (2nd ed.). Gaithersburg, Maryland, USA: Aspen Publishers, Inc.

Kallel, F., Driss, D., Chaari, F., Belghith, L., Bouaziz, F., Ghorbel, R., & Chaabouni, S. E. (2014). Garlic (*Allium sativum L.)* husk waste as a potential source of phenolic compounds: Influence of extracting solvents on its antimicrobial and antioxidant properties. *Industrial Crops and Products*, 62, 34-41.

Kargarzadeh, H., Johar, N., & Ahmad, I. (2017) .Starch biocomposite film reinforced by multiscale rice husk fiber. *Composites Science and Technology*, 151, 147-155.

Lapornik, B., Prosek, M., & Wondra, A. G. (2005). Comparison of extracts prepared from plant by-products using different solvents and extraction time. *Jornal of Food Engineering*, 71, 214-222.

McHugh, T. H., Avena-Bustillos, R., & Krochta, J. M. (1993). Hydrophobic edible films: Modified procedure for water vapour permeability and explanation of thickness effects. Journal of Food Science, 58(4), 899-903.

Meneses, N. G. T., Martins, S., Teixeira, J. A., & Mussatt, S. I. (2013). Influence of extraction solvents on the recovery of antioxidant phenolic compounds from brewer's spent grains. *Separation and Purification Technology*, 108, 152-158.

Montero, B., Rico, M., Rodríguez-Llamazares, S., Barral, L., & Bouza, R. (2017). Effect of nanocellulose as a filler on biodegradable thermoplastic starch films from tuber, cereal and legumes. *Carbohydrate Polymer,* 157, 1094-1104.

Narita, Y., & Inouye, K. (2012). High antioxidant activity of coffee silverskin extracts obtained by the treatment of coffe silverskin with subcritical water. *Food Chemistry*, 135, 943-949.

Ng, H. M., Sin, L. T., Tee, T. T., Bee, S. T., Hui, D., Low, C. Y., & Rahmat, A. R. (2015). Extraction of cellulose nanocrystals from plant sources for application as reinforcing agent in polymers. *Composites Part B Engineering*, 75, 176-200.

Ortega-Toro, R., Contreras, J., Talens, P., & Chiralt, A. (2015). Physical and structural properties and thermal behaviour of starch-poly(e-caprolactone) blend films for food packaging. *Food Packaging and Shelf Life,* 5, 10-20.

Ortega-Toro, R., Collazo-Bigliardi, S., Talens, P., & Chiralt, A. (2016). Influence of citric acid on the properties and stability of starch-polycaprolactone based films. *Journal of Applied Polymer Science*, 42220, 1-16.

Ortega-Toro, R., Bonilla, J., Talens, P., & Chiralt, A. (2017). Starch-based materials in food packaging. In M. A. Villar, S. E. Barbosa, M. A. García, L. A. Castillo, & O. V. López (Eds.), Future of starch-based materials in food packaging (pp. 257-312). Elsevier.

Piñeros-Castro, Y., & Otálvaro, A. M. (2014). Use of lignocellulosic biomass, some research in Colombia. In Y. Piñeros-Castro, & J. Melo (Eds.), Antioxidant activity in liquids from pre-treatments with hot water carried out on rice husk (pp. 237-254). Bogotá. ISBN: 978-958-725-152-4.

Piñeros-Hernandez, D., Medina-Jaramillo, C., López-Córdoba, A., & Goyanes, S. (2017). Edible cassava starch films carrying rosemary antioxidant extracts for potential use as active food packaging. *Food Hydrocolloids*, 63, 488-495.

Sánchez-Maldonado, A. F., Mudge, E., Gänzle, M. G., & Schieber, A. (2014). Extraction and fractionation of phenolic acids and glycoalkaloids from potato peels using acidified water/ethanol-based solvents. *Food Research International*, 65, 27-34.

Shavandi, A., Bekhit, A. E. A., Saeedi, P., Izadifar, Z., Bekhit, A. A., & Khademhosseini, A. (2018). Polyphenol uses in biomaterials engineering. *Biomaterials*, 167, 91-106.

She, D., Nie, X., Xu, F., Geng, Z., Jia, H., Jones, G., & Baird, M. (2012). Physicochemical characterization of different alcohol-soluble lignin from rice straw. *Cellulose Chemistry and Technology*, 46 (3), 207-219.

Singleton, V. L., & Rossi, J. (1965). Colorimetry of total phenolics with phosphomolybdic-phosphotungstic acid reagents. *American Journal of Enology and Viticulture*, 16 (3), 144-158.

Talón, E., Trifkovic, K. T., Nedovic, V. A., Bugarski, B. M., Vargas, M., Chiralt, A., & González-Martínez, C. (2017a). Antioxidant edible films based on chitosan and starch containing polyphenols from thyme extracts. *Carbohydrate Polymers*, 157, 1153-1161.

Talón, E., Trifkovic, K. T., Vargas, M., Chiralt, A., & González-Martínez, C. (2017b). Release of polyphenols from starch-chitosan based films containing thyme extract. *Carbohydrate Polymers*, 175, 122-130.

Vadivel, V., & Brindha, P. (2015). Antioxidant property of solvent extract and acid/alkali hydrolysates from rice hulls. *Food Bioscience*, 11, 85-91.

Valencia-Sullca, C., Vargas, M., Atarés, L., & Chiralt, A. (2018). Thermoplastic cassava starch-chitosan bilayer films containing essential oils. *Food Hydrocolloids*, 75, 107-115.

Wanyo, P., Meeso, N., & Siriamornpun, S. (2014). Effects of different treatments on the antioxidant properties and phenolic compounds of rice bran and rice husk. *Food Chemistry*, 157, 457-463.

Wattanakornsiri, A., Pachana, K., Kaewpirom, S., Traina, M., & Migliaresi, C. (2012). Preparation and properties of green composites based on tapioca starch and differently recycled paper cellulose fibers. *Journal of Polymers and the Environment*, 20, 801-809.

Zainuddin, S. Y. Z., Ahmad, I., Kargarzadeh, H., Abdullah, I., Dufresne, A. (2013). Potential of using multiscale kenaf fibers as reinforcing filler in cassava starch- kenaf biocomposites. *Carbohydrate Polymers*, 92(2), 2299-2305.

Chapter IV

Using grafted poly(ε-caprolactone) for the compatibilization of starch-polylactic acid blends

[1]**Sofía Collazo-Bigliardi;** [2]Rodrigo Ortega-Toro; [1]Amparo Chiralt

Reactive and Functional Polymers. Under Review

[1]Institute of Food Engineering for Development, Universitat Politècnica de València. Valencia, Spain

[2]Food Engineering Program, Faculty of Engineering, Universidad de Cartagena. Cartagena de Indias, Colombia

socol@doctor.upv.es

ABSTRACT

Starch-PLA blend films were obtained by melt blending and compression moulding using grafted polycaprolactone with maleic anhydride and/or glycidyl methacrylate (PCL_{MG} or PCL_G) as compatibilizers. The effect of both the PLA ratio in the blend (20 and 40% with respect to starch) and the amount of both compatibilizers (2.5 and 5%) on the film properties was analysed. Compatibilized blends presented a better dispersion of the PLA in the continuous starch phase, but the use of PCL_G provoked a phase inversion in the matrix when 40% of the starch was substituted by PLA. The compatibilized blend films exhibited higher values of elastic modulus than pure starch films, but were less extensible. The use of compatibilizers did not affect the film's water vapor permeability, which was reduced by up to 33 or 50% for 20 and 40% PLA, respectively, although inverted films with 40% PLA and 5% PCL_G, exhibited marked reduction (67%). Compatibilizers decreased the oxygen permeability of the films by about 50%, regardless of the ratio of PLA and the kind and amount of compatibilizer. Therefore, substituting 20% of the starch by PLA and incorporating 5% of PCL_G would be a good strategy to obtain films useful for food packaging.

Keywords: Starch; Polylactic acid; Grafted polycaprolactone; Compatibilizers; Blend films.

1. INTRODUCTION

Food packaging involves a high consumption of conventional plastics which generate large amounts of waste. These kinds of materials are the most widely used in the food industry due to their great versatility and optimum characteristics for food packaging. Nowadays, an important challenge is to develop different materials that contribute to minimising the environmental impact of petroleum-based plastics, making use of renewable sources, such as biopolymers [1, 2]. One of the most important groups of biodegradable polymers obtained from renewable resources is polysaccharides. These biopolymers are extracted directly from biomass and, depending on their origin, different types of starch, cellulose, chitosan, gums or alginates can be found [3,4]. Another predominant group of bioplastics is those obtained by synthesis from biobased monomers, such as polylactic acid (PLA), or non-biobased monomers, such as poly (ε-caprolactone) (PCL), polyvinyl alcohol (PVA) or polybutylenosuccinate (PBS) [5, 6].

Starch made up of a different amylose-amylopectin ratio is the most widely studied sustainable thermoplastic biopolymer for food packaging applications since it is suitable for food contact, abundant, low cost and can be processed as a thermoplastic polymer. Thermoplastic starch (TPS) exhibits an excellent filmogenic capacity, forming homogeneous and transparent films, with high barrier capacity for oxygen, carbon dioxide or lipids [7]. However, it has certain drawbacks that limit its potential application, such as its high degree of water sensitivity and water vapour permeability, its limited mechanical properties and instability due to retrogradation during storage [8]. Different strategies have been used for the purposes of improving these properties: adding reinforcing agents [9, 10], incorporating cross-linking agents, such as citric acid, adding plasticizers to reduce intermolecular forces and increase flexibility or blending with other polymers [11]. As concerns the blends, the mixtures with more hydrophobic polymers, such as polylactic acid (PLA), have been widely studied in order to minimize the drawbacks of starch, although the lack of polymer compatibility makes the use of compatibilizers necessary [12].

Polylactic acid is linear aliphatic thermoplastic polyester derived from lactic acid, which is obtained from the fermentation of renewable and biodegradable sources (corn or rice starch and raw materials with high sugar content). It can be produced by the chemical conversion of these carbohydrate sources into dextrose; the dextrose is fermented to lactic acid followed by the polycondensation of lactic acid monomers [3]. PLA is biodegradable, renewable and biocompatible; it is also transparent and has excellent water vapor barrier properties [13]; these characteristics are comparable to those of petroleum-based plastics, such as polyethylene terephthalate (PET) or polystyrene (PS). Due to the new technologies available in the area of industrial production, the PLA has a very competitive price on the

market. However, it has certain limitations, such as the fact that it has a low oxygen barrier capacity and is brittle, despite being highly resistant to traction [14].

Both PLA and starch materials have opposite barrier and mechanical properties and the possibility of combining them to obtain matrices with improved properties can counteract the disadvantages shown by pure polymers. However, their thermodynamic immiscibility gives rise to blends with phase separation that limits their effectiveness as packaging materials [15]. To improve the interfacial adhesion between the starch and hydrophobic polymer phases, compatibilizers, with an adequate fraction of polar and non-polar groups, have been added to promote polymer interfacial interaction, thus improving the properties of the blends. For this purpose, S-PLA blends have been compatibilized with citric acid (wheat flour-PLA), methylene diphenyl diisocytane (wheat starch-PLA), stearic acid (corn starch-PLA), maleic anhydride (potato starch-PLA), dicumyl peorxyde and maleic anhydride (corn starch-PLA), adipate or citrate esters (cassava starch-PLA), formamide (corn starch-PLA), maleic anhydride and epoxidized soybean oil (corn starch-PLA), among others [12]. Le Bolay et al. [16], combine PLA and starch in composite materials avoiding the use of compatibilizers or plasticizers through co-grinding, reducing the hydrophilic nature of the blend and the starch's polar energy component.

In previous studies [17], biodegradable polyesters, such as poly-ε-caprolactone (PCL) were functionalized with polar groups, such as epoxide or anhydride, capable of positively interacting with the hydroxyl groups of the starch chains, exerting a positive effect on the polymer's miscibility. These compounds, therefore, act as coupling agents between both materials, improving their compatibility.

The aim of this study was to analyse the effectiveness of PCL, functionalized by grafting with maleic anhydride and/or glycidyl methacrylate, at improving the properties of blend films based on corn starch and PLA, obtained by melt blending and compression moulding. Films were characterized as to their microstructure, thermal behavior and functional properties (mechanical, optical and barrier). The effect of the PLA ratio in the blend, as well as the amount of both compatibilisers, was analyzed in order to select the best formulation for food packaging applications.

2. MATERIALS AND METHODS

2.1. Materials

Corn starch was provided by Roquette (Roquette Laisa, Benifaió, Spain), glycerol was obtained from Panreac Química, S.A. (Castellar del Vallès, Barcelona, Spain) and amorphous

PLA 4060D, density of 1.24 g/cm3, was purchased from Natureworks (U.S.A). For the chemical modification of PCL (pellets ~3 mm, average Mn 80.000 Da, glycidyl methacrylate (G) (purity 97%), maleic anhydride (M) (purity 99.8%) and benzoyl peroxide (BP) were supplied by Sigma (Sigma-Aldrich Chemie, Steinheim, Germany). Phosphorus pentoxide (P_2O_5) and magnesium nitrate-6-hydrate ($Mg(NO_3)_2$), for sample conditioning, were obtained from Panreac Química, S.A. (Castellar del Vallès, Barcelona, Spain).

2.2. Chemical modification of PCL

The chemical modification of PCL by radical grafting reaction was carried out according to the methodology described by Ortega-Toro et al. [17] and Laurienzo et al. [18]. A Brabender plastograph (EC Plus, Duisburg, Germany) was used for the reaction, where 45 g of PCL, 2.5 g of M, 0.5 g of BP and 2.5 g of G were incorporated into the mixer at 100 °C and maintained for 20 min at 32 rpm to functionalise the PCL with maleic anhydride and glycidyl methacrylate (PCL_{MG}). Modified PCL_{MG} was dissolved in 500 mL of chloroform and subsequently re-precipitated in excess of hexane, with the aim of removing any ungrafted reagents. The PCL functionalization with glycidyl methacrylate only (PCL_G) was performed with 45 g of PCL, 0.5 g of BP and 5 g of G. The reaction and purification were carried out following the same process previously described for PCL_{MG} synthesis. Both materials were kept in desiccator under vacuum for 12 h at 25 °C, and frozen stored (-40 °C) before using.

2.3. Experimental design and film preparation

Twelve film formulations were obtained: glycerol plasticized starch (S), pure PLA, and S-PLA blends with and without PCL_G or PCL_{MG} compatibilizers. Two levels of PLA in the blend films were considered (20 and 40% of starch substitution). In all films, glycerol was incorporated as 30 wt% of the starch and compatibilizers (PCL_G or PCL_{MG}) were added as 2.5 or 5% of the total polymers (S plus PLA). The mass fraction of each component in the dry blends and their sample identification codes are shown in Table 1.

The melt blending process was carried out in an internal mixer (HAAKE™ PolyLab™ QC, Thermo Fisher Scientific, Germany) at 160 °C, 50 rpm, for 10 min and 50 g of blend were processed in each batch. The obtained pastes were cut into pellets and conditioned at 25 °C and 53% relative humidity (RH) for one week before the compression moulding to obtain the films. To this end, a hot plate press (Model LP20, Labtech Engineering, Thailand) was used. 4 g of the conditioned pellets were placed onto Teflon sheets and preheated for 3 min at 160 °C and compression moulded for 1 min at 30 bars, followed by 3 min at 130 bars; thereafter,

a 3 min cooling cycle was applied. Films were conditioned at 25 °C and 53% RH for 1 week before their characterisation.

Table 1. Mass fraction (Xi, g compound/g dried Film) of the different components: Starch (S), glycerol (Gly), grafted poly(ε-caprolactone) with glicidyl methacrylate (PCL_G), grafted poly(ε-caprolactone) with maleic anhydride and glycidyl methacrylate (PCL_{MG}) and polylactic acid (PLA) at 20 or 40 wt% of starch.

Formulations	X_S	X_{Gly}	X_{PCL-G}	X_{PCL-MG}	X_{PLA}
S	0.7692	0.2308	-	-	-
PLA	-	-	-	-	1.0000
S PLA_{20}	0.6667	0.200	-	-	0.1333
S($PCL_{2.5G}$)PLA_{20}	0.6536	0.1961	0.0196	-	0.1307
S(PCL_{5G})PLA_{20}	0.6410	0.1923	0.0385	-	0.1282
S($PCL_{2.5MG}$)PLA_{20}	0.6536	0.1961	-	0.0196	0.1307
S(PCL_{5MG})PLA_{20}	0.6410	0.1923	-	0.0385	0.1282
S PLA_{40}	0.5882	0.1765	-	-	0.2353
S($PCL_{2.5G}$)PLA_{40}	0.5764	0.1729	0.0202	-	0.2305
S(PCL_{5G})PLA_{40}	0.5650	0.1695	0.0395	-	0.2260
S($PCL_{2.5MG}$)PLA_{40}	0.5764	0.1729	-	0.0202	0.2305
S(PCL_{5MG})PLA_{40}	0.5650	0.1695	-	0.0395	0.2260

2.4. Film characterisation

2.4.1. Field emission scanning electron microscopy (FESEM)

A Field Emission Scanning Electron Microscope (FESEM Ultra 55, Zeiss, Oxford Instruments, U.K) was used to analyse the cross-section microstructure of the films. Samples were maintained in desiccators with P_2O_5 for 2 weeks at 25 °C, then, film samples were fractured and adequately placed on support stubs and coated with platinum. Observations were carried out at 1.5 kV.

2.4.2. X-Ray diffraction

The X-Ray diffraction patterns of the different samples were obtained by means of a diffractometer (XRD, Bruker AXS/D8 Advance) between 2θ: 5° and 30° with a step size of 0.05, using Kα Cu radiation (λ: 1.542 Å), 40 kV and 40 mA. The degree of crystallinity (Xc) of the samples was estimated from the ratio of crystalline peak areas and the integrated area of XR diffractograms and expressed as a percentage, using OriginPro 8.5 software, assuming

Gaussian profiles for crystalline and amorphous peaks, as was reported by Ortega-Toro et al. [19].

2.4.3. Attenuated Total Reflectance-Fourier Transform Infrared (ATR-FTIR) spectroscopy

The chemical groups in the films were identified through vibration type by the attenuated reflectance ATR-FTIR analysis (Nicolete 5700, Thermo Fisher Scientific Inc., MA, USA) in the range of 4000-400 cm^{-1} with a resolution of 4 cm^{-1}. Samples were recorded as an average of 64 scans.

2.4.4. Thermal behaviour

Differential Scanning Calorimetry (DSC 1 Star^e System, Mettler-Toledo Inc., Switzerland) was performed to analyse the phase transitions in the polymer matrices. Samples (7-9 mg) were placed into aluminium pans and sealed and the lid was perforated to ease the sample water release. They were submitted to a heating cycle from 25 °C to 160 °C; a cooling step from 160 °C to 25 °C, and a second heating cycle till 160 °C, all of which at 10 °C/min. In the first scan, the bonded water in the film was eliminated and, in the second heating cycle, the glass transition of starch and PLA was analysed.

The thermal stability of the samples was examined using a Thermogravimetric Analyzer TGA 1 Star^e System analyser (Mettler-Toledo, Inc., Switzerland). Samples (3-4 mg) were heated from 25 to 600 °C at 20 °C/min under nitrogen atmosphere (gas flow: 10 $mL.min^{-1}$). Initial degradation temperature (T_{Onset}) and peak temperature (T_{Peak}) were studied using the STAR^e Evaluation Software (Mettler-Toledo, Inc., Switzerland), from the first derivative of the resulting weight loss curves.

2.4.5. Tensile properties

A universal test machine (TA.XTplus model, Stable Micro Systems, Haslemere, England) was used to study the tensile properties of the films following the ASTM standard method D882 [20]. Conditioned samples (25 °C, 53% RH) of 25 mm x 100 mm were mounted in the film-extension grips of the testing machine and stretched at 50 mm/min until break. Ten replicates were performed for each film formulation. Elastic modulus (EM), tensile strength at break point (TS) and the elongation at break (ε) of the films were determined from the stress-strain curves. The film thickness was taken into account for the calculations.

2.4.6. Oxygen permeability (OP), water vapour permeability (WVP) and moisture content

Oxygen barrier was determined in samples conditioned at 25 °C and 53% RH by using OX-TRAN equipment, Model 2/21 ML (Mocon Lippke, Neuwied, Germany). A 50 cm^2 film area was used and the thickness was considered in all cases to obtain the OP values. The oxygen transmission values were evaluated every 10 min until equilibrium.

The water vapour permeability (WVP) of the films was determined from a modification of the gravimetric method E96-95 [21, 22]. For this purpose, Payne permeability cups (Elcometer SPRL, Hermelle/s Argenteau, Belgium), 3.5 cm in diameter, were used. 5 mL of bidistilled water was added inside the cups and the film was fitted. Each cup was placed into a desiccator with 53% RH by using a saturated solution of magnesium nitrate. This was placed into a chamber with controlled temperature at 25 °C. The cups were weighed periodically (±0.0001 g) and the water vapour transmission rate (WVTR) was determined from the regression analysis of weight loss data *vs.* time. From this data, WVP was obtained as described by Ortega-Toro et al. [19].

The equilibrium moisture content of the conditioned films was obtained by the sample drying in a natural convection oven (J.P. Selecta, S.A. Barcelona, Spain) for 24 h at 60 °C. Then, they were placed in a desiccator at 25 °C with P_2O_5 (0% RH) for one week to lead the water content to a value of nearly 0. The moisture content of each sample was calculated from the total weight loss of conditioned samples, and expressed as a percentage of dry solids.

2.4.7. Optical properties

The internal transmittance (Ti) of the films, related with the sample transparency, was obtained by applying the multiple scattering Kubelka-Munk theory [23]. Ti (eq. 1) was determined from the reflection spectra (400-700 nm) with a spectorocolorimeter CM-3600d (Minolta Co., Tokyo, Japan) on black and white backgrounds. Internal transmittance at 460 nm was chosen to compare the values of the samples.

$$T_i = \sqrt{(a - R_0)^2 - b^2} \quad (1)$$

where R_0 is the reflectance of the film on the ideal black background. The parameters a and b were calculated by eqs. (2) and (3).

$$a = \frac{1}{2}\left(R + \frac{R_0 - R + R_g}{R_0 R_g}\right) \quad (2)$$

$$b = \sqrt{a^2 - 1} \quad (3)$$

where *R* is the reflectance of the sample layer backed by a known reflectance R_g.

The gloss of the samples was measured at an incidence angle of 85°, following the ASTM standard D523 method [24], using a flat surface gloss meter (Multi-Gloss 268, Minolta, Germany). All results are expressed as gloss units (GU), relative to a highly polished surface of black glass standard with a value near to 100 GU.

2.5. Statistical analysis

Statgraphics Centurion XVI software (Manugistics Corp., Rockville, Md.) was used to perform the statistical analyses of the results by means of analysis of variance (ANOVA). Fisher's least significant difference (LSD) procedure was used at the 95% confidence level.

3. RESULTS AND DISCUSSION

3.1. Micro- and nano-structural properties

Fig. 1 shows the FESEM micrographs of the cross-section of S-PLA blends with and without compatibilizers at both PLA proportions. In almost the all blend films, PLA domains appear dispersed in the continuous starch matrix, except films with 40% PLA and PCL_G at 2.5 and 5%, in which PLA formed the continuous phase while starch domains were dispersed and densely packed in the PLA phase. The PLA phase (dispersed or continuous) exhibited less brittle fracture behaviour than that observed for the starch phase, showing some flakes typical of a more rubbery material. In the non-compatibilized samples, films with 40% PLA show the greatest number of PLA domains with a more flaky structure, interrupting the starch matrix. The lack of a complete adhesion between the S-PLA phases at the interface can be observed in both non-compatibilized blends due to the non-compatible nature of both polymers [25]. The incorporation of both compatibilizers into the blends provoked a positive change in the film structure, with a notable reduction in the size of the PLA domains and with a better adhesion between both polymers, which reveals the flattering effect of the compatibilizers.

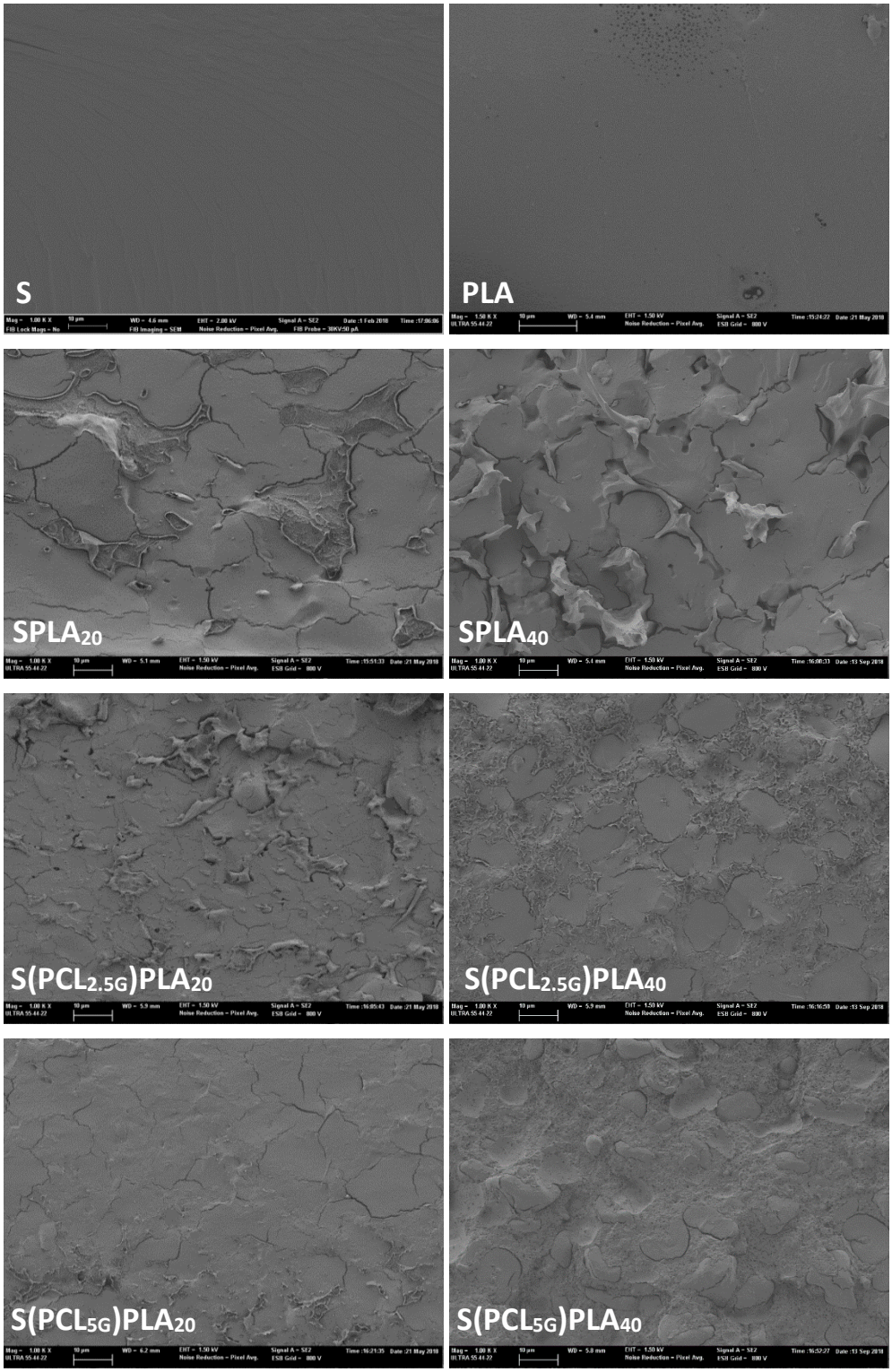

Fig. 1. (Continue).

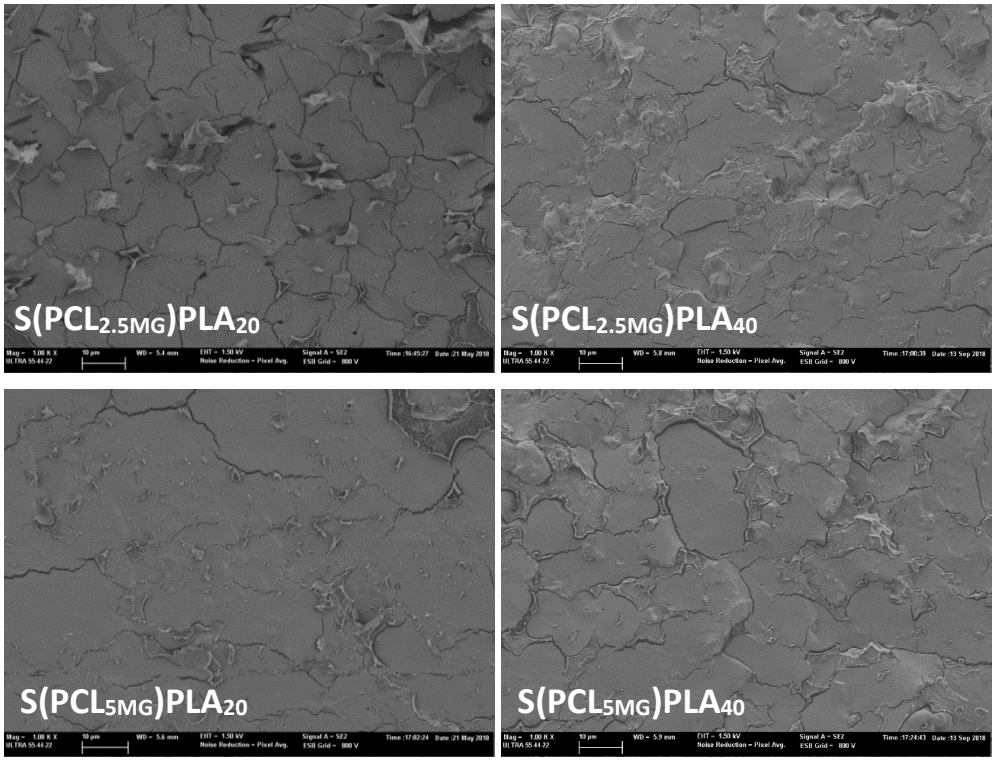

Fig. 1. FESEM micrographs of the cross-section of S-PLA films with 20 or 40 wt% PLA, compatibilized or not with 2.5 and 5% of PCL_G or PCL_{MG}.

In blends with 20% PLA, this effect was more marked for the highest amount of both compatibilizers and films with 5% of PCL_G exhibited the most homogenous structure, with the best dispersion level of PLA in the starch matrix. For films with 40% PLA, different polymer interactions were promoted by PCL_G and PLC_{MG}, provoking a phase inversion in the case of PCL_G. At both concentrations, the incorporation of PCL_G led to a PLA continuous phase where the starch domains were embedded in the PLA matrix, this being clearer at the highest level of compatibilizer. In this case, despite the higher proportion of starch in the blends, its domains appeared well separated, which suggests that a part of the starch was fully compatibilized with PLA. So, the kind of compatibilizer and its percentage in the blends, as well as the polymer ratio, affected the microstructure of the blend films. The interactions between the hydroxyl groups of the starch chains and the hydroxyl, carboxyl or anhydride groups grafted in the PCL chain contributed to polymer compatibilization, as also reported by Ortega-Toro et al. [17] and Haque et al. [26] for other starch-polyester blends compatibilized with PCL_G or PCL_{MG}. Orozco et al. [27] also observed a good compatibilizing effect for PLA functionalized with maleic anhydride on blend films of potato starch and PLA. All the compatibilized blends reflected better adhesion properties between PLA and starch, based on the interactions between the polar groups grafted in the PLA chain and starch.

In order to analyze the effect of compatibilization on polymer crystallization in the films, Fig. 2 shows the X-ray diffraction patterns as well as the percentage of crystallinity of the different films. PLA did not show crystalline peaks, coherent with their initial amorphous nature, whereas starch films exhibited three typical crystalline peaks at 2θ values of around 12.9°, 17.1° and 19.8°, attributed to the crystalline form of amylose type V as reported by other authors [8, 19, 28, 29]. The amylose V-type structure can be Vh (hydrated) with diffraction peaks at 12.6° and 19.4°, and Va (anhydrous) with peaks at 13.2° and 20.6°, which are formed by the crystallization of amylose in single helices involving glycerol or lipids [14, 17]. Blend films only exhibited the crystalline peaks of V-type amylose, thus revealing that only this polymer crystallized in the blends and no induced crystallization of PLA occurred. The characteristic crystalline peaks of PCL are around 2θ of 21.6°, 22.2° and 23.3° [17] and these peaks were not observed in any compatibilized sample. This can be due to the relatively low proportion of PCL in the blends, or to the inhibition of crystallization brought about by the anchoring of the polar groups and their interfacial location. Then, the crystallization pattern of the starch in blend samples was not altered by the presence of amorphous PLA and/or compatibilizers. As regards the degree of crystallinity, the incorporation of PLA with and without compatibilizers slightly enhanced amylose crystallization, since taking the global reduction of the film's starch ratio into account, the degree of crystallinity with respect to that of net starch films increased by about 1% in the blends with 20 or 40% PLA. Likewise, the incorporation of compatibilizers promoted the crystallinity of starch up to about 6 (with 40% PLA) or 7% (with 20% PLA), when referred per mass unit of starch. This could be attributed to a specific nucleating effect of the compatibilizer, enhancing the crystallization capacity of the amylose chains. The degree of crystallinity affects the film properties, such as stiffness, resistance, stretchability or brittleness and barrier properties, among other aspects.

FTIR analysis was carried out to assess potential differences in the chemical interactions between the film components, especially when compatibilizers were present. Fig. 3 shows the FTIR-ATR spectra of pure S and PLA and of the different blend films with and without different ratios of compatibilizers. The starch sample spectrum shows the characteristic broadband at around 3280 cm^{-1} which corresponds to stretching vibration types of -OH groups of amylose, amylopectin, glycerol and adsorbed water. Other bands relative to starch are identified at 2925 cm^{-1} and 1076-923 cm^{-1}, associated with C-H and C-O stretching, respectively; the peaks at 860, 760 and 570 cm^{-1} are assigned to the vibrational absorption peaks of the C-H bond [14, 27]. Another characteristic broad peak at 1645 cm^{-1} was observed, concerning the vibration mode of water molecules that are tightly absorbed in the amorphous regions of starch; this did not appear in the pure PLA sample in line with its more hydrophobic nature and appeared with lower relative intensity in the compatibilized blends [17]. In the PLA spectrum, the C=O stretching vibrations and the vibrations of C-O bonds of ester groups display peaks at 1745 and 1267 cm^{-1}, respectively. The peak at 863 cm^{-1} is

attributed to the -C-C- stretching of the amorphous phase and peaks at 1452 and 1361 cm^{-1} are related to the deformation vibrations of the $-CH_2-$ and $-CH_3$ groups, respectively. The -C-O-C- stretching of the ester groups (1182 cm^{-1}), the C-O stretching (1128 and 1078 cm^{-1}) and the -OH bending (1039 cm^{-1}) are also observed [30, 14].

In S-PLA blend films, the combination of characteristic peaks of each polymer was observed in the same spectrum, with the corresponding changes in the relative intensity. A slight displacement of the carbonyl peak of PLA from 1745 (net PLA) to 1747 or 1749 cm^{-1} (S-PLA films), was observed in non-compatibilized blends. This displacement was more marked in the compatibilized blends (1751-1755 cm^{-1}) and may be attributed to the different chain interactions promoted in the blends with or without compatibilizers and suggests that the presence of functionalized PCL affected the packing of the PLA chains. No peaks associated with the functionalized PCL were observed in the compatibilized samples due to its lower proportion in the blends. The carbonyl PCL peak could overlap with the carbonyl band of PLA and no typical bands of the grafted compounds were observed. The PCL_{MG} spectrum exhibited peaks at 1780 and 1850 cm^{-1} attributed to the stretching of the carbonyl group of the grafted anhydride, and the PCL_G spectrum shows a characteristic peak at 910 cm^{-1} related to the stretching vibration of epoxy ring C-O bonds [30, 17].

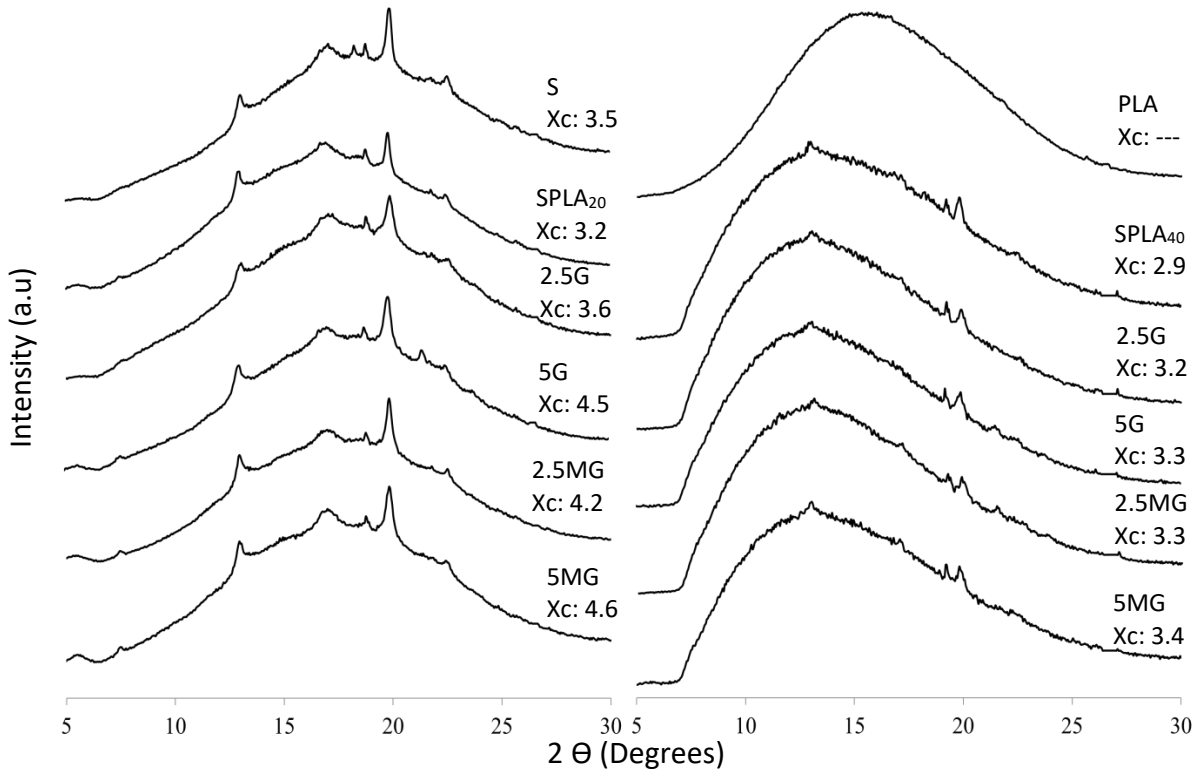

Fig. 2. X-ray diffraction patterns and degree of crystallinity (Xc, %) of S-PLA films with 20 or 40 wt% PLA, compatibilized or not with 2.5 and 5% of PCL_G or PCL_{MG}.

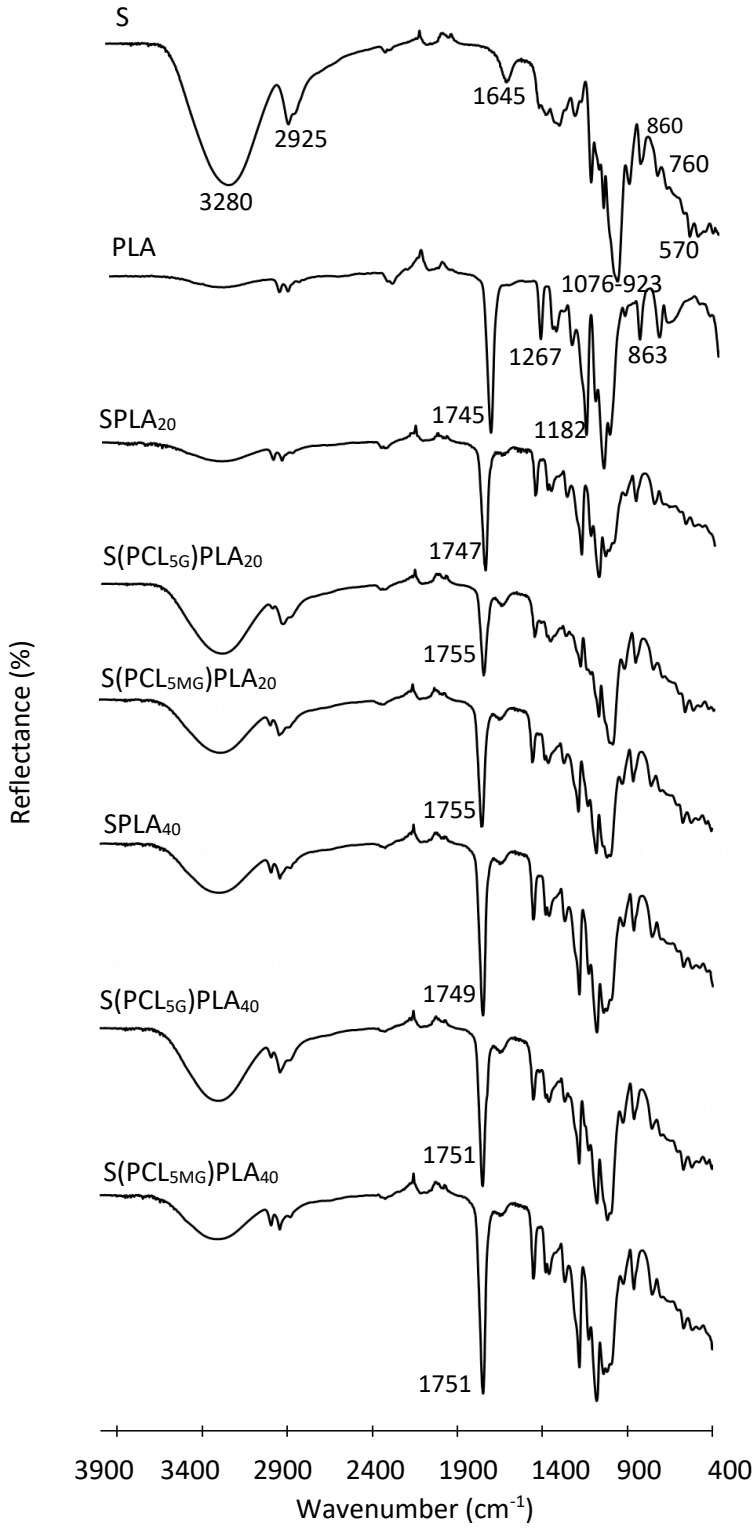

Fig. 3. FTIR-ATR spectra of S-PLA films with 20 or 40 wt% PLA, compatibilized or not with 5% of PCL_G or PCL_{MG}.

3.2. Thermal analysis

The thermogravimetric analysis (TGA) provides information on the thermal stability of polymers, so the maximum temperature that supports the material can be known [9]. Table 2 summarises the initial degradation temperature (Onset) and the temperature at the maximum degradation rate (Peak) of the different film formulations, and TGA and DTG curves are shown in Fig. 4. The initial degradation temperature of the pure starch film is around 264 °C; at this point the weight loss is accentuated, as can be seen in Fig. 4, until reaching the maximum degradation rate at 299 °C. During the degradation process, the dehydration of the hydroxyl groups in the glucose ring takes place; moreover, ether bonds and unsaturated structures are formed by the thermal condensation of the hydroxyl groups of the starch chains, eliminating water and low molecular weight substances [31]. The PLA sample had an initial degradation temperature above that of pure starch, and a maximum degradation rate at 317 °C similar to that previously reported by Sanyang et al. [32]. The S-PLA blends at both ratios, with and without compatibilizers, show three degradation phases of differing intensities, depending on the composition of the mixtures without the complete miscibility of components. The first phase, between 125-205 °C, corresponds to the degradation of low molecular weight components, such as plasticizers (glycerol); the main second phase, between 225-325 °C, is attributable to the overlapped degradation of starch and PLA, since both polymers possess similar degradation temperatures, and the third phase, above 330 °C (in samples with compatibilizers), would mainly correspond to the degradation of the grafted PCL with higher degradation temperatures (341-381 °C, [17]), partially overlapped with the final degradation of PLA. The degradation temperature of the pure PCL is between 300-400 °C and the graft of glycidyl methacrylate and maleic anhydride can partially inhibit the crystallization of the PLC, which promotes degradation at slightly lower temperatures [17].

Table 2 shows that both the initial degradation temperature and the temperature at the maximum degradation rate of the polymers were closer to the corresponding temperatures of the starch, due to its higher ratio in the blends. However, the main peak was wider and extended at higher temperatures, especially when blends contained 40% PLA, reflecting the greater contribution of the PLA degradation to the main peak. For these samples, in fact, the shoulder at about 340 °C, corresponding to the degradation of the grafted PCL, overlapped the PLA final degradation to a greater extent, but at similar temperatures. This behaviour indicates that the thermal degradation of the different polymers is scarcely influenced by the blending effect.

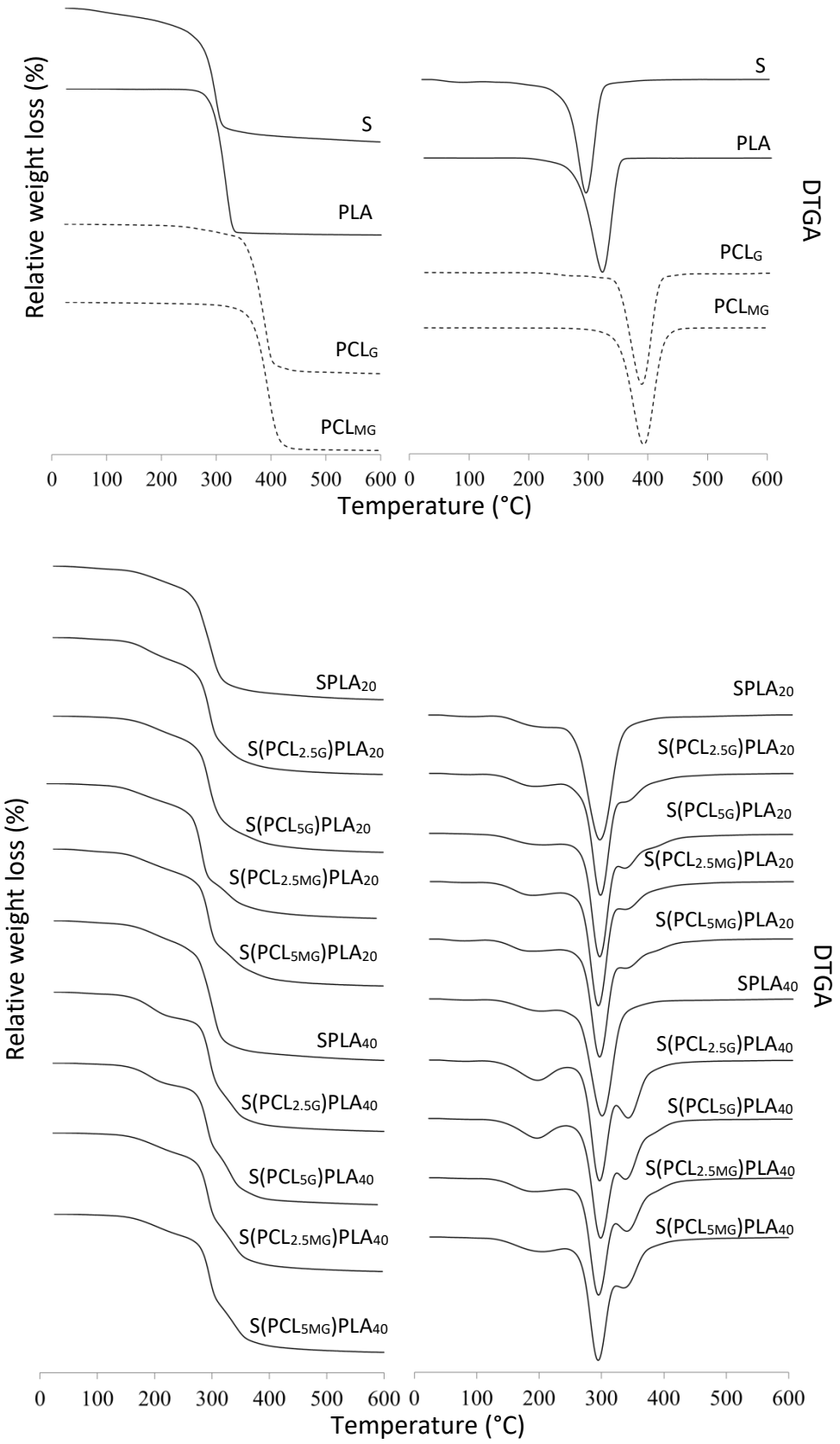

Fig. 4. TGA (a) and DTGA (b) curves of S-PLA films with 20 or 40 wt% PLA, compatibilized or not with 2.5 and 5% of PCL_G or PCL_{MG}.

Table 2. Mean values and standard deviation of onset and peak temperatures of thermal degradation and glass transition temperature (Tg; second heating scan on DSC) of S-PLA dry films compatibilised or not with 2.5 and 5% of PCL_G or PCL_{MG}

Samples	[125-205]°C		[255-360]°C		[339-387]°C	Second heating scan	
	Onset (°C)	Peak (°C)	Onset (°C)	Peak (°C)	Peak (°C)	$T_{g\ Starch}$ (°C)	$T_{g\ PLA}$ (°C)
S	-	-	264 ± 2^{b}	299 ± 4^{c}	-	98.6 ± 0.1^{a}	-
PLA	-	-	278 ± 0.5^{f}	317 ± 5^{b}	-	-	55.3 ± 0.2^{e}
S PLA_{20}	165 ± 3^{g}	201 ± 4^{g}	256 ± 1^{a}	296 ± 0.5^{a}	-	99.3 ± 0.1^{a}	52.8 ± 0.7^{d}
S($PCL_{2.5G}$)PLA_{20}	149 ± 0.2^{f}	185 ± 3^{cd}	271 ± 0.3^{de}	296 ± 1^{a}	341 ± 2^{a}	105.0 ± 3.0^{c}	50.1 ± 0.1^{bc}
S(PCL_{5G})PLA_{20}	146 ± 4^{ef}	195 ± 2^{f}	269 ± 1^{cde}	296 ± 1^{a}	381 ± 6^{b}	105.6 ± 0.8^{c}	49.3 ± 0.7^{ab}
S($PCL_{2.5MG}$)PLA_{20}	129 ± 2^{ab}	180 ± 0.2^{ab}	269 ± 2^{bcde}	292 ± 2^{a}	343 ± 2^{a}	101.1 ± 0.2^{ab}	49.6 ± 0.2^{abc}
S(PCL_{5MG})PLA_{20}	128 ± 3^{a}	176 ± 0.2^{a}	270 ± 0.3^{de}	294 ± 1^{a}	343 ± 0.2^{a}	103.0 ± 4.0^{bc}	50.1 ± 0.1^{bc}
S PLA_{40}	139 ± 0.4^{cd}	189 ± 3^{de}	265 ± 3^{bc}	297 ± 1^{a}	-	98.2 ± 0.3^{a}	52.1 ± 0.9^{d}
S($PCL_{2.5G}$)PLA_{40}	144 ± 1^{def}	195 ± 1^{f}	272 ± 0.2^{e}	294 ± 1^{a}	342 ± 2^{a}	105.0 ± 1.0^{c}	49.9 ± 0.7^{bc}
S(PCL_{5G})PLA_{40}	149 ± 3^{f}	196 ± 2^{fg}	270 ± 4^{de}	293 ± 3^{a}	342 ± 2^{a}	104.4 ± 0.5^{bc}	49.5 ± 0.3^{abc}
S($PCL_{2.5MG}$)PLA_{40}	135 ± 7^{bc}	183 ± 0.2^{bc}	266 ± 5^{bcd}	293 ± 1^{a}	345 ± 4^{a}	103.6 ± 0.4^{bc}	49.4 ± 0.4^{a}
S(PCL_{5MG})PLA_{40}	141 ± 2^{cde}	193 ± 1^{ef}	271 ± 0.2^{de}	294 ± 0.3^{a}	342 ± 2^{a}	103 ± 1^{bc}	50.5 ± 0.3^{c}

Different superscript letters within the same column indicate significant differences between formulations ($p < 0.05$).

Table 2 also shows the glass transition temperatures (T_g) of the starch and the PLA for the different formulations, obtained from the second heating scan. The T_g of the starch is around 100 °C, as reported by other authors [19, 33], and there were no significant differences between the S and S-PLA formulations. However, compatibilizers exert an anti-plasticization effect in the starch phase by increasing its T_g, which was slightly more pronounced for PCL_G. Usually, the addition of plasticizers causes a decrease in the glass transition temperature by increasing the free volume in the matrix, which allows the molecular mobility of the polymers [34]. The increase in the Tg of the starch in the compatibilized blends at both percentage of PLA can be attributed to the chemical interactions between the hydroxyl groups of starch and the grafted polar groups of PCL, which restrict molecular mobility, affecting the glass transition temperature [17]. In contrast, the addition of compatibilizers had a slight plasticizing effect on the PLA phase, provoking a decrease in its glass transition temperature. This behaviour demonstrates the interactions of compatibilizers with both polymers, enhancing their dispersion.

3.3. Mechanical properties

The tensile properties (elastic modulus: EM, tensile strength at break: TS and the elongation at break: ε) of the formulations are shown in Table 3. Starch had the lowest value of EM, which indicates that these films are the least stiff and resistant. However, the starch tends to retrograde during storage, the films becoming stiffer and less flexible due to the formation of crystalline zones [35]. As regards PLA, despite its high tensile strength and elastic modulus, which are comparable with those of conventional polymers such as PET or PS, it is a very brittle material with less than 10% elongation capacity [12]. In blend films without a compatibilizer, an increase in EM and a decrease in ε compared to the pure starch films was observed, which implies an increase in the strength and stiffness of the material, with a reduction in its extensibility. However, the greatest % of PLA implied less resistant, less extensible films with similar stiffness to the films with the lowest PLA ratio. This could be explained in terms of the film microstructure, where the PLA phase was dispersed in a continuous starch matrix. The cohesion force of the continuous matrix greatly contributed to the film's strength and an increase in the volume of the dispersed phase reduced the overall film cohesiveness, despite the higher strength of the dispersed PLA. In compatibilized blends with 20% PLA, a significant increase in EM (~2 times, when using $PCL_{2.5MG}$) and TS (~1.5 times, when using $PCL_{2.5G}$) with respect to the non-compatibilized blends was observed. However, a decrease in the film elongation at break was noted in compatibilized films when PCL_G at 2.5% and PCL_{MG} at 5% were used. Compatibilized samples with 40% PLA exhibited lower values of EM, TS and ε compared to those containing 20% PLA, as commented on for the non-compatibilized blends, which can be attributed to the increase in the volume of the

dispersed phase. This factor is particular for films compatibilised with PCL_G, as commented on above, which provoked the phase inversion in the polymer blend, the PLA becoming the continuous matrix, but with a high amount of dispersed starch that weakened the strength of the PLA continuous phase. As a result of the structural effects, no remarkable differences could be established for the mechanical parameters of films with 40% PLA, regardless of the presence or type of compatibilisers. Therefore, from a mechanical point of view, the greater substitution of starch by PLA did not represent any advantage.

Table 3. Mean values and standard deviation of tensile properties (EM: elastic modulus, TS: tensile strength at break and ε: extensibility) of conditioned (53% RH and 25 °C) S-PLA films compatibilized or not with 2.5 and 5% of PCL_G or PCL_{MG}.

Formulation	EM (MPa)	TS (MPa)	ε (%)	Thickness (mm)
S	77 ± 15^{a}	5.2 ± 1.6^{bc}	64.9 ± 0.5^{h}	0.20 ± 0.02^{bc}
PLA	1370 ± 34^{g}	53.0 ± 2.0^{f}	4.3 ± 0.2^{a}	0.22 ± 0.01^{d}
S PLA_{20}	143 ± 20^{cd}	5.7 ± 0.7^{c}	17.5 ± 3.5^{f}	0.17 ± 0.02^{a}
S($PCL_{2.5G}$)PLA_{20}	312 ± 28^{f}	8.6 ± 0.3^{e}	9.6 ± 1.8^{d}	0.19 ± 0.01^{ab}
S(PCL_{5G})PLA_{20}	195 ± 35^{e}	7.6 ± 0.3^{d}	21.1 ± 1.9^{g}	0.19 ± 0.01^{bc}
S($PCL_{2.5MG}$)PLA_{20}	162 ± 39^{d}	5.9 ± 0.4^{c}	22.3 ± 2.1^{g}	0.17 ± 0.02^{a}
S(PCL_{5MG})PLA_{20}	318 ± 43^{f}	8.1 ± 0.7^{de}	7.2 ± 1.3^{bc}	0.18 ± 0.02^{a}
$S_{60}PLA_{40}$	112 ± 14^{bc}	4.3 ± 0.3^{ab}	6.5 ± 1.3^{b}	0.20 ± 0.01^{bc}
S($PCL_{2.5G}$)PLA_{40}	135 ± 13^{cd}	5.9 ± 0.7^{c}	8.0 ± 1.6^{bcd}	0.23 ± 0.02^{de}
S(PCL_{5G})PLA_{40}	101 ± 15^{ab}	8.1 ± 0.8^{de}	12.9 ± 1.5^{e}	0.24 ± 0.02^{e}
S($PCL_{2.5MG}$)PLA_{40}	98 ± 18^{ab}	4.3 ± 0.9^{ab}	8.9 ± 0.9^{cd}	0.20 ± 0.02^{cd}
S(PCL_{5MG})PLA_{40}	117 ± 14^{bc}	4.1 ± 0.6^{a}	5.8 ± 0.5^{ab}	0.21 ± 0.02^{bc}

Different superscript letters within the same column indicate significant differences among formulations ($p < 0.05$).

In blends with 20% PLA, the values of elongation at break were higher than those found by Zuo et al. [36], by compatibilizing S-PLA blends by means of starch esterification with maleic anhydride; however they obtained TS values of around 38 MPa. The improved mechanical behaviour of blend films with grafted-PCL compatibilizers reflects the better dispersion and interfacial adhesion of the polylactic acid in the starch matrix, depending on the concentration and type of compatibilizer, as shown in the FESEM micrographs. Ortega-Toro

et al. [17] also used grafted PCL with G and MG to compatibilize S-PCL blends in an 80:20 ratio and obtained improved mechanical properties as the concentration of compatibilizer in the mixture increased.

3.4. Moisture content and barrier properties

The moisture content, water vapor permeability (WVP) and oxygen permeability of the films are shown in Table 4. The moisture content of the films was consistent with the different hydrophilic character of the polymers, although starch substitution by PLA did not lead to the expected reduction in the water sorption capacity of the films, whose equilibrium water content values were similar to those of the net starch film.

Table 4. Mean values and standard deviation of moisture content, water vapour permeability (WVP) and oxygen permeability (OP) of S-PLA conditioned (53% RH and 25 °C) films compatibilised or not with 2.5 and 5% of PCL_G or PCL_{MG}.

Formulation	Moisture content (g water/g dried film)	WVP ($g \cdot mm \cdot kPa^{-1} \cdot h^{-1} \cdot m^{-2}$)	OP x10^{14} ($cm^3 \cdot m^{-1} \cdot s^{-1} \cdot Pa^{-1}$)
S	0.096 ± 0.007^{bc}	14.9 ± 0.4^{f}	10.3 ± 0.1^{a}
PLA	0.0025 ± 0.0004^{a}	0.158 ± 0.01^{a}	466.0 ± 3.0^{e}
S PLA_{20}	0.071 ± 0.003^{b}	10.2 ± 0.3^{de}	39.0 ± 1.0^{d}
S($PCL_{2.5G}$)PLA_{20}	0.068 ± 0.005^{b}	10.7 ± 0.7^{e}	24.0 ± 4.0^{bc}
S(PCL_{5G})PLA_{20}	0.065 ± 0.004^{b}	10.1 ± 0.4^{de}	19.9 ± 0.6^{b}
S($PCL_{2.5MG}$)PLA_{20}	0.074 ± 0.002^{b}	9.76 ± 1.0^{de}	20.9 ± 0.8^{bc}
S(PCL_{5MG})PLA_{20}	0.0649 ± 0.0014^{b}	9.4 ± 0.3^{d}	19.9 ± 0.3^{b}
S PLA_{40}	0.097 ± 0.010^{bc}	7.6 ± 0.3^{c}	43.4 ± 1.5^{d}
S($PCL_{2.5G}$)PLA_{40}	0.086 ± 0.004^{b}	7.5 ± 0.2^{c}	24.7 ± 3.3^{c}
S(PCL_{5G})PLA_{40}	0.088 ± 0.005^{b}	5.1 ± 0.2^{b}	22.1 ± 1.9^{bc}
S($PCL_{2.5MG}$)PLA_{40}	0.125 ± 0.003^{de}	7.1 ± 0.4^{c}	23.5 ± 0.5^{bc}
S(PCL_{5MG})PLA_{40}	0.137 ± 0.006^{e}	7.1 ± 0.8^{c}	22.6 ± 0.3^{bc}

Different superscript letters within the same column indicate significant differences among formulations ($p < 0.05$).

Pure starch films showed the highest values of WVP in the range previously reported by other authors [19, 37]. The partial substitution of starch by PLA in the blends, with and without compatibilizers, implied a WVP reduction of about 33 or 50% for 20 and 40% PLA, respectively. However, in films with 40% PLA and 5% PCL_G, the reduction was more marked (67%); this can be attributed to the greater continuity of the more hydrophobic PLA phase, as can be observed in Fig. 1, which limited the transport of water molecules. This decrease in WVP can be associated with the increase in the tortuosity factor for mass transfer caused by the dispersion of the hydrophobic PLA domains within the continuous starch phase [17].

As concerns the oxygen permeability, blend films were more permeable than net starch films, but much lesser permeable than net PLA films. No significant differences in OP were observed for 20 and 40% PLA in the non-compatibilized blends, whose higher values with respect to the starch can be explained by the presence of a less polar phase in the matrix which promote the oxygen solubility. The incorporation of compatibilizers significantly decreases the OP for both PLA ratios with respect to non-compatibilized samples. The reduction was about 40% in every case regardless of the ratio of PLA and the kind and amount of compatibilizer. This decrease could be attributed to the better dispersion of polymers which enhanced the tortuosity factor of the matrix, thus limiting the diffusion of the gas molecules through the matrix. Likewise, as reported by Ortega-Toro et al. [17], the interfacial location of the grafted PCL and interactions with PLA can hinder the diffusion of the gas molecules into the PLA domains, thus affecting the overall permeability of the films.

3.5. Optical properties

Fig. 5 shows the internal transmittance (Ti) of the films in the wavelength range of 400-700 nm as an indicator of the film transparency to VIS radiation. The mean values and standard deviation of Ti at 460 nm (Ti) and gloss at 85° are shown in Fig. 6. The S-PLA blend films with and without compatibilizer exhibited lower values of Ti than pure PLA or starch films, coherently with the formation of a heterogeneous system with a polymer dispersed phase in a continuous phase of the other polymer; both phases have a different refractive index, which implies light scattering effects with the consequent increase in the film opacity. This can be considered positive for food applications as it is potentially able to protect the food, reducing the light induced oxidation reactions. In most cases, the addition of compatibilizers had no significant effect on the Ti values, except for three blends which exhibited the lowest Ti values and the highest gloss. These samples were the blend with 20% PLA and 5% PCL_G and the two blends with 40% PLA and PCL_G at 2.5 and 5%. These differences must be associated with the particular film microstructure.

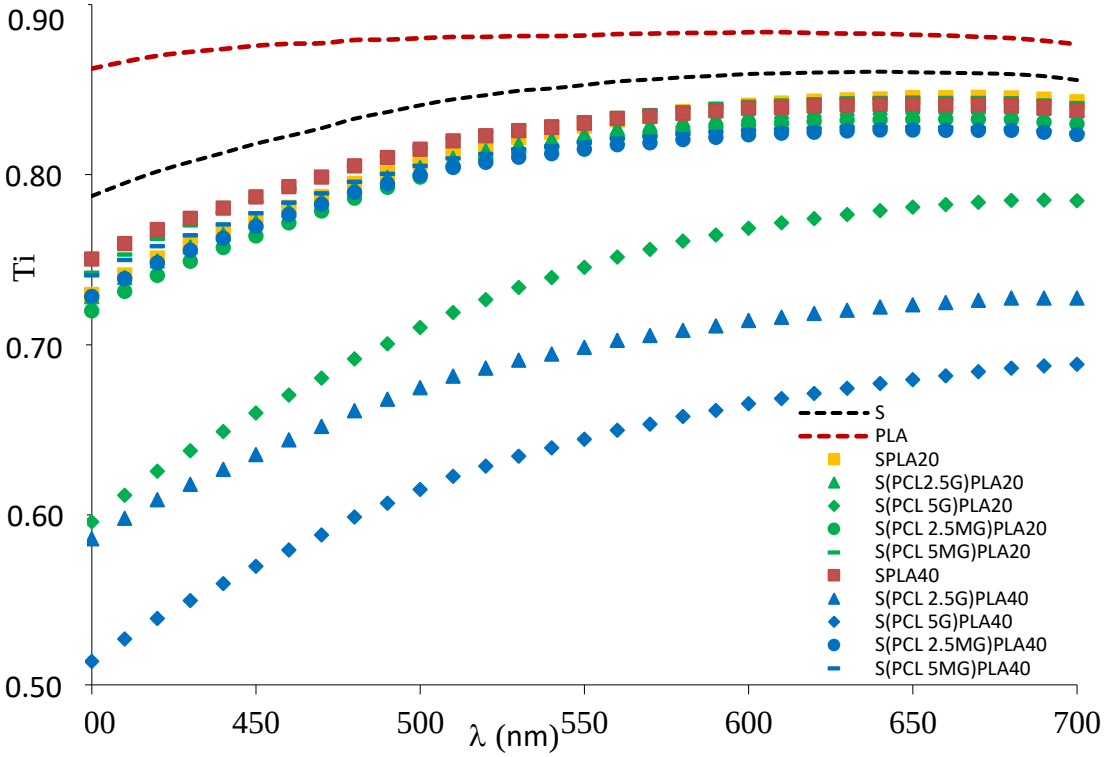

Fig. 5. Internal transmittance (Ti) spectra of TPS-PLA films with 20 or 40 wt% PLA, compatibilized or not with 2.5 and 5% of PCL_G or PCL_{MG}.

In the first case, the better PLA dispersion in the starch matrix, with the reduced size of PLA domains, as shown in FESEM micrographs, will cause a greater light scattering effect; this will give rise to less transparency in the films, at the same time as the better PLA dispersion will promote lower surface irregularities and higher gloss in the films.

The two samples with 40% PLA with lower transparency corresponded to the inverted structures, where PLA constituted the continuous phase with a high amount of dispersed starch phase, which will provoke a more marked light scattering effect, reducing the film transparency. In these cases, the continuity of the PLA phase enhanced the film gloss. Similar effects have been found by other authors for blends of PLA and plasticized starch [15].

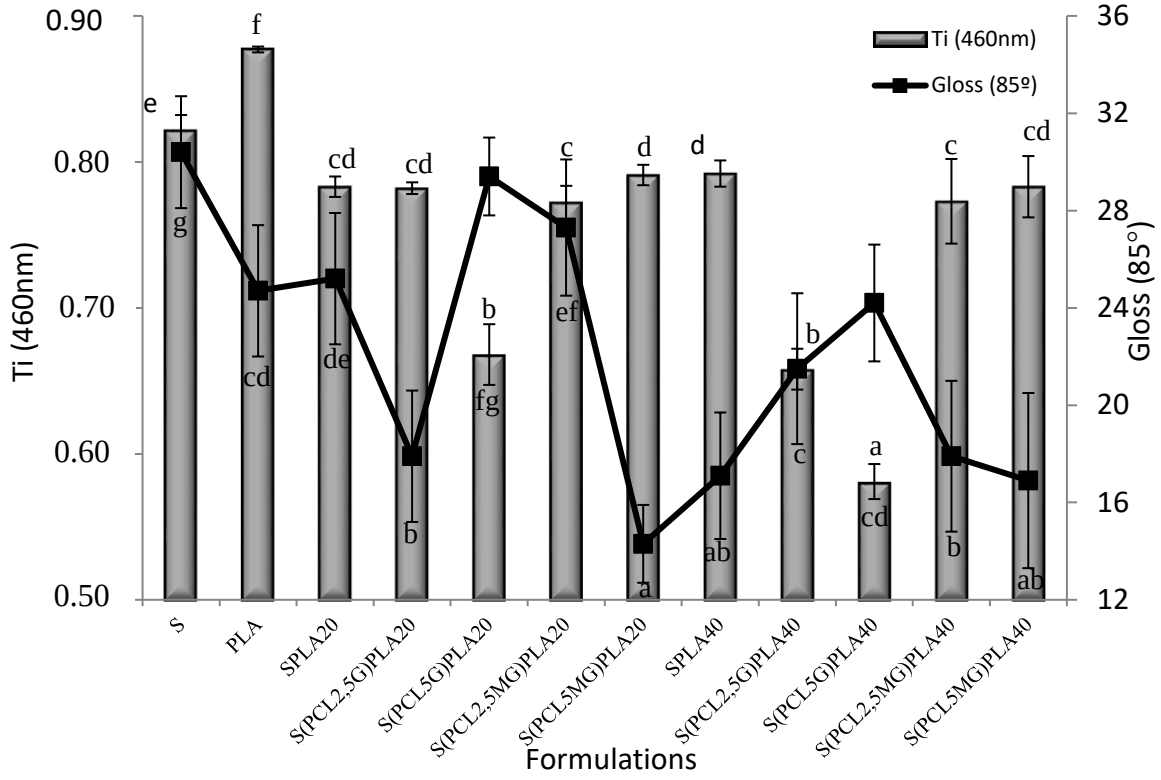

Fig. 6. Mean values and standard deviation of internal transmittance at 460 nm (Ti) and gloss (85°) values of S-PLA films with 20 or 40 wt% PLA, compatibilized or not with 2.5 and 5% of PCL_G or PCL_{MG}.

4. CONCLUSIONS

The starch-PLA matrices compatibilized with grafted PCL presented a better dispersion of the PLA in the continuous starch phase, especially for the highest amount of compatibilizer. The use of PCL_G provoked a phase inversion in the matrix when 40% of starch was substituted by PLA. Interactions between polymers and compatibilizers could be deduced from microstructural, thermal and spectral data. The compatibilized blend films exhibited higher values of elastic modulus than pure starch films, but they were less extensible, with similar tensile strength at break, the values depending on the PLA ratio and the type and concentration of compatibilizer. From the mechanical point of view, the film formulation containing 20% PLA and 5% PCL_G exhibited good tensile strength and great extensibility, being suitable for packaging purposes. The WVP was reduced by blending up to 33 or 50% for 20 and 40% PLA, respectively, although films with 40% PLA and 5% PCL_G, exhibited a marked reduction (67%). The incorporation of compatibilizers significantly decreased the OP

by about 40% respect to non-compatibilized samples, regardless of the % of PLA and the kind and amount of compatibilizer. Therefore, substituting 20% of the starch by PLA and incorporating 5% PCL_G would be a good strategy to obtain films that are useful for food packaging; the starch phase provided the films with an excellent oxygen barrier capacity, while PLA enhanced the mechanical resistance and reduced the water vapour permeability. In particular, dry or partially dehydrated products and fatty or oxidation-sensitive foods could be adequately packaged with these films, thus improving their preservation.

Acknowledgements

The authors thank the Ministerio de Economía y Competitividad (Spain) for the financial support provided through Project AGL2016-76699-R. The authors also wish to thank the Electron Microscopy Service of the UPV for their technical assistance.

REFERENCES

[1] C. Brigham, Biopolymers: Biodegradable alternatives to traditional plastics, in: B. Török, T. Dransfield (Eds.), Green chemistry, Elsevier Inc., Amsterdam, 2018, pp. 753-770.

[2] C. Ingrao, V. Siracusa, Quality- and sustainability-related issues associated with biopolymers for food packaging applications: a comprehensive review, in: N. Gopal Shimpi (Ed), Biodegradable and Biocompatible Polymer Composites, Woodhead Publishing, 2018, pp. 401-418.

[3] A.B. Balaji, H. Pakalapati, M. Khalid, R. Walvekar, R, H. Siddiqui, Natural and synthetic biocompatible and biodegradable polymers, in: N. Gopal Shimpi (Ed.), Biodegradable and biocompatible polymer composites, Woodhead Publishing, United Kingdom, 2017, pp. 3–32.

[4] M.J. Fabra, A. López-Rubio, J.M. Lagarón, Biopolymers for food packaging applications, in: M. R. Aguilar De Armas, J. S. Román (Eds.), Smart polymers and their applications, Woodhead Publishing, United Kingdom,2014, pp. 476-509.

[5] M. Bassas-Galia, S. Follonier, M. Pusnik, M. Zinn, Natural polymers: a source of inspiration, in: G. Perale, J. Hilborn (Eds.), Bioresorbable polymers for biomedical applications, Woodhead Publishing**.** United Kingdom, 2017, pp. 31-64.

[6] L. Jiang, J. Zhang, Biodegradable and biobased polymers, in: M. Kutz (Ed.), *Applied Plastics Engineering Handbook,* William Andrew, New York, 2017, pp. 127-143.

[7] K. Koch, K. Starch-based film. In M. Sjöö, L. Nilsson (Eds), Starch in food, Woodhead Publishing, 2018, pp. 747-767.

[8] R. Ortega-Toro, J. Contreras, T. Talens, A. Chiralt, Physical and structural properties and thermal behaviour of starch-poly(e-caprolactone) blend films for food packaging, Food Packag. and Shelf Life 5 (2015) 10-20.

[9] S. Collazo-Bigliardi, R. Ortega-Toro, A. Chiralt, Isolation and characterisation of microcrystalline cellulose and cellulose nanocrystals from coffee husk and comparative study with rice husk, Carbohydr. Polym. 191 (2018) 205-215.

[10] S. Collazo-Bigliardi, R. Ortega-Toro, A. Chiralt, Properties of Micro- and nano-reinforced biopolymers for food applications, in: T. Gutiérrez (Ed.), Polymers for food applications, Springer, 2018, pp. 61-99.

[11] R. Ortega-Toro, J. Bonilla, P. Talens, A. Chiralt, Starch-based materials in food packaging, in: M. A. Villar, S.E. Barbosa, M.A. García, L.A. Castillo, O.V. López (Eds.), Future of starch-based materials in food packaging, Aspen Publishers, 2017, pp. 257-312.

[12] J. Muller, C. González-Martínez, A. Chiralt, A. Combination of poly(lactic) acid and starch for biodegradable food packaging, *Mater.* 10 (2017) 952-974.

[13] M. Murariu, P. Dubois, PLA composites: From production to properties, Adv. Drug Deliv. Rev. 107 (2016) 17-46.

[14] J. Muller, C. González-Martínez, A. Chiralt, Poly(lactic) acid (PLA) and starch bilayer films, containing cinnamaldehyde, obtained by compression moulding. Eur. Polym. J. 95 (2017) 56-70.

[15] P. Müller, J. Bere, R. Fekete, J. Móczó, B. Nagy, M. Kállay, B. Gyarmati, B. Pukánszky, Interactions, structure and properties in PLA/plasticized starch blends. Polym. 103 (2016) 9-18.

[16] N. Le Bolay, A. Lamure, N. Gallego, A. Subhani, How to combine a hydrophobic matrix and a hydrophilic filler without adding a compatibilizer-Co grinding enhances use properties of renewable PLA-starch composites, Chem. Eng. and Process. 56 (2012) 1-9.

[17] R. Ortega-Toro, G. Santagata, G. Gomez d'Ayala, P. Cerruti, P. Talens, A. Chiralt, M. Malinconico, Enhancement of interfacial adhesion between starch and grafted poly(ε-caprolactone), Carbohydr. Polym. 147 (2016) 16-27.

[18] P. Laurienzo, M. Malinconico, G. Mattia, G. Romano, Synthesis and characterization of functionalized crosslinkable poly(ε-caprolactone), Macromol. Chem. and Phys. 207 (2006) 1861-1869.

[19] R. Ortega-Toro, S. Collazo-Bigliardi, P. Talens, A. Chiralt, Influence of citric acid on the properties and stability of starch-polycaprolactone based films, J. Appl. Polym. Sci. 42220 (2016) 1-16.

[20] ASTM, Standard test method for tensile properties of thin plastic sheeting. Standard Designations: D882, Annual book of ASTM standards. Philadelphia, PA: American Society for Testing and Materials (2001).

[21] ASTM, Standard test methods for water vapor transmission of materials. Standard Designations: E96-95, In Annual books of ASTM, Philadelphia, PA: American Society for Testing and Materials, 1995, pp. 406-413.

[22] T.H. McHugh, R. Avena-Bustillos, J.M. Krochta, J. M, Hydrophobic edible films: Modified procedure for water vapour permeability and explanation of thickness effects. J.l of Food Sci. 58(4) (1993) 899-903.

[23] J.B. Hutchings, Food color and appearance (2nd ed.), Gaithersburg, Maryland, Aspen Publishers Inc., USA, 1999.

[24] ASTM, Standard test method for specular gloss. In Designation (D523).annual book of ASTM standards, vol. 06.01. PA: American Society for Testing and Materials Philadelphia, 1999.

[25] M. Akrami, I. Ghasemi, H. Azizi, M. Karrabi, M. Seyedabadi, A new approach in compatibilization of the poly(lactic acid)/thermoplastic starch (PLA/TPS) blends. Carbohydr. Polym. 144 (2016) 254-262.

[26] M. Haque, M.E. Errico, G. Gentile, M. Avella, M. Pracella, Functionalization and compatibilization of poly(ε-caprolactone) composites with cellulose microfibres: morphology, thermal and mechanical properties, Macromolecular Mater. and Engi. 297(10) (2012) 985-993.

[27] V.H. Orozco, W. Brostow, W. Chonkaew, B.L. Lopez, Preparation and characterization of poly (Lactic acid)-g-maleic anhydride + starch blends, Macromol. Symp. 277 (2009) 69-80.

[28] L. Castillo, O. López, C. López, N. Zaritzky, M.A. García, S. Barbosa, M. Villar, Thermoplastic starch films reinforced with talc nanoparticles, Carbohydr. Polym. 95(2) (2013) 664-674.

[30] S.M. Davachi, B.S. Heidari, I. Hejazi, J. Seyfi, E. Oliaei, A. Farzaneh, H. Rashedi, Interface modified polylactic acid/starch/poly ε-caprolactone antibacterial nanocomposite blends for medical applications, Carbohydr. Polym. 155 (2017) 336-344.

[31] O.V. López, L.A. Castillo, S.E. Barbosa, M.A. Villar, M. A. García, Processing–properties–applications relationship of nanocomposites based on thermoplastic corn starch and talc, Polym. Compos. 39(4) (2018) 1331-1338.

[32] M.L. Sanyang, S.M. Sapuan, M. Jawaid, M.R. Ishak, J. Sahari, Development and characterization of sugar palm starch and poly (lactic acid) bilayer films. Carbohydr. Polym., 146 (2016) 36-45.

[33] A. Tampau, C. González-Martínez, A. Chiralt, Release kinetics and antimicrobial properties of carvacrol encapsulated in electrospun poly-(ε-caprolactone) nanofibres. Application in starch multilayer films, Food Hydrocoll. 79 (2018) 158-169*.*

[34] P.Y. Mikus, S. Alix, J. Soulestin, M.F. Lacrampe, P. Krawczak, X. Coqueret, P. Dole, Deformation mechanisms of plasticized starch materials, Carbohydrate Polym. 114 (2014) 450-457.

[35] R. Ortega-Toro, A. Jiménez, P. Talens, A. Chiralt, Properties of starch-hydroxypropyl methylcellulose based films obtained by compression molding. Carbohydr. Polym. 109 (2014) 155-165.

[36] Y. Zuo, J. Gu, L. Yang, Z. Qiao, H. Tan, Y. Zhang, Preparation and characterization of dry method esterified starch/polylactic acid composite materials, Intern. J. of Biol. Macromol. 64 (2014) 174-180.

[37] S. Collazo-Bigliardi, R. Ortega-Toro, A. Chiralt, Reinforcement of thermoplastic starch films with cellulose fibres obtained from rice and coffee husks, J. Renew. Mater. 6(6) (2018) 599-610.

Chapter V

Using lignocellulosic fractions of coffee husk to improve properties of compatibilized starch-PLA blend films

[1]**Sofía Collazo-Bigliardi;** [2]Rodrigo Ortega-Toro; [1]Amparo Chiralt

Food Packaging and Shelf Life. Under Review

[1]Institute of Food Engineering for Development, Universitat Politècnica de València. Valencia, Spain

[2]Food Engineering Program, Faculty of Engineering, Universidad de Cartagena. Cartagena de Indias, Colombia

socol@doctor.upv.es

ABSTRACT

The effectiveness of the incorporation of cellulosic reinforcing agents and antioxidant aqueous extract (AE) from coffee husk at improving the functional properties of compatibilized starch-PLA blend films was studied. Tensile and barrier properties, crystallization pattern and thermal behaviour were analysed in films containing 1 wt% of cellulosic fibres (CF) or cellulose nanocrystals (CNC) incorporated by two different methods or 5.8 wt% of antioxidant extract. The antioxidant properties of the films were also tested through their efficacy at preserving sunflower oil from oxidation. Of the cellulosic fractions, CF were not adequate for enhancing the functionality of the blend films, but CNC directly blended with the starch phase were effective at reinforcing tensile properties of the material (148% and 45% increase in elastic modulus and tensile strength, respectively) and at reducing their water vapour (WVP) and oxygen permeability (OP) (28% and 42% reduction, respectively in WVP and OP). The AE did not improve the mechanical performance of the blend films, but conferred antioxidant capacity useful for food packaging applications.

Keywords: Coffee husk; cellulose fillers; antioxidant extracts; starch; polylactic acid; grafted polycaprolactone.

1. INTRODUCTION

Nowadays, it is a challenge to develop materials able to substitute the conventional petroleum-derived polymers with high environmental impact due to their accumulation and difficult management (Balaji, Pakalapati, Khalid, Walvekar, &, Siddiqui, 2017). This is especially convenient in the food packaging area where there is a very high consumption of plastic materials. In this sense, biodegradable materials should substitute synthetic plastics since they represent an attractive solution to this issue, being abundant and mostly obtained from renewable resources. Different groups of biodegradable polymers have been studied, such as those directly obtained from biomass (polysaccharides, proteins and those produced by microbial action) and those synthesised from bio-based monomers (polylactic acid: PLA) or from petrochemical products (poly (ε-caprolactone): PCL) (Brigham, 2018; Collazo-Bigliardi, Ortega-Toro, & Chiralt, 2018a). These materials can also be used in combination, forming multilayer packaging systems (Requena, Vargas, & Chiralt, 2018; Tampau, González-Martínez, & Chiralt, 2018) or composites (Ortega-Toro, Collazo-Bigliardi, Talens, & Chiralt, 2016a) with optimized mechanical and barrier properties for food packaging.

Starch and PLA are the most widely-studied biomaterials for food packaging applications. Starch from different sources (rice, potato, corn, cassava, wheat, etc.) can be transformed into thermoplastic starch (TPS) by thermo-mechanical treatment in combination with the action of plasticizers (Koch, 2018). Despite its hydrophilic nature and water sensitivity, its limited mechanical performance and retrogradation during storage, starch is an interesting polymer for food packaging development due to its suitability for food contact, competitive price and high oxygen barrier capacity (Ortega-Toro, Bonilla, Talens, & Chiralt, 2017). Likewise, starch modification through the reaction of hydroxyl groups (-OH) provides several possibilities for modulating its properties (Ogunsona, Ojogbo, & Mekonnen, 2018). As concerns PLA, it is synthesized from lactic acid obtained in the dextrose fermentation, using renewable sources, such as corn starch, rice starch or raw materials with high sugar content. This biodegradable aliphatic polyester is commonly produced by the ring-opening polymerization (ROP) of lactide monomers formed from lactic acid (Balaji et al., 2017; Muller, González-Martínez, & Chiralt, 2017a). PLA is easy to process, transparent and has excellent water vapour barrier permeability (Murariu & Dubois, 2016), with characteristics comparable to those traditional petrochemical-based polymers (such as polystyrene: PS or polyethylene terephthalate: PET). However, PLA exhibits low oxygen barrier capacity in line with its hydrophobic nature and limited toughness, despite the fact that it is resistant to traction (Hamad, Kaseem, Ayyoob, Joo, & Deri, 2018).

TPS-PLA blends have been studied to make the most of their complementary properties for the purposes of designing packaging materials. Nevertheless, these polymers are not thermodynamically compatible and their blends exhibit phase separation, which limits their

effectiveness (Müller et al., 2016). Then, it is necessary to improve their interfacial adhesion in order to obtain TPS-PLA blends with better functional properties. To this end, the use of compatibilizers has been widely studied (Hamad et al., 2018). Different compounds, such as citric acid, stearic acid, maleic anhydride, dicumyl peroxide or citrate esters, have been used to enhance the mechanical, thermal and barrier properties of the blends (Muller et al., 2017a). Ortega-Toro et al. (2016b) studied the use of compatibilizers based on the melt grafting of poly(ε-caprolactone) (PCL) with reactive polar groups from glycidyl methacrylate (epoxide) or maleic anhydride (anhydride), as reported by Laurienzo, Malinconico, Mattia and Romano (2006), in TPS-PCL blends. These compatibilizers have also been used in TPS-PLA blends leading to films with improved functional properties (Collazo-Bigliardi, Ortega-Toro & Chiralt, Unpublished results). Particularly, films with 20% substitution of starch by PLA, containing 5% of grafted PCL with glycidyl methacrylate exhibited high resistance to break and reduced water vapour permeability with respect to the starch films, with very high oxygen barrier capacity. The incorporation of cellulosic fibres and antioxidant compounds into this matrix might still improve the film characteristics for their application in food packaging.

Micro- or nano-fillers from different sources have been studied to improve the functional properties of biopolymer films (Collazo-Bigliardi et al., 2018a). In particular, lignocellulosic agro-wastes have been commonly used to isolate microcrystalline cellulose and cellulose nanocrystals. These fillers have been incorporated into starch-based blends (Azeredo, Rosa, & Mattoso, 2017; Berthet et al., 2015; Collazo-Bigliardi, Ortega-Toro, & Chiralt, 2018b; Patel & Parsania, 2017) and provided great thermal resistance, improving the elastic modulus and barrier properties of composites. The presence of the hydroxyl groups of the cellulose favours its interaction with the polymer matrix, thus contributing to its reinforcement.

Lignocellulosic materials are also a source of phenolic compounds, which exhibit active properties to control microbial or oxidative processes in food matrices (Cong-Cong, Bing, Yi-Qiong, Jian-Sheng, & Tong; Shavandi et al., 2018). The antioxidant character of polyphenols is related with their ability both to act as free radical scavengers, inhibiting lipoxygenase enzyme activity, and to chelate metals (Talón, Trifkovic, Vargas, Chiralt, & González-Martínez, 2017).

In this context, coffee husk (endocarp of coffee beans) is an interesting raw material produced in coffee processing, with high content of both cellulosic and phenolic components that can be valued through its use for packaging material development (Alves, Rodrigues, Nunes, Vinha, & Oliveira, 2017). This residue can be submitted to hydrothermal treatments to extract active compounds (Piñeros-Castro & Otálvaro, 2014), and to different chemical treatments in order to isolate cellulose fibres, whose subsequent acid hydrolysis produces cellulose nanocrystals (Collazo-Bigliardi et al 2018b and 2018c).

The aim of this work was to analyse the effectiveness of the incorporation of cellulosic reinforcing agents (cellulose fibres and cellulose nanocrystals) and antioxidant aqueous extract from coffee husk at improving the functional properties of compatibilized starch-PLA blend films. The antioxidant properties of the films were tested through their efficacy at preserving sunflower oil from oxidation. The effect of the incorporation method of cellulose nanocrystals into the blend films was also analysed.

2. MATERIALS AND METHODS

2.1. Materials

Corn starch (S) was supplied by Roquette (Roquette Laisa, Benifaió, Spain) and amorphous PLA 4060D, density of 1.24 g/cm^3, was purchased from Natureworks (U.S.A). Glycerol was obtained from Panreac Química, S.A. (Castellar del Vallès, Barcelona, Spain). For the chemical modification of PCL (pellets ∼3 mm, average Mn 80.000 Da), glycidyl methacrylate (G) (purity 97%) and benzoyl peroxide (BP) were supplied by Sigma (Sigma-Aldrich Chemie, Steinheim, Germany). Coffee husks were provided by Universidad Jorge Tadeo Lozano (Bogotá, Colombia) and maltodextrin 18 DE used in spray drying of extracts was from Tecnas S.A., Colombia.

2.2. Preparation of grafted PCL

The grafting reaction of glycidyl methacrylate (G) to PCL was performed following the methodology described by Ortega-Toro et al. (2016b) and Laurienzo et al. (2006). To this end, 45 g of PCL, 0.5 g of BP and 5 g of G were incorporated into the Brabender plastograph (EC Plus, Duisburg, Germany) and melt blended at 100 °C and 32 rpm for 20 min to obtain PCL_G. Modified PCL_G was dissolved in 500 mL of chloroform, subsequently re-precipitated in excess of hexane for the purposes of removing any ungrafted reagents (oligomers and monomers residuals), and kept in a desiccator under vacuum for 12 h at 25 °C, and stored under freezing till its use.

2.3. Extraction of antioxidant compound and isolation of cellulosic materials from coffee husk

The extraction of the antioxidant fraction was carried out with 650 g of coffee husk and 3 L of distilled water in a 5 L capacity pilot scale reactor (A2423 model, Amar Equipment, India) by pressurised hot water (180 °C and 9.5 bar) for 60 min, according to previous studies (Piñeros-Castro & Otálvaro, 2014). The extracts were separated from the solid fraction which

was dried for the purposes of subsequently extracting the cellulose fillers. The extract was concentrated at 90 °C under continuous stirring and then spray dried using a Vibrasec pilot dryer model Pasalab 1.5 (Universidad Nacional de Colombia, Medellin), operating at 180 °C and 90 °C outlet temperature, at an atomiser disk speed of 24,000 rpm. Maltodextrin (18 DE) at 29.8 wt% was added as drying coadjuvant.

The process of isolating cellulose reinforcing agents from coffee husks was carried out following the methodology reported by Collazo-Bigliardi et al. (2018b). The solid residue from the hydrothermal treatment was alkali treated with 4 wt% of NaOH at 80 °C for 3 h. Then, the sample was washed with distilled water until the alkali solution was removed. The bleaching process to obtain cellulose fibres (CF) was completed by adding equal parts of acetate buffer solution, sodium chlorite (1.7 wt%) and distilled water to the alkali- treated solid at reflux temperature (~100 °C) for 4 h, under mechanical stirring. This process was repeated 4 times until the samples were completely white. Then, the fibres were washed with distilled water several times, dried and ground in a Moulinex grinder DJ200031 350W. Cellulose nanocrystals (CNC) were prepared by acid hydrolysis of the obtained bleached fibres by 64% wt/wt sulphuric acid, at 50 °C for 40 min. The hydrolysed sample was washed with distilled water by centrifugation at 14,000 rpm for 30 min. Then, the suspension was dialysed against distilled water until constant pH and neutralised with 10 wt% ion resin (Dowex Marathon MR-3) for 24 h. Finally, the CNC suspension was sonicated for 30 min using a tip sonicator (Vibra-Cell™ VCX 750, Sonics & Materials, Inc., Newton, USA) and kept refrigerated.

2.4. Obtaining compatibilised films

Films were obtained by melt blending the different components by using an internal mixer (HAAKE™ PolyLab™ QC, Thermo Fisher Scientific, Germany) at 160 °C and 50 rpm, for 10 min. The different film formulations and the mass ratio of the respective components are shown in Table 1. In all cases, 30 wt% of glycerol and 20 wt% of PLA with respect to starch were used and 5 wt%, with respect to the total polymer, of compatibiliser PCL_G. Cellulosic material (CF or CNC) was added at 1 wt% and dry antioxidant extract (AE) was added at 5.8 wt%. The incorporation of 1 wt% of CNC into the films required specific previous steps, as commented on below. The obtained blends were cut into pellets and conditioned at 25 °C and 53% relative humidity (RH) for one week before the film performance.

The films were obtained by compression moulding using a hot plate press (Model LP20, Labtech Engineering, Thailand). 4 g of the conditioned pellets were put onto Teflon sheets, preheated for 3 min at 160 °C and compression moulded for 1 min at 30 bars, followed by 3 min at 130 bars; thereafter, a 3 min cooling cycle was applied. Films were conditioned at 25 °C and 53% RH for 1 week before their characterisation.

Table 1. Mass fraction (Xi, g compound/g dried film) of the different components: Starch (S), glycerol (Gly), glycidyl methacrylate grafted polycaprolactone (PCL_G), polylactic acid (PLA), cellulose nanocrystals (CNC) from coffee husk, cellulose fibres from coffee husk (CF) and antioxidant extract from coffee husk (AE).

Formulations	X_S	X_{Gly}	X_{PCLG}	X_{PLA}	$X_{CNC/CF}$	X_{AE}
$S(PCL_{5G})PLA_{20}$	0.6410	0.1923	0.0385	0.1282	-	-
$S(PCL_{5G})PLA_{20}$-CNC	0.6346	0.1904	0.0381	0.1269	0.0100	-
$S(PCL_{5G})PLA_{20}$ -CF	0.6346	0.1904	0.0381	0.1269	0.0100	-
$S(PCL_{5G})PLA_{20}$ -AE	0.6410	0.1346	0.0385	0.1282	-	0.0577

2.4.1. The incorporation of CNC

Since the obtained CNC were in aqueous dispersion (at 1 wt%) to prevent their aggregation (Brinchi, Cotana, Fortunati, & Kenny, 2013; Ng et al., 2015), their incorporation into the blend films required different strategies aimed at dispersing CNC within the polymer matrix. Since no water could be included in the internal mixer used for polymer melt blending to prevent overpressure, two different strategies were used: method 1) the initial transference of CNC to the glycerol, following the method described by Dorris & Gray (2012) and method 2) the prior thermoprocessing of the aqueous dispersion of CNC containing glycerol and starch granules in a two-roll mill to obtain CNC-TPS pellets.

In method 1 (M1), the aqueous CNC suspension after sonication was mixed with the corresponding amount of glycerol under continuous stirring for 30 min (Dorris & Gray, 2012) and the water was subsequently removed by evaporation in an oven at 74°C. The CNC-glycerol blend, starch, PLA and PCL_G were melt blended in the internal mixer as described above. In method 2 (M2), starch and glycerol were dispersed in the aqueous CNC suspension and then thermoprocessed in a two-roll mill (Model LRM-M-100, Labtech Engineering, Thailand roller) at 160 °C for 15 min. The obtained pellets were melt blended with PLA and PCL_G in the internal mixer under the same conditions as for M1.

To evaluate the effect of the CNC incorporation method on the film properties, two pure thermoplastic starch films were additionally prepared, plasticised with 30% of glycerol respect to starch, containing or not 1 wt% of CNC in the films incorporated by methods 1 and 2 (samples S-CNC-M1 and S-CNC-M2). The compatibilised starch-PLA blend films with 1 wt% of CNC were also prepared by methods 1 and 2 (samples $S(PCL_{5G})PLA_{20}$-CNC-M1 and $S(PCL_{5G})PLA_{20}$-CNC-M2).

2.5. Characterisation of the films

2.5.1. Field emission scanning electron microscopy (FESEM) and X-Ray diffraction pattern

Microstructural analyses of the cross-section of the films were carried out in a Field Emission Scanning Electron Microscope (FESEM Ultra 55, Zeiss, Oxford Instruments, U.K). Samples were conditioned in desiccators with P_2O_5 for 2 weeks at 25 °C, and afterwards adequately put on support stubs and coated with platinum. Observations were carried out at 1.5 kV.

An X-Ray diffraction analysis of the different samples was performed using a diffractometer (XRD, Bruker AXS/D8 Advance) at 40 kV and 40 mA. Scattered radiation was detected in an angular range 2θ: 5-30° with a step size of 0.05°. The degree of crystallinity (Xc) of the samples, expressed as a percentage, was calculated with OriginPro 8.5 software from the ratio of crystalline peak areas and the integrated area of XRD diffractograms, assuming Gaussian profiles for crystalline and amorphous peaks (Collazo-Bigliardi et al., 2018b; Ortega-Toro et al., 2016b).

2.5.2. Thermal behaviour

A thermogravimetric analyser (TGA 1 Star^e System analyser, Mettler-Toledo, Inc., Switzerland) was used to study the thermal stability of the samples. The measurements of the thermal weight loss were taken over a temperature range of 25 to 600 °C at 20 °C/min, under nitrogen atmosphere (gas flow: 10 mLmin^{-1}). The initial degradation temperature (T_{Onset}) and peak temperature (T_{Peak}) were obtained using the STAR^e Evaluation Software (Mettler-Toledo, Inc., Switzerland), from the first derivative of the resulting weight loss curves.

The phase transitions in the polymer matrices were evaluated by means of Differential Scanning Calorimetry (DSC 1 Star^e System, Mettler-Toledo Inc., Switzerland). Film samples of 7-9 mg were placed into aluminium pans and sealed. The thermograms were obtained in a heating cycle from 25 °C to 160 °C at 10 °C/min, cooled until 25 °C, and then heated in a second cycle under the same conditions. In the first scan, the bonded water in the film was eliminated, and in the second heating scan, the glass transition of starch and PLA was analysed.

2.5.3. Mechanical properties

The mechanical performance of the samples was analysed following the ASTM standard method D882 (ASTM, 2001). A universal test machine (TA.XTplus model, Stable Micro Systems, Haslemere, England) was used to obtain the stress-strain curves. From these curves, the elastic modulus (EM), tensile strength at break point (TS) and the elongation at break (ε) of the films were determined. The film thickness was taken into account for the calculations. Conditioned (25 °C, 53% RH) samples of 25 x 100 mm were mounted in the film-extension grips of the testing machine and stretched at 50 mm/min until break. Ten replicates were made for each formulation.

2.5.4. Moisture content, water vapour permeability (WVP) and oxygen permeability (OP)

The samples conditioned at 53% RH were dried in a natural convection oven (J.P. Selecta, S.A. Barcelona, Spain) for 24 h at 60 °C to determine the equilibrium moisture content of the films. Then, they were placed in a desiccator at 25 °C with P_2O_5 for a week to adjust the relative humidity to close to 0%. The moisture content of the samples was calculated by varying the weight between the wet sample (53% RH) and the dry sample (0% RH).

The water vapour permeability (WVP) of the films was determined following the gravimetric method, E96-95 (ASTM, 1995; McHugh, Avena-Bustillos, & Krochta, 1993), with some modifications. Payne permeability cups (Elcometer SPRL, Hermelle/s Argenteau, Belgium), 3.5 cm in diameter, were used with 5 mL of bidistilled water and the adjusted film. Each cup was placed into a desiccator equilibrated with $Mg(NO_3)_2$ saturated solution (53% HR, 25 °C) and inserted into a chamber at 25 °C. The cups were weighed periodically (±0.0001 g) until the steady state was reached. The WVP was calculated from the slope of the curves of weight loss versus time as reported by Ortega-Toro et al. (2016a).

The oxygen permeability of the films (50 cm^2 film area) was determined using OX-TRAN equipment, Model 2/21 ML (Mocon Lippke, Neuwied, Germany) in samples conditioned at 25 °C and 53% RH. Film thickness was considered in all cases in order to obtain the OP values. The oxygen transmission values were evaluated every 10 min until equilibrium.

2.5.5. Optical properties

The film transparency was measured through the internal transmittance (Ti), applying the Kubelka-Munk theory of multiple scattering (Hutchings, 1999), using the film reflection spectra obtained on both black and white backgrounds, as described by Talón et al. (2017). Reflection spectra from 400 to 700 nm were obtained by using a spectro-colorimeter CM-3600d (Minolta Co., Tokyo, Japan).

2.6. Antioxidant performance of the films on sunflower oil

To evaluate the antioxidant properties of the S-PLA compatibilised films with antioxidant extract, their potential positive effect on the retardation of sunflower oil oxidation was analysed. To this end, the method described by Galarza, Haas, de Oliveira, & Hickmann (2017) was used. Film samples (area of 7.5 cm × 4 cm) were thermosealed to form bags using a vacuum packing machine (SAECO Vacio Press Elite, Barcelona, Spain). 5 mL of commercial sunflower oil were placed into each bag and thermo-sealed. How effective the films were at delaying sunflower oil oxidation was evaluated in comparison to S-PLA compatibilised blend films without antioxidant extract. As the control sample, an open glass Petri dish containing 10 mL of sunflower oil was considered. All of the samples were stored at 30 °C and 53% RH and exposed to fluorescent light at an intensity of 1000-1500 lux (measured using a digital Luxometer; model RS Pro ILM1332A, RS Components, Madrid, Spain). The oxidative stability of sunflower oil was measured in terms of peroxide index after 5, 9, 14, 19 and 23 days of storage. For that purpose, a titrimetric method was employed (IUPAC, 1987), using an automatic titrator (Titrando, Metrohm Ion Analysis, Switzerland). 1 g of oil was dissolved in 10 mL of solvent (glacial acetic acid:1-decanol at 3:2 volume ratio, containing 10-15 $mg \cdot L^{-1}$ of iodine) and mixed with 200 µL of saturated KI solution and kept in the dark for 1 min. Then, 50 mL of distilled water was added, and the solution was titrated with 0.01 M or 0.001 M $Na_2S_2O_3$, depending on the expected peroxide index. A blank control sample (without sunflower oil) was prepared by the same procedure.

2.7. Statistical analysis

Statgraphics Centurion XVI software (Manugistics Corp., Rockville, Md.) was used to perform the statistical analyses of the results by means of analysis of variance (ANOVA). Fisher's least significant difference (LSD) procedure was used at the 95% confidence level.

3. RESULTS AND DISCUSSION

3.1. Effect of the CNC on the film functional properties as affected by the incorporation method

The incorporation method of CNC from their aqueous dispersion into the polymeric matrices is critical since water content must be reduced in the internal mixer to prevent overpressure during the polymer melt blending or polymer hydrolysis. The CNC dispersion could be dried before the incorporation process and drying methods that are effective at maintaining the inherent nano-scale dimensions, such as freeze drying, spray drying or supercritical drying,

have been described (Ng et al., 2015). Nevertheless, CNC are aggregated in the dry form and re-dispersion in the polymer melt represents a challenge, on top of the difficulty involved in handling them in dry form (Brinchi et al., 2013). In this work, two different methods were used to transfer CNC to the polymer blend: their previous transference to the glycerol used as plasticizer (M1) and the previous thermoprocessing of the starch phase suspended in the initial CNC dispersion in an open two-roll mill, which favours water evaporation while the starch gelatinization occurs (M2). In this sense, 1 wt% of CNC was incorporated into both S-PLA compatibilised blends and net TPS films, for comparison purposes. Tables 2 and 3 include the tensile properties (elastic modulus: EM, tensile strength: TS and elongation at break: ε), thickness, barrier properties (water vapour permeability: WVP and oxygen permeability: OP) and moisture content of the obtained films.

Table 2. Tensile properties (EM: elastic modulus, TS: tensile strength, ε: elongation at break point) of pure thermoplastic starch (S) and containing CNC incorporated by different methods (M1: glycerol transference, M2: direct thermoprocessing in two-roll mill), compatibilised S-PLA blends containing CNC incorporated by M1 and M2, cellulose fibres (CF) and antioxidant extract (AE) from coffee husk (films conditioned at 53% RH and 25 °C).

Formulation	EM (MPa)	TS (MPa)	ε (%)	Thickness (mm)
S	77 ± 15^{b}	5.2 ± 1.6^{b}	64.9 ± 0.5^{f}	0.20 ± 0.02^{bc}
S-CNC-M1	45 ± 3^{a}	3.8 ± 0.2^{a}	55.3 ± 1.4^{e}	0.20 ± 0.02^{b}
S-CNC-M2	179 ± 4^{d}	6.6 ± 0.4^{c}	35.1 ± 4.7^{d}	0.20 ± 0.01^{bc}
S(PCL_{5G})PLA_{20}	195 ± 35^{d}	7.6 ± 0.3^{de}	21.1 ± 1.9^{b}	0.19 ± 0.01^{ab}
S(PCL_{5G})PLA_{20}-CNC-M1	140 ± 16^{c}	8.0 ± 0.5^{e}	28.3 ± 3.9^{c}	0.20 ± 0.02^{b}
S(PCL_{5G})PLA_{20}-CNC-M2	515 ± 29^{g}	11.0 ± 0.3^{f}	12.6 ± 2.0^{a}	0.21 ± 0.01^{c}
S(PCL_{5G})PLA_{20}-CF	132 ± 15^{c}	7.0 ± 0.3^{cd}	20.5 ± 1.4^{b}	0.18 ± 0.01^{a}
S(PCL_{5G})PLA_{20}-AE	183 ± 13^{d}	6.9 ± 0.9^{cd}	19.8 ± 2.3^{b}	0.18 ± 0.01^{a}

Different superscript letters within the same row indicate significant differences among formulations ($p<0.05$).

Significant differences in tensile properties were obtained for films with the same composition obtained by using both methods for the CNC transference. Using M1, reductions in the EM of the films, with respect to that of the corresponding film without CNC, of about 42 and 33%, respectively for starch and starch-PLA blend, was obtained. However, a significant increase in EM was detected when CNC were directly incorporated

into the starch phase in the open two-roll mill (132 and 148%, respectively for the starch and starch-PLA blend). A similar effect was observed on the TS, while the film extensibility was only notably reduced when using M2 for CNC incorporation. This indicates the different reinforcing effect of CNC on the matrix depending on the transference method. The greater improvement in the film resistance and stiffness when CNC were directly incorporated into the starch phase from the water dispersion points to the strong interfacial interaction between crystalline cellulose and starch during the melt blending through the great surface area of the CNC (Collazo-Bigliardi et al., 2017b). In contrast, the previous transference of the CNC to the glycerol could lead to the formation of glycerol-CNC complexes through hydroxyl hydrogen bonds. CNC-glycerol interactions would favour the glycerol carbon exposure on the outside of the molecular complex, giving particles with a more hydrophobic surface and lower ability to disperse in the hydrophilic starch continuous phase of the film, where their reinforcing capacity would be more appreciable. Dispersion of the more hydrophobic CNC-glycerol particles in the starch phase would contribute to a reduction in the cohesion forces of the matrix, thus reducing the films' stiffness and resistance to break. In the S-PLA blend, the CNC-glycerol complexes would exhibit more affinity with the less-polar molecules of PLA than with the continuous polar starch phase and so, the glycerol-CNC particles could be better dispersed in the PLA domains, which, in turn, are dispersed in the starch matrix. Fig.1 shows the FESEM micrograph of compatibilised blend films, where the good interfacial adhesion between the dispersed PLA domains and continuous starch phase may be observed, as well as the reduced size of the PLA domains, as discussed in previous studies (Collazo-Bigliardi et al., Unpublished results).

Fig.1 also shows the FESEM micrographs of the compatibilised blend films with CNC transferred by both methods, where no CNC aggregates could be observed at the used magnification level, while qualitative differences may be appreciated at the PLA-starch interface. M2 led to lower interfacial adhesion of the polymers than M1. This could be due to the different location of CNC, which can also contribute to the interfacial interactions, depending on their prevalent distribution in each phase and their association, or not, with the glycerol molecules. In the S-PLA blend, the CNC-glycerol particles dispersed within the PLA domains could improve the interfacial affinity of both polymers.

Kargarzadeh, Johar, & Ahmad (2017) also observed an increase in EM (up to 70%) and TS (up to 52%) with the addition of 6% of CNC from rice husk to cassava starch films obtained by casting. Savadekar & Mhaske (2012) also incorporated CNC from cotton fibres into thermoplastic starch blends at 0.4 wt% with good reinforcement efficiency. The formation of a percolation network favours the enhancement of the film mechanical properties because of the interaction among the CNC by intra- and inter-molecular hydrogen bonds and/or the mutual entanglement between the CNC and the starch matrix. Moreover, the intrinsic stiffness of crystalline cellulose, associated with the crystalline structure, could also contribute to the increase in EM.

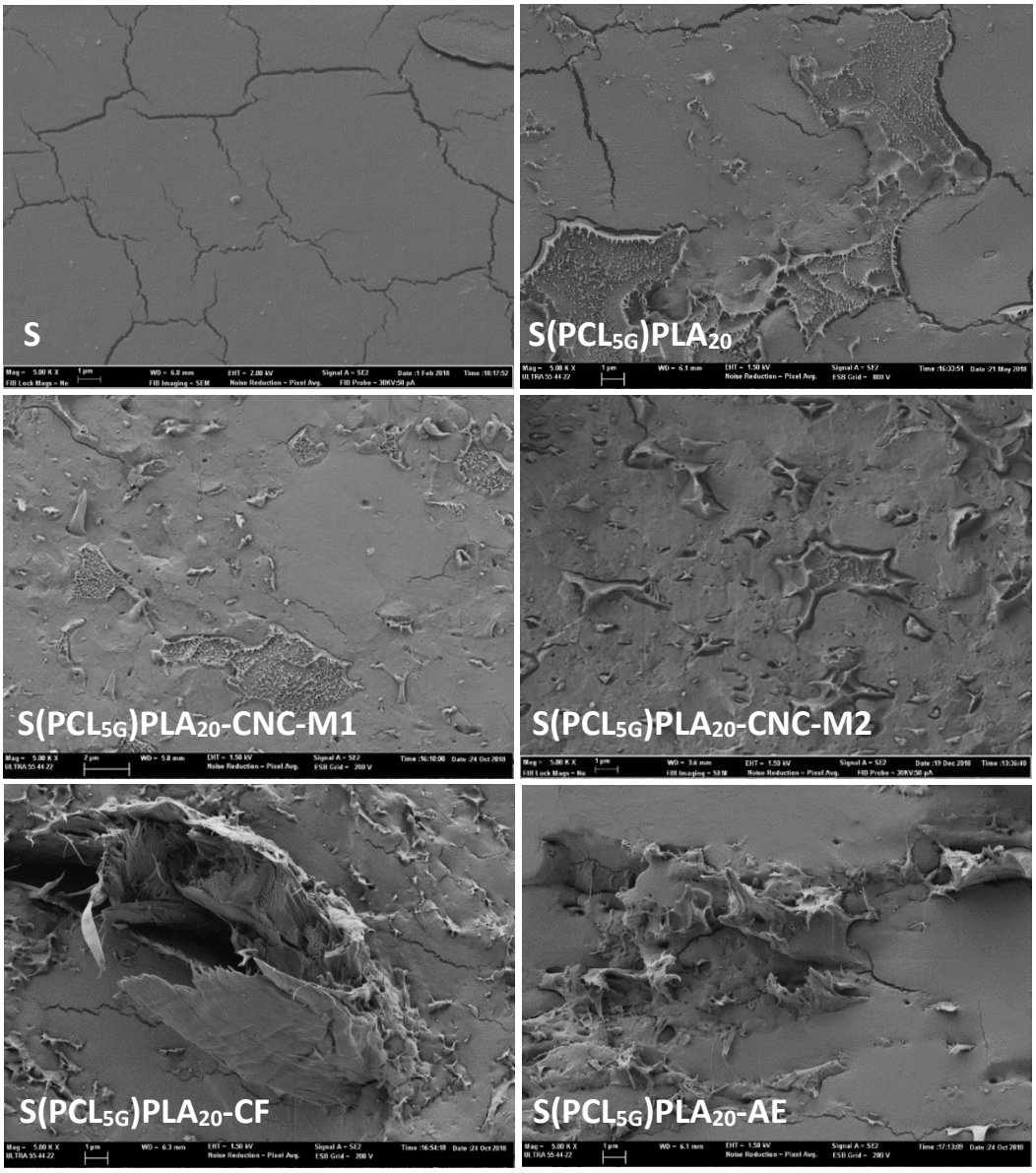

Fig. 1. FESEM micrographs of the cross-section of pure thermoplastic starch (S) and compatibilised S-PLA blends containing or not CNC incorporated by different methods (M1: glycerol transference, M2: direct thermoprocessing in two-roll mill), cellulose fibres (CF) and antioxidant extract (AE) from coffee husk.

This fact was also reported by Sung, Chang, & Han (2017) for PLA matrices obtained by extrusion process when freeze-dried CNC from coffee silverskin were incorporated. Authors also reported that the stiffening effect of the filler led to significant local stress concentrations and reduced strain to failure. Karkarzadeh et al. (2017) and Sung et al. (2017) indicated that the main factors determining the reinforcing effect of nano-scale fillers are the good dispersion and adhesion between the filler and the polymer matrix, which, in turn, are affected by the CNC load in the blend (Dhar, Tarafder, Kumar, & Katiyar, 2016).

Barrier properties were also affected by the CNC incorporation method. In starch films, WVP was reduced by 28 and 36% when CNC were incorporated by methods 1 and 2, respectively. In contrast, OP was only significantly reduced (by 40%) when using M2. Reduction in WVP was also reported by Fabra, López-Rubio, Ambrosio-Martín, & Lagaron (2016) for thermoplastic corn starch films with different contents of bacterial cellulose nanowhiskers. The different effect of the CNC on barrier properties, depending on the transference method, agrees with the different film microstructure and the prevalent location of the CNC in each case.

Table 3. Mean values and standard deviation of barrier properties (water vapor permeability: WVP, oxygen permeability: OP) and moisture content of pure thermoplastic starch (S) containing or not CNC incorporated by different methods (M1: glycerol transference, M2: direct thermoprocessing in two roll mill) and compatibilised S-PLA blends containing CNC incorporated by M1 and M2, cellulose fibres (CF) and antioxidant extract (AE) from coffee husk (films conditioned at 53% RH and 25 °C).

Formulation	Moisture content (g water/g dried film)	WVP ($g \cdot mm \cdot kPa^{-1} \cdot h^{-1} \cdot m^{-2}$)	OP x10^{14} ($cm^3 \cdot m^{-1} \cdot s^{-1} \cdot Pa^{-1}$)
S	0.096 ± 0.007^{c}	14.9 ± 0.4^{d}	10.3 ± 0.1^{b}
S-CNC-M1	0.098 ± 0.005^{c}	10.7 ± 0.6^{c}	11.8 ± 0.9^{c}
S-CNC-M2	0.097 ± 0.006^{c}	9.3 ± 1.3^{bc}	6.2 ± 0.8^{a}
S(PCL_{5G})PLA_{20}	0.065 ± 0.004^{a}	10.1 ± 0.4^{bc}	19.9 ± 0.6^{e}
S(PCL_{5G})PLA_{20}-CNC-M1	0.091 ± 0.006^{bc}	10.8 ± 1.2^{c}	25.9 ± 0.7^{f}
S(PCL_{5G})PLA_{20}-CNC-M2	0.092 ± 0.005^{bc}	7.3 ± 0.9^{a}	11.6 ± 0.8^{bc}
S(PCL_{5G})PLA_{20}-CF	0.104 ± 0.003^{d}	8.9 ± 1.0^{ab}	28.1 ± 0.4^{g}
S(PCL_{5G})PLA_{20}-AE	0.086 ± 0.001^{b}	8.4 ± 0.9^{ab}	17.2 ± 0.2^{d}

Different superscript letters within the same row indicate significant differences among formulations ($p < 0.05$).

In starch-PLA compatibilised films, WVP was only reduced (by 28%) by method 2, whereas OP increased by 30% by method 1 and decreased by 42% by method 2. These different effects are coherent with the more hydrophobic nature of the CNC particles when transferred from the glycerol and their prevalent location in the dispersed PLA domains, whereas CNC incorporated into the starch phase (method 2) provided a more efficient barrier capacity, similar to that observed in the net starch films.

The role of CNC at improving barrier properties is mainly related with their crystalline structure, which hinders the diffusion of molecules (O_2, CO_2, H_2O) through the biopolymer matrix. The formation of hydrogen-bonded structures and a percolation network promotes the tortuosity factor of the matrix (Collazo-Bigliardi et al., 2018b; Luzi et al., 2016), which mainly depends on the matrix-filler adhesion, degree of dispersion, aspect ratio of filler and polymer chain immobilization (Sung et al., 2017). In polymer blends with phase separation, the percolation network in the continuous phase will be more effective than that in the dispersed domains, which also points to the different distribution of CNC (in the continuous or dispersed phase), according to the incorporation method.

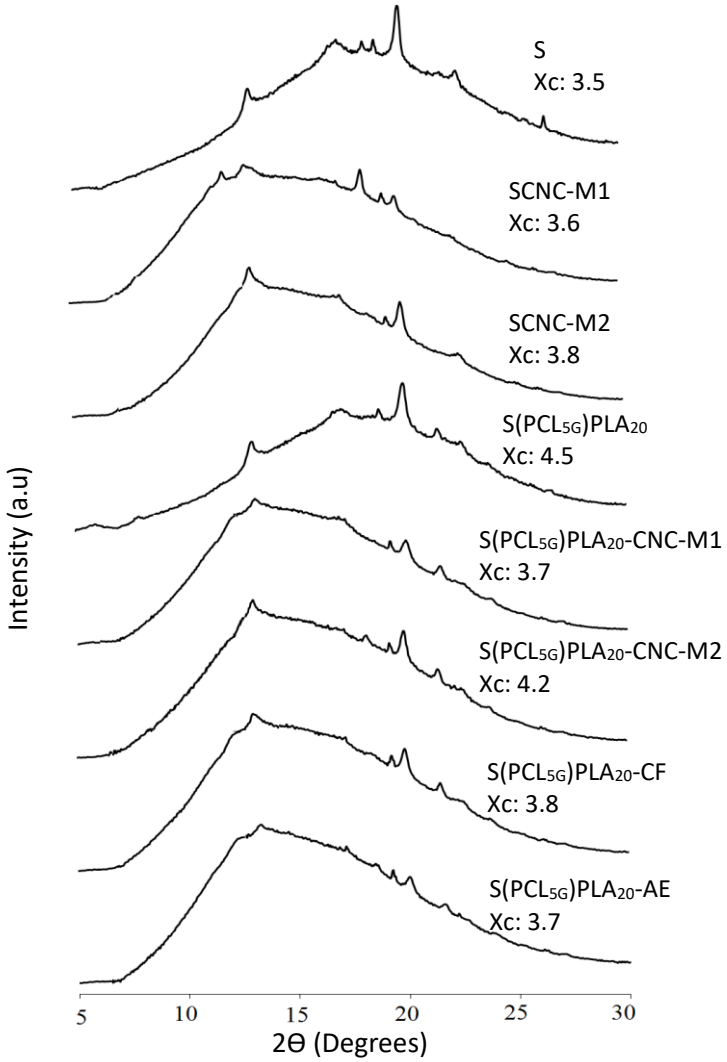

Fig. 2. X-ray diffraction patterns and crystallinity degree (Xc, %) of pure thermoplastic starch (S) and compatibilised S-PLA blends containing or not CNC incorporated by different methods (M1: glycerol transference, M2: direct thermoprocessing in two roll mill), cellulose fibres (CF) and antioxidant extract (AE) from coffee husk.

As regards crystallization, Fig. 2 shows X-ray diffraction pattern and degree of crystallinity (Xc) of the different samples containing CNC incorporated by the two methods. The main characteristic crystalline peaks of starch were detected in all samples at 2θ values of around 12.9° and 19.8°, which are associated with the crystalline structure of amylose type V (Castillo et al., 2013; Ortega-Toro, Contreras, Talens, & Chiralt, 2015), although some peaks associated with A form (2θ: 18-18.5°) could also be observed. The characteristic peak of crystalline PLA on 2θ of 17° (Muller et al., 2017b) was not observed, coherent with its amorphous nature. Likewise, no peaks of crystalline PCL (2θ: 21.6°, 22.2° and 23.3°; Ortega-Toro et al., 2016b) were detected for the grafted PCL, either because of its low concentration in the blend or its crystallization inhibition by the anchoring of the polar groups (Ortega-Toro et al., 2016b). Cellulosic micro- or nano-fillers exhibited typical crystalline peaks of type I cellulose at 2θ: 17° and 21.4° (Collazo-Bigliardi et al., 2018b) but they were not observed, probably due to their low content in the film. The incorporation of CNC directly into the starch phase (method 2) slightly promoted the amylose crystallization in starch films, which could be due to the favoured interaction of amylose and crystalline cellulose, which can act as nucleating agents, as reported by other authors (Ferreira et al., 2018). However, this effect was not observed in the starch-PLA blend.

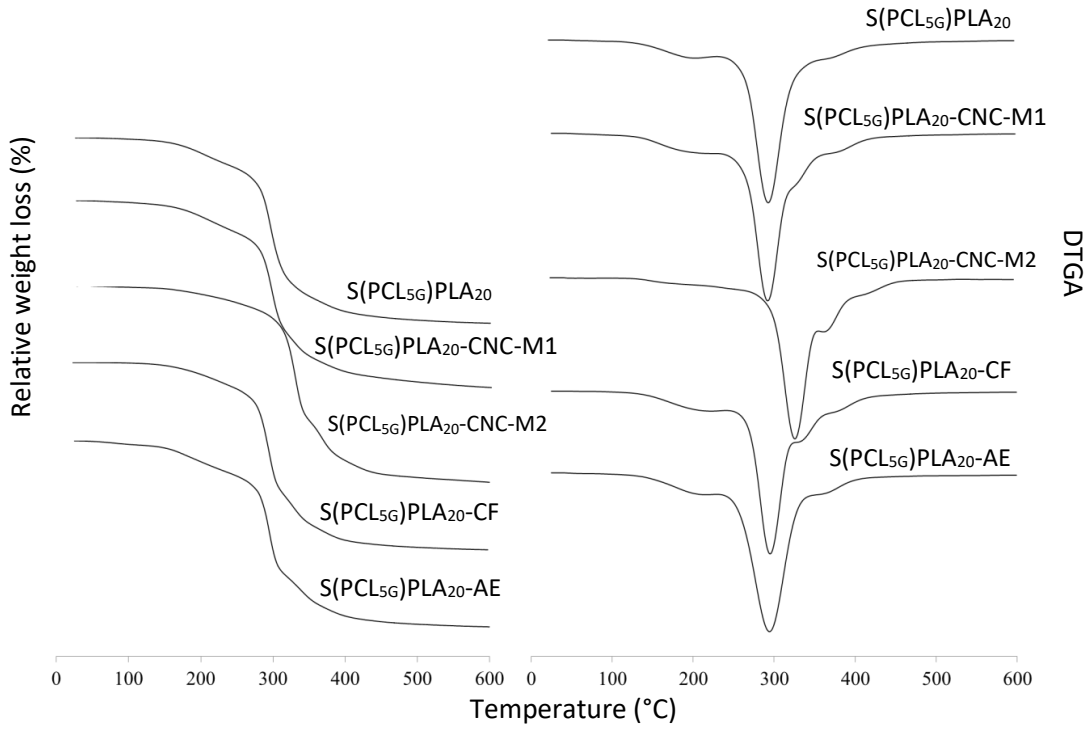

Fig. 3. TGA and DTGA curves of compatibilised S-PLA blends containing or not CNC incorporated by different methods (M1: glycerol transference, M2: direct thermoprocessing in two roll mill), cellulose fibres (CF) and active extracts (AE) from coffee husk.

Table 4. Mean values and standard deviation of onset and peak temperatures for thermal degradation and glass transition temperature (Tg; second heating scan on DSC) of S-PLA films with cellulosic material and antioxidant extract from coffee husk, conditioned in P_2O_5.

Samples	[138-205]°C		[250-400]°C			Second heating scan	
	Onset (°C)	Peak (°C)	Onset (°C)	Peak (°C)	Endset (°C)	Tg (°C) Starch	Tg (°C) PLA
S(PCL$_{5G}$)PLA$_{20}$	146 ± 4^{a}	195 ± 2^{bc}	269 ± 1^{b}	296 ± 1^{a}	392 ± 2^{a}	106 ± 1^{a}	49.3 ± 0.7^{b}
S(PCL$_{5G}$)PLA$_{20}$-CNC-M1	141 ± 3^{a}	193 ± 8^{b}	268 ± 1^{b}	294 ± 2^{a}	400 ± 0.3^{b}	107 ± 2^{a}	48.2 ± 0.9^{ab}
S(PCL$_{5G}$)PLA$_{20}$-CNC-M2	145 ± 2^{a}	171 ± 0.2^{a}	305 ± 0.2^{c}	329 ± 1^{b}	438 ± 4^{c}	107 ± 2^{a}	48.3 ± 0.9^{ab}
S(PCL$_{5G}$)PLA$_{20}$-CF	151 ± 5^{ab}	204 ± 0.5^{c}	270 ± 1^{b}	296 ± 0.2^{a}	400 ± 2^{b}	108 ± 1^{a}	49.5 ± 0.6^{b}
S(PCL$_{5G}$)PLA$_{20}$-AE	156 ± 3^{b}	200 ± 0.1^{bc}	258 ± 0.2^{a}	295 ± 1^{a}	404 ± 2^{b}	110 ± 1^{b}	47.7 ± 0.3^{a}

Different superscript letters within the same column indicate significant differences between formulations ($p < 0.05$).

Fig. 3 shows TGA and derivate (DTGA) curves obtained for the studied formulations. TGA curves exhibited several degradation phases of differing intensities for every sample; the first phase can be attributed to the bonded water evaporation and the degradation of low molecular weight components and, afterwards, the partially overlapped thermal degradation of the polymers, starch, PLA and PCL_G, and the cellulosic fraction, took place. These different phases are reflected in the DTGA curves as peaks or shoulders. The shoulder in the main peak at about 380 °C would mainly correspond to the degradation of the grafted PCL with higher degradation temperatures (341-381 °C, Ortega-Toro et al., 2016b), partially overlapped with the final degradation of PLA. The comparison of samples containing CNC incorporated by both methods and control sample (free of lignocellulosic fractions) reflects differences in the peak and shoulder temperatures in both the first and the main peak. No differences were found between control sample and that processed by method 1, but samples processed by method 2 exhibited a lower temperature for the first peak and a higher temperature for the main peak, with temperature displacements for the shoulders. This can be attributed to the different interactions of CNC with the polymers in both cases, resulting in changes in the degradation behaviour of the different blend components (Kargarzadeh et al., 2018). Table 4 also shows the glass transition temperature (Tg) of S and PLA in the different blend films. This is an important parameter since it indicates the maximum temperature of use of the packaging material before its softening (Ortega-Toro et al., 2017). The addition of CNC by method 1 or 2 did not affect the values of Tg of any of the polymers.

As concerns transparency (Fig. 4), the control sample (free of lignocellulosic fractions) exhibited relatively low transparency that can be attributed to the dispersion of the PLA domains in the starch matrix, as observed in the FESEM images, which implies an increase in the dispersive component of light. The incorporation of CNC into the blend slightly modified film transparency, depending on the incorporation method. This agrees with the microstructural observations that reflect differences in the component arrangement mainly at interfacial level, which may affect the light dispersion pattern and so, the film transparency, as reported by Muller et al. (2017b).

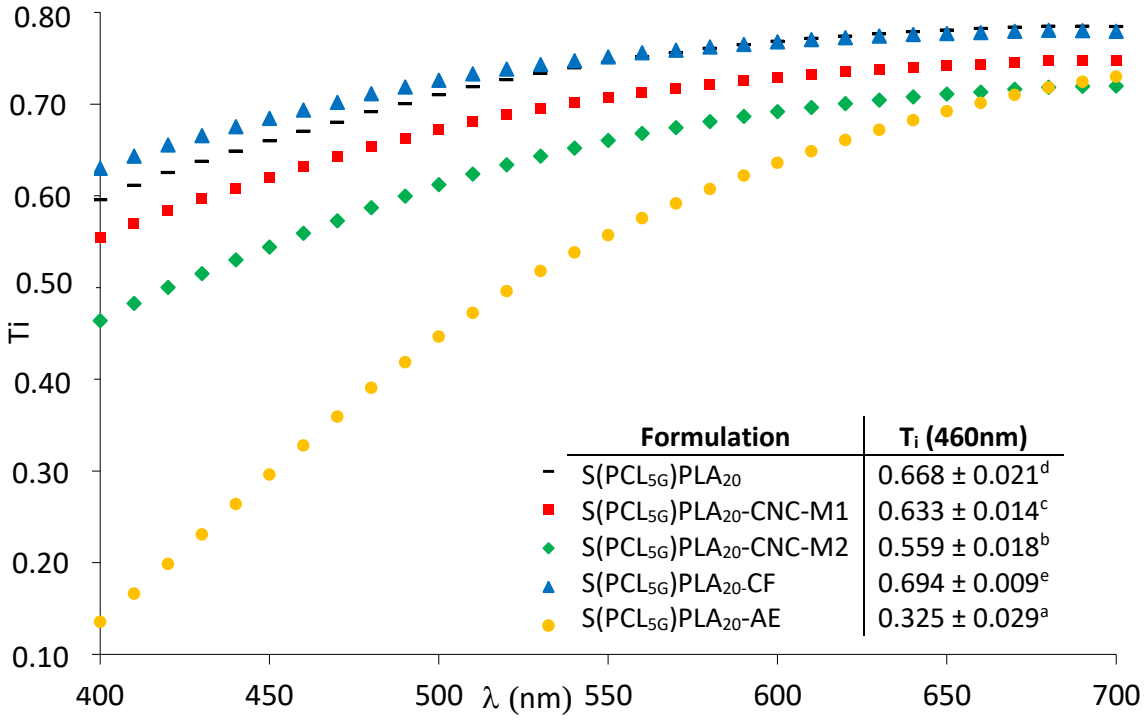

Fig. 4. Internal transmittance (Ti) spectra of compatibilised S-PLA blends containing or not CNC incorporated by different methods (M1: glycerol transference, M2: direct thermoprocessing in two roll mill), cellulose fibres (CF) and active extracts (AE) from coffee husk. Embedded table shows the Ti values at 460 nm.

3.2. Effect of cellulosic fibres on the film's functional properties

The microstructural impact of cellulosic fibres from coffee husk on the S-PLA compatibilised matrix can be observed in Fig. 1, where the FESEM micrographs of the film cross-section are shown. The CF could be clearly seen embedded in the film matrix with good interfacial adhesion. However, CF provoked a weakening effect on the film matrix reflected in the fact that the EM values were lower than in the control film, although they did not provoke significant changes in the film resistance to break and extensibility. Likewise, the barrier properties of the films were negatively affected by CF; no significant changes in the WVP were observed, but OP increased by 40% with respect to the control film.

The addition of CF did not provoke notable changes in the film transparency, polymer crystallization pattern or in the degree of crystallinity; neither did it influence the thermal behaviour of the blend in terms of the thermodegradation of components or the polymer glass transition. Then, CF behaved as a quasi-inert filler that, at the used ratio, did not improve film properties. However, CF incorporated at 1% in net starch films increased their

elastic module by 50% with respect to the control film, with no changes in barrier properties (Collazo-Bigliardi et al., 2018a). The lack of effect brought about by CF in the compatibilised starch-PLA blend could be explained by the starch film that is already reinforced by the dispersed PLA that makes the fibre effect less appreciable. Likewise, in terms of barrier properties, fibres do not seem to lead to a notable increase in the tortuosity of the path to permeation of the water and gas molecules, with respect to that promoted by the PLA dispersed in the starch matrix, and the expected improvement in the film barrier capacity was not observed.

3.3. Effect of antioxidant extract on the film's functional properties

The incorporation of the active extract into the blend films led to morphological changes in both the continuous starch phase and the PLA dispersed phase, as compared with the control sample, as shown in Fig. 1. In fact, the ability of the extract compounds to interact with the starch matrix, contributing to the formation of a more compact and homogeneous matrix, has previously been reported in other studies (Collazo-Bigliardi et al., in press; Talón et al., 2017). Likewise, PLA in the dispersed phase could also interact with these compounds. The acid nature of phenolic acids could even partially hydrolyse the polyester chains. Caffeic and chlorogenic acids were the main phenolic compounds present in coffee husk, and vanillic, gallic, tannic and protocatechuic acids were also found in small quantities (Aguiar, Estevinho, & Santos, 2016).

The tensile properties of the blend films were not significantly affected by the presence of the antioxidant extract, despite the fact that this had a great reinforcement effect in net starch films. This suggests that compounds could interact better with the dispersed PLA than with the starch, which dilutes the potential reinforcing effects in the film's continuous phase. As concerns barrier properties, no significant effect was observed on the WVP, but the OP was reduced by 15% respect to that of the control film. OP reduction brought about by the extract incorporation was also observed in net starch films, which was attributed to the oxygen scavenging capacity of the compounds in line with their antioxidant capacity (Collazo-Bigliardi et al., in press).

The incorporation of the extract did not modify the crystallization pattern of the films, but slightly reduced the degree of crystallinity in line with its amorphous nature. The thermodegradation behaviour was also slightly modified by the extract, due to the presence of low molecular compounds which degrade at low temperature. Likewise, the Tg of starch and PLA changed with respect to the control film, thus indicating the interactions of the extract compounds with both polymers. The Tg value of starch increased, as previously observed for net starch films containing this extract (Collazo-Bigliardi et al., in press) and the

Tg of PLA decreased, according to a plasticizing effect of the compounds in this polymer phase or to the possible partial de-polymerization of PLA provoked by phenolic acids, as previously mentioned.

The films containing active extract exhibited the lowest transparency level which is mainly caused by the selective light absorption of the extract compounds, mainly at low wavelengths. This could be considered positive because of the potential protection capacity of the films for use in food applications, reducing the light-induced oxidation reactions (Collazo-Bigliardi et al., 2018c).

The antioxidant capacity of these films was evaluated through their ability to preserve sunflower oil from oxidation. The antioxidant capacity of this film formulation was compared to that of the control film and to an open oil sample. The PV values reflect the initial oxidation stage of oil since it is related with the presence of peroxides derived from the polyunsaturated fatty acids existing in the sample (Galarza et al., 2017). Hydroperoxides are produced as primary oxidation products that could be derived into secondary products. The progress of the PV in the different samples throughout 23 days is shown in Fig. 5.

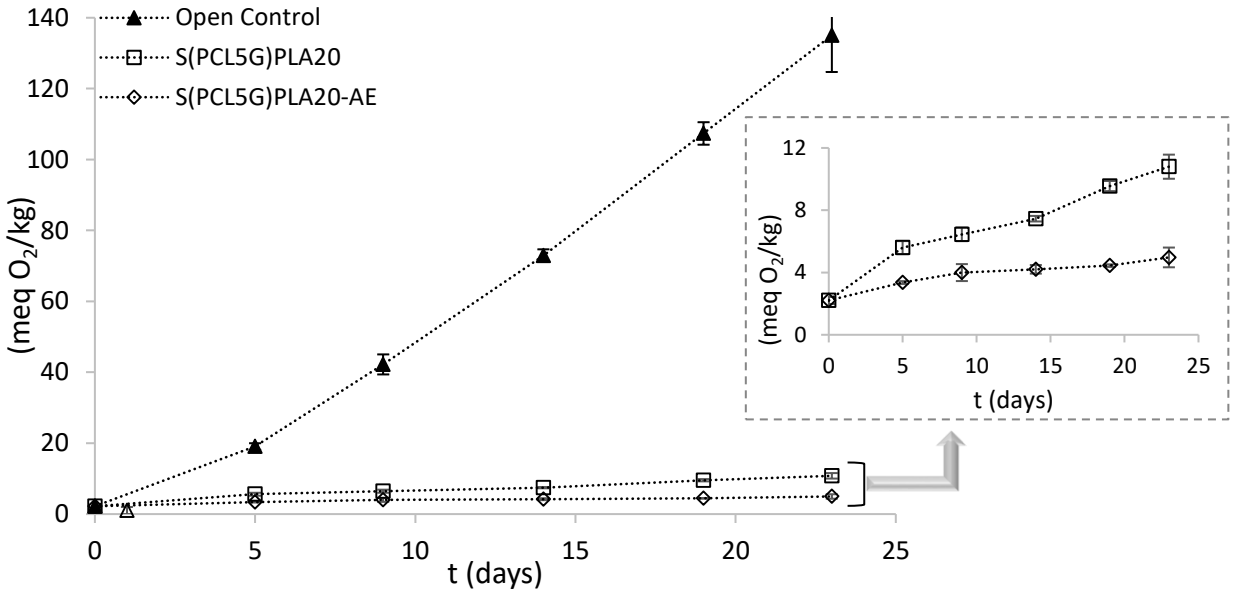

Fig. 5. Peroxide Index (mEq O_2/kg), B) of sunflower oil packaged in films of compatibilised S-PLA blends containing or not antioxidant extract (AE), compared with the control open samples.

The PV of sunflower oil in the initial stage was 2.2 mEq O_2/kg, as also reported by other authors (Kiralan et al., 2017; Mohdaly, Sarhan, Mahmoud, Ramadan, & Smetanska, 2010). A remarkable increase in this value was found for the open control sample (135 mEq O_2/kg in the final stage). However, the samples with and without antioxidant compound were kept below the required limits, even for the control film, at the end of the experiment (~5 mEq O_2/kg). The Codex Alimentarius established a limit of PV in 10 mEq O_2/kg for refined oils (Codex-Alimentarius, 1999). This behaviour is attributable to the great oxygen barrier capacity of the films, mainly made up of starch. The lowest PV was obtained in the sample packaged in the film with AE, wherein the presence of the antioxidant compounds from coffee husk prevented the oxidation of sunflower oil. Similar results were described by Reis, de Souza, da Silva, Martins, Nunes, & Druzian (2015) analysing the incorporation of mango pulp and yerba mate extract into cassava starch films, which were effective at preserving palm oil. Galarza et al. (2017) also reported a good preservation of sunflower oil oxidation when packaged in bags formed with glycerol-plasticised films from rice flour (RRF) and red rice starch (RRS) in a 9:1 RRF:RRS ratio.

4. CONCLUSIONS

Lignocellulosic fractions of coffee husk could be used to improve the functional properties of compatibilised starch PLA films, depending on their final use. Of the cellulosic fractions, CF was not adequate to enhance the functionality of the blend film, but CNC previously incorporated into the starch phase were effective at reinforcing the tensile properties of the material (148% and 45% increases in EM and TS, respectively) and at reducing the WVP and OP of the films (28% and 42% reductions, respectively in WVP and OP). Likewise, the antioxidant extract did not impart a better mechanical performance to the blend films, but reduced their oxygen permeability and conferred antioxidant capacity, promoting their usefulness for the purposes of preventing food oxidation reactions.

Acknowledgements

The authors thank the Ministerio de Economía y Competitividad (Spain) for the financial support provided through Project AGL2016-76699-R. The authors also wish to thank the Electron Microscopy Service of the UPV for their technical assistance.

REFERENCES

Aguiar, J., Estevinho, B. N., & Santos, L. (2016). Microencapsulation of natural antioxidants for food application - The specific case of coffee antioxidants - A review. *Trends in Food Science & Technology*, 58, 21-39.

Alves, R. C., Rodrigues, F., Nunes, M. A., Vinha, A. F., & Oliveira, M. B. P. P. (2017). State of the art in coffee processing by-products. In C. M. Galanakis (Ed.). *Handbook of coffee processing by-products* (pp. 1–26). Cambridge: Academic Press.

ASTM. (1995). Standard test methods for water vapor transmission of materials. Standard Designations: E96-95. In Annual books of ASTM. pp. 406-413. Philadelphia, PA: American Society for Testing and Materials.

ASTM (2001). Standard test method for tensile properties of thin plastic sheeting. Standard Designations: D882. Annual book of ASTM standards. Philadelphia, PA: American Society for Testing and Materials.

Azeredo, H., Rosa, M. F., & Mattoso, L. H. (2017). Nanocellulose in bio-based food packaging applications. *Industrial Crops and Products*, 97, 664-671.

Balaji, A. B., Pakalapati, H., Khalid, M., Walvekar, R., & Siddiqui, H. (2017). Natural and synthetic biocompatible and biodegradable polymers. In N. Gopal Shimpi (Ed.). *Biodegradable and biocompatible polymer composites* (pp. 3-32). United Kingdom: Woodhead Publishing.

Berthet, M. A., Angellier-Coussy, H., Machado, D., Hilliou, L., Stabler, A., Vicente, A., & Gontard, N. (2015). Exploring the potentialities of using lignocellulosic fibres derived from three food by-products as constituents of biocomposites for food packaging. *Industrial Crops and Products*, 69, 110-122.

Brigham, C. (2018). Biopolymers: Biodegradable alternatives to traditional plastics. In B. Török, & T. Dransfield (Eds.). *Green chemistry* (pp. 753-770). Amsterdam: Elsevier Inc.

Brinchi, L., Cotana, F., Fortunati, E., & Kenny, J. M. (2013). Production of nanocrystalline cellulose from lignocellulosic biomass: Technology and applications. *Carbohydrate Polymers*, 94, 154–169.

Castillo, L., López, O., López, C., Zaritzky, N., García, M. A., Barbosa, S., & Villar, M. (2013). Thermoplastic starch films reinforced with talc nanoparticles. *Carbohydrate Polymers*, 95(2), 664-674.

Codex-Alimentarius. (1999). Codex-Standards for fats and oils from vegetable sources (Vol. 210, p. 1).

Collazo-Bigliardi, S., Ortega-Toro, R., & Chiralt, A. (2018a). Properties of Micro- and nano-reinforced biopolymers for food applications. In T. Gutiérrez (Ed.), *Polymers for food applications* (pp. 61-99). Springer.

Collazo-Bigliardi, S., Ortega-Toro, R., & Chiralt, A. (2018b). Isolation and characterisation of microcrystalline cellulose and cellulose nanocrystals from coffee husk and comparative study with rice husk. *Carbohydrate Polymers*, 191, 205-215.

Collazo-Bigliardi, S., Ortega-Toro, R., & Chiralt, A. (2018c). Reinforcement of thermoplastic starch films with cellulose fibres obtained from rice and coffee husks. *Journal of Renewable Materials*, 6, 599-610.

Collazo-Bigliardi, S., Ortega-Toro, R., & Chiralt, A. Using grafted poly(ε-caprolactone) for the compatibilization of starch-polylactic acid blends. Carbohydrate Polymers, Unpublished results.

Collazo-Bigliardi, S., Ortega-Toro, R., & Chiralt, A. Improving properties of thermoplastic starch films by incorporating active extracts and cellulose fibres isolated from rice or coffee husk. Food Packaging and Shelf Life. In press.

Cong-Cong, X., Bing, W., Yi-Qiong, P., Jian-Sheng, T., & Tong, Z. (2017). Advances in extraction and analysis of phenolic compounds from plant materials. *Chinese Journal of Natural Medicines*, 15(10), 721-731.

Dhar, P., Tarafder, D., Kumar, A., & Katiyar, V. (2016). Thermally recyclable polylactic acid/cellulose nanocrystal films through reactive extrusion process. *Polymer*, 87, 268-282.

Dorris, A., & Gray, D. G. (2012). Gelation of cellulose nanocrystals suspensions in glycerol. *Cellulose,* 19, 687-694.

Fabra, M. J., López-Rubio, A., Ambrosio-Martín, J., & Lagaron, J. M. (2016). Improving the barrier properties of thermoplastic corn starch-based films containing bacterial cellulose nanowhiskers by means of PHA electrospun coatings of interest in food packaging. *Food Hydrocolloids*, 61, 261-268.

Ferreira, F. V., Dufresne, A., Pinheiro, I. F., Souza, D. H. S., Gouveia, R. F., Mei, L. H. I., & Lona, L. M. F. (2018). How do cellulose nanocrystals affect the overall properties of

biodegradable polymer nanocomposites: A comprehensive review. *European Polymer Journal*, 108, 274-285.

Galarza, C., Costa, T. M. H., de Oliveira Rios, A., & Flôres, S. H. (2017). Comparative study on the properties of films based on red rice (Oryza glaberrima) flour and starch. *Food Hydrocolloids*, 65, 96-106.

Hamad, K., Kaseem, M., Ayyoob, M., Joo, J., & Deri, F. (2018). Polylactic acid blends: The future of green, light and tough. *Progress in Polymer Science*, 85, 83-127.

Hutchings, J. B. (1999). Food color and appearance (2nd ed.). Gaithersburg, Maryland, USA: Aspen Publishers, Inc.

IUPAC (International Union of Pure and Applied Chemistry). (1987). Standard method for the analysis of oils, fats and derivatives; Paquot, C., Hautfenne, A. London, U.K: Blackwell Scientific Publications.

Kargarzadeh, H., Johar, N., & Ahmad, I. (2017). Starch biocomposite film reinforced by multiscale rice husk fiber. *Composite Science and Technology*, 15, 147–155.

Kargarzadeh, H., Huang, J., Lin, N., Ahmad, I., Mariano, M., Dufresne, A., Thomas, S., & Galeski, A. (2018). Recent developments in nanocellulose-based biodegradable polymers, thermoplastic polymers, and porous nanocomposites. *Progress in Polymer Science*, 87, 197-227.

Kiralan, M., Ulaş, M., Özaydin, A., Özdemır, N., Özkan, G., Bayrak, A., & Ramadan, M. F. (2017). Blends of cold pressed black cumin oil and sunflower oil with improved stability: a study based on changes in the levels of volatiles, tocopherols and thymoquinone during accelerated oxidation conditions. *Journal of Food Biochemistry*, 41(1).

Koch, K. (2018). Starch-based film. In M. Sjöö & L. Nilsson (Eds), *Starch in food* (pp. 747-767). Woodhead Publishing.

Laurienzo, P., Malinconico, M., Mattia, G., & Romano, G. (2006). Synthesis and characterization of functionalized crosslinkable poly(ε-caprolactone). *Macromolecular Chemistry and Physics*, 207, 1861-1869.

Luzi, F., Fortunati, E., Jiménez, A., Puglia, D., Pezzolla, D., Gigliotti, G., Kenny, J. M., Chiralt, A., & Torre, L. (2016). Production and characterization of PLA_PBS biodegradable blends reinforced with nanocrystals extracted from hemp fibres. *Industrial Crops and Products*, 93, 276–289.

McHugh, T. H., Avena-Bustillos, R., & Krochta, J. M. (1993). Hydrophobic edible films: Modified procedure for water vapour permeability and explanation of thickness effects. *Journal of Food Science*, 58(4), 899-903.

Mohdaly, A. A. A., Sarhan, M. A., Mahmoud, A., Ramadan, M. F., & Smetanska, I. (2010). Antioxidant efficacy of potato peels and sugar beet pulp extracts in vegetable oils protection. *Food chemistry*, 123(4), 1019-1026.

Müller, P., Bere, J., Fekete, R., Móczó, J., Nagy, B., Kállay, M., Gyarmati, B., & Pukánszky, B. (2016). Interactions, structure and properties in PLA/plasticized starch blends. *Polymer*, 103, 9-18.

Muller, J., González-Martínez, C., & Chiralt, A. (2017a). Combination of poly(lactic) acid and starch for biodegradable food packaging. *Materials*, 10, 952.

Muller, J., González-Martínez, C., & Chiralt, A. (2017b). Poly(lactic) acid (PLA) and starch bilayer films, containing cinnamaldehyde, obtained by compression moulding. *European Polymer Journal*, 95, 56-70.

Murariu, M., & Dubois, P. (2016). PLA composites: From production to properties. *Advanced drug delivery reviews*, 107, 17-46.

Ng, H. M., Sin, L. T., Tee, T. T., Bee, S. T., Hui, D., Low, C. Y., et al. (2015). Extraction of cellulose nanocrystals from plant sources for application as reinforcing agent in polymers. *Composites Part B Engineering,* 75, 176–200.

Ogunsona, E., Ojogbo, E., & Mekonnen, T. (2018). Advanced material applications of starch and its derivatives. *European Polymer Journal*, 108, 570-581.

Ortega-Toro, R., Contreras, J., Talens, P., & Chiralt, A. (2015). Physical and structural properties and thermal behaviour of starch-poly(e-caprolactone) blend films for food packaging. *Food Packaging and Shelf Life* 5, 10-20.

Ortega-Toro, R., Collazo-Bigliardi, S., Talens, P., & Chiralt, A. (2016a). Influence of citric acid on the properties and stability of starch-polycaprolactone based films. *Journal of Applied Polymer Science*, 42220, 1-16.

Ortega-Toro, R., Santagata, G., Gomez d'Ayala, G., Cerruti, P., Talens, P., Chiralt, A., & Malinconico, M. (2016b). Enhancement of interfacial adhesion between starch and grafted poly(ε-caprolactone). *Carbohydrate Polymers*, 147, 16-27.

Ortega-Toro, R., Bonilla, J., Talens, P., & Chiralt, A. (2017). Starch-based materials in food packaging. In M. A. Villar, S. E. Barbosa, M. A. García, L. A. Castillo, & O. V. López (Eds.), *Future of starch-based materials in food packaging* (pp. 257-312). Aspen Publishers.

Patel, J. P., & Parsania, P. H. (2018). Characterization, testing, and reinforcing materials of biodegradable composites. In N. G. Shimpi (Ed.). *Biodegradable and biocompatible polymer composites* (pp. 55–79). United Kingdom: Woodhead Publishing.

Piñeros-Castro, Y., & Otálvaro, A. M. (2014). Use of lignocellulosic biomass, some research in Colombia. In Y. Piñeros-Castro, & J. Melo (Eds.), Antioxidant activity in liquids from pre-treatments with hot water carried out on rice husk (pp. 237-254). Bogotá. ISBN: 978-958-725-152-4.

Reis, L., De Souza, C., Da Silva, J., Martins, A., Nunes, I., & Druzian, J. (2015). Active biocomposites of cassava starch: The effect of yerba mate extract and mango pulp as antioxidant additives on the properties and the stability of a packaged product. *Food and Bioproducts Processing*, 94, 382-391.

Requena, R., Vargas, M., & Chiralt, A. (2018). Obtaining antimicrobial bilayer starch and polyester-blend films with carvacrol. *Food Hydrocolloids,* 83, 118-133.

Savadekar, N. M., & Mhaske, S. T. (2012). Synthesis of nano cellulose fibers and effect on thermoplastics starch based films. *Carbohydrate Polymers*, 89, 146–151.

Shavandi, A., Bekhit, A. E. A., Saeedi, P., Izadifar, Z., Bekhit, A. A., & Khademhosseini, A. (2018). Polyphenol uses in biomaterials engineering. *Biomaterials*, 167, 91-106.

Sung, S. H., Chang, Y., & Han, J. (2017). Development of polylactic acid nanocomposite films reinforced with cellulose nanocrystals derived from coffee silverskin. *Carbohydrate Polymers*, 169, 495-503.

Talón, E., Trifkovic, K. T., Nedovic, V. A., Bugarski, B. M., Vargas, M., Chiralt, A., & González-Martínez, C. (2017). Antioxidant edible films based on chitosan and starch containing polyphenols from thyme extracts. *Carbohydrate Polymers*, 157, 1153-1161.

Tampau, A., González-Martínez, C., & Chiralt, A. (2018). Release kinetics and antimicrobial properties of carvacrol encapsulated in electrospun poly-(ε-caprolactone) nanofibres. Application in starch multilayer films. *Food Hydrocolloids,* 79, 158-169.

GENERAL DISCUSSION

The field of food packaging involves a high consumption of oil-derived synthetic plastics, which generates a serious environmental problem due to their very low rates of biodegradation, at the same time as the consumption of a non-renewable source (oil) represents a significant limitation. The development of biodegradable packaging that contributes to minimising the environmental impact, making use of renewable sources, is one of the most interesting approaches to reducing this problem. Starch and poly-lactic acid (PLA) are biodegradable polymers obtained from natural resources which could be used for food packaging purposes due to their ability to form food-contact plastic materials with a competitive cost. Nevertheless, some of their functional properties, such as water sensitivity (starch), low oxygen barrier capacity (PLA) or mechanical performance, need to be adapted in order to meet the packaging requirements. Likewise, lignocellulosic residues constitute a source of reinforcing materials (cellulose fibres or nanocrystals) and active compounds (antioxidant/antimicrobial) which can be used to improve the functional properties of biodegradable plastics. This Doctoral Thesis has focused on the isolation and characterisation of cellulosic materials and active extracts from rice and coffee husks, and their incorporation into starch films and starch-PLA compatibilised blend films, in order to improve their functional properties as food packaging materials.

Lignocellulosic agro-waste is one of the most important natural sources of renewable non-polymeric and polymeric compounds, which are attractive materials due to their biodegradability and good mechanical properties. They contain a high fraction of cellulose, from which micro- and nano-cellulose fibres can be isolated, which can act as reinforcing agents, as well as other constituents, such as phenols linked to the hemicellulose or lignin fractions, which can provide different functional properties (antioxidant or antimicrobial capacity) to the developed materials. In this sense, rice and coffee husks have been used to isolate cellulosic fractions and to obtain active extracts through a green method, such as hydrothermal treatment.

The cellulose fibres were obtained through alkali and bleaching treatment with a final yield of 41 and 53 g fibres/100 g husk, respectively for rice and coffee husks. Cellulose nanocrystals were isolated from the bleached fibres by acid hydrolysis. The final yield of the isolation process was around 5%, with respect to bleached fibres, in both cases. This yield depends on the initial raw material and process conditions and the latter could be optimized in further studies. Despite the low yield, they possessed a high capacity to accomplish their function as reinforcing agents (**Chapter I**), such as high crystallinity (90 and 92% for CNC from rice and coffee husks), thermal resistance (T_{Peak}: ~300 °C) and aspect ratio (L/d: 20-40).

The active compounds from different types of agro-waste are usually extracted using organic solvents, such as ethanol or methanol. Nevertheless, the extraction by hydrothermal treatments is a better option because hot-water at high-pressure extraction (180 °C, 9.5 bar,

60 min; **Chapter III**) is an environmentally-friendly process. The concentrated and spray dried extracts, yielded 17 and 18 g of extract solids/ 100 g of rice or coffee husks, and were brown in colour. The total phenolic content of rice and coffee husk extracts ranged between 60-70 mg GAE/g extract solids, with a small reduction in this content during the spray-drying process probably associated with the partial oxidation of some components. Likewise, extracts exhibited antioxidant properties with similar capacity in both samples. In terms of Trolox equivalence (TE), it was 12.5 mg TE/g extract solid, while the EC_{50} parameter showed values of 5.37-5.29 mg extract solids/mg DPPH, in the range of other active lignocellulosic residues. The powdered extracts from coffee and rice husks also exhibited antibacterial activity against *L. innocua* and *E. coli,* which were quantified in terms of the minimal inhibitory concentration (MIC, mg powder/mL). The powdered coffee extract exhibited a greater inhibitory effect (lower MIC values) against both bacteria (*L. innocua*: 48; *E. coli*: 50) than that obtained from rice husk (*L. innocua*: 52; *E. coli*: 66). Therefore, the incorporation of these extracts into biodegradable films can enhance their functional properties, while could confer colour to the films.

In the present study, the changes induced by the addition of the isolated lignocellulosic fractions to pure thermoplastic starch films and compatibilised starch-PLA blend films were analysed, all of which were processed by melt blending (using a two-roll mill or internal mixer) and compression moulding. Table 1 summarises the composition of each of the considered formulations throughout the different chapters. Mechanical and barrier properties were chosen as the most relevant indicators with which to analyse the films' ability for food packaging purposes. Figure 1 shows the plot of TS (Tensile Strength, MPa) vs. ε (Elongation at break point, %) where of all the film formulations are located, while Figure 2 shows the values of their elastics modulus (EM, MPa). In both figures, the values of tensile properties of some conventional polymers are also shown. Likewise, Figure 3 shows the map of barrier properties (OP vs. WVP) where the different film formulations are located for comparison purposes.

The first analysis used to check the effectiveness of the cellulose reinforcing agents was to incorporate them at 1 wt% into pure thermoplastic starch matrices, by melt blending process using the two-roll mill with subsequent compression moulding (**Chapter I**). The values of mechanical properties were affected by both micro- and nano-fillers, where the EM were considerably increased, especially when cellulose particles were in the nanoscale (from 258 MPa in net starch film to 740 MPa in films with CNC from rice husk). In parallel, the elongation at break decreased more than 50% compared to pure starch films, as previously observed for composites.

Table 1. Summary of all formulations developed in the present doctoral thesis organized by chapters.

Chapter	Description	Film composition (g compound/ g dried film)						Processing method	Notation	Sample code in the maps
		S	Gly	PLA	PCL_G/PCL_{MG}	CNC/CF	AE			
I	Corn starch films reinforced with 1 wt% of cellulose fibres or CNC from rice and coffee husk	0.769	0.231	-	-	-	-	Two roll mill and compression moulding	S'	1
		0.762	0.228	-	-	0.010	-		S-RF	2
		0.762	0.228	-	-	0.010	-		S-RC	3
		0.762	0.228	-	-	0.010	-		S-CF	4
		0.762	0.228	-	-	0.010	-		S-CC	5
II	Films based on corn starch containing different quantity of cellulose fibres from rice or coffee husk	0.731	0.219	-	-	0.050	-	Two roll mill and compression moulding	S-RF5	6
		0.692	0.208	-	-	0.100	-		S-RF10	7
		0.731	0.219	-	-	0.050	-		S-CF5	8
		0.692	0.208	-	-	0.100	-		S-CF10	9
III	Corn starch films with different ratio glucerol:active compound from rice or coffee husk. Cellulose fibres from rice or coffee husk was also incorporated at the optimal formulation	0.769	0.231	-	-	-	-	Internal mixer and compression moulding	S''	10
		0.769	0.185	-	-	-	0.046		S-80:20C	11
		0.769	0.162	-	-	-	0.069		S-70:30C	12
		0.769	0.138	-	-	-	0.092		S-60:40C	13
		0.769	0.185	-	-	-	0.046		S-80:20R	14
		0.769	0.162	-	-	-	0.069		S-70:30R	15
		0.769	0.138	-	-	-	0.092		S-60:40R	16
		0.731	0.219	-	-	0.050	-		S-CF'	17
		0.731	0.153	-	-	0.050	0.066		S-70:30C-CF	18
		0.731	0.219	-	-	0.050	-		S-RF'	19
		0.731	0.153	-	-	0.050	0.066		S-70:30R-RF	20

Table 1. (Continued).

Chapter	Description	Film composition (g compound/ g dried film) S	Gly	PLA	PCL_G/PCL_{MG}	CNC/CF	AE	Processing method	Notation	Sample code in the maps
IV	Films based on corn starch and PLA blends compatibilised with grafted poly(ε-caprolactone) at 2.5 or 5 wt%	-	-	1.000	-	-	-	Internal mixer and compression moulding	PLA	21
		0.667	0.200	0.133	-	-	-		$SPLA_{20}$	22
		0.654	0.196	0.131	0.019	-	-		$S(PCL_{2.5G})PLA_{20}$	23
		0.641	0.192	0.128	0.038	-	-		$S(PCL_{5G})PLA_{20}$	24
		0.654	0.196	0.131	0.019	-	-		$S(PCL_{2.5MG})PLA_{20}$	25
		0.641	0.192	0.128	0.038	-	-		$S(PCL_{5MG})PLA_{20}$	26
		0.588	0.176	0.235	-	-	-		$SPLA_{40}$	27
		0.576	0.173	0.231	0.020				$S(PCL_{2.5G})PLA_{40}$	28
		0.565	0.169	0.226	0.040				$S(PCL_{5G})PLA_{40}$	29
		0.576	0.173	0.231	0.020				$S(PCL_{2.5MG})PLA_{40}$	30
		0.565	0.169	0.226	0.040				$S(PCL5_{MG})PLA_{40}$	31
V	Starch-PLA compatibilised blends containing cellulosic fractions and active compound from coffee husk. CNC were incorporated by two methods (M1 and M2)	0.762	0.228	-	-	0.010	-	M1: glycerol transference M2: direct thermoprocessing in two roll mill Internal mixer and compression moulding	S-CNC-M1	32
		0.762	0.228	-	-	0.010	-		S-CNC-M2	33
		0.635	0.190	0.127	0.038	0.010	-		$S(PCL_{5G})PLA_{20}$-CNC-M1	34
		0.635	0.190	0.127	0.038	0.010	-		$S(PCL_{5G})PLA_{20}$-CNC-M2	35
		0.635	0.190	0.127	0.038	0.010	-		$S(PCL_{5G})PLA_{20}$-CF	36
		0.641	0.135	0.128	0.038	-	0.058		$S(PCL_{5G})PLA_{20}$-AE	37

S': processed in two-roll mill; S'': processed in the internal mixer; S-CF': 5 wt% of cellulose fibres from coffee husk processed in the internal mixer; S-RF': 5 wt% of cellulose fibres from rice husk processed in the internal mixer.

Due to the positive effect of the fillers on the mechanical performance of the films, a more in-depth analysis of the effect of the fibres, obtained with high yield from the husks, was carried out through the incorporation of 5 and 10 wt% cellulose fibres into the starch films (**Chapter II**). This study showed a considerable increase in the film strength (EM and TS) as the amount of fibres rose.

The incorporation of active extract, from both rice and coffee husks, into the thermoplastic starch matrix (**Chapter III**) had a positive effect on the oxygen permeability of the films, since it was reduced by between 85-86% with respect to the control sample, at the highest incorporation ratio (9.2 wt.%). The mechanical properties were also improved with the active extract; TS increased compared to the control film when 4.6 and 6.9 wt % of extract solids were incorporated, although the highest ratio led to the opposite effect, giving rise to very brittle, less stretchable films. Therefore, the formulation with 6.9 % of extract solids (with the highest values of EM, TS, and ε) was chosen to incorporate 5 wt% of cellulose fibres in order to further enhance their tensile or barrier properties. These composites maintained adequate elongation with slightly higher EM and TS and very low values of OP, although they exhibited higher WVP. Then, reinforcing films containing active extracts with cellulose fibres did not represent a notable improvement in the film's characteristics compared to the fibre-free sample. In comparison with commercial synthetic polymers, these films were more extensible than PS or PP (polypropylene), but with not as stiff.

When the net starch films processed by two different melt processes (two-roll mill and internal mixer) were compared, notable differences in tensile behaviour was observed. The ε increased by 440% in the sample processed in the internal mixer, which, in turn was less stiff and resistant to break, with lower barrier capacity to water vapour and oxygen. This could be attributed to a varying degree of starch depolymerisation during the different processes. Other authors report that starch chains depolymerise during thermoprocessing, depending on the process conditions (Koch, 2018). In the internal mixer, components are submitted to overpressure in the closed chamber whereas in the open two-roll mill, atmospheric starch gelatinisation occurred at atmospheric pressure. This factor could imply a higher degree of starch depolymerisation, giving rise to shorter polymer chains, with less ability to strengthen the films and to limit the mass transfer phenomenon (permeation of water and oxygen molecules). Similar behaviour was observed for the starch formulations with 5 wt% of cellulose fibres obtained by processing with the two-roll mill (S-CF5/S-RF5) or the internal mixer (S-CF'/S-RF').

Blending starch with PLA led to changes in the film's tensile and barrier properties, enhancing its stiffness and resistance to break, but reducing stretchability. Almost all of the films exhibited a starch continuous phase where PLA domains were dispersed, with lower particle size and better interfacial adhesion when grafted PCL were included as

compatibilisers. However, films with 40 % substitution of starch by PLA presented a PLA continuous phase with dispersed starch when grafted PLC_G was used at 2.5 or 5 % (**Chapter IV**). The characteristics of PLA (EM: 1370 MPa, TS: 53 MPa; ε: 4%; WVP: 0.2 $g \cdot mm \cdot kPa^{-1} \cdot h^{-1} \cdot m^{-1}$; OP: 466 $cm^3 \cdot m^{-1} \cdot s^{-1} \cdot Pa^{-1}$) are comparable to some petroleum-based plastics, such as polyethylene terephthalate (PET; EM: 1700 MPa; WVP: 0.3 $g \cdot mm \cdot kPa^{-1} \cdot h^{-1} \cdot m^{-1}$; OP: 455 $cm^3 \cdot m^{-1} \cdot s^{-1} \cdot Pa^{-1}$) or PS (EM: 2800 MPa, TS: 45 MPa; ε: 1-4%; WVP: 0.3 $g \cdot mm \cdot kPa^{-1} \cdot h^{-1} \cdot m^{-1}$).

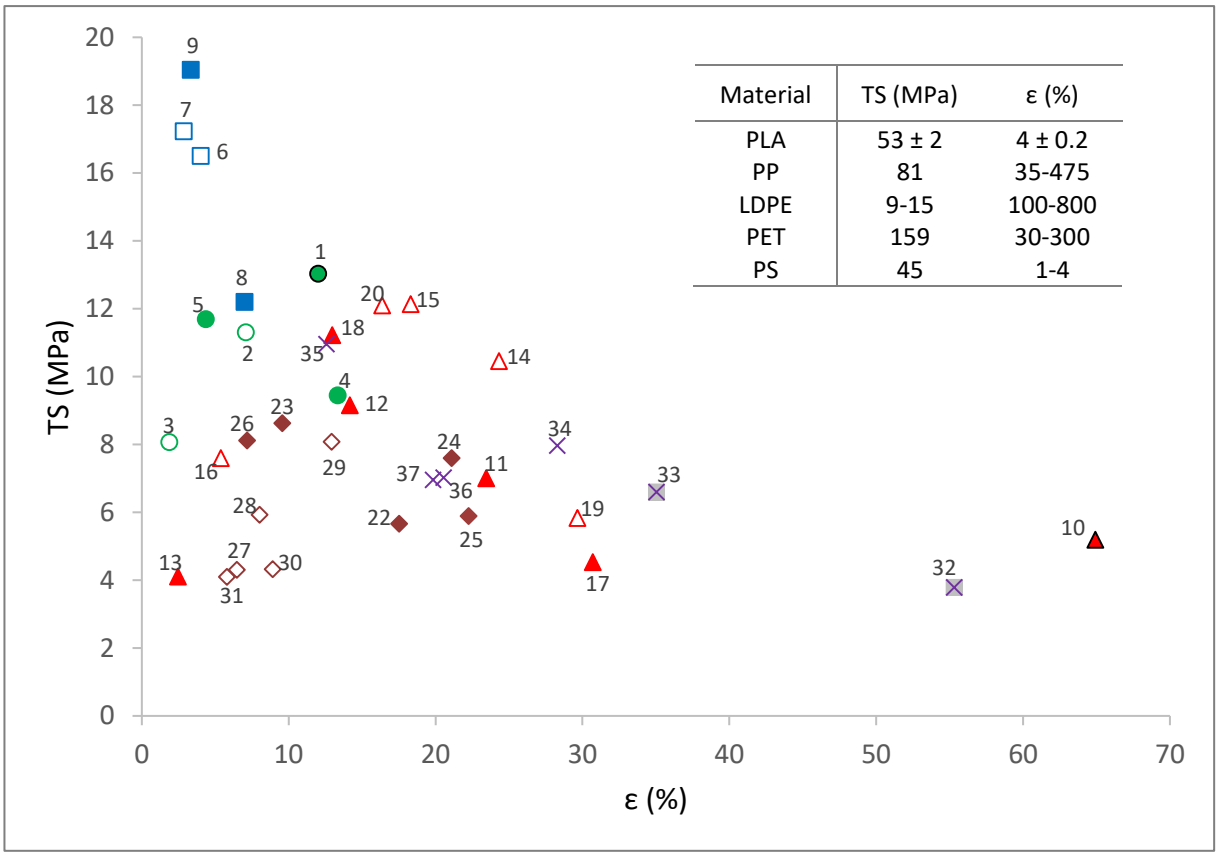

Figure 1. Map of mechanical properties (Tensile Strength vs. Elongation at break) showing the location of the different film formulations and some synthetic plastics commonly used in food packaging (PP, LDPE, PET, PS; Mark, 1999; Ortega-Toro et al. 2017).

Then, although PLA incorporation provided the blends with lower water vapour permeability, it promoted their oxygen permeability. The OP increased in all of the blend formulations, especially in the blend with 40% starch substitution without compatibilisers (43 $cm^3 \cdot m^{-1} \cdot s^{-1} \cdot Pa^{-1}$). Nonetheless, a reduction of about 40% was observed in every case, regardless of the ratio of PLA, with respect to blends without compatibilisers. The WVP was reduced by about 33 or 50% in blends where starch was substituted by 20 and 40% PLA,

respectively. This reduction was greater than that obtained with cellulose fibres or active extracts in the starch films due to the hydrophobic nature of the PLA. As concerns tensile properties, compatibilised samples with 40% starch substitution exhibited lower values of EM, TS and ε than those with 20% starch substitution, which can be attributed to the increase in the volume fraction of the dispersed phase. Compatibilised blends with 20% starch substitution showed a significant increase in EM (~2 times, when using $PCL_{2.5MG}$) and TS (~1.5 times, when using $PCL_{2.5G}$) with respect to the non-compatibilised blends. However, a decrease in the film elongation at break was observed in compatibilised films when PCL_G and PCL_{MG} were used, at 2.5% and 5%, respectively. Based on these results, S-PLA_{20} compatibilised with 5% of PCL_G was considered the most suitable formulation for food packaging purposes, although blends with 40 % of starch substitution by PLA and 5% of PCL_G exhibited the lowest WVP and, in spite of being less extensible, could also be selected for specific food packaging with these requirements.

Cellulose fibres (1 wt %), cellulose nanocrystals (1 wt%) or antioxidant extracts (6.9 wt%) from coffee husk were used to enhance the functional properties of compatibilised starch-PLA blend films (**Chapter V**). The method of CNC incorporation from their aqueous dispersion into the polymeric matrices was studied, due to the fact that the water content must be reduced in the internal mixer to prevent overpressure during the polymer melt blending or polymer hydrolysis. Significant differences in tensile properties were observed for films with the same composition obtained by using both methods for the CNC transference. A considerable increase in EM was detected when CNC were directly incorporated into the starch phase in the open two-roll mill (e.g. from 140 MPa to 515 MPa in S(PCL_{5G})PLA_{20}-CNC blend). A similar effect was observed on the TS, while the film extensibility was only notably reduced when using M2 for CNC incorporation. Barrier properties were also affected by the CNC incorporation method. In starch-PLA compatibilised films, WVP was reduced (by 28%) whereas OP decreased by 42% when using method 2.

Cellulose fibres and antioxidant extracts provoked a weakening effect on the film matrix reflected in the EM values, which were lower than in the control film, even though both compounds had a significant reinforcement effect on net starch films. Moreover, they did not provoke significant changes in the film resistance to break and extensibility. This phenomenon could be explained by the fact that the dispersed PLA already reinforces starch films, but introduces a dispersed phase in the matrix, which could limit the effect of both fibres and active compounds. As concerns the barrier properties, although neither was observed to have a significant effect on the WVP, the presence of antioxidant extracts brought about a 15% reduction in OP with respect to the control film.

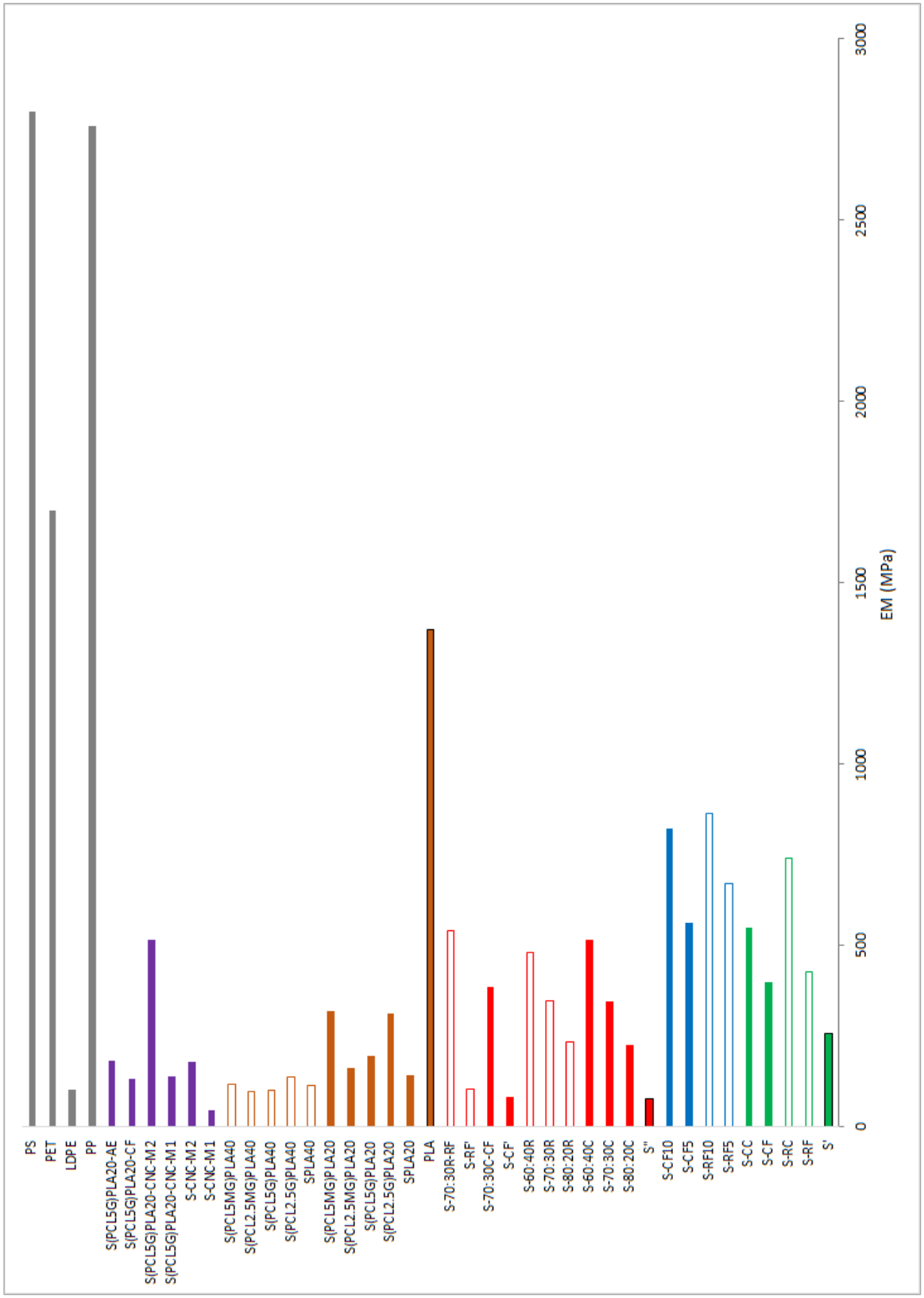

Figure 2. Elastic modulus values of the different film formulations and some synthetic plastics commonly used in food packaging (PP, LDPE, PET, PS; Mark, 1999; Ortega-Toro et al. 2017).

An OP reduction caused by extract incorporation was also observed in net starch films, which was attributed to the oxygen scavenging capacity of the compounds in line with their antioxidant activity. In contrast, the addition of fibres to the S-PLA compatibilised matrix increased the OP by 40%.

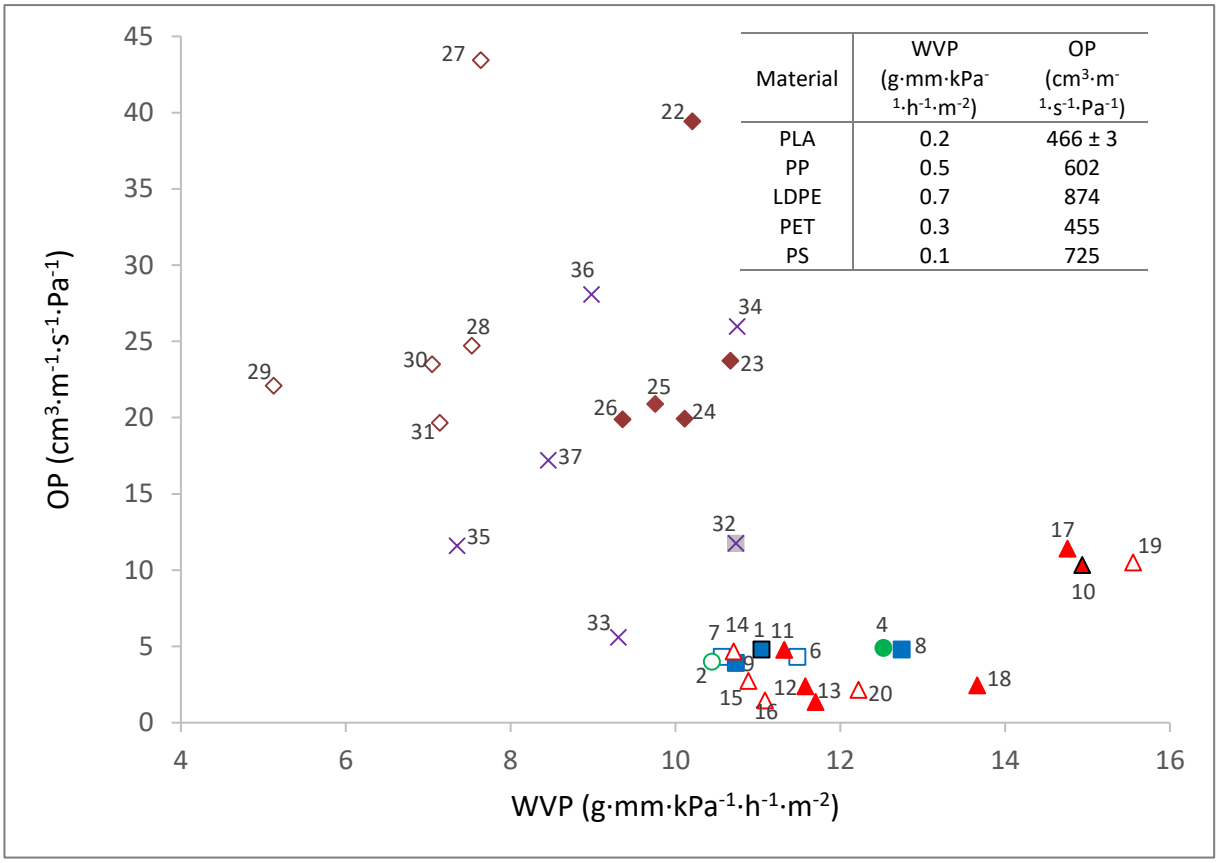

Figure 3. Map of barrier properties showing the location of the different film formulations and some synthetic plastics commonly used in food packaging (PP, LDPE, PET, PS; Ortega-Toro et al. 2017).

All the formulations based on S-PLA blends showed higher water vapour permeability values than commercial synthetic polymers because they are hydrophobic materials. However, they presented considerably lower OP values. As regards the mechanical properties, these materials had a lower elastic modulus than the synthetic materials, except for the LDPE. The TS and ε values are higher than the LDPE and PS, but lower compared to PP and PET. To sum up, lignocellulosic fractions or PLA incorporation allowed for an improvement in the properties of starch materials so they may be used for food packaging purposes. All of these maintain very low oxygen permeability, which is an important function for preserving foods

from oxidation, while the mechanical performance was notably improved. However, given the limited reduction in the water vapour permeability, their use will be restricted to low or intermediate moisture foods where the oxidation process can limit their shelf life, such as fatty foods. In this sense, the use of antioxidant extracts from lignocellulosic residues is of particular interest since they provide the films with antioxidant capacity (and possiblyantibacterial activity) which efficiently contribute to an enhancement in the film functionality. Likewise, the valorisation of these residues in biodegradable materials for food packaging lies within the framework of circular economy and provides interesting sustainable materials for food packaging applications. Specific application studies into different kinds of food products should be carried out in order to validate their usefulness.

References

Koch, K. (2018). Starch-based film. In M. Sjöö & L. Nilsson (Eds), *Starch in food* (pp. 747-767). Woodhead Publishing.

Mark, E. J. (Ed.) (1999). *Polymer Data Handbook*. New York: Oxford university press.

Ortega-Toro, R., Bonilla, J., Talens, P., & Chiralt, A. (2017). Starch-based materials in food packaging. In M. A. Villar, S. E. Barbosa, M. A. García, L. A. Castillo, & O. V. López (Eds.), *Future of starch-based materials in food packaging* (pp. 257-312). Aspen Publishers.

CONCLUSIONS

1- The cellulose contents of rice and coffee husks were similar in the range of 34-35 %, which make them a good source of cellulosic material for different industrial uses. Purification of cellulose, using the classical alkali and bleaching treatments was effective at removing hemicellulose and lignin, providing white fibres with about 50% crystallinity degree and 60-500 μm length, with good thermal stability. Coffee fibres were flatter and more helically folded than rice fibres. Acid hydrolysis of both fibres gave rise to CNCs, with small morphological differences. CNCs from coffee husk were slightly thinner (20 against 39 nm, in average diameter), but with similar aspect ratio (higher than 10). The CNCs exhibited slightly lower thermal stability than the cellulose fibres. The properties of cellulosic fractions from rice and coffee husk make them very adequate as reinforcing materials in biopolymer composites, especially nano-sized reinforcement which increased the elastic modulus of TPS films by 186% and 121%, respectively. So, coffee husk represents an interesting source of cellulosic reinforcing material, whose use in different applications, such as packaging materials, could boost the value of this waste.

2- Coffee and rice husk cellulosic fibres provoked a relevant reinforcing effect on glycerol plasticised TPS films, this being higher (more than 200%) when the fibre content increased till 10 wt%, while reduced the film stretchability. However, CF better maintained the film ductility than RF at 1 and 5 wt%. This reinforcing effect was maintained during film storage (28 weeks). A network of fine oriented fibres was observed in the surface of the films, which could contribute greatly to the increase in the resistance to deformation of the films. The fibres distributed in the internal part of the matrix exhibited a good adherence to the polymer network as revealed by the FESEM analysis of the film cross-section. WVP of TPS films was not reduced in composites, although OP was lowered by about 17%. Film transparency decreased by fibre addition in the UV-VIS range, which could be interesting to preserve foods from light-induced oxidation reactions. Thermal stability of composites was slightly higher than net TPS films. These results indicate the excellent capacity of fibres from coffee and rice husks to improve functional properties of TPS films while representing a good alternative to give added value to these agricultural wastes.

3- The incorporation of aqueous extracts and cellulose fibres from rice and coffee husks into thermoplastic starch films leads to improved functional properties as packaging materials, while exploiting these by-products. Both hydrothermal aqueous extracts exhibited antioxidant and antibacterial activity against *L. innocua* and *E. coli*, which provide the films with active properties. The active extracts improved the tensile properties of the starch films, mainly when they were incorporated by substituting 30% of the plasticizing glycerol. Although the films became less stretchable, a relevant reinforcing effect was observed, with the EM increasing by about 350% for rice and coffee husk extracts. The incorporation of cellulosic fibres from both residues was more effective in films containing extract solids than in net starch films in terms of the reinforcing effect. This can be attributed to a certain

compatibilizer effect of the extract compounds that allows for a better integration of the fibres in the starch matrices. Likewise, active extracts led to a 30% reduction in the WVP of starch films and a 50-85% reduction in the OP, depending on the amount of extract. However, cellulose fibres at 5% were observed to have no effect on barrier properties. So, the incorporation of extracts and fibres produced films with improved tensile and barrier properties, which, in turn, were less transparent and brown. Then, they could have specific applications in the preservation of foods from light induced oxidation, which may be enhanced by their antioxidant activity. Specific *in vivo* tests would be required to assess their antibacterial action in different food matrices.

4- The starch-PLA matrices compatibilized with grafted PCL presented a better dispersion of the PLA in the continuous starch phase, especially for the highest amount of compatibilizer. The use of PCL_G provoked a phase inversion in the matrix when 40% of starch was substituted by PLA. Interactions between polymers and compatibilizers could be deduced from microstructural, thermal and spectral data. The compatibilized blend films exhibited higher values of EM than pure starch films, but they were less extensible, with similar tensile strength at break, the values depending on the PLA ratio and the type and concentration of compatibilizer. From the mechanical point of view, the film formulation containing about 20% PLA and 5% PCL_G exhibited good tensile strength and great extensibility, being suitable for packaging purposes. The WVP was reduced by blending up to 33 or 50% for about 20 and 40% PLA, respectively, although films with 40% PLA and 5% PCL_G, exhibited a more marked reduction (67%). The incorporation of compatibilizers significantly decreased the OP by about 40% with respect to non-compatibilized samples, regardless of the % of PLA and the kind and amount of compatibilizer. Therefore, substituting 20% of the starch by PLA and incorporating 5% PCL_G would be a good strategy to obtain films that are useful for food packaging; the starch phase provided the films with an excellent oxygen barrier capacity, while PLA enhanced the mechanical resistance and reduced the water vapour permeability. In particular, dry or partially dehydrated products and fatty or oxidation-sensitive foods could be adequately packaged with these films, thus improving their preservation.

5- Lignocellulosic fractions of coffee husk could be used to improve the functional properties of compatibilised starch PLA films, depending on their final use. Of the cellulosic fractions, CF was not adequate to enhance the functionality of the blend film, but CNC previously incorporated into the starch phase were effective at reinforcing the tensile properties of the material (148% and 45% increases in EM and TS, respectively) and at reducing the WVP and OP of the films (28% and 42% reductions, respectively in WVP and OP). Likewise, the antioxidant extract did not impart a better mechanical performance to the blend films, but reduced their oxygen permeability and conferred antioxidant capacity, promoting their usefulness for the purposes of preventing food oxidation reactions.

As a general conclusion, coffee and rice husks represent an interesting source of cellulose reinforcing material and active compounds, with antioxidant and antibacterial properties (tested on *L. Innocua* and *E. coli*). Both reinforcing and active agents isolated from both residues were effective at improving the functional characteristics of starch films. The elastic modulus and resistance to break were enhanced, especially when using nano-sized reinforcements and active extracts, while the film stretchability was reduced. Active extracts provide the films with higher oxygen barrier capacity and antioxidant activity and, as in the case of the fillers, reduced the film transparency in the UV-VIS range, all of which is of interest for the purposes of preserving foods from light-induced oxidation reactions. Blending of starch and PLA with functionalised PCL also enhanced the functionality of starch films, increasing their mechanical resistance while promoting their barrier capacity for water vapour. The incorporation of lignocellulosic fractions into blend films was less effective in terms of mechanical reinforcement than in net starch films but enhanced their water vapour barrier capacity, while active extracts also conferred antioxidant activity. Therefore, the use of lignocellulosic fractions of rice and coffee husks allows for an improvement in the functionality of starch-based films, making them more suitable to meet the food packaging requirements. Considering the biodegradable nature of the used materials and the valorisation of by-products, the developed films lie within the framework of circular economy and provide interesting sustainable materials for food packaging applications. Specific application studies into different kinds of food products should be carried out to validate their usefulness.

"Sé el cambio que quieres ver en el mundo"